

7-

Late Cenozoic Stratigraphy of the Feather and Yuba Rivers Area, California, with a Section on Soil Development in Mixed Alluvium at Honcut Creek

U.S. GEOLOGICAL SURVEY BULLETIN 1590-G



AVAILABILITY OF BOOKS AND MAPS OF THE U.S. GEOLOGICAL SURVEY

Instructions on ordering publications of the U.S. Geological Survey, along with prices of the last offerings, are given in the current-year issues of the monthly catalog "New Publications of the U.S. Geological Survey." Prices of available U.S. Geological Survey publications released prior to the current year are listed in the most recent annual "Price and Availability List." Publications that are listed in various U.S. Geological Survey catalogs (see back inside cover) but not listed in the most recent annual "Price and Availability List" are no longer available.

Prices of reports released to the open files are given in the listing "U.S. Geological Survey Open-File Reports," updated monthly, which is for sale in microfiche from the U.S. Geological Survey, Books and Open-File Reports Section, Federal Center, Box 25425, Denver, CO 80225. Reports released through the NTIS may be obtained by writing to the National Technical Information Service, U.S. Department of Commerce, Springfield, VA 22161; please include NTIS report number with inquiry.

Order U.S. Geological Survey publications by mail or over the counter from the offices given below.

BY MAIL

Books

Professional Papers, Bulletins, Water-Supply Papers, Techniques of Water-Resources Investigations, Circulars, publications of general interest (such as leaflets, pamphlets, booklets), single copies of Earthquakes & Volcanoes, Preliminary Determination of Epicenters, and some miscellaneous reports, including some of the foregoing series that have gone out of print at the Superintendent of Documents, are obtainable by mail from

**U.S. Geological Survey, Books and Open-File Reports
Federal Center, Box 25425
Denver, CO 80225**

Subscriptions to periodicals (Earthquakes & Volcanoes and Preliminary Determination of Epicenters) can be obtained ONLY from the

**Superintendent of Documents
Government Printing Office
Washington, D.C. 20402**

(Check or money order must be payable to Superintendent of Documents.)

Maps

For maps, address mail orders to

**U.S. Geological Survey, Map Distribution
Federal Center, Box 25286
Denver, CO 80225**

Residents of Alaska may order maps from

**Alaska Distribution Section, U.S. Geological Survey,
New Federal Building - Box 12
101 Twelfth Ave., Fairbanks, AK 99701**

OVER THE COUNTER

Books

Books of the U.S. Geological Survey are available over the counter at the following Geological Survey Public Inquiries Offices, all of which are authorized agents of the Superintendent of Documents:

- **WASHINGTON, D.C.**--Main Interior Bldg., 2600 corridor, 18th and C Sts., NW.
- **DENVER, Colorado**--Federal Bldg., Rm. 169, 1961 Stout St.
- **LOS ANGELES, California**--Federal Bldg., Rm. 7638, 300 N. Los Angeles St.
- **MENLO PARK, California**--Bldg. 3 (Stop 533), Rm. 3128, 345 Middlefield Rd.
- **RESTON, Virginia**--503 National Center, Rm. 1C402, 12201 Sunrise Valley Dr.
- **SALT LAKE CITY, Utah**--Federal Bldg., Rm. 8105, 125 South State St.
- **SAN FRANCISCO, California**--Customhouse, Rm. 504, 555 Battery St.
- **SPOKANE, Washington**--U.S. Courthouse, Rm. 678, West 920 Riverside Ave..
- **ANCHORAGE, Alaska**--Rm. 101, 4230 University Dr.
- **ANCHORAGE, Alaska**--Federal Bldg, Rm. E-146, 701 C St.

Maps

Maps may be purchased over the counter at the U.S. Geological Survey offices where books are sold (all addresses in above list) and at the following Geological Survey offices:

- **ROLLA, Missouri**--1400 Independence Rd.
- **DENVER, Colorado**--Map Distribution, Bldg. 810, Federal Center
- **FAIRBANKS, Alaska**--New Federal Bldg., 101 Twelfth Ave.

Chapter G

Late Cenozoic Stratigraphy of the Feather and Yuba Rivers Area, California, with a Section on Soil Development in Mixed Alluvium at Honcut Creek

By ALAN J. BUSACCA, MICHAEL J. SINGER, and
KENNETH L. VEROSUB

U.S. GEOLOGICAL SURVEY BULLETIN 1590

SOIL CHRONOSEQUENCES IN THE WESTERN UNITED STATES

DEPARTMENT OF THE INTERIOR

MANUEL LUJAN, JR., Secretary

U.S. GEOLOGICAL SURVEY

Dallas L. Peck, Director



Any use of trade, product, or firm names in this publication is for descriptive purposes only and does not imply endorsement by the U.S. Government

UNITED STATES GOVERNMENT PRINTING OFFICE, WASHINGTON : 1989

For sale by the Books and
Open-File Reports Section,
U.S. Geological Survey
Federal Center, Box 25425
Denver, CO 80225

Library of Congress Cataloging in Publication Data

Busacca, Alan J.

Late Cenozoic stratigraphy of the Feather and Yuba Rivers area, California :
with a section on soil development in mixed alluvium at Honcut Creek / by
Alan J. Busacca, Michael J. Singer, and Kenneth L. Verosub.

p. cm. — (Soil chronosequences in the western United States;)
(U.S. Geological Survey bulletin ; 1590-G)

Bibliography: p.

Supt. of Docs. no.: I 19.3:1590-G

1. Geology, Stratigraphic—Cenozoic. 2. Geology—California—Feather
River Region. 3. Geology—California—Yuba River Region. 4. Soil
formation—California—Honcut Creek Region. I. Singer, Michael J. (Michael
John), 1945- . II. Verosub, Kenneth L. III. Title. IV. Series. V. Series:
U.S. Geological Survey bulletin; 1590-G.

QE75.B9 no. 1590-G
[QE690]

557.3 s-dc20
[551.7'8'097943]

89-600086
CIP

FOREWORD

This series of reports, "Soil Chronosequences in the Western United States," attempts to integrate studies of different earth-science disciplines, including pedology, geomorphology, stratigraphy, and Quaternary geology in general. Each discipline provides information important to the others. From geomorphic relations we can determine the relative ages of deposits and soils; from stratigraphy we can place age constraints on the soils. Field investigations and mineralogic and sedimentologic studies provide information on the nature and types of deposits in which soils form. As a result of our work, we have estimated rates of soil formation, inferred processes of soil formation from trends in soil development with increasing age, and obtained information on the types of weathering that occur in various areas. In return, soil development and soil genesis have provided data on the age of landforms, the timing and duration of sedimentation, and, in some cases, the history of climatic fluctuations.

Between 1978 and 1983, a coordinated and systematic study was conducted on soil development in different types of geologic deposits in the Western United States. The goals of this project, led by the late D.E. Marchand and subsequently by M.N. Machette, were to learn whether rates of chemical, physical, and mineralogic transformations could be determined from soil chronosequences; how these rates vary in different mineralogic and climatic environments; and how accurately soils can be used for such problems as estimating the ages of deposits, periods of landscape stability, and timing of fault movements. This series of reports presents data from several soil chronosequences of that project.

More than 100 analyses on more than 1,000 samples were performed on soils collected in the Western United States. Some results have appeared in various books, journals, and maps (for example, Harden and Marchand, 1977, 1980; Burke and Birkeland, 1979; Dethier and Bethel, 1981; Marchand and Allwardt, 1981; Meixner and Singer, 1981; Busacca, 1982; Harden, 1982a,b; Harden and Taylor, 1983; Machette, 1983; Machette and Steven, 1983; Busacca and others, 1984; Machette and others, 1984; Reheis, 1984). In the reports in this series, the basic field information, geologic background, and analytical data are presented for each chronosequence, as well as some results additional to the previous publications.

One of the most significant aspects of these chronosequence studies is that in every study area, many soil parameters change systematically over time, or with the age of deposits. As Deming (1943) emphasized, it is this recurrence of correlation in such different conditions that is most significant to geologic and pedologic studies. In relatively moist areas, such as coastal and central California, such soil properties as percent clay or reddening of soil colors change most systematically over time. In more arid regions, such as in the Bighorn basin of Wyoming, calcium carbonate and gypsum contents best reflect relative ages of the deposits. A few parameters—for example, elemental composition of sands or clays—appear to be comparable between areas so diverse in climatic setting.

Numeric age control has enabled us to estimate rates of soil development. In some places, we have been able to compare rates between different areas. For example, in central California, rates of clay accumulation were found to be most rapid during the initial stages of soil development; the rates declined with increasing age. The straightest lines for regression were on a log-log scale. In coastal California, rates of clay accumulation appeared to be much higher than in central California. This difference in rates could be due to parent material (the coastal soils that we studied formed on reworked shale and sandstone, whereas central California soils were developed in granitic alluvium), and (or) the differences in rates could be due to eolian additions of clay. In the Bighorn basin of Wyoming, rates of clay accumulation, as well as most other soil properties, increased linearly over time, with no apparent decrease in initial rates.

The data we present here suggest many opportunities for further interpretation. For example, we may learn how climate, vegetation, and mineralogy affect the rates of clay formation or organic-matter accumulation. In some study areas, we present data for rare-earth elements, which could be used to examine how each element reacts in different weathering environments. These examples are only a fraction of the possible future studies that could be conducted on the data presented here.

J.W. Harden
Editor

CONTENTS

Foreword	III	
Abstract	G1	
Introduction	G2	
Diagnostic stratigraphic criteria and methods		G5
Stratigraphic criteria	G5	
Dating methods	G5	
Paleomagnetic stratigraphy		G5
Radiocarbon dating	G5	
Potassium-argon radiometric dating		G5
Tephrochronology	G5	
Geologic mapping	G6	
Geographic and geologic setting		G6
Geographic setting	G6	
Geologic setting	G7	
Stratigraphy	G7	
Previous work	G7	
Description of stratigraphic units		G10
Basin deposits	G14	
Holocene alluvium	G14	
Soil landscapes	G15	
Geochronology and correlation		G15
Modesto Formation	G16	
Upper member	G16	
Lower member	G16	
Soil landscapes	G18	
Geochronology and correlation		G19
Riverbank Formation	G19	
Upper member	G20	
Lower member	G20	
Soil landscapes	G21	
Geochronology and correlation		G22
Laguna Formation	G23	
Upper member	G25	
Lower member	G27	
Nomlaki Tuff member	G28	
Post-Laguna, pre-Riverbank erosion		G29
Soil landscapes	G29	
Geochronology and correlation		G30
Dacite unit	G33	
Geochronology and correlation		G35
Pre-dacite Cenozoic units	G36	
Deformation and tectonism	G37	
Summary and discussion of geologic history and tectonics		G39
Soil chronosequence site selection, excavation, and sampling		G41
Characteristics of the soil chronosequence	G43	
Review of state factors	G44	
Climate	G44	
Organisms	G45	
Parent material	G45	
Soil development	G48	
Soil development index	G48	

Mineralogy of the clay fraction	G55
Elemental composition of silt-size fractions	G56
Summary of trends in soil development and their use in soil correlation	G62
References cited	G63
Supplementary tables	G68

FIGURES

1. Index map of study area	G3
2. Generalized geologic map of study area	G8
3. Schematic cross sections on and south of Honcut Creek	G15
4. Schematic cross sections showing inferred extension of Prairie Creek and Magalia lineament fault zone	G24
5. Correlation of samples with an established magnetic polarity time scale	G31
6. Index map showing sample sites of chronosequence soil profiles	G42
7. Plots of estimated rainfall from Miocene to Quaternary time in west-central California and central Sierra Nevada	G44
8–16. Plots of:	
8. Percent clay-free sand versus depth in replicate soil profiles formed in Holocene alluvium	G46
9. Horizon index versus depth of soil horizons in replicate soil profiles formed in alluvium of chronosequence members	G51
10. Composite depth showing soil development quantified by average values of horizon indices of replicate profiles calculated at 10-cm intervals for soils	G53
11. Age trend of soil development showing profile indices versus soil age	G54
12. Relative abundance of clay minerals determined by X-ray diffraction versus soil age	G55
13. SiO ₂ in coarse-silt fraction of surface horizons versus soil age	G58
14. Ratio of Fe ₂ O ₃ in percent to Zr in ppm × 100 in fine-silt fraction of surface horizons versus soil age	G58
15. Fraction of original content of elemental oxides remaining in fine-silt fraction versus soil depth	G61
16. Fraction of original content of elemental oxides remaining in fine-silt fraction of surface horizons versus soil age	G62

TABLES

1. Stratigraphic correlations	G4
2. Comparison of areally and stratigraphically important soils in the project area with soil series designated in soil surveys	G11
3. Age control for alluvial units in the Feather and Yuba Rivers area, and correlation of units to the northeastern San Joaquin Valley	G12
4. Comparison of stratigraphic interpretations of an exposure in the Thermalito Power Canal at Cherokee Bridge	G36
5. Site locations, assumed ages, and taxonomic subgroups of the soils sampled for the chronosequence study	G43
6. Comparison of the effect of stratification in a Holocene soil profile on texture versus elemental composition	G47
7. Comparison of the effect of textural stratification on elemental composition of coarse versus fine silt in a soil profile on the lower member of the Modesto Formation	G48
8. Average values of element concentration in coarse and fine silt fractions of BC and C horizons of the chronosequence soils	G49
9. Selected morphological and physical properties of the chronosequence soils	G50

10. Comparison of profile indices for soils from Honcut Creek and the Merced River that are approximate stratigraphic equivalents **G52**
11. Relative enrichment and depletion of elements in the fine silt fraction of A horizons of the chronosequence soils **G56**
12. Ratios of elements to zirconium in fine-silt fraction of selected horizons of soil formed on lower member of the Laguna Formation **G57**
13. Concentration ratios for zircon in fine- and coarse-silt fraction of chronosequence soils **G58**
14. Effect of stratification on the calculation of percentage of original content of elements remaining in the fine-silt fraction of a Holocene soil using Zr as a stable index **G59**
15. Percentage of original content of elements remaining in the fine-silt fraction, calculated using Zr as a stable index **G60**
16. Percentage of original content of elements remaining in the coarse-silt fraction, calculated using Zr as a stable index **G60**

SUPPLEMENTARY TABLES

1. Site locations and field descriptions **G68**
2. Physical properties **G80**
3. Extractive chemical analyses **G84**
4. Clay mineralogy of the coarse and fine fractions **G86**
5. Total chemical analyses of the fine fraction by X-ray fluorescence **G94**
6. Total chemical analyses of the 2–20 μm fraction and the 20–50 μm fraction by X-ray fluorescence for major oxides and trace elements **G98**
7. Total chemical analyses of the fine fraction by instrumental neutron activation **G114**
8. Calculated values of the Soil Development Index **G126**
9. Radiocarbon ages and K-Ar radiometric ages of dacite blocks from lahar of the dacite unit **G128**
10. Tephra correlation **G130**
11. Paleomagnetic determinations **G131**

SUPPLEMENTARY FIGURE

1. Stereographic projections of data from paleomagnetic studies **G132**

Late Cenozoic Stratigraphy of the Feather and Yuba Rivers Area, California, with a Section on Soil Development in Mixed Alluvium at Honcut Creek

By Alan J. Busacca, Michael J. Singer, and Kenneth L. Verosub

Abstract

We describe a sequence of upper Tertiary and Quaternary alluvial deposits for the area of the Feather and Yuba Rivers in the Sacramento Valley, California, and we correlate these deposits with existing stratigraphic units to the south in the northeastern San Joaquin Valley. We also describe our studies of relict and exhumed soils formed on six of these deposits at Honcut Creek in the center of the project area. The soils were examined in order to establish a soil chronosequence to evaluate the systematic changes in soil profile properties with increasing age of the deposits, and to evaluate the use of soils as correlation and dating tools for deposits of the upper Cenozoic.

Methods employed in developing the local stratigraphy and in correlating deposits to the San Joaquin Valley included: (1) stratigraphic superposition of deposits, several of which are separated by buried soils, (2) relative elevation and degree of dissection of original surfaces of deposits, (3) contrasting development of soils on relatively uneroded surfaces of the deposits, (4) tephra correlation, (5) magnetostratigraphy, and (6) radiometric dating.

The alluvial deposits form a poorly expressed set of inset terraces along the edge of the valley that open to the south and west to form a fan flood plain in which successive deposits are buried in normal stratigraphic superposition. Some of the deposits therefore can be observed in both relict-surface and buried positions. Buried soils mark substantial periods of stability between episodes of aggradation. We recognize seven principal alluvial units and we correlate these with members and informal units of the Modesto, Riverbank, and Laguna Formations, plus Holocene alluvium. We did not recognize an alluvial deposit equivalent to the middle Pleistocene Turlock Lake Formation. We suggest that a major hiatus in deposition occurred between the upper Pliocene and lower Pleistocene Laguna Formation and the middle Pleistocene Riverbank Formation.

Tephra correlation and magnetostratigraphy provide new information on the age of the Laguna Formation. Glass from fluviially laid tephra at or near the base of the lower member is correlated with the Nomlaki Tuff Member of the Tehama and Tuscan Formations and provides an age of 3.4 Ma for inception of alluvial deposition in the

project area. We associate a normal-to-reversed transition in magnetic polarity in the upper member of the Laguna with the boundary between the Gauss Normal- and Matuyama Reversed-Polarity Chrons dated elsewhere at 2.48 Ma.

A lahar and volcanic sediments that contain dacitic clasts underlie the Laguna Formation and have only limited surface exposure. Previous workers interpreted this volcanic unit to lie stratigraphically below the Miocene Lovejoy Basalt (basalt of Table Mountain) and attributed a Miocene age to it. Blocks of dacite from the lahar have a mean whole-rock K-Ar age of 3.2 Ma. New stratigraphic and geomorphic data plus the radiometric dating suggest a late Pliocene age and further constrain the time of inception of alluvial valley filling.

The volcanic unit and the Laguna Formation are monoclinaly folded or faulted along the edge of the foothills. Deformation occurred between about 3.0 and 1.5 Ma and is perhaps a southerly extension of the Chico monocline, which terminates 20 km to the north of the Feather River. Aligned north-south drainages in the Riverbank Formation suggest more recent minor deformation.

Distinctive soils are associated with relict surfaces of each formation and member. The most recognizable field properties that develop systematically with increasing soil age are soil color, soil depth, and argillic B horizons. Soils formed in Holocene alluvium have 10 YR brown color hues and A horizons that are less than 0.5 m thick. In contrast, soils formed on the lower member of the Laguna Formation have 10 R red color hues and strong argillic B horizons that extend more than 5 m deep. We analyzed the soils to determine their morphologic, physical, chemical and mineralogic properties. Properties that develop most systematically with soil age are total profile development, as quantified from field properties by the Harden's soil development index, and depletion of major elements from silt-size fractions as determined by X-ray fluorescence spectroscopy. Changes in clay mineralogy with soil age also are distinctive but are qualitative data. Nonconstancy of other soil-forming factors, principally parent material composition and topographic position, introduces important variation in the age trends that we observed and limits the certainty with which soils can be used to correlate and date alluvial deposits. Nevertheless,

systematic change in soil properties over the 1.6 million year estimated age span of the chronosequence provides insight into near-surface weathering processes and provides a means to use soils as a tool in geologic studies.

INTRODUCTION

The 1975 earthquake near Oroville, California, which had a Richter magnitude of 5.7, awakened strong interest and controversy about the late Cenozoic seismic and geologic history of the eastern margin of the Sacramento Valley and adjacent foothills of the Sierra Nevada. This area had not previously been considered to be one of active faulting, and several large engineering structures, most notably the Oroville Dam and reservoir complex and the proposed Auburn Dam, are located on or very near conspicuous topographic lineament-fault zones. Seismic and geologic studies made in the Oroville area after the 1975 earthquake (California Department of Water Resources, 1979; Woodward-Clyde Consultants, 1977; Sherburne and Hauge, 1975) were hampered by a lack of information on the ages and stratigraphic sequence of the alluvial deposits along the margin of the Sacramento Valley. Several photolineaments and, possibly, active faults trend through the alluvium in the Oroville area, but the significance of this cannot be assessed without information on the ages and identity of the deposits. Thick upper Cenozoic alluvial and basin deposits that fill the Sacramento and San Joaquin Valleys have been studied in detail in several locations (Janda, 1966; Marchand and Allwardt, 1981; Helley and others 1981; Harwood and others, 1981). Until this study, however, the deposits in the Oroville area had been the subject of only reconnaissance-level geologic mapping (Davis and Olmsted, 1952; Olmsted and Davis, 1961; California Department of Water Resources, 1979; R. Ford, unpub. data of California Department of Water Resources, 1966).

We undertook this project to develop a coherent stratigraphy for the upper Tertiary and Quaternary deposits of the Feather and Yuba Rivers near Oroville (fig. 1). In addition, we wanted to study in detail the relict soils formed on the surfaces of these deposits, using the increasing degree of soil development with age as a means to correlate and approximately date the deposits. Relict and buried soils have become an important tool for Quaternary studies in recent years (Birkeland, 1984; Morrison, 1978), especially because Quaternary surficial deposits often lack datable horizons, and because correlation based on traditional stratigraphic methods can be difficult.

Using stratigraphic, pedologic, paleomagnetic, and radiometric evidence, we have subdivided the alluvial fill into a sequence of terrace, flood plain, and basin deposits which are derived from the Feather and Yuba Rivers and which span a period of 3 million years. We correlate these deposits with the type Modesto, Riverbank, and Laguna Formations found in the northeastern San Joaquin Valley (Marchand and Allwardt, 1981) and thereby extend the late

Cenozoic stratigraphy of the San Joaquin Valley to the Feather and Yuba Rivers area. Within the description of stratigraphic units, we discuss the characteristic soil landscapes and the typical soil series found on relict and eroded parts of each unit.

In this report we describe the Modesto, Riverbank, and Laguna Formations as they occur in the project area, and we describe reference stratigraphic sections for the Laguna and Riverbank Formations. The Nomlaki Tuff Member of the Laguna, Tehama and Tuscan Formations (Russell and VanderHoof, 1931; Everndon and others, 1964; Harwood and others, 1981; Helley and Harwood, 1985) is bedded at or near the base of the Laguna Formation in the project area. Tephra correlation, paleomagnetic stratigraphy, and new radiometric dates described here provide a better picture of the age and history of the Laguna Formation than we have had before.

We present new radiometric and stratigraphic evidence to show that the part of the volcanoclastic Mehrten(?) Formation of Creely (1965) that lies south of Table Mountain (fig. 1) is actually an independent and much younger stratigraphic unit and is of late Pliocene, not Miocene age. This newly described unit consists of dacitic lahars and volcanoclastic sedimentary rocks. It underlies virtually the entire upper Cenozoic alluvial pile in the project area and for this reason is an important stratigraphic marker. From its age and stratigraphic position, we infer that the dacitic unit may have been an early part of the eruptive sequence that also produced the Nomlaki Tuff Member of the Laguna, Tehama, and Tuscan formations. Table 1 shows the relationship of stratigraphic units used in this report to those used previously in the Sacramento and San Joaquin Valleys.

We use the outcrop distribution of the stratigraphic units, their ages, their surface and subsurface elevations, and the slopes on marker beds and contacts of the units to reconstruct the history of late Cenozoic deformation in the area.

In the second major part of the report, we discuss our rationale for describing, sampling, and analyzing the sequence of soils formed on the alluvial deposits at Honcut Creek (fig. 1). The soils differ greatly in age or time of development but have formed under similar conditions of climate, vegetation, topography, and parent material; thus they constitute a soil chronosequence. We describe the morphology of the soils and discuss the major trends in soil development with increasing age of the deposits. The discussion of soil development is intentionally short and is meant primarily to introduce the reader to the extensive data on the morphology, chemistry, elemental composition, and mineralogy of the soils that are included in the supplementary tables.

Acknowledgments.—Our work was performed as a part of the U.S. Geological Survey Soil Correlation and Dating Project of the late Denis E. Marchand, which has as its major goals, first, to use soils as tools for correlation and dating of Quaternary surficial deposits in the Western

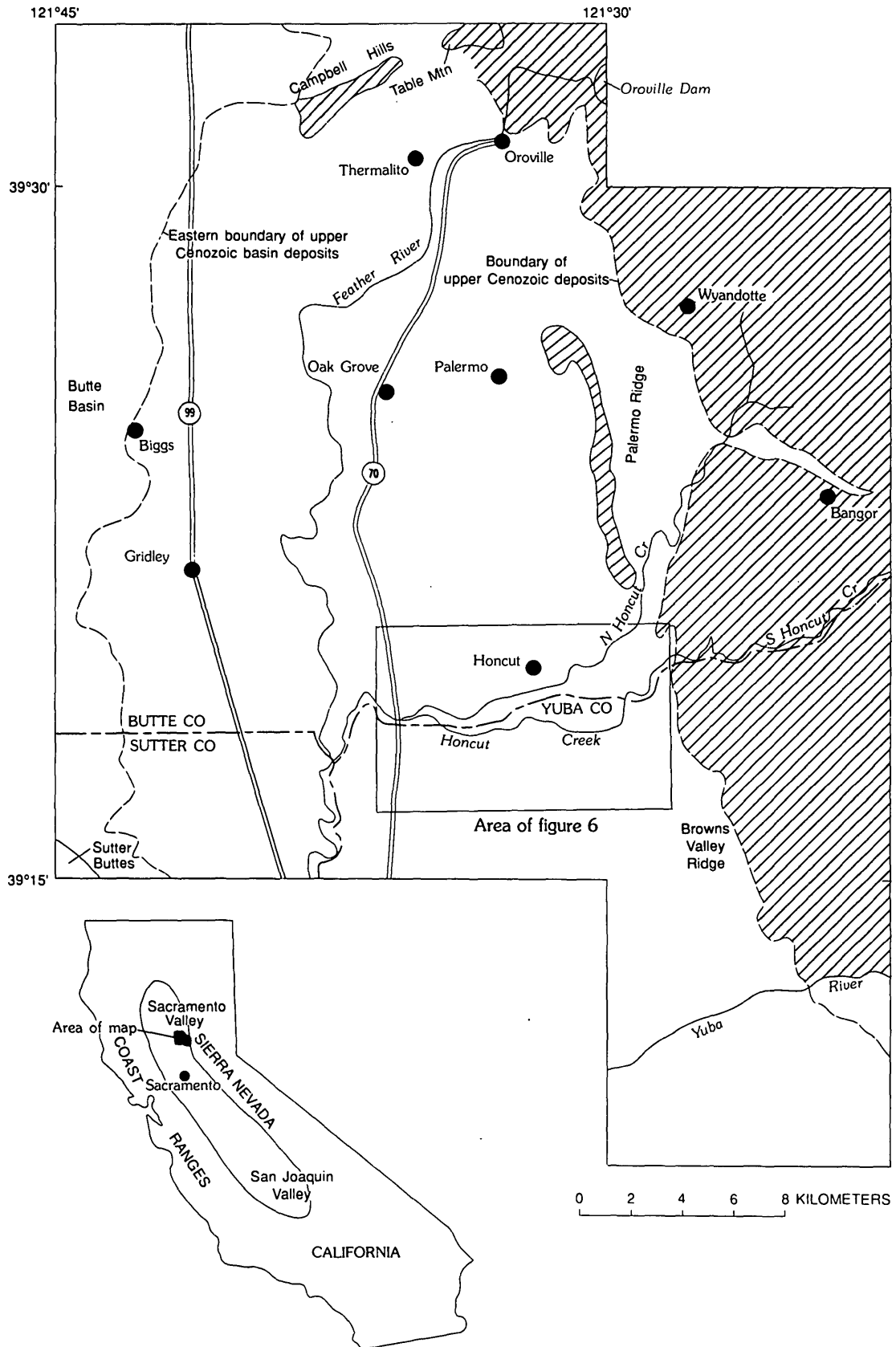


Figure 1. Index map of study area. Lined pattern is pre-upper Cenozoic bedrock.

Table 1. Stratigraphic correlations

GEOLOGIC PERIOD AND EPOCH	SAN JOAQUIN VALLEY							AGE ¹ Ma	SACRAMENTO VALLEY																
	MOKELUMNE RIVER AREA	MERCED RIVER AREA	EAST STANISLAUS AND NORTH MERCED	MERCED RIVER AREA	SAN JOAQUIN RIVER FAN	N.E. SAN JOAQUIN VALLEY			FEATHER AND YUBA RIVER AREA	OROVILLE AREA	OROVILLE AREA	OROVILLE AREA	OROVILLE QUADRANGLE	CHICO MONOCLINE AND N.E. SAC. VALLEY	N.W. SACRAMENTO VALLEY	SAC. CO., NORTH OF AMERICAN RIVER	SAC. CO., SOUTH OF AMERICAN RIVER	S.E. SACRAMENTO VALLEY	SUTTER AND YUBA COUNTY						
	Gale and others (1939)	Arkley (1954)	Davis and Hall (1959)	Arkley (1962)	Janda (1965, 1966)	Marchand and Allwardt (1981)			This report	Helley and Harwood (1985)	C.D.W.R. ² (1979)	C.D.M.G. ³ (1975)	Creely (1965)	Harwood and others (1981)	Steele (1979)	Shlemon (1967b, 1972)	Shlemon (1967b, 1972)	Olmsted and Davis (1961)	Davis and Olmsted (1952)						
QUATERNARY	HOLOCENE	Alluvium	Flood-plain alluvium	Alluvium and sand dunes	Alluvium and sand dunes	Alluvium	Post-Modesto	IV III II (M) I (L)	.006 (O) .003 (M) .004-.009 (L)	Alluvium (O) and basin deposits	Alluvium and basin deposits			Alluvium and basin deposits	Alluvium	Alluvium and basin deposits	Alluvium and basin deposits	Alluvial fan and river deposits	Young alluvial deposits						
		PLEISTOCENE	Young alluvial fan	Modesto Fm.	Modesto Fm.	Modesto Fm.	Modesto Fm.	Younger Mbr. Older Mbr.	Upper Mbr. (I) Lower Mbr. (H)	.009-.014 (I) .029-.042 (H)	Modesto Fm.	Upper Mbr. Lower Mbr.	Modesto Fm.	Lower Mbr.	Alluvium	Alluvium	Alluvium	Modesto Fm.	Upper Mbr. Lower Mbr.	Modesto Fm.	Upper Mbr. Lower Mbr.	Victor Fm.	Intermediate alluvial deposits		
				Low terraces and older fans	Riverbank Fm.	Riverbank Fm.	Riverbank Fm.	Riverbank Fm.	Riverbank Fm.	Upper unit (G) Middle unit (N) Lower unit (J)	.103-.130 (G) .260 (N) .340-450 (J)	Riverbank Fm.	Upper Mbr. Lower Mbr.	Riverbank Fm.	Upper Mbr. Lower Mbr.	Alluvium	Alluvium	Alluvium	Modesto Fm.	Upper Mbr. Lower Mbr.	Modesto Fm.			Upper Mbr. Lower Mbr.	
			High terraces	Turlock Lake Fm.	Turlock Lake Fm.	Turlock Lake Fm.	Turlock Lake Fm.	Younger Mbr. Friant P. Corcoran Older Mbr.	Upper unit Friant P. (E) Corcoran Lower unit	.450 (F) .60 (E)															
	TERTIARY	PLIOCENE	Arroyo Seco gravel			North Merced gravel		North Merced gravel		1.08 (D)															
			Laguna Fm.			China Hat gravel			China Hat Mbr. Upper unit	2.4 (B)															
			Mehrten Fm.			Mehrten Fm.			Lower unit	3.4 (A) 3.2 (P)															
	MIOCENE																								

¹Letters refer to the sources of ages used: To find the source reference for a date in the "Age" column, locate the index letter at that stratigraphic level in one of the reference columns. Time scale of Palmer (1982).

²California Department of Water Resources.

³California Division of Mines and Geology.

⁴The "ash of Mt. Maiku" has been renamed the "Rockland ash bed."

⁵Red Bluff Formation of Helley and Harwood (1985) in the Oroville area correlates physically with the uppermost gravel bed of this report; the Turlock Lake Formation of Helley and Harwood (1985) in the Oroville area correlates physically with part of the Laguna Formation of this report.

United States, and second, to establish a data base for soils from the chronosequences studied. We are indebted to Denis Marchand for the help that he gave so freely and to the U.S. Geological Survey for its financial support of this project.

DIAGNOSTIC STRATIGRAPHIC CRITERIA AND METHODS

Stratigraphic Criteria

The delineation of a local stratigraphic sequence for the alluvial deposits of the Feather-Yuba Rivers area presents problems that are similar to those encountered elsewhere in the Great Valley. Units of widely varying age are often lithologically similar. The source areas and thus the characteristics of the gravel, sand, silt, and clay derived from a single drainage basin have not changed markedly over the time of deposition of the alluvium. Conversely, within a single mappable stratigraphic unit, nonsystematic lateral lithologic variation is commonly as great as the variation between units. Classical stratigraphic concepts are difficult to apply. Younger stratigraphic units in the project area locally lie in normal superposition over older units, but more often the younger units are inset into the older units, and therefore are topographically lower.

In this study, five principal characteristics were used to differentiate stratigraphic units: (1) disconformities that could be recognized and traced laterally, such as truncation or incision of one alluvial fill by another or the presence of buried soils on former surfaces of older units; (2) distinctive lithology and stratigraphic superposition (for example, dacitic lahars overlain by cobbly, mixed-source alluvium); (3) relative elevation or position of geomorphic surfaces; (4) surface form and the degree of erosional dissection of original surfaces; and (5) contrasting degrees of development of surface soils on little-eroded remnant surfaces of different topographic elevations. Using these characteristics, and the relative and absolute dating methods discussed below, we define a local stratigraphic sequence that we correlate with the late Cenozoic stratigraphy of the northern Sacramento Valley (Helley and Harwood, 1985) and the northeastern San Joaquin Valley (Marchand and Allwardt, 1981).

Dating Methods

Two methods of absolute radiometric dating and two methods of relative dating provided a limited chronologic framework in which to place the stratigraphic units. The four methods used were paleomagnetic stratigraphy, tephrochronology, K-Ar radiometric dating, and radiocarbon dating. Analytical results and the location of sampling sites are given in the supplementary tables. The interpretation of the results is discussed in the section titled "Stratigraphy."

Paleomagnetic Stratigraphy

Approximately 50 oriented sediment samples were collected by standard methods for paleomagnetic polarity determination. Several sandy samples were lost because of disaggregation. All magnetic studies were performed in the paleomagnetism laboratory of the Geology Department of the University of California, Davis. Paleomagnetic measurements were performed on a Schonsted SSM-1 spinner magnetometer operating in a six-spin mode. Alternating field demagnetization of the samples was done with a Schonsted GSD-1 demagnetizer.

Behavior of the samples during demagnetization is discussed and stereographic projections of paleomagnetic data for the samples are given in supplementary table 11.

Radiocarbon Dating

Eight samples of wood or charcoal were collected from streambank exposures for radiocarbon (^{14}C) dating. Individual samples consisted of one or more of the following: pieces of charcoal in individual sand lenses, remnants of bark, or conifer cone scales. One subsample was cut from a charred, transported tree stump. Samples were wrapped in aluminum foil at the site. Conventional ^{14}C analyses were made on whole, hand-concentrated samples by Beta Analytic Incorporated, Coral Gables, Florida.

Potassium-Argon Radiometric Dating

Three large blocks of fresh, biotite-bearing dacite from the lahar bed of the dacite unit were collected at two locations east and southeast of the town of Oroville. Potassium-argon ages were determined on both whole rock samples and biotite and hornblende separates of the dacites by Wendy Hillhouse of the U.S. Geological Survey.

Tephrochronology

Several samples of the "unnamed rhyolitic pumice tuff" of Creely (1965) from the Oroville area and of a rhyolitic tuff from near the Yuba River were collected by U.S. Geological Survey geologists between 1975 and 1978. We collected samples of tuffaceous and pumiceous sediments from the project area, and the California Department of Water Resources gave us two additional samples collected from test wells in the Thermalito area west of Oroville. Andrei Sarna-Wojcicki of the U.S. Geological Survey analyzed glass from these tephra samples by geochemical methods for the purpose of correlating them with recognized, dated tephra at other locations.

Geologic Mapping

Geology was mapped at 7.5-minute scale (1:24,000) and compiled at 15-minute scale (1:62,500) (Busacca, 1982). Soil surveys for the Oroville area (Carpenter and others, 1926), Yuba County (Herbert and Begg, 1969), and Sutter County (Lytle, in press) were particularly useful in the detailed mapping of stratigraphic units because of the general correspondence of soil associations to individual stratigraphic units. Black and white vertical aerial photographs of Yuba and Butte Counties, at 1:20,000 scale and dated 1962, were used for landform mapping; however, they predated only part of the large-scale land leveling of the low and intermediate terraces (Modesto and Riverbank Formations). Land leveling posed the most serious difficulty in subdividing and mapping members of the Modesto and Riverbank Formations. Both Landsat images and U-2 high altitude vertical color photographs were used to map photolineaments and other broad landform features.

The Project Geology Branch of the California Department of Water Resources made available a wide range of drillers' records and stratigraphic descriptions of test wells and excavation sites from engineering and geologic studies of the Thermalito Forebay and Afterbay complexes of the Oroville Dam Project. Subsurface correlations and part of the stratigraphic reconstruction discussed below arose from use of these materials and from access that the department provided to excavation sites.

GEOGRAPHIC AND GEOLOGIC SETTING

Geographic Setting

The study area extends from Table Mountain north of the Feather River, southeastward along the terrace sequence at the eastern edge of the Sacramento Valley, to a point about 7 km south of the Yuba River (fig. 1). The western boundary of the area is the eastern border of the Butte basin. The project area included all of the Honcut, Palermo, Gridley and Biggs 7.5-minute quadrangle maps and parts of the Shippee, Oroville, Bangor, Loma Rica, and Browns Valley 7.5-minute quadrangle maps. Elevations in the project area range from 18 m on the Feather River at the south edge of the area to 293 m on the highest point of upper-Tertiary gravel near the town of Bangor.

The project area is underlain principally by unconsolidated alluvial deposits that form fan-shaped flood plains and uplifted, dissected terraces. These deposits are grouped with the valley-fill sediments of Cenozoic age that occur in other parts of the Sacramento Valley, and together form the Sacramento Valley geologic province (Olmsted and Davis, 1961). Remnants of several distinct high terraces are visible to the southeast from the flood plain of Honcut Creek. To the north near Oroville, the alluvial landscape has a stepped appearance that suggests multiple terrace

levels. The deposits in the Feather and Yuba Rivers area record a complex cycle of alluvial fan and flood plain deposition followed by incision and erosional modification that has been repeated throughout late Tertiary and Quaternary time. Adding to the complexity, the deposits have been tectonically deformed.

The drainage basins of the Feather and Yuba Rivers and of Honcut Creek lie within the Sierra Nevada geologic province. From the Sierran crest to the foothills, the Feather and Yuba basins drain primarily a sequence of weakly metamorphosed marine shale, phyllite, schist, slate, and quartzite of probable Mesozoic age (California Department of Water Resources, 1979); granodiorite, tonalite, and granite of Mesozoic age; and metamorphosed volcanic rocks, primarily andesite and basalt, which are interpreted as a Mesozoic ophiolite, that is, a remnant of subducted oceanic crust and sea floor (Schweickert and Cowan, 1975). Approximately 65 percent of the drainage basin of Honcut Creek is underlain by basic metavolcanic rocks, and the remainder is tonalite or granodiorite. The Feather and Yuba basins also drain remnants of Pliocene andesitic rocks, and all three basins contain remnants of early and middle Cenozoic auriferous gravels. The Cenozoic volcanic rocks and gravels cap ridges on the long western slope of the Sierra.

The Feather River has a drainage basin area of 9,350 km² above the town of Oroville (Davis and Olmsted, 1952). Within the Sacramento Valley, the Feather River maintains a southerly course for 78 km from Oroville south to its confluence with the Sacramento River at Verona. The southerly course allows the Feather River to act as a trunk stream along the eastern margin of the Sacramento Valley. To the east of the river lies the sequence of elevated, dissected alluvial terraces which are the subject of this study; to the west lie the recent basin deposits of the Butte, Sutter, and Yuba basins.

Honcut Creek, with a drainage basin area above the town of Honcut of approximately 290 km², drains the foothill area between the Feather and Yuba basins. The Yuba River, with a drainage basin area of 3,092 km² (Davis and Olmsted, 1952), flows west-southwest for 24 km from the mountain front to its confluence with the Feather River at Marysville.

The present climate in the project area is a Mediterranean type. Summers are hot and dry, and winters are cool and wet. Mean annual temperature (MAT) at Marysville is 16.7 °C (108 years of record); mean January temperature is 7.5 °C and mean July temperature is 26 °C; more than 80 percent of the mean annual precipitation (MAP) of 550 mm occurs between November and March (National Oceanographic and Atmospheric Administration, 1979).

The MAT at Honcut Creek is nearly identical to that reported at Marysville. The MAP at Honcut Creek increases from 570 mm at its confluence with the Feather River to 680 mm 13 km to the east at the valley edge (California Department of Water Resources, 1963).

There is a strong orographic effect on cyclonic storms that approach from the Pacific Ocean to the west and rise to pass over the Sierran crest. MAP increases systematically to 1,050 mm in the upper reaches of the Honcut Creek drainage, and to more than 2,000 mm in the upper Yuba River drainage; the maximum MAP in the Feather River drainage is more than 2,350 mm at Bald Eagle Mountain near Bucks Lake (National Oceanographic and Atmospheric Administration, 1979).

Geologic Setting

The alluvial deposits of the Feather River, and to a lesser extent those of the Yuba River and Honcut Creek, occur as a sequence of nested terraces that open into fans to the southwest and west toward the axis of the Sacramento Valley (fig. 2). Tectonic uplift and westward tilting of the Sierra Nevada has continued from the early Miocene to the present (Huber, 1981). As a consequence, the original depositional gradients of Tertiary and Quaternary volcanic and alluvial units increase with increasing age. For example, the present-day gradient on the Feather River below Oroville is 0.5–1.8 meters per kilometer, whereas the slope on the Miocene Lovejoy Basalt at Table Mountain is 22–33 m/km. A similar pattern was documented in the Merced River area by Marchand (1977) and Arkley (1962).

The uplift and westward tilting of the Sierra Nevada have combined with cyclical or episodic deposition of sediments to produce a distinctive pattern of alluvial landforms. Near the mountain front, successively older deposits stand at higher elevation than younger deposits, are more dissected, and bear soils of stronger profile development. Younger deposits are inset into older deposits to form a series of nested terraces. The surfaces of the deposits gradually converge to the southwest and west because older deposits have a steeper gradient than the younger ones; a few kilometers west of the mountain front the alluvial deposits occur in normal stratigraphic superposition with younger units progressively burying older. Buried soils mark the tops of some of the units in the subsurface. Several of the units thus have both surface and subsurface expression. Tectonic deformation of the alluvium along the mountain front during the Pliocene and Pleistocene has increased the complexity of this pattern, and gold dredging and agricultural land leveling serve to further obscure the geomorphic sequence.

Marchand (1977) postulated that the regular cycles of alluvial fan building, river incision, and soil formation in the northeastern San Joaquin Valley were keyed to Pleistocene glacial-interglacial climatic change in the Sierra Nevada. He cited several lines of evidence from his own previous work as well as that of Arkley (1962), Janda (1965, 1966), and Janda and Croft (1967) to support this view. In brief, he envisioned the deposition of fine granitic rock flour during glacial advance as the initial stage in a cycle of fan-flood plain deposition. This was followed

by deposition of unweathered cobbly alluvium during glacial retreat, as formerly glacier-filled valleys were flushed of coarse sediment. Finally, river incision occurred during interglacial periods or early in the next glacial cycle when streamflow was high but sediment load was low. This hypothesis is consistent with the observation that coarse sediments overlie fine in many of the alluvial units of the eastern San Joaquin Valley. Alluvial cycles in the Feather River and Yuba River basins may also have been controlled by glacial-interglacial climatic change, although the lower elevations in the northern Sierra compared to the central and southern Sierra may have modified the degree or timing of the response of the alluvial system to climate change.

Alluvial deposits younger than the Pliocene dacitic volcanoclastic rocks in the project area primarily have a mixed mineralogy. This is a reflection of the several rock types in each drainage basin. In general, however, dark metavolcanic rocks and blue and white siliceous metasedimentary rocks are dominant in the gravelly alluvium. Clasts of various Mesozoic granitic and Tertiary volcanic rocks are less abundant. Specific variations in lithology are due to local differences in source area, to reworking of alluvium, and to differential weathering of gravels within the deposits. Young alluvium along intermittent streams that drain from old deposits is commonly more weathered and redder than is alluvium of the same age along main rivers that drain from relatively unweathered bedrock.

STRATIGRAPHY

Previous Work

Alluvial fan and dissected terrace deposits of late Cenozoic age in the Sacramento Valley were mentioned in some of the earliest geologic studies of this region. For example, Lindgren (1911) described a system of three so-called gravel benches near Oroville along the Feather River, although he stressed that the threefold division of gravels was difficult to trace southward to the Yuba and Bear Rivers. Bryan (1923) recognized two broad terrace levels throughout the Sacramento Valley and hypothesized a tectonic or climatic origin. Russell (1931) identified but did not study in detail four terrace levels on the west side of the Sacramento Valley that are younger than the Pliocene Tehama Formation.

In the early geologic studies, more attention was given to the prominent Pliocene alluvial and volcanoclastic deposits than to those of Pleistocene age. Russell (in Russell and VanderHoof, 1931) gave the name Tehama Formation to a thick sequence of fluvial sediments on the west side of the Sacramento Valley. Anderson and Russell (1939) described the Red Bluff Formation as a coarse, brick-red, gravelly alluvial deposit of variable thickness that unconformably overlies the Tehama. In subsequent years, the name Red Bluff has been used extensively in the Sacramento Valley, both formally and informally, to describe red gravelly



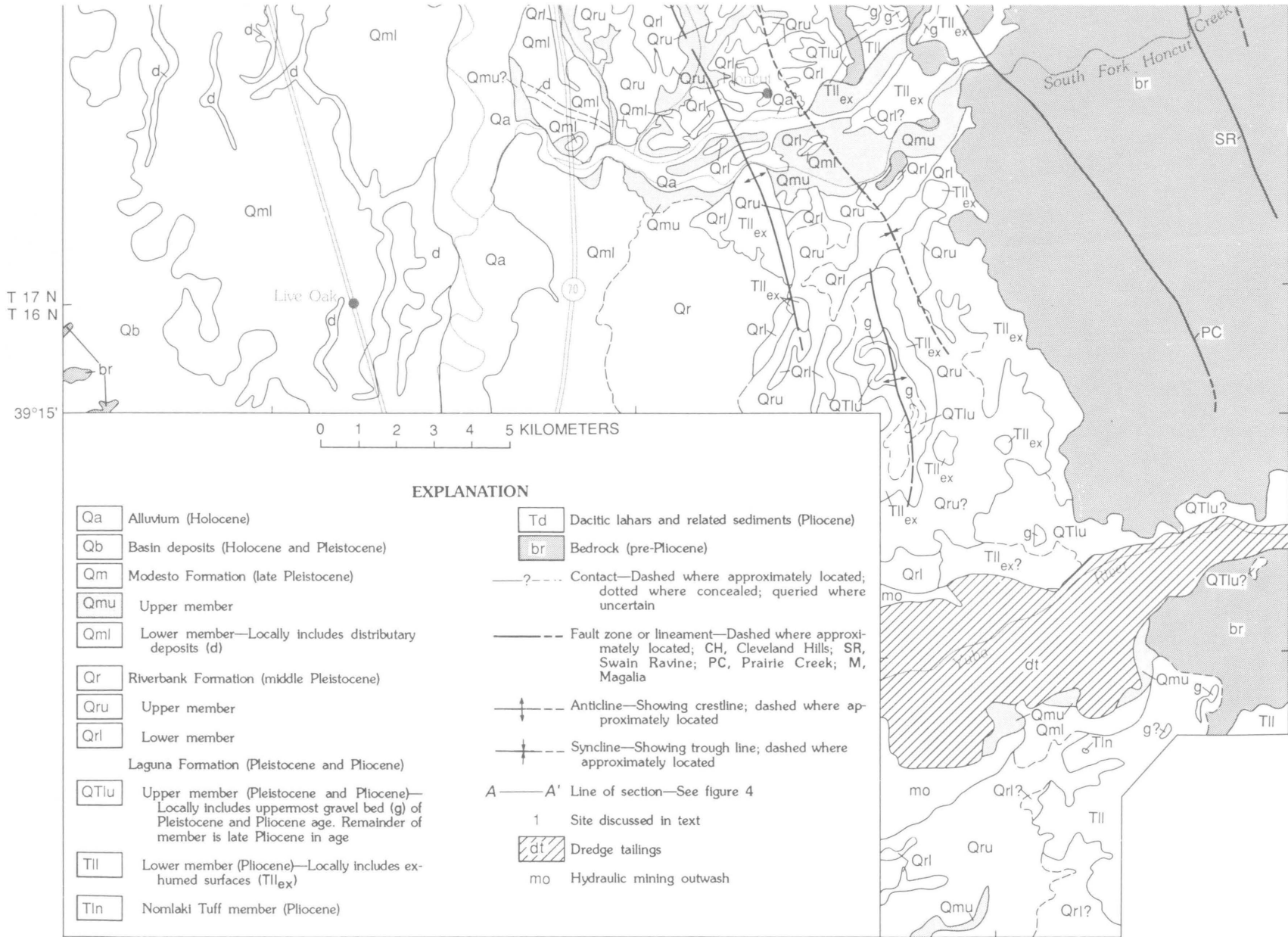


Figure 2. Generalized geologic map of study area.

alluvium derived from diverse sources and of probable different ages. For example, Creely (1965) extended the Red Bluff Formation into the Oroville area, using the name for all older uplifted terrace deposits. More recently, Helley and Harwood (1985), Harwood and others (1981), and Helley and others (1981) used radiometric and stratigraphic evidence to correlate the older, coalescing gravelly fan remnants on the east side of the Sacramento Valley with the Red Bluff Formation on the west side.

Anderson (1933) described the Tuscan Formation as a series of volcanic mudflow breccias and volcanic conglomerates that blanket the west slope of the northern Sierra and extend into the Sacramento Valley. The Tuscan and the Tehama are both Pliocene in age, and the two formations interfinger in the subsurface of the Sacramento Valley (Anderson and Russell, 1939). The Nomlaki Tuff Member is interstratified at or near the base of both formations. Evernden and others (1964) dated a sample of the welded dacite tuff from Bear Creek Falls, which Anderson and Russell (1939) correlated with the type Nomlaki Tuff Member on the west side of the Valley, and reported a K-Ar age of 3.3 ± 0.4 Ma.¹

Pliocene and Pleistocene alluvial deposits have been studied in the greatest detail in the northeastern San Joaquin Valley in conjunction with investigations of ground-water resources, and more recently, tectonic stability. Gale and others (1939) recognized and named three extensive deposits in the Mokelumne area: the Victor Formation (now obsolete), the Arroyo Seco Gravel, and the Laguna Formation. Arkley (1962) and Davis and Hall (1959) subdivided the Victor Formation into the Modesto, Riverbank, and Turlock Lake Formations. More recently, Shlemon (1967a, b; 1972) subdivided the upper Cenozoic alluvial deposits of the American and Mokelumne Rivers near Sacramento. Shlemon used a combination of existing and new formation names. Extensive mapping and detailed investigation of late Cenozoic alluvial deposits in the eastern San Joaquin Valley is summarized in Marchand (1977) and Marchand and Allwardt (1981). Marchand and Allwardt (1981) presented a comprehensive revision and updating of stratigraphic units in the northeastern San Joaquin Valley. From youngest to oldest, they recognized four distinct deposits of Recent age, two members of the Modesto Formation and three members of the Riverbank, two members of the Turlock Lake Formation, the North Merced Gravel, and two members of the Laguna Formation, including the China Hat Gravel member as the uppermost gravel unit of the Laguna. Helley (1979), Harwood and others (1981) and Helley and Harwood (1985) extended the formations and stratigraphy of Marchand and Allwardt (1981), with some modification, into the Sacramento area and throughout much of the Sacramento Valley. Shlemon and Begg (1972) delineated, but did not correlate, five sets of channel systems of

different ages, all younger than the Red Bluff Formation, on Stony Creek in the western Sacramento Valley. Steele (1979) recognized at least six strath terraces and fill terraces, all younger than the Red Bluff Formation, on the west side of the northern Sacramento Valley.

In the Feather-Yuba Rivers area, Olmsted and Davis (1961) provisionally assigned the names alluvial deposits, Victor Formation, and Laguna Formation (following Gale and others, 1939) to young, intermediate, and old alluvial fan and terrace deposits, respectively. Their Laguna Formation corresponds approximately to deposits in the vicinity of Oroville assigned by Creely (1965) to the Red Bluff Formation. The different stratigraphic concepts and formation names that were developed independently in the Sacramento and the San Joaquin Valleys unfortunately overlap and conflict in the Feather-Yuba area. Recent mapping by the California Department of Water Resources (1979) and by the Division of Mines and Geology (Sherburne and Hauge, 1975), following the Oroville earthquake, was concentrated in the foothill areas where ground rupture occurred, and no attempt was made to revise or update the alluvial stratigraphy.

Description of Stratigraphic Units

In this section we describe the stratigraphic units and the common soil landscapes on relict and eroded areas of each unit. We list in table 2 the correspondence between soils that are areally and stratigraphically important and official soil series designated in soil surveys of the local area. The taxonomic classification of these soils is also given in table 2. The soils that we selected for the chronosequence study met a very specific set of conditions in order to best express the age or time of soil development on each unit; therefore, we describe and discuss the characteristics of these chronosequence soils in a separate section later in this report.

We present current information on the ages of the units (table 3) and we correlate several of the informal members with informal members of formations used by Marchand and Allwardt (1981) in the northeastern San Joaquin Valley (table 1). Holocene basin deposits and alluvium, two members of the Modesto Formation and two members of the Riverbank Formation are described. Two informal members and one formal member of the Laguna Formation are recognized and supplemental reference sections are described. These we correlate, respectively, with the post-Modesto deposits, upper and lower members of the Modesto Formation, upper and middle units of the Riverbank Formation, and upper and lower units of the Laguna Formation of Marchand and Allwardt (1981). Dacitic lahars and volcanoclastic rocks that underlie the alluvial sequence are described and reference sections are presented for them. We did not recognize an equivalent deposit to the Turlock Lake Formation of Marchand and Allwardt (1981). We describe the stratigraphic units in age order from young to

¹ Recalculated to 3.4 ± 0.4 Ma, using the revised decay constants of Steiger and Jaeger (1977).

Table 2. Comparison of areally and stratigraphically important soils in the project area with soil series designated in soil surveys

This report		Soil survey of the Oroville area, California (Carpenter and others, 1926)	Soils of the Yuba area, California (Herbert and Begg, 1969)	Soil survey of Sutter County, California (Lytle, in press)
Geologic unit	Informally designated soil series ¹			
Holocene and modern alluvium	<i>Honcut</i> (Typic Xerorthents)	Honcut loam	Honcut series (Typic Xerorthents)	— ²
Modesto Formation	<i>Wyman variant</i> (Typic Haploxerolls)	Honcut loam, compact substratum phase	Wyman series (Mollic Haploxeralfs)	— ²
	Ryer series (Mollic Haploxeralfs) ³	Gridley clay loam	Ryer series (Mollic Haploxeralfs) ³ Loam and clay loam deep over substratum	Marcum series, 40–60 in. (Typic Argixerolls)
			Loam and clay loam, moderately deep over substratum	Gridley series, 20–40 in. (Typic Argixerolls)
	<i>Ryer duripan variant</i> (Abruptic Durixeralfs)	Gridley clay	— ²	Yuvas series (Abruptic Durixeralfs)
	<i>Ryer coarse variant</i> (Typic Haploxerolls)	Honcut sand	— ²	Liveoak series (Typic Haploxerolls)
	<i>Wyman series</i> (Mollic Haploxeralfs) ³	Wyman loam	<i>Wyman series</i> (Mollic Haploxeralfs) ³	Conejo series (Pachic Haploxerolls)
Riverbank Formation	<i>Kimball series</i> (Mollic Paleixeralfs)	Rocklin fine sandy loam	<i>Kimball series</i> (Mollic Paleixeralfs)	— ⁴
	<i>Yokohl series</i> (Abruptic Durixeralfs)		<i>Yokohl series</i> (Abruptic Durixeralfs)	— ⁴
	<i>Kimball deep variant</i> (Mollic Paleixeralfs)	Kimball loam	<i>Ramona series</i> on Yuba River only (Typic Haploxeralfs)	— ⁴
Laguna Formation	<i>Redding series</i> (Abruptic Durixeralfs)	Redding gravelly sandy loam	<i>Redding series</i> (Abruptic Durixeralfs)	— ⁴
	<i>Red Bluff strong variant</i> (Palexerults)	— ²	— ^{2,4}	— ⁴

¹Soils in italics sampled for the chronosequence study.
²No equivalent soil series mapped in this area.
³Official series classification for Ryer and Wyman is Typic Haploxeralfs.
⁴No equivalent landform or geologic formation.

old rather than the conventional old to young because this order is more compatible with our studies of the soils formed on these units. A generalized geologic map is presented in figure 2. A detailed geologic map of the project area at 1:62,500 scale can be found in Busacca

(1982). This geologic mapping, modified somewhat for the purposes of map compilation throughout the Sacramento Valley, also can be found in Helley and Harwood (1985). Table 3 presents the age control for the stratigraphic units to be described below.

Table 3. Age control for alluvial units in the Feather and Yuba Rivers area, and correlation of units to the northeastern San Joaquin Valley

Geologic unit	Radiometric ages from the Central Valley (ka)			Inferred correlation to NE San Joaquin Valley (Marchand and Allwardt, 1981)	Remarks	Chrono-sequence soils, this study	Age of surfaces assumed for chronosequence (ka)	Uncertainty of age estimates (ka), comments
	Stratigraphically above unit (limiting minimum)	Within unit	Stratigraphically below unit (limiting maximum)					
Holocene alluvium On Honcut Creek	0	¹ 0.450±0.45 ¹ 1.775±0.110	² 3.020±0.160	Post-Modesto III	Well-vegetated natural levee and back-levee deposits. These deposits are incised into major flood plain surface on Feather River, and grade to similar deposits on Feather River.	HON-1 HON-2 HON-3	³ 0.6	0–3.0 ka, range in ¹⁴ C ages from comparable sites suggest true age range from 0.45 to 1.8 ka.
Major high flood plain on Feather River	¹ 1.775±0.110	² 3.020±0.160	⁴ 8.230±0.80	Post-Modesto II		not sampled	—	—
Basin deposits	0	N.A. ⁵	N.A. ⁵	No correlative unit	Stratigraphic position of of base of unit is not known	not sampled	—	—
Modesto Formation Upper member	² 3.020±0.160 ⁴ 8.230±0.80	N.A. ⁵ ⁷ 14.1±0.203	⁴ 31.24±0.32 ² 9.41±2.03	Modesto Formation upper member		HON-5 HON-6	10.0	3.0–29.0
Lower member	14.1±0.20	N.A. ⁵ ⁷ 29.41±2.03 ⁷ 42.4±1.0 ⁴ 42.0±16.0 ⁴ 43.0±34.0	⁸ 103±6	Modesto Formation lower member		HON-9 HON-10 HON-11	40.0	14.0–100.0, soil development suggests that true age is 40,000 but range of estimate is large because deposition not radiometrically dated in project area.
Riverbank Formation Upper member	⁵ N.A. ⁸ 103±6 ⁴ 120±40 ⁴ 140±40 ⁴ 145±20	⁹ <730	Riverbank Formation upper unit	Ages of 103 and 120 ka are from upper unit in Sacramento area, and geomorphic surface of that deposit can be traced to Oroville area.		HON-13 HON-14	130	50–250 ka, soil development suggests that true age of the surface is approximately 100 ka but range of estimate is large because deposit is not radiometrically dated in project.

Geologic unit	Radiometric ages from the Central Valley (ka)			Inferred correlation to NE San Joaquin Valley (Marchand and Allwardt, 1981)	Remarks	Chrono-sequence soils, this study	Age of surfaces assumed for chronosequence (ka)	Uncertainty of age estimates (ka), comments
	Stratigraphically above unit (limiting minimum)	Within unit	Stratigraphically below unit (limiting maximum)					
Riverbank Formation— <i>Continued</i>								
Lower member	⁸ 103±6	⁹ <730 ⁴ 260±45	¹¹ 2,470	Riverbank Formation middle unit	Alluvium of middle member on Honcut Creek has normal magnetic polarity and thus is less than about 730 ka.	HON-17 HON-18 HON-19 HON-20	250	100–450
Laguna Formation Upper member	⁹ 730	¹¹ 1,800 ¹¹ 2,470	¹² 3,400±400	Laguna Formation upper unit	Correlation with members of Laguna Formation in Merced River area must be considered tentative.	not sampled	—	0.9–3.2 Ma, ¹⁰ normal polarity of uppermost gravel bed may be associated with Jaramillo (0.9 Ma) or Olduvai (1.8 Ma) normal-polarity subchron; see text for complete discussion.
Lower member	¹¹ 2,470	¹² 3,400±0.400 3,200±100	3,200±100	Laguna Formation lower unit	We consider inversion of dates within and below this unit to be analytical, not stratigraphic, uncertainty.	HON-21 HON-22	1,600	ca. 0.5–3.2 Ma, age of 1.6 Ma for chronosequence soil profile is derived from estimate of total time surface has been exposed to soil development: 3.2 to 2.6 m.y. and ca. 1.0 m.y. to the present.
Dacite unit	¹² 3,400±400	¹³ 3,200±100 2,800±300 ¹⁴ 3,400±200	— —	No correlative unit	This unit underlies all upper Cenozoic alluvial units in Feather-Yuba Rivers area.	not sampled	—	ca. 0.5–3.2 Ma

¹See supplementary table 9 and text for full listing and discussion of ¹⁴C ages.

²E.L. Begg, oral commun. 1982.

³Carbon-14 age of 605±45 yr B.P. obtained from wood collected at 1.2 m depth at site HON-4.

⁴Harden (1987).

⁵None available from immediate project area.

⁶Atwater and others (1986).

⁷Marchand and Allwardt (1981).

⁸Hansen and Begg (1970); American River area.

⁹See text for discussion. Normal magnetic polarity in the lower member, along with stratigraphic relationships, suggest an age <730 ka, the currently accepted age of the Matuyama-Brunhes reversal (Mankinen and Dalrymple, 1979).

¹⁰Ma is millions of years before present.

¹¹Currently accepted ages of the Olduvai subchron and Gauss-Matuyama boundary (Mankinen and Dalrymple, 1979) with which we associate the normal polarity of the uppermost gravel bed and the prominent reverse over normal polarity zonation in the upper member, respectively.

¹²Published age of the tuff at Bear Creek Falls (Evernden and others, 1964) to which the exposures of the Nomlaki Tuff Member of the Laguna Formation in the Oroville area have been correlated.

¹³Whole-rock K-Ar age on dacite; see supplementary table 9.

¹⁴Range of five K-Ar ages on biotite or hornblende from dacite; see supplementary table 9.

Basin Deposits

Clay-rich alluvium forms sheetlike basin deposits to the west of the Feather River and extends beyond the project area into the Butte and Sutter basins. The clays, which are flood-basin sediments, were deposited from major distributary channels that splay away from the Feather River (fig. 2), and from local intermittent streams that drain land underlain by the Modesto, Riverbank, and Laguna Formations to the west and northwest of the Feather River. The basin deposits are 1 to 2 m thick in the project area and thicken gradually to the west. The surface is smooth and slopes to the west-southwest at approximately 1 m/km.

Clay, silty clay, and minor lenses of sand and fine gravel compose the deposits. Exposure is poor. Dark-brown to black Vertisol soil profiles have formed on the deposits in most places.

The stratigraphic relationship of the basin deposits to other units is known only from a limited number of shallow exposures. We have observed that (1) the upper part of the basin deposit overlies a conspicuous silt substratum within the lower member of the Modesto Formation; (2) the upper part of the basin deposit interfingers with the part of the lower member of the Modesto Formation that lies above the silt layer; (3) in years with heavy stream runoff before flood control structures were built on the Feather and Yuba Rivers, the basin received flood water and sediment from intermittent streams and distributary channels (Carpenter and others, 1926). The upper part of the basin deposits lap onto dissected surfaces of the Riverbank and Laguna Formations. In T. 19 N., R. 2 E., to the east of Richvale (fig. 2), the basin deposits bury a truncated remnant of a hardpan soil formed on the Riverbank Formation. From this we conclude that the basin deposits interfinger with at least the deposits of the Modesto Formation and Holocene alluvium. We speculate that farther to the west and deeper in the subsurface, the lower part of the basin deposits may also interfinger with the alluvium of the Riverbank and Laguna Formations.

We have no radiometric ages on the basin deposits. The near-surface part of the deposits can be no older than the age of the lower member of Modesto Formation, because basin clay overlies the silt substratum in the lower member. The top of the deposits is probably of modern age, having received deposition of sediment in recorded time. Basin sediments may well have been filling the Butte and Sutter basins intermittently at least from the late Pleistocene, and likely from the late Pliocene to the present (Olmsted and Davis, 1961).

Holocene Alluvium

Alluvium that postdates the Modesto Formation deposits is confined to narrow flood plains along the Feather and Yuba Rivers and along Honcut Creek. The deposits are inset into channels that were cut into the Modesto and older formations; in the project area Holocene alluvium does not

expand into extensive fan-shaped flood plains comparable to those of the older formations. We did not subdivide the Holocene deposits, although multiple topographic surfaces exist in some areas, and radiometric dating indicates age differences. On the Feather River, the alluvium forms a flood plain 1 to 2 km wide that lies 2 to 6 m below adjacent surfaces of older deposits. On the average, the main, broad Holocene flood plain lies 6 m above the low flow level of the river. In this reach of the Feather River, there is little evidence of natural levee deposits of Holocene age on the edge of the terraces of the lower member of the Modesto Formation, indicating that before debris from hydraulic mining altered the flow regime, the Feather River did not regularly send floodwaters to the west across the lower Modesto surface into the Butte basin. The Holocene flood plain of the Feather River is hummocky and deeply channeled; backfilled meander loops share the flood plain with anastomosing interdistributary channels in various stages of activity. A bluff exposure in the county park due east of the town of Live Oak, on the boundary between T. 16 N. and T. 17 N. (fig. 2), displays an 8-m-thick section of large-scale trough-crossbedded sand, overlain by flat-bedded, finely interstratified sand and silt. The crossbed sets have amplitudes of 1 to 3 m. The crossbedded sand is underlain by coarse gravel to the base of the exposure. We interpret this sequence as a gravel channel and sandy point bar deposit of lateral accretion that is topped by a stratified overbank deposit of vertical accretion. Holocene deposits on Honcut Creek and smaller creeks consist of interstratified sand, gravel, and silt that have cut-and-fill and cross-cutting channel-fill structures.

On Honcut Creek the Holocene alluvium is less extensive; it fills channels cut across and into the flood plain of upper member of the Modesto Formation (fig. 3A). At the upper end of the Honcut Creek flood plain, Holocene alluvium lies in discrete, narrow channels cut into the flood plain of the upper member. Downstream to the confluence of the Feather River, natural levee and overbank deposits of Holocene age progressively bury the alluvium of the upper member of the Modesto.

Interpretation of the distribution of Holocene deposits on the Yuba River is difficult, because most of the Holocene flood plain and flood plain of the upper member of the Modesto Formation have been destroyed either by mining activity or, in the Yuba River basin, by being buried under several meters of debris from hydraulic mining.

The Holocene sediments are of mixed mineralogy. Those on the Feather River are micaceous with nearly equal amounts of quartz, feldspar, and lithic grains. The sediments on Honcut Creek are not micaceous and generally are reddish brown rather than brown or gray, which characterizes the Feather and Yuba River sediments. The Holocene deposits of the Feather River flood plain are at least 8 m thick, although they may be much thicker. On Honcut Creek, channel deposits are less than 3 m thick, and overbank sediments are no more than 1 to 2 m thick. On

intermittent streams that drain the low foothills and older terraces, the Holocene sediments are red because they are reworked from older deposits. They range in thickness from 1 to 2 m.

Soil Landscapes

Soils formed in Holocene alluvium of Honcut Creek are simple ones that have developed only A horizons. The *Honcut* soil series (*Typic Xerorthents*) is an example. On the Feather River, dominant soils of the Holocene flood plain are the medium-textured *Columbia* soils (*Aquic Xerofluvents*). They occur generally in a high flood plain or overbank position, and the coarse-textured *Tujunga* soils (*Typic Xeropsamments*) occur slightly above but adjacent to active channels of the Feather River. From site to site, differences in thickness of A horizons and in depth of mixing (biologic churning) of stratified materials are common in the Honcut, Columbia, and Tujunga soils, and the variations are related to differences in the age of individual

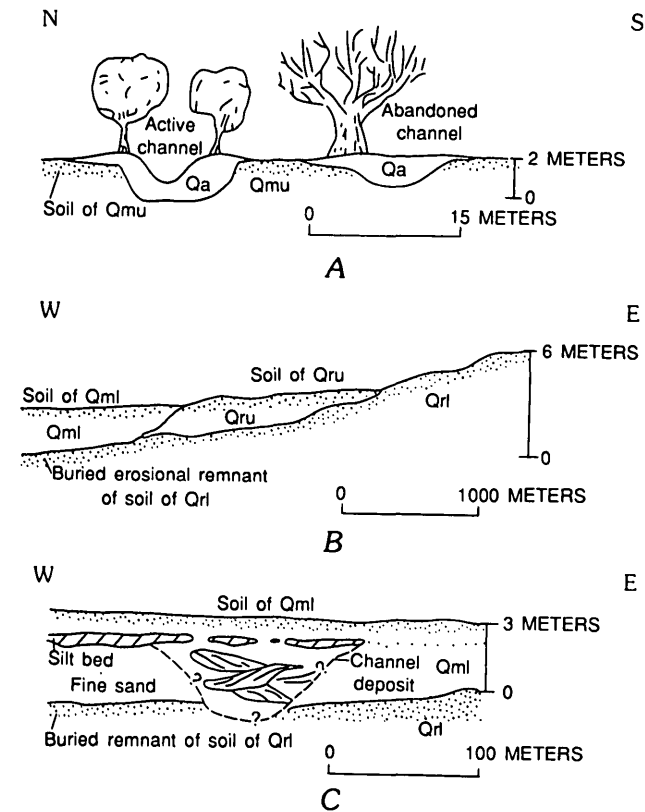


Figure 3. Schematic cross sections on and south of Honcut Creek. Vertical and horizontal scales are approximate; see figure 2 for explanation. A, Overbank deposits (Qa) cut into and overlie deposits of the upper member of the Modesto Formation (Qmu) on Honcut Creek. B, Stratigraphic relations between lower member of Modesto Formation (Qml), upper (Qru) and lower (Qrl) members of the Riverbank Formation, and surface and buried soils. C, Reconstruction from series of backhoe trenches of lower member of Modesto Formation (Qml) and lower member of Riverbank Formation (Qrl) in SW¼ sec. 1, T. 16 N., R. 3 E., south of Honcut Creek.

deposits, channels, and flood plain levels, and to the relative stability of particular sites with respect to continued deposition. Buried A horizons are also common within the flood plain deposits.

Geochronology and Correlation

The ages of Holocene deposits in the project area were deduced from radiocarbon dating of wood and charcoal samples collected on Honcut Creek and the Feather River. The ages range from $3,020 \pm 160$ yr B.P. to 450 ± 45 yr B.P. The ages may represent true fluctuations in Holocene alluvial activity, random sampling of more or less continuous activity throughout the Holocene, or older charcoal and wood reworked into younger strata.

The oldest age, $3,020 \pm 160$ yr B.P., came from charcoal collected by Gene Begg 1.6 m beneath a soil of the Columbia series on the prominent high flood plain of the Feather River northeast of Gridley (fig. 2, sec. 28, T. 18 N., R. 3 E.) (E.L. Begg, oral commun., 1982). Based on age, extensiveness of the deposit, and geomorphic position, the major flood plain surface of the Feather River is here correlated with the post-Modesto II terrace-flood plain deposit of Marchand and Allwardt (1981) in the northeastern San Joaquin Valley.

The oldest ages of $1,775 \pm 110$ and $1,625 \pm 90$ yr B.P. on Honcut Creek are from charcoal found 47 cm beneath stratified sand on upper South Honcut Creek and from a burned stump at a depth of 2.5 m beneath the surface farther downstream.

Charcoal fragments from depths of 1.8 and 1 m on the Honcut Creek flood plain gave ages of $1,045 \pm 95$ and $1,110 \pm 95$ yr B.P., respectively. Four additional samples collected from three other locations on Honcut Creek gave ages of 450 ± 45 , 595 ± 70 (2 dates), and 605 ± 45 yr B.P. The fragment of wood that yielded the age of 605 yr B.P. was collected 1.2 m beneath the surface of a natural levee that was the sampling site for one of the soils of the chronosequence, a *Honcut* series soil (*Typic Xerorthents*), sampling site HON-4.

The deposits from which these charcoal and wood fragments were taken have a well-preserved constructional form of natural levees and back-levee depressions, and they are well vegetated and have weak soils developed on them. They are part of the modern flood plain but stand slightly above the active channels and bars. Based on the radiocarbon ages and geomorphic position, these deposits on Honcut Creek are broadly correlative with the post-Modesto III deposits of Marchand and Allwardt (1981).

The Holocene channel fills of Honcut Creek that gave ages of 1,775 to 450 yr B.P. are incised into the upper, channeled surface of the major Feather River flood plain terrace, implying that the dominant episode of flood plain building on the Feather River took place as much as 3,000 yr ago and that this major deposit has been modified by channeling of its surface since about 1,700 yr ago.

Modesto Formation

The deposits of the Modesto Formation are present in the project area as a set of little-dissected fan-shaped flood plains. The sediments of the Modesto Formation are asymmetric (fig. 2) in plan view because they were deposited by both the south-flowing Feather River and by southwest-flowing distributary flood channels that drain to the Butte and Sutter basins. Near the mountain front at Oroville, on Honcut Creek, and on the Yuba River, Modesto deposits are inset as terraces into and topographically below the Riverbank Formation and older formations. Deposits of the Modesto Formation are, in turn, incised by Holocene streams and rivers and locally are buried by Holocene sediments. Farther west of the mountain front, the deposits of the Modesto Formation spread into fan-shaped flood plains that progressively bury sediments and soils of the Riverbank Formation. Extensive agricultural development, particularly the planting of orchards, has taken place on the young, fertile soils of the Modesto Formation.

We recognized the Modesto Formation by its well-preserved fan-shaped flood plain form, by minimal erosional dissection and minimal development of surface drainage channels, by its close association with modern streams and rivers, by its slight to moderate soil development, and by stratigraphic position. The formation has been divided into an upper and lower member. The lower member is by far the more extensive in the project area.

Upper Member

The upper member of the Modesto Formation is not extensive in the project area; the largest remnants lie along Honcut Creek and the small intermittent streams that drain the terrace lands and low foothills. On the Feather River, the bulk of the upper member must have been deposited on a confined flood plain that was inset into the deposits of the lower member of the Modesto. During Holocene time, the Feather River seems to have reoccupied and enlarged this confined flood plain of the upper member of the Modesto Formation, and deposits of the upper member were largely removed in this process. Little, if any, of the alluvium or soils of the upper member were preserved in this scouring, and as a consequence we did not find deposits of the upper member along the Feather River itself. A large area adjacent to the Feather River southwest of Oroville that may have contained deposits of the upper member at one time was dredged long ago for gold. Deposits of the upper member are partly preserved beneath a thin veneer of young alluvium that is inset 3 m below the depositional surface of the lower member near the crossing of Highway 70 over Honcut Creek (secs. 23 and 24, T. 17 N., R. 3 E. Honcut 7.5-minute quadrangle). Several kilometers upstream on Honcut Creek, deposits of the upper member are more extensive and are little dissected.

The areas along the Yuba River which most logically would have contained deposits of the upper member either have been dredged for gold or are covered by several meters of debris from hydraulic mining.

On lower Honcut Creek (secs. 23 and 24, T. 17 N., R. 3 E.) there is a conspicuous abandoned oxbow meander loop that was formed during a period of downcutting which must have occurred between deposition of the lower and upper members. Rapid downcutting by the Feather River, perhaps during interglacial time, apparently led to an oversteepening of the gradient on lower Honcut Creek. This downcutting in turn may have resulted in entrenchment of the meander on Honcut Creek near its confluence with the Feather River. Alluvium of the upper member then back-filled the abandoned meander.

The upper member is primarily composed of fine silt and silty fine sand on Honcut Creek. Gravel that we associate with a basal channel of the upper member was encountered at a depth of 3.5 m beneath the flood plain surface. Assuming that the deep gravel represents a basal channel, the upper member on Honcut Creek is 4 to 5 m or more thick. Because of erosion and mining activity, little is known of the thickness or extent of the upper member on the Feather or Yuba Rivers.

Lower Member

The lower member of the Modesto Formation consists of alluvial and possible lacustrine sediments deposited by the Feather and Yuba Rivers, by Honcut Creek and intermittent streams draining the terrace lands and low foothills, and by distributary flood channels that diverted flood-stage overbank flows of the Feather River to the west into the Sutter and Butte basins. We were able to recognize and map separately these relict distributary channels because of their preserved channel form, their coarse-textured sediments, and their characteristic soil profile development (fig. 2).

The lower member of the Modesto Formation is extensive in the project area. The relative youth of the deposit is attested to by the lack of erosional dissection of its surface, which contrasts strongly with the moderate to extensive dissection of all older deposits: between Marysville and Honcut Creek, in a distance of 15 km, only one intermittent stream channel cuts its surface (secs. 1 and 2, T. 16 N., R. 3 E., and sec. 35, T. 17 N., R. 3 E., Honcut 7.5-minute quadrangle). To the west of the Feather River, the smooth surface of the lower member is interrupted only by the slight undulations of the relict distributary channels. The lower member of the Modesto Formation is inset into older deposits near the mountain front and spreads into a fan-shaped flood plain that flanks the Feather and Yuba Rivers and also extends westward into the Sutter and Butte basins (fig. 2).

Along the Feather River from Oroville to the settlement of Oak Grove, remnants of the lower member of the Modesto are inset into the older deposits. The surface on

which the older part of Oroville is located (SE corner sec. 7 and NE corner sec. 18, T. 19 N., R. 4 E., Oroville 7.5-minute quadrangle) is underlain by a probable remnant of the lower member, although this land was dredged for gold in the late 1800's. Near Oak Grove (NW¼ sec. 11, T. 18 N., R. 3 E., Palermo 7.5-minute quadrangle) a small remnant of the lower member of the Modesto is inset approximately 3 m below the surface of the middle member of the Riverbank Formation.

On the upper part of Honcut Creek, only a single outcrop of probable alluvium of the lower member of the Modesto was found (near W¼ corner sec. 22, T. 17 N., R. 4 E. Honcut 7.5-minute quadrangle) where it nestles against the upstream side of a remnant of the Riverbank Formation, which presumably protected it from erosion and removal. This outcrop of alluvium of the lower member of the Modesto lies 2 m below the surface of the Riverbank remnant and 1 m above the surface of the upper member of the Modesto Formation. The lower member appears to have been poorly preserved on the upper part of Honcut Creek because incision and lateral planation during late Modesto and Holocene time scoured out the flood plain to its contacts with the Riverbank Formation on the north and south. The distribution of the lower member of the Modesto Formation on the Yuba River near the mountain front is unknown because of gold dredging and overwash from hydraulic mining.

Downstream on the Feather River from Oak Grove to Marysville and westward into the Butte basin, alluvium of the lower member of the Modesto spreads as a sheet that thickens and progressively buries the older units. Along the east side of the Feather River in this reach, the lower member of the Modesto overlies the upper and lower members of the Riverbank Formation in a very slight unconformity. A topographic break of 1 to 2 m separates the deposits between Oak Grove and Honcut Creek. No discernible topographic break separates the two formations south of Honcut Creek; there the boundary is recognized by strongly contrasting soil properties.

In some places around and to the north of Honcut Creek (for example, near the SE corner sec. 13, T. 17 N., R. 3 E., Honcut 7.5-minute quadrangle), alluvium of the lower member of the Modesto overlies the eroded remnants of a duripan soil formed on the upper member of the Riverbank Formation (fig. 3B). Along Honcut Creek and in backhoe trench exposures to the south (for example, SW¼ sec. 24, T. 17 N., R. 3 E., and SW¼ sec. 1, T. 16 N., R. 3 E., Honcut 7.5-minute quadrangle), the lower member of the Modesto Formation unconformably overlies the soil profile formed on the middle member of the Riverbank Formation (fig. 3B, C) at depths of 2 to 3 m. The Modesto Formation progressively buries the Riverbank Formation to the west of the Feather River; Modesto age and younger alluvium must thicken substantially to the west and southwest, because we found no trace of the buried soils on the Riverbank Formation in excavations as deep as 6 m. Davis and

Olmsted (1952) showed brown and crumbly red zones at depths of 10 to 20 m at several points along a north-south cross section of well logs drawn between the towns of Live Oak and Marysville. We interpret these as a soil or soils on the buried surfaces of the Riverbank Formation to the west of the Feather River.

Sediments in the lower member are unweathered and grains are subangular; those from the Feather River are micaceous. Quartz, feldspar, and lithic fragments dominate in the sand. Coarse-sand lenses commonly carry a few percent of fine gravel; the gravel is dominated by a blue, siliceous metamorphic rock. Modesto age sand from the Feather and Yuba Rivers is neutral gray below the zone of pedogenic alteration.

A layer of compact silt forms a very prominent marker of uniform thickness within the lower member. The silt is light gray and micaceous, and from petrographic analysis consists of more than 70 percent silt-size aggregates of birefringent clay (Dennis Lytle, oral commun. of the result of petrographic analysis by the Soil Conservation Service, Lincoln Laboratories, 1981). The clay is not pedogenic but is primary in the deposit. The balance of the silt fraction consists of fresh quartz, feldspars, and ferromagnesian minerals. The silt is compact and very hard, but no cementing agent has been recognized; it is referred to as "hardpan" by local orchardists although it is not a pedogenic feature. It breaks with blocky fracture and, in most places, it has many fine tubular pores that may be former root channels or insect burrows formed soon after deposition. The silt occurs as a sheet, or in sheetlike form, over an area of more than 390 km² in Butte, Sutter, and Yuba Counties. The silt sheet is encountered at depths of 1 to 2 m beneath the surface of the fan-shaped flood plain of the lower member of the Modesto (fig. 3C), and although it thickens and thins locally, it has an average thickness of 1 to 2 m. It can be traced to the west, where it is interstratified in the clays of the Sutter and Butte basins. The stratum contains micaceous fine- or medium-grained sand or silty sand near its base, and it fines upward to a very compact clayey silt. The uniform thickness over a wide area and the upward fining of texture suggest that this is the deposit of a single, large flood event that spread out over the entire flood plain. The silt overlies sandy distributary channel and overbank deposits, and is in turn overlain by channel and overbank materials (fig. 3C). The processes of flood plain accretion apparently were going on before and continued after the postulated flood event.

Cordell Durrell recognized a thick sequence of glacial lacustrine deposits of probable late Pleistocene age in Mohawk Valley at high elevation in the upper Feather River basin, and he gathered evidence that the lake was catastrophically breached and drained (Durrell, oral commun., 1981). The relationship of the lacustrine deposits to two sets of Wisconsin age moraines is not clear, but the strand lines of the lake may cut the older moraines but not the younger ones. If so, breaching of the low natural dam that im-

pounded the lake may have taken place after the maximum advance of the older (Tahoe) glaciation. The lake may not have existed at the time of the younger (Tioga) glacial advance. It is a speculative but intriguing possibility that the silt sheet resulted directly from the breaching of a glacial Lake Mohawk.

Alternatively, the silt may have been deposited as a lacustrine or prodelta facies of the prograding alluvial fan of the lower member of the Modesto Formation on the Feather River. Cherven (1984) has proposed such an explanation for the widespread occurrence of finely bedded silt on the distal parts of several ages of Pleistocene alluvial fans in the eastern San Joaquin Valley. Cherven explained the apparent coarsening upward from silt to sand to gravel within these alluvial deposits, noted by Marchand and Allwardt (1981), as resulting from westward progradation of glacial outwash fans into proglacial lakes. Our observation of laminated silt and apparent coarsening upward of alluvium in not only the lower member of the Modesto but also in the Riverbank and Laguna Formations lends support to Cherven's explanation of the origin of the laminated silt.

A second unusual feature is the relict distributary channels on the surface of the fan-shaped flood plain of the lower member of the Modesto. In many cases, the channels have retained their surface form, including natural levees and channel beds, even though these features may have formed on a flood plain that was abandoned as much as 40,000 years ago. Some of the best preserved channels do have a thin veneer of fresh sand, but this was probably deposited around the turn of the century, after sediment from hydraulic mining had raised the bed of the Feather River more than 4 m at Yuba City (Lindgren, 1911, p. 17). Lindgren (1911) stated that before mining debris raised the river bed, the Feather River was not subject to widespread overflow except at a point below Yuba City. Even today, after sedimentation, the surface of the flood plain of the lower member of the Modesto lies 7.5 to 9 m above the low-flow level of the Feather River. The distributary channels appear not to have carried floodstage flows from the Feather River since early Modesto time. This conclusion is strengthened by the observation that soil profiles with strong cambic, or weak argillic horizons (*Live Oak* series *Typic Haploxerolls*, or *Ryer* series *coarse variant*, *Typic Haploxerolls*) have formed in the sandy materials both on the levees and in the bottoms of the relict channels. Stability and nondeposition (or very rare deposition) are required for such soils to have formed. In this case, the channels must have carried principally surface runoff from the local area of the surface of the lower member itself since the time that it ceased functioning as an active flood plain. The well-preserved form also suggests that eolian deposition onto this surface has been minimal since the channels were formed.

All of the sediments of the lower member that we observed are stratified sand and silt deposited as overbank sediments or in distributary channels. The distributary

channels of the lower member of the Modesto radiate from the axis of the present-day Feather River. Based on these observations, we suggest that the north-south course of the Feather River, paralleling the mountain front, had been established by early Modesto time, and that the Feather River has followed essentially the same course from that time to the present.

Soil Landscapes

We have informally designated soils formed on the upper member of the Modesto Formation on the flood plain of Honcut Creek as *Wyman variant* soils (*Typic Haploxerolls*) (table 2). They have brown (7.5YR 5/4D) loam or silt loam A horizons and cambic B horizons with strong brown (7.5YR 4/6 and 5/5D) colors, strong blocky structure, and a very small increase in pedogenic clay (less than 1 to 2 percent absolute). Parent material color is 10YR 4/3M and 6/3D.

Soils formed on the lower member of the Modesto Formation are quite variable laterally across the landscape, and they have been difficult to map accurately. The widespread compact silt substratum within this deposit (fig. 3C) has impeded vertical water movement in the soil profile. At least two distinct soil profiles can be recognized in alluvium containing the substratum. The *Ryer* series (*Mollic Haploxeralfs*)² soil profiles have brown or pale-brown (10YR 5/3 or 6/3D) loam or clay loam A horizons that overlie yellowish-brown (10YR 5/4D), strong angular blocky clay loam or clay argillic B horizons. The argillic horizons of the *Ryer* soils display a net increase in clay of up to 12 percent. Phases of this soil have been delineated during soil-survey mapping (see table 6) based on differences in surface texture and depth to the silt substratum. A second distinct soil has formed over the substratum where internal drainage has been further impeded. The *Ryer duripan variants* (*Abruptic Durixeralfs*) have similar features in the upper profile to those of the *Ryer* series, but argillic horizons are more clay rich and are underlain by light yellowish-brown (10YR 6/4D) silica- and calcium carbonate-cemented duripans formed near the interface with the substratum. Parts of the soil landscape that lack the silt substratum display less strongly developed soils of the *Wyman* series (*Mollic Haploxeralfs*)³ with brown (10YR 5/3D) loam A horizons overlying brown (7.5YR 5/4D) clay loam argillic B horizons that have an average net increase in pedogenic clay of 5 or 6 percent. In addition, small areas of soils on the lower member, usually associated with the *Wyman* series, have little or no increase in clay content from the A to the B horizon, and therefore are similar to the

² This is the series classification assigned in the Yuba area soil survey. While it is probably correct, it is at variance with the official series classification for *Ryer*, which is *Typic Haploxeralfs*.

³ This is the series classification assigned in the Yuba area soil survey; the official *Wyman* series classification is *Typic Haploxeralfs*.

Wyman variant soils of the upper member of the Modesto Formation. In general, these more weakly developed soils occur near the Feather River (D. Lytle, oral commun., 1982). Although there is no topographic evidence, it is possible that areas of the terrace of the lower member of the Modesto near the river were subject to scour and erosion to a depth of less than 1 m after early Modesto time, and were subsequently backfilled to an accordant level.

We have informally designated soils formed on coarse distributary channel deposits of the lower member of the Modesto Formation as *Ryer coarse variants* (*Typic Haploxerolls*). These soils display just less than the 3 percent absolute increase in clay content required to meet the definition of an argillic horizon set forth in Soil Taxonomy (Soil Survey Staff, 1975), yet they have all the evidence of argillic character. The soils have brown (7.5YR 5/2D) sandy loam A horizons with about 10 percent clay, and brown to strong brown (7.5YR 5/4 to 5/5D) argillic horizons that have about 13 percent clay, abundant clay films bridging grains and coating pebbles, and moderate angular blocky structure. On the soil-geomorphic surface of the lower member of the Modesto Formation, soils range from weakly developed on coarse, somewhat excessively drained materials, to moderately strongly developed with duripans and strong argillic horizons on finer, silt loam and clay loam parent materials that overlie a restrictive substratum.

Geochronology and Correlation

We recognize and differentiate two members of the Modesto Formation in the project area based on stratigraphic relations and differences in soil development. We have correlated these units with the two members of the Modesto Formation in the northeastern San Joaquin Valley (Marchand and Allwardt, 1981) by tracing similar geomorphic surfaces from the project area to the Sacramento area, and by comparison of soil profile characteristics between areas.

The ages of the two members of the Modesto Formation were not determined in the project area; no datable materials were found even though a great deal of time was spent searching natural and manmade exposures. Marchand and Allwardt (1981) and Harden (1987) summarized available radiometric ages of the two members: The upper member of the Modesto Formation is bracketed by radiocarbon ages from the San Joaquin Valley of about 8 to 9 ka and 27 to 31 ka (Atwater and others, 1986). Marchand and Allwardt (1981) and Harden (1987) associated deposition of alluvium of the upper member of the Modesto Formation with the Tioga glaciation in the Sierra Nevada, which ended by about 9,000 years ago. The close association of the upper member of the Modesto Formation with Holocene channels on Honcut Creek, the total absence of surface dissection, and the relatively undeveloped soils on the member suggest that the age of the surface of the deposit is

in the young end of this range of ages. Pending radiocarbon dating of the upper member in the project area, we have adopted an age of 10 ka for the upper part and soils of the upper member (table 3).

The age of the lower member of the Modesto Formation is not well established. Marchand and Allwardt (1981) pointed out that deposits correlated with the lower member could represent two episodes of alluvial deposition in early and middle Wisconsin time. Marchand and Allwardt (1981) reported a uranium-series age on bone of about 29 ka as a probable minimum age for the lower member, and they cited a radiocarbon age of 42.4 ka from wood near the base of the lower member. Harden (1987) revised uranium-trend ages, reported by Marchand as 95 ± 45 ka, to about 42 ka using new calibrations. Atwater and others (1986) estimated the age of the lower member of the Modesto Formation at 20 to 26 ka based on work in the southern San Joaquin Valley. We have adopted a tentative age of 40 ka for the upper surface and soils of the lower member, although the deposit has not been dated in the project area; the true age may range from 14 to 100 ka (table 3).

Riverbank Formation

The Riverbank Formation underlies a prominent, rolling, moderately dissected landscape that occurs as a belt along the valley margin between the high terraces to the east and Modesto Formation to the west. Remnants of the Riverbank Formation are inset into deposits of the Laguna Formation near the mountain front on the Feather and Yuba Rivers. To the west and southwest, alluvium of the Riverbank Formation spreads out to form a fan flood plain, now dissected, that buries the eroded surface of the Laguna Formation. The Modesto Formation deposits, in turn, bury the surfaces and soils formed on the Riverbank Formation. We subdivided the Riverbank Formation in the project area into two members on the basis of stratigraphic superposition, geomorphic expression, and surface and buried soils. We have named these the upper and lower members of the Riverbank Formation, and correlate these deposits with the upper and middle units, respectively, of the Riverbank Formation in the northeastern San Joaquin Valley (Marchand and Allwardt, 1981). We do not recognize the lower unit of the Riverbank Formation of Marchand and Allwardt (1981) in the project area.

The relationship between the two members of the Riverbank Formation over most of the project area is one in which alluvium of the upper member is inset into and topographically below high remnants of the rolling, dissected surface of the lower member. This results in a pattern of "islands" of the lower member that project 1 to 5 m topographically above the surface of the upper member. The dual surfaces of the Riverbank Formation are well expressed on Honcut Creek near the town of Honcut and on the Feather River to the east and southeast of Oak Grove. At

these places the topographic separation of the two members is about 5 m. The topographic separation of the members diminishes to the south on the Feather River and to the west on Honcut Creek, because the lower member dips more steeply to the west-southwest than does the younger upper member. Just to the north and east of the confluence of the Feather River and Honcut Creek, the separation is about 1 m, and to the south of Honcut Creek the upper member overtops and buries the lower member. This pattern is difficult to confirm on the Feather River above Oak Grove, and on the upper Yuba River, because very little Riverbank-age alluvium has been preserved along their channels, both of which have been deeply incised into the high terraces of the Laguna Formation.

The rolling surfaces of the Riverbank Formation can be traced at least as far south as Sacramento County. The soils formed on the Riverbank are locally referred to as "red clays" because of their strong, brightly colored argillic B horizons. Until recent years, these lands were dry-farmed to wheat and barley, but today they are being leveled to grow irrigated rice.

Upper Member

The upper member of the Riverbank Formation is most extensive to the east of the Feather River between the towns of Palermo and Honcut, and south from there to the Yuba River. To the west of the Feather River most of the upper member of the Riverbank Formation has been buried by alluvium of the Modesto Formation; however, small areas of the upper member of the Riverbank crop out to the east and northeast of the town of Biggs (fig. 2).

The upper member of the Riverbank Formation was deposited over a wide area as a veneer 1 to 3 m thick on the rolling, dissected surface of the lower member of the Riverbank. This veneer is generally composed of silt and sand. Coarser sandy and gravelly deposits greater than 3 m thick were found adjacent to the modern Honcut Creek.

The upper member of the Riverbank is separated from the lower member in some places by a buried soil on the surface of the lower member. For example, a buried soil on the lower member can be seen in the channel of Honcut Creek (SE $\frac{1}{4}$ NE $\frac{1}{4}$ sec. 19, T. 17 N., R. 4 E., Honcut 7.5-minute quadrangle). The buried soil has some characteristics like the modern-day *Alamo* series (*Typic Duracquolls*) soils which form in clayey sediments. This buried soil on the lower member appears to have formed in fine-textured sediment in a depression on an erosional surface that must predate deposition of the alluvium of the upper member. Additional evidence of an unconformity and hiatus between the two Riverbank members was found at Honcut Creek near the Highway 70 triple bridges, and in backhoe trenches in the Modesto Formation 4 km to the south (S $\frac{1}{2}$ sec. 24, T. 17 N., R. 3 E.; and NW $\frac{1}{4}$ SW $\frac{1}{4}$ sec. 1, T. 16 N., R. 3 E., respectively, Honcut 7.5-minute quadrangle). At these locations, part of a red argillic

horizon is buried beneath deposits of the Modesto Formation. The soil remnant is topographically lower than the projection of the surface of the upper member, and we infer that it is a remnant of an older, stratigraphically lower, buried soil formed on the eroded surface of the lower member (fig. 3B).

In the central area between Palermo and Honcut Creek, alluvium of the upper member is 1 to 2 m thick and it unconformably overlies a compact silt layer in the lower member. The soil profile that has formed on the upper member in this area extends through the alluvium of the upper member and into the silt layer in the lower member. A silica-cemented duripan has formed along the unconformity because of restricted water movement into the underlying silt stratum.

The upper member of the Riverbank Formation can be differentiated from the lower member on the basis of degree of erosional dissection. Surface relief on the upper member averages 1 m and a partially integrated drainage pattern results in a subtle mound and swale topography. Small intermittent streams are incised as much as 2 m below the surface of the upper member, Honcut Creek is incised as much as 3 m, and the Feather River is incised as much as 9 m below the surface of the upper member.

Lower Member

The surface extent of the lower member of the Riverbank Formation is not as great as that of the upper member: it crops out discontinuously and adjoins the Laguna Formation in an arc from northeast of Biggs on the north to the Yuba River on the south (fig. 2). It also crops out in the central and south-central project area as isolated remnants that are surrounded by deposits of the upper member of the Riverbank Formation and the Modesto Formation.

On the Feather River north of the town of Oak Grove, the lower member was deposited within a deep channel cut into deposits of the Laguna Formation. Small remnants of the lower member are inset against the Laguna Formation a few kilometers to the southeast and south of Oroville. The topographic separation between the surfaces of the lower member of the Riverbank Formation and the upper member of the Laguna Formation decreases from about 20 m near Oroville to less than 5 m near Oak Grove, because the older unit dips more steeply to the southwest than does the younger.

Downstream from Oak Grove on the Feather River, the lower member of the Riverbank spread from its confining canyon within the Laguna Formation to form a wide fan-shaped flood plain which almost completely buried the dissected surfaces of the Laguna Formation. The remnants of this flood plain of the lower member occur now as the isolated outcrops in the central project area. To the southwest and south of Oak Grove, the lower member of the Riverbank Formation is in turn buried by alluvium of the upper member of the Riverbank Formation and of the

Modesto Formation. On Honcut Creek and the Yuba River, alluvium of the lower member of the Riverbank spread to the west as fan-shaped flood plains from points very close to the mountain front. Very few remnants of the lower member exist in the narrow channels upstream from these points. Downstream or westward from the mountain front on these waterways, the lower member of the Riverbank Formation almost completely buries the dissected remnants of the Laguna Formation.

The landscape of the lower member is distinctly rolling, with up to 5 m of relief. An integrated drainage network is well developed. The outcrop pattern of the lower member appears to conform more closely to the drainage-ways of the present-day creeks and rivers than does that of the Laguna Formation.

There are few exposures in the Riverbank Formation; however, the reference section described below is typical of the lower member:

Reference section location: South Honcut Creek; description taken at an exposure in the south bluff; S¼ corner NE¼NE¼ sec. 27, T. 17 N., R. 4 E.; Honcut 7.5-minute quadrangle.

Elevation of top of bluff is approximately 125 ft (37 m).⁴

Riverbank Formation:

Lower member:

	<i>Approximate thickness (m)</i>
4. Medium and coarse sandy clay, with occasional fine gravel, weathered reddish brown to red; Kimball series soil profile formed in these sediments is poorly exposed, hilltop convex	~ 2.0
3. Medium to fine subangular sand; gradational to overlying unit; feldspars are highly weathered; cross-bedded, individual cross-bed sets up to 0.7 m in height; weathered brown to red brown	1.0
2. Medium to coarse sand; similar to unit above but forms a distinct channel cut into underlying unit..	0-1.5
1. Silt; finely laminated and cross-laminated; very compact; weathered gray to buff	~ 2-3
Total thickness	<u>5.0-7.5</u>

Base of bluff, stream channel underlain by modern deposits.

The coarse overlying fine sequence is typical of the deposits of the lower member of the Riverbank on the Feather River and on Honcut Creek.

The thickness of the lower member is not known directly; maximum exposure is about 6 m on Honcut Creek (description above). A driller's log from a California Department of Water Resources test well on Highway 99 at the Thermalito Afterbay (79-107A) records what may be a complete aggradational unit of the lower member that is 9.5 m thick. This was described by the geologist in charge as a probable fill in the eroded surface of the "Red Bluff" (Laguna Formation) because a distinct pumiceous tuff bed at 4 m in this unit is not reported in any other nearby wells (R. Bartlett, California Department of Water Resources, oral commun., 1981).

⁴ Elevations are stated in feet, with metric equivalents in parentheses, because topographic maps for this area use English units.

Riverbank Formation alluvium consists largely of mixed, well-sorted, subangular quartz, feldspar, and lithic sand and silt that is similar in physical appearance to alluvium of the older units. Gravel is less common than in the older units, except locally where there has been a source of cobbles that are reworked from the older units. Trough crossbeds as much as 1 m in amplitude are present in Riverbank alluvium. Silt and silty sand is finely laminated and cross laminated. The beds of silt are very compact, and their appearance is that of a siltstone, although no cementing agent is obvious. The silt weathers neutral gray to light tan. Gravel clasts, including those of granitic composition, are fresher than those in the older units.

Soil Landscapes

Soils formed on the Riverbank Formation are deeper, redder, and more strongly developed than those formed on the Holocene alluvium and on the Modesto Formation. The *Yokohl* series (*Typic Durixeralfs*) duripan soils have reddish-brown (5YR 4/3D) loam A horizons that abruptly overlie reddish-brown or yellowish-red (5YR 5/4 or 5/6D) clay-textured argillic B horizons. The argillic horizons overlie strongly cemented reddish-brown (5YR 5/4D) iron- and silica-cemented duripans at about 1.1 m. *Yokohl* series soils are dominant on the surfaces of the upper member of the Riverbank in the vicinity of the Feather River and Honcut Creek, where alluvium of the upper member is thin and overlies compact silt of the lower member. Along the Yuba River, the *San Joaquin* series (*Abruptic Durixeralfs*) replaces the *Yokohl* series where alluvium of the upper member has a larger granitic component. Soils of the *Kimball* series (*Mollic Palexeralfs*) are found in areas where the alluvium of the upper member is thicker, as near the town of Honcut, or where the unconformity on the alluvium of the lower member is not abrupt texturally. These are the soils that we sampled to represent soil development on the surface of the upper member of the Riverbank. These soils are quite strongly developed and they have brown or reddish-yellow (7.5YR 4/4 or 6/6D) loam or silt loam A horizons that abruptly overlie dense, reddish-brown or yellowish-red (5YR 5/4 or 5/6D) claypan argillic horizons at about 70 cm. The argillic horizons extend deeper than 1.2 m, and transitional BCt horizons may extend as deep as 2.5 m. Skeletans (coatings of clean sand and silt grains on the surfaces of prismatic or blocky peds) are well developed in the BA horizon of these soils, indicating strong leaching of the upper part of the Bt horizon probably as a result of lateral flow of water through these profiles from adjacent higher-elevation surfaces of the lower member of the Riverbank. The landscape of the upper member of the Riverbank displays as much as 1 to 2 m of relief, and a mound and swale microrelief is well developed on undisturbed sites. Soils of the mound areas tend to have thicker A and BA horizons, and locally soils of the *Landlow* series occur in swales.

Remnants of the lower member of the Riverbank Formation generally rise 2 to 5 m above the level of the landscape of the upper member. Soils on the least eroded surfaces of the lower member are distinctive, and we have informally designated them as *Kimball deep variants (Mollic Palexeralfs)* (table 2). These soils have argillic horizons that are deeper and redder than those of the Kimball series, although they have lower maximum clay contents than do the argillic horizons of the Kimball or Yokohl series formed on the upper member. The deep-variant soils have reddish-brown (5YR 5/4D) loam A horizons, thick transitional BA horizons, and red (2.5YR 5/6D) clay loam argillic horizons that extend from 0.9 to 1.6 m in the profile. These soils also have very thick transitional BCt horizons that extend to 3 m and beyond. Soils on erosional hillslopes between the lower and upper members of the Riverbank have properties that are transitional between the two Kimball soils. On the Yuba River, soils of the *Ramona* series (*Typic Haploxeralfs*) replace the Kimball deep variant in parent materials that are largely granitic.

Geochronology and Correlation

Within the local stratigraphic sequence, the two alluvial deposits that we correlate with the Riverbank Formation are distinctive and unique in several ways compared to both younger and older alluvial deposits. They are intermediate between deposits of the Modesto and Laguna Formations in stratigraphic position, degree of surface dissection, and degree of soil development. The two deposits together compose a distinctive geomorphic unit that has 1 to 5 m of rolling relief. The profile index of soils formed on these two deposits is significantly different from the profile indices of either the Modesto or Laguna Formations (see table 10).

Within the local stratigraphic sequence, the two deposits that we correlate with the two members of the Riverbank Formation are separate alluvial units as shown by an unconformable contact between them, marked by a strongly developed buried soil, and by differences in erosional relief. No radiometric ages are available from either member in the project area; however, we use two lines of evidence to establish a correlation to the type locality of the Riverbank Formation in the northeastern San Joaquin Valley and to assign probable ages for the two members. First, the distinctive geomorphic surface and characteristic soils of the Riverbank Formation can be traced from Sacramento County (Helley, 1979), where radiometric ages are available, into the project area. Second, the soils formed on the two members of the Riverbank Formation in the project area and at the type locations on the Merced River (Harden, 1987) are similar in degree of soil profile development. For example, both the absolute values of the profile index and the small difference in the profile index between members seem characteristic of the Riverbank Formation in both areas (see table 10).

Marchand and Allwardt (1981) and Huntington (1980) described three separate alluvial units within the Riverbank Formation in several areas of the eastern San Joaquin Valley. The oldest unit in the San Joaquin Valley is the least extensive of the three, and has very little preservation of surface form, or surface exposure (Marchand and Allwardt, 1981). It is found primarily in the subsurface. The middle unit is extensive and is highly dissected (as much as 5 m of relief), and the upper unit, which is of intermediate extent, has much lower (<2 m) relief (Marchand and Allwardt, 1981). Shlemon (1967a, b, 1972) recognized two rather than three alluvial fills of Riverbank age associated with the ancestral American River in Sacramento County. Harwood and others (1981) and Helley and Harwood (1985) also recognized two rather than three alluvial units of the Riverbank Formation in the northern Sacramento Valley. The reason why three units were recognized in the San Joaquin Valley and only two in the Sacramento Valley is not known. Two rather than three episodes of alluviation may have occurred in the north because the physical response of the northern Sierra to Pleistocene climatic change and tectonism was different from that in the central and southern Sierra.

We provisionally correlate the upper and lower members of the Riverbank Formation in the Feather and Yuba rivers area with the upper and middle units of the Riverbank Formation of Marchand and Allwardt (1981), respectively. We base this on similar degree of soil development of the members between areas (see table 10), on similar geomorphic expression of the members between areas, on physical tracing of the geomorphic surface between areas, and on similarities in extensiveness of the two members between areas.

We have only limited information from the project area on the age of the Riverbank. Two oriented samples collected from the reference section of the lower member on Honcut Creek had normal magnetic polarities, which, in conjunction with stratigraphic relationships, suggests deposition during the Brunhes Normal-Polarity Chron, and an age of less than about 730 ka.

Andrei Sarna-Wojcicki determined the concentration of major and trace elements in a sample of pumiceous sand from a depth of 6 m in an alluvial deposit near the perimeter of the Thermalito Afterbay that we correlate with the lower member of the Riverbank Formation. Similarity coefficients determined by Sarna-Wojcicki on the basis of the elemental suite are 0.9 for comparison of this pumice with the informal Rockland ash bed (0.45 Ma) and 0.85–0.9 for comparison with the Nomlaki Tuff member of the Tehama Formation (3.4 Ma). Neither coefficient is high enough to permit reasonable correlation with these well-known tephra units (A. Sarna-Wojcicki, oral commun., 1984). The eruptive source and age of the pumiceous sand are not known at this time.

The age of the Riverbank Formation in the northeastern San Joaquin Valley is known from several lines of evi-

dence. Hansen and Begg (1970) reported a minimum age of 103 ± 6 ka for the younger(?) Riverbank deposits in Sacramento County. This age was based on uranium-series dating of mineralized vertebrate fossils. All units of the Riverbank Formation in the Merced River area are much younger than 600 ka because there was time to develop a strong soil on the radiometrically dated Turlock Lake Formation before the lower unit of the Riverbank Formation was deposited (Marchand and Allwardt, 1981, p. 41).

Marchand (1977) correlated the three units of the Riverbank with marine cold-water isotope stages 6, 8, and 10 or 12, dated at 127–190, 247–276, and 336–356 or 425–457 ka, respectively (Hays and others, 1976). Harden (1987) reported uranium-trend ages of 140 ± 40 ka and 145 ± 20 ka for the upper unit, and 260 ± 45 ka for the middle unit of the Riverbank in the Merced River area. Harden also reported a uranium-trend age of 120 ± 40 ka on upper member alluvium at a site near the quarry where Hansen and Begg's (1970) bone was recovered to yield the uranium-series age of 103 ka.

The radiometric ages of the upper member from the Sacramento area and Merced River and the age of the end of oxygen-isotope stage 6 are in reasonable agreement. We have adopted an age of 130 ka for the upper surface of the upper member of the Riverbank Formation in the project area. We believe it is reasonable, given the similarity of the geomorphic surfaces and soils between the Sacramento area and the project area. We have adopted an age of 250 ka for the upper surface of the lower member. The erosional relief and strong soils that developed on the lower member before deposition of the upper member are consistent with the long time interval postulated between members. Because we lack radiometric dating of the lower member in the project area, we must allow the possibility that our lower member is correlative with the lower unit of Marchand and Allwardt (1981) and has an age of 330–450 ka (correlative with the ends of marine cold-water isotope stages 10 or 12).

Laguna Formation

Deposits associated here with the Laguna Formation underlie the rolling, deeply dissected hills east of Oroville, the prominent high terraces that flank the Feather and Yuba Rivers at the margin of the valley, and the isolated remnants of high terraces that lie several kilometers west of the valley margin between the Feather and Yuba Rivers.

The Laguna Formation occurs above the older dacitic unit, and it is truncated by a complex of erosional surfaces that are difficult to trace or correlate laterally. The Laguna Formation is unconformably overlain by the Riverbank Formation (fig. 4A, C).

The Laguna Formation consists of a tuff and two distinct alluvial units of different ages that have a complex relationship to each other. The alluvial units are here designated the lower and upper members of the Laguna Formation. The Nomlaki Tuff Member, a distinctive time

marker in the Sacramento Valley, occurs at or near the base of the lower member and provides the basis for correlating the Laguna Formation in part with the Tuscan and Tehama Formations, which also include the Nomlaki as a member. A thick gravel bed caps the upper member in most places. We use the informal term uppermost gravel bed for this layer. The formation displays relict, exhumed, and erosional surfaces that are marked by distinctive surface and buried soils. A complex interplay of deposition, erosion, and tectonics must be invoked to explain the outcrop patterns now seen.

The two alluvial members of the Laguna are apparently superposed in normal stratigraphic order in the subsurface beneath the massive high terrace west and northwest of Oroville. Drill logs from this area show two fining-upward sequences above the dacitic unit. Each sequence begins with a basal gravel (as much as 10 m thick) and fines upward into stratified sand, silt, and clay. The relict surface of the upper member is represented by remnant knolls such as the hill at the Butte County Administrative Center (SW $\frac{1}{4}$ sec. 6, T. 19 N., R. 4 E., Oroville 7.5-minute quadrangle). The buried surface of the lower member, just beneath the basal gravel of the upper member, contains what appears in the drill records to be a soil profile that is as thick as 6 m. The buried soil on the lower member is exposed at an elevation of 140 ft (43 m) on the southwest wall of the large borrow pit 2 km south of the Oroville airport. The soil profile exposed there is more than 5 m and possibly 8 to 10 m thick, has prominent reticulate mottling, and is similar to the *Red Bluff strong variant* surface soil (*Palaxerults*) recognized on exhumed surfaces of the lower member of the Laguna. To the southeast, across the Feather River in the area between Oak Grove and Palermo, and at other sites such as near Honcut Creek, the upper member of the Laguna has been stripped away by erosion, exhuming the lower member (fig. 4A, C). The soil profiles seen at these sites vary in their properties and are the result of re-exposure of remnants of the soil originally formed on the surface of the lower member of the Laguna before burial by the upper member, and of renewed soil development since the time of exhumation. East of Oroville and Palermo, at elevations of as much as 600 ft (183 m), dissected remnants of the lower member of the Laguna Formation crop out that were never buried by the upper member. A few hillcrests in this position bear relict soils that have developed over a span of as much as 3 million years. The area west of Palermo Ridge that demonstrates normal superposition of the two Laguna members, and the area to the east where the younger deposit is inset topographically below the older, are apparently related across a zone of monoclinical flexure or high-angle reverse faulting, or both, that was active at the time one or both members were deposited.

It is not possible to recognize and separate the two alluvial members of the Laguna Formation on the basis of lithology alone. Their separation is based on distinct topographic position (for example, east of Oroville where the

lower member has never been buried); on recognition of the unique, extremely strong relict soil profile that is preserved on infrequent high-elevation remnants of the lower mem-

ber, or of the anomalously strong soil profiles displayed where the lower member has been exhumed by erosion of the upper member; and on the subsurface expression of the

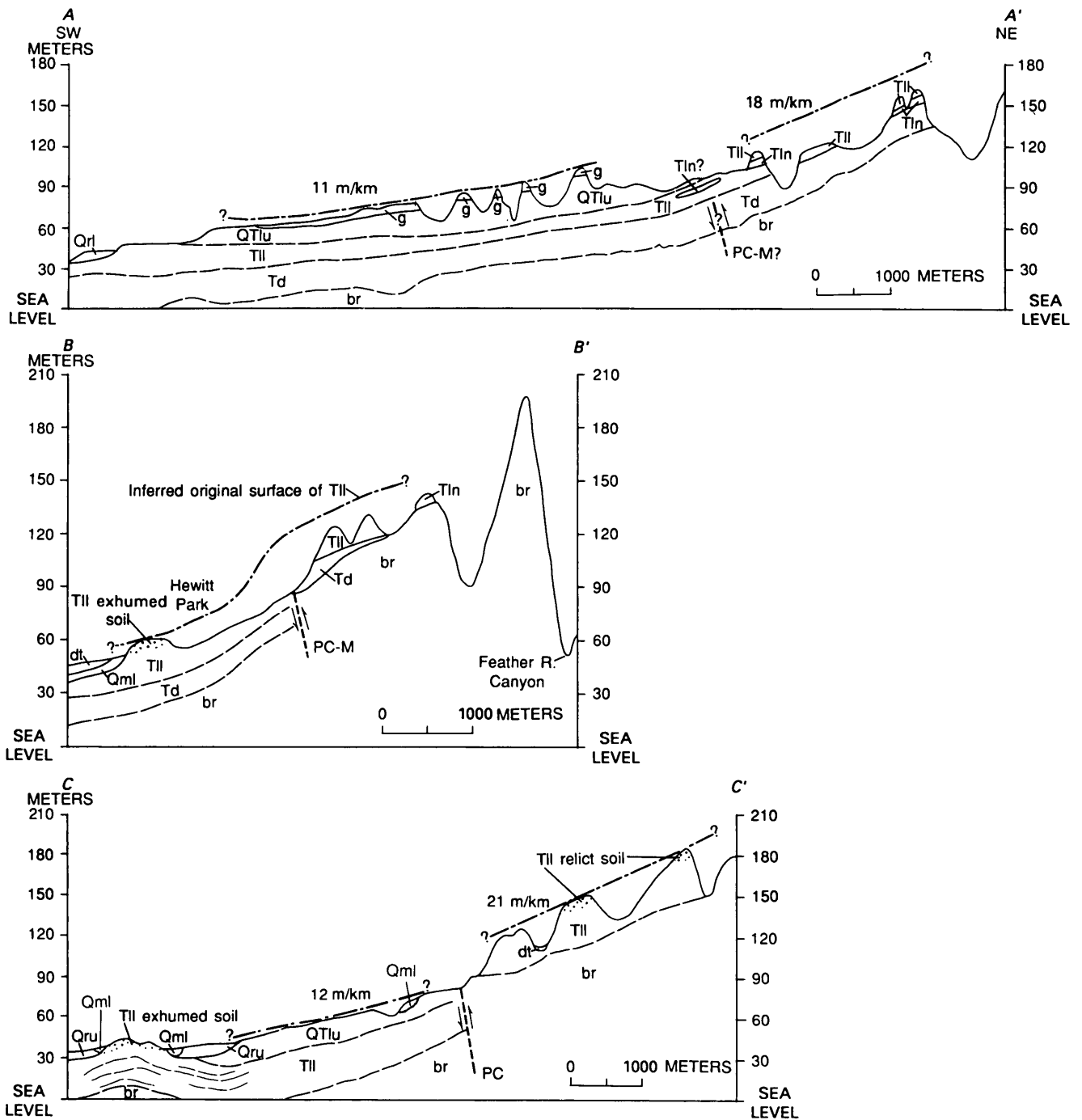


Figure 4. Schematic cross sections showing inferred extension of Prairie Creek (PC) and Magalia (M) lineament fault zones; arrows show probable direction of movement. See figure 2 for locations and description of map unit symbols. Contacts dashed where approximately located; heavy dash/dot line above units represents reconstructed surfaces of upper and lower members of the Laguna Formation indicating inferred monoclinial flexure; vertical exag-

geration $\times 20$. A, Section A-A' showing a slope of 18 m/km on reconstructed TII surface and slope of 11 m/km on the unit g surface. B, Section B-B' showing reconstructed apparent uplift of northeastern block as inferred from discussion of deformation. C, Section C-C' showing relations of relict, buried, and exhumed surfaces of TII and apparent uplift of northeastern block.

superposition of two fining-upward alluvial cycles separated by a strongly developed buried soil. In places where these clues are lacking, one cannot say with certainty which of the two members is displayed.

Upper Member

The upper member of the Laguna Formation comprises most of the deposits underlying the rolling high terrace surface in the Thermalito area west of Oroville, the haystack hills and bluffs south of Oroville on Highway 70, and the upper part of the isolated terrace remnants between Honcut Creek and the Yuba River. These are the principal landforms that Olmsted and Davis (1961) correlated with the Laguna Formation.

The upper and lower contacts of the upper member are unconformable in the map area. The base of the upper member rests, in various places, on metamorphic bedrock, on the eroded surface of the older dacite unit, and on the soil profile or sediments of the lower member. Relief on the underlying units may exceed 45 m. Basal gravel of the upper member rests on bedrock at 160 ft (50 m) elevation near the Feather River Fish Hatchery, but 1 km to the north, the upper member rests on the top of the dacite unit at 295 ft (90 m) elevation. A valley apparently was cut into sediments of the lower member and older deposits by the ancestral Feather River, in approximately its present position, before deposition of the upper member began. Flexure or faulting along the mountain front during Pliocene time may have controlled the erosional pattern. Near the Yuba River, the upper member was apparently deposited unconformably on the lower member.

The upper member consists of fluviially deposited gravel, sand, and silt of mixed lithology and mineralogy. Beds of sand and silt appear to dominate over gravel within the upper member, although lateral variability is great and exposures are few. The composition of gravel in the upper member is similar to that in the lower member. Several types of blue silicic metamorphic rocks are common, as are clasts of quartzite, dark metavolcanic rocks, and a pale greenish-white felsic metavolcanic(?) rock. Volcanic and granitic rocks are generally only minor components of the gravel, except at a few outcrops where individual gravel beds carry a large proportion of andesitic cobbles. The gravels and cobbles are subrounded or rounded and average 10 to 15 cm in diameter, although cobbles in the basal part of the upper member on the Feather River and in the uppermost gravel bed south of the river are coarser, as much as 40 cm in diameter. The conglomerates are matrix supported, and most show imbrication of the cobbles. Conglomerate beds encountered in the subsurface west of the Feather River carry mixed gravel that is 5 to 12 cm in diameter.

Sand in the upper member is composed of subangular or subrounded quartz with a high proportion of lithic grains and weathered feldspar. Sand tends to be fresher in the

upper member than in the lower member. Individual sandy beds vary from flat and well-bedded to trough-crossbedded forms with amplitudes of more than 2 m.

Finely bedded and laminated silt and clay with a tuffaceous appearance is interbedded with sandy beds in the upper member. Individual beds of silt drape over undulating surfaces of underlying crossbed sets. Silt beds also contain thin flat laminae and fine crosslamination.

A striking feature of the upper member of the Laguna Formation is the tuffaceous appearance of many sandy and silty beds, and the local appearance of abundant volcanic clasts in gravel beds. Exposures of the upper member along Highway 70 and in a railroad cut illustrate these lithologic variations (NE $\frac{1}{4}$ sec. 36, T. 19 N., R. 3 E., and NE $\frac{1}{4}$ sec. 31, T. 19 N., R. 4 E., respectively, Palermo 7.5-minute quadrangle). At the Highway 70 site, individual beds in the section alternate between lithic volcanic sand and mixed sand; high in the cut, one gravel bed has abundant cobbles of andesite(?) in a sandy, tuffaceous matrix. At the railroad site, some silty beds appear to be highly weathered tuff. Exposures such as these have led some geologists (Lindgren, 1911; R. Ford, unpub. mapping) to assign these sediments to older volcanic units. An alternative explanation, based on the fact that these sediments were deposited contemporaneously with part of the volcanic activity that formed the Tuscan Formation to the north, is preferred. Volcanic mudflows did not come down the Feather River drainage to the Sacramento Valley, although the Tuscan Formation directly abuts the west branch of the Feather River. We propose that airfall ash, lapilli, and possibly volcanic blocks were deposited in, then eroded from, the upper watershed of the Feather River and that these became interbedded with the more typical mixed sediments in the resulting deposits.

Because of poor exposure and lateral heterogeneity, the gross stratigraphy of the upper member is not well known. From the outcrops and drill records examined, the lower part of the upper member of the Laguna Formation in the Feather River area consists of coarse basal channel deposits of gravel that thicken to the west or southwest. Deep exposures along the north and west sides of the river, near where Highway 70 crosses it, show these deposits. The upper member here appears to have filled the deepest trough cut in older deposits and in bedrock. In this exposure the gravel is coarse, crudely bedded, and because it is more than 24 m thick, probably represents more than one aggradational cycle. The basal gravel lies on metavolcanic bedrock and on the eroded surface of the dacite unit in these exposures. Five kilometers to the south, in a railroad cut (NE $\frac{1}{4}$ sec. 31, T. 19 N., R. 4 E., Palermo 7.5-minute quadrangle), a coarse basal gravel bed 4 m thick rests on dacitic sediment. In the subsurface 10 km to the west, along Highway 99, a basal gravel of the upper(?) member is 9 m thick and rests on the buried soil of the lower member.

In the few places where the middle section of the upper member is exposed, it is generally composed of crossbed-

ded sand and finely laminated silt or silty clay. At least two buried soils have been recognized in this part of the section, one at the Thermalito Power Plant and another in a roadcut on Ophir Road (NE $\frac{1}{4}$ sec. 31, T. 19 N., R. 4 E., Palermo 7.5-minute quadrangle). The soils are moderately to strongly developed, with red or reddish-brown argillic B horizons, and in aggregate they may represent tens to hundreds of thousands of years of landscape stability and nondeposition within the upper member.

At several places in the Oroville area, the dissected surface of the upper member forms knobs or haystack hills that rise 10 to 20 m above the general landscape of more eroded parts of the upper member: the Butte County Administrative Center, the canal crossing at Cherokee bridge, and the haystack hills south of Oroville are examples (SW $\frac{1}{4}$ sec. 6, and sec. 5, Oroville 7.5-minute quadrangle; and secs. 29 and 31, Palermo 7.5-minute quadrangle; respectively, T. 19 N., R. 4 E.). These are underlain by a coarse gravel lag or channel deposit that appears to be the uppermost bed of the upper member. The prominent high-terrace outliers in the valley between Honcut Creek and the Yuba River are capped by the same coarse gravel deposit. At this time, we do not know whether this uppermost gravel bed is a pedimentlike veneer on an erosional surface, or whether it is merely the stratigraphically highest gravelly fan or flood plain deposit of the upper member of the Laguna Formation. Arkley (1962) and Marchand and Allwardt (1981) recognized that the Laguna Formation and younger alluvial deposits in the northeastern San Joaquin Valley coarsen upward and that gravel beds cap several of them, including the Laguna. These and other authors have variously interpreted the capping gravel as pedimentlike veneers or as the final stage of deposition of upward-coarsening alluvial fan building. Cherven (1984) interpreted the capping gravel on the Laguna Formation as an upper fan facies (a facies deposited near the mountain front) of westward-prograding glacial outwash fans. He noted that the gravelly, upper fan facies of the Laguna Formation is found as a sheet deposit near the Sierra foothills and as linear ridges to the west that are either erosional remnants of the sheet deposit or preserved channel thalwegs. Although there are several possible correlative formations, for example the Red Bluff Formation, the Arroyo Seco Gravel, the China Hat Gravel Member of the Laguna Formation, and the North Merced Gravel, we refer to the gravel bed in this report as the uppermost gravel bed of the upper member of the Laguna Formation, because our information on the probable age and stratigraphic significance of the bed is not precise enough to suggest a definite correlation.

A reference section in the upper member of the Laguna Formation that includes the uppermost gravel bed and part of the underlying dacite unit (the lower member is not represented at this exposure) is located south of Oroville and is described below:

Reference section location: Site 2 of figures 2 and 5. Composite section includes roadcut in Ophir Road (north face), southeast sideslope of the adjacent hill where we cut back the surface soil to expose sediments, the Western Pacific Railroad cut, and exposures in Baggett-Palermo Road, NE $\frac{1}{4}$ sec. 31, and SE $\frac{1}{4}$ SE $\frac{1}{4}$ sec. 30, T. 19 N., R. 4 E., Palermo 7.5-minute quadrangle.

Top of the uppermost gravel bed in roadcut is at approximately 275 ft (85 m) in elevation. The surface is somewhat stripped and only the hardpan (silica-cemented duripan of pedogenic origin) remains from what was probably a Redding series (*Abrupt Durixeralfs*) soil profile. The central part of the section is poorly exposed on the side hill and descriptions are brief and approximate.

Approximate
thickness (m)

Laguna Formation:

Upper Member:

14. Coarse mixed gravel, channeled into underlying beds; subrounded to rounded gravel in a coarse reddish sand matrix; cobbles average 10 to 15 cm in diameter but cobbles up to 40 cm are common; bears remnants of a soil profile with a duripan; basal contact quite flat with less than 1 m of relief	2-3
13. Fine sandy sediment, thin-bedded; weathered buff to brown	1.5
12. Coarse sand, thin- to medium-bedded; fills a distinct channel cut into underlying sediments; neutral gray in color; channel approximately 6-8 m wide	0-1.5
11. Fine sand, as in bed 13; weathered buff	~1
10. Paleosol formed in fine silty sediments; strong brown to reddish-brown color; silty clay loam texture; fine and medium angular blocky structure; moderately thick patchy clay films coating ped; former argillic horizon with A horizon apparently removed by erosion; sharp upper contact, wavy, gradual lower boundary; paleosol appears to dip slightly to the west	1
9. Silty fine sand; thin- to medium-bedded; weathered brown	1.5
8. Slightly gravelly sand; medium sand at base with a few fine, subrounded gravel clasts; grades upward to fine sand and silty fine sand; weathered brown to buff	2
7. Silt, with very fine sand; thinly bedded; weathered chocolate brown; tuffaceous appearance, fine white (1 mm) pumice(?) fragments; root casts and animal burrows(?); section poorly exposed on sideslope; cobbly lag gravel mantles lower hillslope and flat area near intersection of road	~3.5
6. Silty fine sand and sand; thin to medium bedded; weathered gray to brown	3
5. Dense silt; thin bedded to very thin bedded; buff to gray; tuffaceous(?)	1
4. Sand; medium to coarse; in trough crossbed sets with amplitudes approximately 2 m; interbedded tight-packed tuffaceous(?) silt is draped over crossbeds; sand may have a component of blue lithic volcanic fragments; thin lenses of fine gravel also interbedded; individual bodies of sand are lens shaped but the unit persists laterally; sand-size weathered dacite(?) in silts	~3-4
3. Mixed coarse gravel; massive; coarse sand matrix; with a few sand lenses; gravel subrounded	4
Unconformity.	
Dacite unit:	
2. Fine sand; tuffaceous; contains lithic fragments of dacite; weathered gray to buff	2
1. Medium sand; tuffaceous; contains angular quartz, and euhedral hornblende and biotite, lithic fragments of dacite, and a few dacite pebbles; weathered medium gray	2
Total thickness	29-31

This sequence of beds in the upper member appears to have been deposited in a meandering-river environment much like that of the modern Feather River. From the foregoing description it would appear that unit 3 is a channel-lag gravel, units 4 through 6 are point bar deposits, and unit 7 is an overbank silt of vertical accretion. At the Highway 70 cut 1.5 km to the west, units 1 through 7 appear to be present, but above unit 7 is a thick gravel that may be the base of a new fill sequence.

The thickness of the upper member varies. In the Thermalito Power Canal the upper member is represented solely by the uppermost gravel unit, with a single deeper channel beneath it at one point along the exposure. At this site, the upper member was deposited on an erosional surface cut into the underlying dacite unit. Here the total thickness varies from 9 to 15 m, and the basal elevation of the upper member is approximately 260 ft (80 m). Along the present Feather River 1.5 km south, gravel deposits belonging to the upper member are at least 30 m thick in a channel that was cut much deeper into underlying rocks than at the Thermalito Canal. In the subsurface due west of Oroville, along Highway 99, the section that we attribute to the upper member is approximately 23 m thick. The deposits on the Yuba were not as closely studied, but sediments of the upper member in the prominent terrace outliers are approximately 15 to 21 m thick.

Lower Member

East of Oroville, the lower member of the Laguna was deposited unconformably on surfaces eroded into Jurassic bedrock and into the dacite unit. The fan-shaped flood plain of the lower member of the Laguna issued from an apex centered near Sycamore Hill (NW $\frac{1}{4}$ sec. 3, T. 19 N., R. 3 E., Oroville 7.5-minute quadrangle) at an elevation of approximately 500 ft (150 m). The ancestral Feather River apparently flowed to the southwest or south, because south-trending remnants of the lower member cap the bedrock ridge that lies to the east of Oroville and Palermo and continue south to Honcut Creek (fig. 2).

Along the ancestral Yuba River the lower member of the Laguna Formation was also deposited unconformably over the dacite unit and older rocks. Beds of gravel and sand that contain the Nomlaki Tuff Member overlie thin remnants of a dacitic mudflow and also overlie bedrock in a series of exposures along the Smartsville Road (SE $\frac{1}{4}$ sec. 3, T. 15 N., R. 5 E., Browns Valley 7.5-minute quadrangle). The ancestral Yuba River appears to have been flowing to the west at this time.

The lower member consists of fluvially deposited gravel, sand, and silt of mixed lithology and mineralogy. The gravel contains several rock types including common clasts of blue silicic metamorphic rocks and white quartzite and several different types of metavolcanic rock, including

a pale-greenish-white felsic metavolcanic(?) rock that is commonly very highly weathered. Metasedimentary rocks locally dominate metavolcanic rocks in the cobbles by 2 or 3 to 1. Volcanic rocks—andesite, basaltic andesite, basalt, and dacite—make up less than 20 percent of the gravel. Tonalite or granodiorite usually makes up less than 5 percent of the gravel. Gravel exposed near the base of the section contains as much as 20 percent dacite blocks, indicating that the dacite was reworked into basal sediment of the lower member of the Laguna at the contact (for example, an exposure 150 m west of the intersection of Foothill Boulevard and Olive Highway, SW $\frac{1}{4}$ sec. 16, T. 19 N., R. 4 E., Palermo and Oroville 7.5-minute quadrangles). Gravel higher in the section includes less than 1 percent dacite cobbles.

Gravel and cobbles are subrounded or rounded and, east of Oroville, nearer the ancestral mountain front, they average 10 to 15 cm in diameter. The largest are about 30 cm in diameter. Gravel of the lower member is fresh or highly weathered, with the more weathered gravel generally nearer the original upper surface of the deposit. Clasts of granite are weathered in place to grus, although the biotite in them appears unaltered. Metavolcanic and volcanic gravel can be quite weathered and commonly respond with a dull thud when struck. Clasts of siliceous metamorphic rocks are fresh.

Sand of the lower member is dominated by quartz and feldspar, with a large component of lithic grains derived from all of the rock types also represented in the gravel. Sand tends to be coarse, subrounded, and like the gravel, highly weathered. Sand of the lower member can generally be crushed to a powder in the hand. The lower member of the Laguna is not well exposed. No reference section is designated, but some of the best exposures of the lower member can be seen at several sites in secs. 10, 15, and 16, T. 19 N., R. 4 E. Remnants of the lower member of the Laguna Formation east of Oroville and extending south toward Honcut Creek are dominated by coarse gravel to cobble conglomerate with a few lenticular sandy beds. These coarse conglomerate beds occur near the postulated apex of the fan-shaped flood plain at the mouth of the ancestral canyon. West of Oroville, in the subsurface at greater distance from the apex, the deposit consists of 17 m of basal fine gravel and fine gravelly sand overlain by stratified silt and silty clay (California Department of Water Resources drill record 79-107A).

As we have represented them, all of the conglomerate deposits at higher elevations in the eastern part of the project area are included in the lower member of the Laguna Formation. These include the deposits near the town of Bangor at elevations up to 960 ft (290 m). The conglomerate that trends west from Bangor appears to have occupied an ancestral channel of the North Fork of Honcut Creek. The composition of this gravel is mixed and includes

metasedimentary, metavolcanic, volcanic, and granitic rocks. Cobbles here are as much as 80 cm in diameter and are well rounded but poorly sorted. The lithology is similar to other deposits of the lower member of the Laguna and unlike the older Tertiary auriferous gravels, which tend to be dominated by chert, quartzite, and(or) volcanic rocks. The channel fill appears to be as much as 80 m thick, although this may be an overestimate because the cobbles may be mantling erosional sideslopes. Although the deposit is deeply eroded, reconstruction of the original surface of the deposit shows it to be roughly continuous with the more extensive remnants of the lower member 3 to 5 km to the west. Because of similar cobble lithologies and the reconstructed surface extent, this deposit has been included with the lower member of the Laguna. It is conceivable that it represents deposition over an extended period from early Miocene(?) time to Laguna time. No definitive evidence is available on the age of these high gravels.

The most extensive area of conglomerate in the lower member of the Laguna lies south and west of the town of Wyandotte at elevations averaging 500 to 600 ft (150–180 m). These exposures are generally bounded on the west and separated from the Sacramento Valley by a north-south-trending bedrock ridge, and bounded on the east by the canyons of North Honcut and Fine Gold Creeks. These exposures of conglomerate are grouped with the lower member of the Laguna Formation for several reasons. First, the dissected topography is strikingly similar to that underlain by the lower member of the Laguna Formation east of Oroville that contains the Nomlaki Tuff Member. The deposits in question are in fact laterally continuous with the lower member east of Oroville. The elevations of both the basal contact and the reconstructed upper surface of the deposit are essentially the same as corresponding surfaces of the lower member of the Laguna. In addition, the highest hilltops of the deposit display the striking soil profile that we associate with relict surfaces of the lower member of the Laguna Formation. The deposits near Wyandotte may overlie remnants of older gravel deposits, and along North Honcut and Fine Gold creeks the gravel deposits may include younger fills of gravel inset into the main deposit. It is thus possible that the deposit may be more diverse in age and origin than we have shown in the correlation of map units (fig. 2).

The thickness of the lower member of the Laguna can be estimated from topographic maps and drill logs. In the foothill area east of Oroville, the base of the lower member may be as low as 450 ft (135 m): an exposure on Oro-Dam Boulevard (200 m north-northwest of the center sec. 10, T. 19 N., R. 4 E., Oroville 7.5-minute quadrangle) contains basal gravel of the lower member in a channel cut into metamorphic bedrock. At other locations in the area, the basal contact is at elevations of 400 to 500 ft (120 to 150 m) and either gravel or the Nomlaki Tuff Member locally forms the basal part of the lower member. At the east corner SW $\frac{1}{4}$

sec. 4, T. 19 N., R. 4 E. (Oroville 7.5-minute quadrangle) just off Long Bar Road, the Nomlaki Tuff Member lies directly on metamorphic bedrock at an elevation of 450 ft (135 m); on Meadowview Road (site 3 of figs. 2 and 5, NW $\frac{1}{4}$ NE $\frac{1}{4}$ sec. 15, T. 19 N., R. 4 E., Oroville 7.5-minute quadrangle) the Nomlaki Tuff Member lies on a transition zone of reworked dacitic sediments above dacite lahars. The highest hilltops associated with the lower member are at an elevation of 600 ft (180 m). Thus, while the maximum thickness may be 60 m in the area east of Oroville, 45 m is probably the average thickness. Similar thicknesses occur to the south in the Wyandotte area. In the subsurface 13 km due west of Oroville, sediments that we interpret as within the lower member have a preserved thickness of 26 m. In contrast, only 15 to 18 m of sediment of the lower member is preserved on Honcut Creek where it overlies dacitic sediments (possibly reworked). The lower member does appear to thicken substantially to the west. The thickness of the lower unit on the Yuba River is difficult to estimate, but from limited surface exposures, it appears to be 7 to 12 m in the vicinity of Beale Air Force Base where an unknown thickness has been removed by erosion.

Nomlaki Tuff Member

A widespread time-stratigraphic marker, the Nomlaki Tuff Member occurs at or near the base of the lower member of the Laguna Formation. Positive correlation was made by Andrei Sarna-Wojcicki (oral commun. 1980) of the U.S. Geological Survey from samples collected east of Oroville during fieldwork following the 1975 Oroville earthquake. He also identified bedded ash collected in a roadcut along Smartsville Road south of the Yuba River as correlative with the Nomlaki Tuff Member (NE $\frac{1}{4}$ sec. 8, T. 15 N., R. 5 E., Browns Valley 7.5-minute quadrangle).

The Nomlaki Tuff Member exposed in the area is a fluviially derived, crystal vitric tuff interbedded with layers containing abundant, subrounded pumice pebbles that range in size from 0.5 to 5 cm. The pumice pebbles are composed of vesicular, transparent to white glass that contains angular and euhedral quartz, feldspar, hornblende, and orthopyroxene(?). Individual tuff beds are thinly bedded (3 to 10 cm) in alternating layers of tuffaceous sand, silt, and pumice-pebble sand. The sand is flat bedded and crossbedded; silt is finely laminated. Beds of the tuff are neutral gray, chalky white, or pale tan in outcrop.

Creely (1965, p. 64–66) included a very complete description of the Nomlaki Tuff Member from similar outcrops. Although he stated that the tuff was probably similar in source and age to the Nomlaki, he stopped short of making the direct correlation and called it instead the “unnamed rhyolitic pumice tuff,” placing it at the same position as the Nomlaki Tuff Member in his stratigraphic correlation table. Creely measured the refractive index of glass from the Oroville exposures and obtained values of

1.500 to 1.511 ± 0.003 , indicating a silica content of 67 to 69 percent and a rhyodacitic composition (1965, p. 65). These values are very close to those of 1.500 to 1.502 ± 0.001 measured by Sarna-Wojcicki (1976, p. 13) on glass from the Nomlaki Tuff Member of the Tehama Formation.

The Nomlaki appears to lie at or near the base of the lower member of the Laguna. At Meadowview Road (site 3 of figs. 2 and 5, NW $\frac{1}{4}$ NE $\frac{1}{4}$ sec. 15, T. 19 N., R. 4 E., Oroville 7.5-minute quadrangle) at an elevation of 500 ft (150 m), the Nomlaki Tuff Member lies on dacitic sediments of the dacite unit with an apparent gradational contact. One kilometer to the north, at an elevation of 450 ft (135 m), gravel of the lower member of the Laguna rests directly on metamorphic bedrock. The Nomlaki Tuff Member appears to be underlain locally by mixed gravel. The lithologic similarity between, and the stratigraphic association of, the Nomlaki Tuff Member and the dacite unit draws attention to the possibility that they are different phases of the same eruptive cycle.

Post-Laguna, Pre-Riverbank Erosion

The complex of erosional surfaces cut into the Laguna Formation near Oroville, and especially those cut into the upper member of the Laguna Formation, are important to the interpretation and regional correlation of deposits. These high terrace surfaces present a strikingly stepped appearance, particularly southwest of Oroville. It is difficult, however, to identify corresponding surfaces across the Feather River and to the south along the margin of the valley, because they generally have different slopes and elevations and are not as clearly expressed. For example, on the south side of the Feather River (secs. 29, 31, T. 19 N., R. 4 E., and sec. 36, T. 19 N., R. 3 E., Palermo 7.5-minute quadrangle), the uppermost gravel bed of the upper member of the Laguna has a reconstructed slope of 9–11 m/km (fig. 4A), based on a N. 20° W. strike, and a maximum elevation of 346 ft (105 m). Corresponding remnants, on strike to the north of the Feather River, have a slope of approximately 5 m/km and rise to barely 300 ft (90 m) in elevation. The stepped appearance, particularly southwest of Oroville, led Lindgren (1911) and geologists from the Division of Mines and Geology (Sherburne and Hauge, 1975) to postulate that the high terrace surfaces represent as many as four separate inset alluvial fills (within our Laguna Formation). We found no evidence for multiple inset alluvial fills corresponding to these geomorphic surfaces. Our interpretation, as described here and below, involves tectonically related erosional dissection of the Laguna Formation in post-Laguna but pre-Riverbank time that exhumed the buried surface and the buried paleosol on the lower member of the Laguna.

At least two major erosional surfaces were cut into the deposits of the Laguna Formation between deposition of the

uppermost gravel bed of the upper member of the Laguna and the deposition of the Riverbank Formation (fig. 4A). These erosional features predate and do not include incision that immediately preceded deposition of the Riverbank Formation. The older of the two erosional events resulted in the shaping of the major surface of the Thermalito area west of Oroville. Remnants of the resulting surface are also visible as a 200-ft-elevation (60 m) surface on Highway 70 southwest of Oroville (secs. 35 and 36, T. 19 N., R. 3 E. and sec. 1, T. 18 N., R. 3 E., Palermo 7.5-minute quadrangle). North of Oroville, the elevation of this surface is approximately 260 ft (80 m), and it decreases to the west-southwest with a slope of about 5 m/km. The most widespread average elevation for this erosional surface in the Thermalito area is about 200 ft (60 m). For example, the Oroville airport is on this surface. In part, the elevation of this surface is controlled by resistant units such as gravel beds within the Laguna. The surface, where cut in nongravely sediments, appears to be strictly erosional; where cut in gravelly beds, such as the uppermost gravel bed, the erosional surface is mantled by a lag of gravel as much as several meters thick. This appears to be the case in sec. 36, T. 19 N., R. 3 E. where a large erosional surface at approximately 200 ft (60 m) in elevation is mantled by a lag of gravel derived from the uppermost gravel bed. We cannot definitely associate any thicker, more continuous deposits with this erosional surface, although exposure is poor.

The second and younger surface is prominent at an elevation of approximately 160 ft (50 m) between Oak Grove and Palermo (fig. 2), and as a series of outliers that crop out south to Honcut Creek. This erosional episode exhumed at least part of the lower member of the Laguna Formation and its buried soil, and consequently, the surface displays a soil profile that in places is much more strongly developed than soils on topographically higher surfaces. The soil profile that exists on this exhumed surface in the lower member of the Laguna may be the net result of two periods of soil formation, one before burial by the upper member and the other after exhumation. We have not found evidence of alluvial fills on this geomorphic surface that are equivalent in age to the erosional episode.

Soil Landscapes

The great age and complex erosional and depositional history of the Laguna Formation produced a large array of different soils on various parts of the formation. Few remnant surfaces exist on the uppermost gravel bed of the upper member of the Laguna, and no soil was sampled from this surface for the chronosequence study. The soils found on little-eroded parts of the uppermost gravel bed of the upper member are commonly quite strong representatives of the Redding series (*Abruptic Durixeralfs*) or those of the Red Bluff series (*Ultic Palixeralfs*). The Redding soils have

yellowish-red (5YR 5/6D) very gravelly loam A horizons, and red (2.5YR 4/6D) gravelly clay Bt horizons at depths of 0.5 to 1 m that overlie reddish-brown or yellowish-red (5YR 4/4 or 5/6D) strongly cemented iron-silica duripans 1 to 1.5 m thick. Sediments beneath the soils are weathered and red gravelly clay loams to a depth of 4 to 5 m. A particularly complete example of the Redding soil on the uppermost gravel bed occurs on the south side of the Thermalito Canal 300 m east of Cherokee Bridge in the SW $\frac{1}{4}$ sec. 5, T. 19 N., R. 4 E. (Oroville 7.5-minute quadrangle). Most of the surfaces of the uppermost gravel bed have been stripped to the duripan of the Redding soil. A good example of this is displayed south of Oroville at the 283-ft (85 m) hill in the NE $\frac{1}{4}$ sec. 31, T. 19 N., R. 4 E. (Palermo 7.5-minute quadrangle).

Multiple erosional surfaces descend from the highest remnants of the upper member of the Laguna Formation. Flat and rolling erosional surfaces cut at elevations below the uppermost gravel bed have Redding and *Corning* series (*Typic Palexeralfs*) soils. Extensive examples of this soil landscape surround the Oroville airport and the Thermalito Afterbay area. A well-developed mound and swale microrelief exists in areas of the Redding soils. Soils on steeper sideslopes in mixed materials of the upper member of the Laguna Formation have been mapped as the less strongly developed *Cometa* series (*Typic Palexeralfs*). The *Agate variant* (*Typic Durochrepts*) has also been mapped on steep sideslopes. Erosional sideslopes underlain by finer materials bear soils of the *Altamont* series (*Typic Chromoxererts*). In Yuba County, the *Burriss* series (*Chromic Pelloxererts*) has been mapped on colluvial sideslopes and toeslopes of the Laguna Formation.

Well-preserved, never-buried remnants of the soil originally formed on the lower member of the Laguna Formation are rare. We have informally named this soil the *Red Bluff strong variant* (*Palexerults*). Most commonly the profile of this soil has been partially eroded, but the near-total weathering of nonsiliceous clasts, 10R color hues, the presence of red and pinkish-gray to white reticulate mottling, and the great depth of soil formation serve to identify this soil. Over broad areas east of Palermo and Oroville, erosional surfaces are cut deeply into the lower member of the Laguna Formation and brown, gravelly, *Newville variant* soils (*Typic Haploxeralfs*) have formed. These soils have formed in the colluvial mantle of the erosional sideslopes. On Lower Wyandotte Road in the SW $\frac{1}{4}$ sec. 35, T. 19 N., R. 4 E. (Bangor 7.5-minute quadrangle), a roadcut exposes a deeply eroded remnant of the Red Bluff strong variant soil. As much as 5 m of the upper profile has been removed by erosion at this site. The modern rolling hillslopes very obviously truncate this extreme soil profile, and the sideslopes are mantled by colluvium on which the *Newville variant* soil has formed.

Exhumed remnants of the lower member of the Laguna bear a variety of soils. Most commonly, strong variants of

the Redding series or of the *Corning* series cap the exhumed surfaces, and these older soils may be partially truncated by the present-day topography. Because of ongoing erosion, the older soils show a range in the thickness and completeness of the upper profile, but the 10R color hues, great depth of soil formation, and extreme weathering of cobbles are diagnostic.

Less commonly, exhumed remnants of the lower member of the Laguna bear the complete Red Bluff strong variant soil profile that is very similar to the soil profile found on parts of the lower member of the Laguna that were never buried. These soils apparently underwent little erosion of their deep soil profile prior to burial by alluvium of the upper member of the Laguna Formation, and soil formation resumed after re-exposure in pre-Riverbank time. This is the case on Honcut Creek at the site sampled for the chronosequence study. Here the soils have reddish-brown (2.5YR 4/4D) loam A horizons over dark-red (10R 3/6D), clay argillic (Bt) horizons that begin at about 0.4 to 0.6 m and extend to a depth of almost 3 m. Pale-white and dark-red reticulate mottling is conspicuous near the base of the Bt horizons and extends to more than 5 m in BCt horizons. Total depth of weathering of this ancient soil may exceed 10 m.

Geochronology and Correlation

The paleomagnetic stratigraphy of the Laguna Formation and the dacite unit, and radiometric ages of the Nomlaki Tuff Member and dacite unit, allow us to correlate the Laguna Formation in this area with the Laguna Formation in its type location and to estimate the age of the formation. The most complete section sampled for magnetic polarity zonation extended through 30 m of sediments at the reference section described above for the upper member of the Laguna (site 2); 29 samples were collected at approximately 1-m intervals. In addition, the magnetic polarity of the Nomlaki Tuff Member was measured at two sites (sites 3 and 4 of figs. 2 and 5). Six samples of the Nomlaki Tuff Member from two separate exposures yielded reverse polarities with strong magnetizations. The radiometric age of the Nomlaki, using the new decay constant, is 3.4 m.y. This age corresponds to the end of the Gilbert Reversed-Polarity Chron. The paleomagnetic and radiometric ages are consistent. The Nomlaki appears to lie at or near the base of the lower member of the Laguna Formation. The base of the lower member, therefore, is less than 3.4 Ma, but the age of the upper part is not known directly.

Radiometric dating of the blocks of dacite within a lahar in the dacite unit gave ages that range from 2.8 to 3.4 Ma (supp. table 9). The dacite unit underlies the Nomlaki, therefore these dates and the age of the Nomlaki Tuff Member are reversed compared to their stratigraphic sequence. The analytical uncertainty associated with the dates

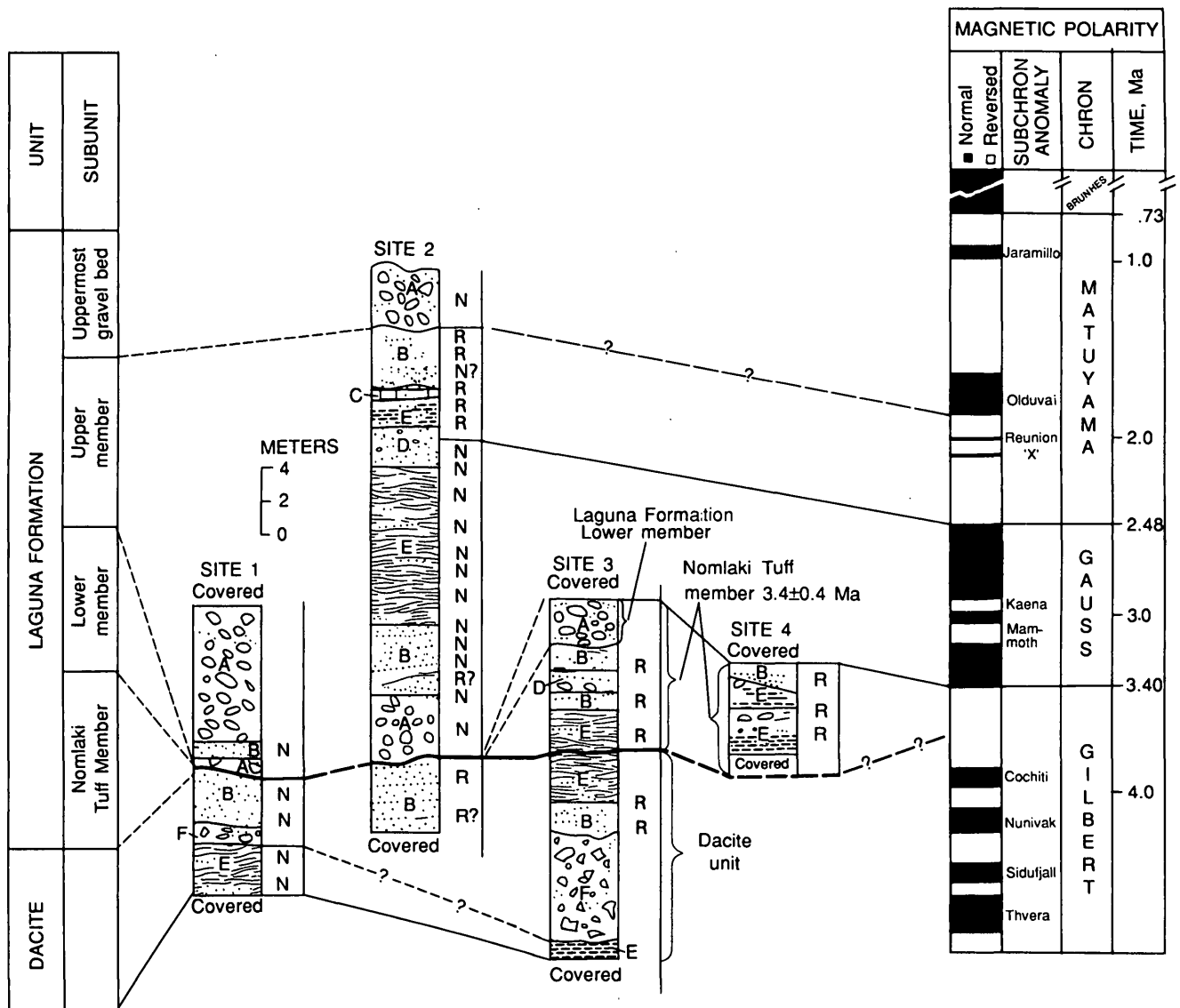


Figure 5. Correlation of samples with an established magnetic polarity time scale (Mankinen and Dalrymple, 1979) for site 1, Feather River; site 2, Western Pacific Railroad; site 3, Meadowview Road; site 4, Wyandotte Road. Normal (N) and reverse (R) magnetic polarity of samples is shown on right side of sections. See figure 2 for locations; see text for interpretation.

for the two units overlap, however, so the ages are statistically indistinguishable.

The magnetic polarity of the upper member of the Laguna at the reference location is normal in the lower two-thirds of the section (units 3 through 8 of the description) to a point 2 m below the buried paleosol, and reversed from there to the base of the uppermost gravel bed (fig. 5). A coarse channel fill within the reversed zone (unit 12) has a questionable normal polarity, possibly indicating a brief polarity event. A single sample from a sand lens within the uppermost gravel bed also yields a questionable normal polarity. We know that this section is younger than the lower member of the Laguna, which in turn is younger than 3.4 Ma. The strength of development of the soil formed on the lower member of the Laguna where buried by the upper member, or where exhumed, argues for a long period of time between deposition of the two members. Even with the effect of a wetter Pliocene climate the time must have been 0.5 million years or more.

Based on these considerations, we associate the normal-to-reversed transition in the upper member with the normal-to-reversed boundary between the Gauss Normal-Polarity and Matuyama Reversed-Polarity Chrons. This boundary is presently dated at 2.48 Ma (Mankinen and Dalrymple, 1979). If this correlation is correct, then the normally polarized channel fill in the upper reversed zone might represent the Reunion Normal-Polarity Subchron or "X" polarity event at about 2 to 2.1 Ma. Furthermore, if the uppermost gravel bed of the upper member of the Laguna is normally magnetized, as is suggested by our single measurement, it may have been deposited during the Olduvai Normal-Polarity Subchron or possibly during the Jaramillo Normal-Polarity Subchron presently dated at about 1.75 and 0.9 Ma, respectively.

Harwood and others (1981) reported bracketing ages of 0.45 and 1.1 Ma for a gravel deposit along the front of the Chico monocline that they correlated with the Red Bluff Formation. Helley and Harwood (1985), in a regional map of Tertiary and Quaternary deposits, correlated the uppermost gravel bed of the upper member of the Laguna in the Feather River area with the Red Bluff Formation. This correlation, and an age of 0.45 to 1.1 Ma for the uppermost gravel bed of the Laguna, is not precluded by the evidence we present. We favor instead the interpretation that the uppermost gravel bed was deposited during the Olduvai and thus has an age of about 1.75 Ma, because 1.4 million years or more (2.48 minus 1.1) seems an excessive period of time to deposit the upper few meters of the upper member of the Laguna Formation.

We correlate the two alluvial members of the Laguna Formation in the Feather-Yuba Rivers area with the two members of the Laguna that were recognized by Marchand and Allwardt (1981) in the San Joaquin Valley. Our correlation is provisional but is based on similarities in geomorphic expression, radiometric ages, and magnetic polarity zonation in the units in the two areas: Marchand

and Allwardt (1981) recognized an unconformable contact separating two units of the Laguna in the Merced River area by the presence of a strongly developed buried soil on the surface of the older unit. The deposits of the Laguna Formation are the oldest nonvolcanic alluvial units in both areas; they present the most highly elevated and dissected remnants of mixed alluvium in both areas. In the Kings River area of the southern San Joaquin Valley, gravel deposits correlated with the Laguna by Marchand and Allwardt (1981) contain clasts of a basalt with a K-Ar age of 3.76 ± 0.08 Ma. Marchand and Allwardt (1981) also reported, from preliminary paleomagnetic studies of the Laguna, that the lower unit is magnetically reversed and the upper unit is normal, and they suggested that the boundary between the two might correlate with the Gilbert-Gauss boundary at 3.4 Ma (Mankinen and Dalrymple, 1979).

A preliminary study of paleomagnetic zonation in the Laguna Formation in a series of roadcuts near Sloughouse in Sacramento County showed that the upper part of the section had reverse polarity, while the thicker, lower part displayed normal polarity (R.J. Shlemon, oral commun., 1981). This suggests that the reference section of the upper member at Oroville and the section in Sacramento County are correlative, but such a correlation does not place direct time limits on the units.

Our best estimate of the ages of the Laguna Formation at Oroville, based on tephrochronology, paleomagnetic stratigraphy, and soil development, are: deposition of the lower member of the Laguna from about 3.4(?) to 3.2 Ma; deposition of the upper member, possibly beginning about 2.6 Ma and concluding with deposition of the uppermost gravel bed about 1.7 Ma or possibly 0.9 Ma.

The Laguna Formation as described near the Feather River thus is broadly coeval with the Tehama Formation (Russell, 1931) and possibly the Red Bluff Formation, both of which occur extensively along the west side of the Sacramento Valley. The Tehama, as the Laguna described here, contains the Nomlaki Tuff Member near its base, but the age of the upper part of the Tehama is not known. No major hiatus is recognized within the Tehama. The similarity of time of inception of these major alluvial deposits (Tehama and Laguna) suggests a synchronous regional control on deposition, probably either climatic or tectonic. We favor the concept of tectonic control of the initiation of the major alluviation in the Sacramento Valley.

In our interpretation, the geomorphic surfaces below the uppermost gravel bed of the upper member of the Laguna are primarily erosional, not depositional features. These surfaces may be coeval with the Arroyo Seco Gravel and "gravels of uncertain age" (Gale and others, 1939) in the American-Mokelumne Rivers area. Gale described the Arroyo Seco as a series of erosional surfaces cut into the Laguna Formation and veneered with pedimentlike gravel. Shlemon (1967a, b; 1972) disagreed with Gale's interpretation of the Arroyo Seco and stated instead that the Arroyo Seco surfaces in the American River area are actually a

flight of terraces underlain by distinct alluvial deposits younger than, and cut into, the Laguna Formation. The most recent mapping of Quaternary deposits in the American River area, by Helley (1979), follows Gale's interpretation once again, and the Arroyo Seco is shown as one or more erosional surfaces cut into the Laguna Formation.

One of the two erosional surfaces that we recognize here might also be coeval with the Red Bluff Formation, which has been extended into the Chico area by Harwood and others (1981), and which is now bracketed by radiometric ages of 0.45 and 1.1 Ma.⁵ The erosional surface(s) may also be coeval with the North Merced Gravel recognized in the northeastern San Joaquin Valley (Marchand and Allwardt, 1981).

The Turlock Lake Formation and the Fair Oaks Formation (partially equivalent) (Marchand and Allwardt, 1981; Shlemon, 1967a, b) are major deposits of middle Pleistocene age in the northeastern San Joaquin Valley that lie in the stratigraphic interval between the Laguna and Riverbank formations. We have not recognized any extensive depositional units equivalent to the Turlock Lake or Fair Oaks Formations in the Feather-Yuba Rivers area.

Dacite Unit

A sequence of dacitic lahars interstratified with related volcanoclastic sediments underlie the alluvial terrace deposits throughout much of the project area. Although this unit is distinctive and widespread in the project area, it has not been recognized north of Oroville near Table Mountain, nor south of the Bear River (the next drainage south of the Yuba River). The unit is generally poorly exposed; it crops out in a few places in the foothills east and northeast of Oroville and in exposures near channel level on the Feather River, Wyandotte Creek, Honcut Creek, and the Yuba River. It has been penetrated by many research and test wells drilled by the California Department of Water Resources in the Oroville area, and it also appears in artificial exposures such as the Thermalito Power Canal.

The dacite unit has been recognized by earlier workers, albeit with different extents and interpretations. Lindgren's (1911) "Tuffs of Oroville" appear to have included the dacite unit and a part of the alluvial sediments that we correlate with the Laguna Formation. Creely (1965) grouped andesitic mudflows and conglomerates that lie beneath the Lovejoy Basalt with the dacite unit, and he provisionally correlated all of these with the Miocene and Pliocene Mehrten Formation (he used the term Mehrten(?) Formation). Dalrymple (1964) reported a K-Ar age of 23.8 Ma from a tuff bed within the andesitic conglomerates beneath the Lovejoy Basalt, and this age has been assumed

by more recent workers to apply to the dacite unit as well as the andesites. Excavation of the Thermalito Power Canal north of Oroville in the 1960's exposed a thick section in the dacite unit. Geologists from the California Department of Water Resources referred to these rocks as "unnamed Upper Pliocene(?) volcanic sediments" in early reports (California Department of Water Resources, 1968), but in later reports they adopted Creely's correlation of the dacite unit as part of the Mehrten(?) Formation.

Evidence gathered by Busacca (1982) and summarized here demonstrates that the dacite unit is not related to the andesitic Mehrten(?) Formation of Creely, which indeed lies beneath the Lovejoy Basalt, but that instead it is a separate, younger volcanoclastic deposit. The reinterpretation is based on topographic, stratigraphic, lithologic, and radiometric evidence. The term dacite has been applied to these rocks based on elemental composition and mineralogy. Two blocks of the dacite have whole-rock compositions of about 60 percent SiO₂, 16.5 percent Al₂O₃, 3 percent each Na₂O and MgO, 1.5 percent K₂O, 5.5 percent CaO, and 6 percent total Fe as Fe₂O₃. Plagioclase, hornblende, and biotite are the dominant minerals seen in hand specimen and thin section. Quartz and pyroxene are not in the rock.

The dacite unit crops out at elevations of 300 to 500 ft (90 to 150 m) in the hills east and northeast of Oroville. This contrasts strongly with the Mehrten(?) Formation under the Lovejoy Basalt (Oroville Table Mountain), which crops out at elevations of 850 to 950 ft (260 to 290 m) projected along a strike of N. 20° W. (regional tilt axis). Similarly, exposures of the dacite in the Thermalito Power Canal are at elevations of 225 to 300 ft (70 to 90 m), while 2.5 km to the north along the regional strike the Mehrten(?) Formation crops out under Table Mountain at 600 to 650 ft (180 to 200 m). If the dacite unit and Mehrten(?) Formation are part of the same deposit, two parallel paleovalleys would have had to exist less than 3 to 5 km apart, but with 350 to 500 ft (110 to 150 m) of elevation difference at comparable points along their length. This situation is not impossible in itself; what is improbable is that, subsequent to deposition of the dacite and valley filling, the higher valley then filled with lavas of the Lovejoy Basalt while the lower valley did not.

The slope of the Mehrten(?) Formation and that of the dacite unit are markedly different. The base of the Mehrten(?) Formation beneath South Table Mountain has a slope of 29 to 33 m/km; that of the lahar unit of the dacite unit averages 4.6 to 17 m/km. While these slopes probably have been affected by local tectonics, the dominant effect is the regional tilting of the Sierra, and the difference indicates a significant difference in age between the two.

Although the Mehrten(?) Formation under South Table Mountain is at a higher elevation than the dacite unit, it has a much greater slope. At about the position of the Campbell Hills (fig. 1), the tops of the two units are at nearly equal elevations. Farther to the southwest, in the subsurface, the

⁵ In Helley and Harwood (1985), the uppermost gravel bed of the upper member of the Laguna, as described here, was correlated with the Red Bluff Formation. This is not precluded by the evidence we present, but our interpretation differs from that of Helley.

tops of the two units converge and then cross over in relative elevation.

We studied contact and stratigraphic relations of the dacite to underlying and overlying units in the Thermalito Power Canal and at other outcrops in the project area. In the Thermalito Power Canal, the dacite unit unconformably overlies gravel that is dominated by clasts of Lovejoy Basalt. This is the only known location where the base of the dacitic section is exposed. The basal contact is relatively smooth over the length of the 600-m exposure. The upper contact of the dacite unit is unconformable with overlying sand and gravel of the Laguna Formation. At the east end of the Thermalito Canal a channel-fill deposit of mixed gravel of the Laguna Formation is cut almost 9 m into dacitic sediments. At other locations, such as at Meadowview Road east of Oroville (site 3 of figs. 2 and 5, NW $\frac{1}{4}$ NE $\frac{1}{4}$ sec. 15, T. 19 N., R. 4 E., Oroville 7.5-minute quadrangle), the dacitic section is not well exposed but appears to grade upward into the Nomlaki Tuff Member of the Laguna Formation. At Honcut Creek there is also a mixed transition zone at the contact. There, about 2 m of dacitic sand and silt lies on metavolcanic bedrock in the creek bottom (N $\frac{1}{2}$ sec. 23, T. 17 N., R. 4 E., Loma Rica 7.5-minute quadrangle). These deposits are overlain by a westward-thickening section of gravel and sand of the lower member of the Laguna Formation that contains an upward-decreasing percentage of dacitic pebbles and sand.

On the Yuba River, fine dacitic silt and sand is unconformably overlain by coarse gravel of the Laguna Formation. The contact is sharp, with less than 0.5 m of reworked material between units.

The dacite unit is very distinctive and recognizable in most exposures because it contrasts strongly with overlying mixed alluvial sediments. The laharic beds within this unit are light gray to medium brownish gray, massive, and compact or cemented. The matrix is poorly sorted, silty and clayey, and it contains abundant sand-size crystal, lithic, and possibly vitric fragments. Plagioclase, hornblende, and biotite are the dominant materials in the matrix. Sand- and fine-gravel-size lithic fragments derived from the dacite are ubiquitous. Blocks of subangular, blue-gray dacite that average 10 to 15 cm in diameter are set in the tuffaceous matrix of the lahar. Some outcrops of the lahar contain blocks as large as 60 cm; other outcrops, such as at the Feather River, are dominated by dacite pebbles 3 to 6 cm in size.

The most common of several textural variants of the dacite blocks in the lahars is a fine- to medium-grained, equigranular rock with euhedral biotite, subhedral hornblende, zoned plagioclase, and a small amount of glassy matrix. Other variants observed included one with elongated hornblende laths (to 2 cm), one with a frothy, vesicular, pumiceous matrix, and one with equant plagioclase crowded in a slightly glassy matrix. The most distinct feature of both the blocks of dacite and of sand-size lithic fragments in the matrix is their chalky white appearance when weathered.

The two stratigraphic sections of the dacite unit with the best exposure are described below. The second one displays a basal contact with underlying units.

Reference section location: Site 3 of figures 2 and 5. Meadowview Road exposure, begins at the intersection of Meadowview and Oro-Quincy Roads and extends eastward on Meadowview Road; NW $\frac{1}{4}$ NE $\frac{1}{4}$ sec. 15, T. 19 N., R. 4 E., Oroville 7.5-minute quadrangle.

The Nomlaki Tuff Member extends at least 3 m above roadway level at the intersection. Gravel of the lower member of the Laguna Formation overlies the Nomlaki Tuff Member and extends to the hilltop at 551 ft (168 m). Elevation of the intersection approximately 510 ft (155 m).

	<i>Approximate thickness (m)</i>
Laguna Formation:	
Nomlaki Tuff Member:	
4. Tuffaceous sand and silt; weathered neutral gray to buff; upper part more sandy; flat bedded to cross-bedded, with lenses of rounded rhyolitic pumice pebbles to 2 to 3 cm in diameter; lower part fine tuffaceous sand and silt; sediments are a mixture of vitric and crystal fragments; water laid; grades downward into silt derived from the dacite, contact not apparent	~ 5-6
Unconformity, or possible gradational contact.	
Dacite Unit:	
3. Mixed, tuffaceous sand and silt derived from dacite, weathered tan to gray; finely bedded at top; becomes coarser and more obviously derived from the dacite toward the base; coarser sand is a mixture of lithic, crystal, and vitric (?) fragments; section partially covered; abrupt contact with mudflows below	4
2. Dacite mudflow(s); unsorted, matrix-supported blocks of subangular dacite set in a matrix derived almost exclusively from dacitic material; sand and fine gravel-size lithic and crystal fragments dominate in the matrix; hard or indurated; gray to tan in color; 80-95 percent of the blocks are one of two or three slight textural variants of the dacite; blocks range in size from a few cm to more than 50 cm; dacite blocks bear euhedral hornblende and biotite.	5-7
1. Mixed, flat-bedded and crossbedded tuffaceous sand and silty sand; gray to tan; apparently derived from dacitic material; poorly exposed, base not exposed.....	2-4
Total Thickness.....	16-21

Reference section location: Thermalito Power Canal exposure; south face of the canal, east side of the Cherokee bridge; SW $\frac{1}{4}$ sec. 5, T. 19 N., R. 4 E., Oroville 7.5-minute quadrangle.

Top of bluff is approximately 305 ft (91 m).

	<i>Approximate thickness (m)</i>
Laguna Formation:	
Upper member:	
Uppermost gravel bed:	
4. Coarse, mixed, subrounded to rounded gravel in medium sand matrix; thick, red, Redding-series soil profile extends well into the gravel; basal contact is quite flat, but 600 m to the east a 10-m-thick channel fill of mixed sand and gravel is interposed between this unit and the underlying dacite unit	~3
Unconformity.	
Dacite unit:	
3. Coarse cobbly sediments composed of dacitic gravel; apparently fluvial but exposure is poor and slope has been disturbed; 80-95 percent of cobbles are composed of dacite; other volcanic rocks and siliceous metamorphic rocks compose 5-20 percent; some cobbles are of very frothy, pumiceous	

Dacite unit—*Continued*

- variant of the dacite rarely seen elsewhere; weathers to a neutral gray; dips 1° west..... 10
- 2. Top of this unit appears to be capped by a dark-brown soil profile; strongly weathered sediments are silt, clay, and sand exhibiting a variety of colors including gray, brown, yellowish brown, and tan; sand- and fine-gravel-size lithic fragments derived from the dacite throughout; a second, brown soil profile (?) occurs near the base 10

Unconformity.

New Era(?) Formation of Creely (1965):

- 1. Coarse gravel in a channel scoured into the underlying hard bedrock; clasts are subangular to sub-rounded, 10–20 cm in diameter, and composed almost wholly of basalt derived from the Lovejoy Formation 8
- Total thickness..... 31
- Paved below this point.

Along Long Bar Road, just northeast of downtown Oroville (SE¼NW¼ sec. 9, T. 19 N., R. 4 E., Oroville 7.5-minute quadrangle), sand and silt derived from the dacite is overlain by a thick lahar, which is overlain in turn by a thin section of dacitic sediments. On Linda Avenue 500 m to the east, 4 m of the mudflow unit is exposed, capped by gravel assigned to the Laguna Formation. Directly under the mudflow is a possible soil profile formed in dacitic silt. This soil profile may correlate with the upper soil in a similar stratigraphic position in the Thermalito Canal. Along the Feather River due east of Thermalito, laminated silt is overlain by a thin (2 m) mudflow(?) with small dacitic pebbles, which in turn is overlain by bedded gray dacitic sand. Exposures on Honcut Creek and the Yuba River are generally of bedded, dacitic sand and silt. On the Smartsville Road, south of the Yuba River, a thin (2 m) dacitic mudflow crops out (SE¼ sec. 3, T. 15 N., R. 5 E., Browns Valley 7.5-minute quadrangle). The dacite unit described here is thickest in the Feather or ancestral Feather River basin, is thinner to the south, and has not been recognized to the north of the Feather River. Honcut Creek, a small drainage of the middle foothill elevations, has only several meters of dacitic sediment. The undetermined source area appears to have been in the upper Feather River basin bordering the basins of the ancestral Yuba and possibly American Rivers. The stratigraphic evidence already discussed, the physical continuity with the Nomlaki Tuff Member in at least one exposure (the only exposure in the project area where the base of the Nomlaki is exposed), and gross compositional similarity between the dacite unit and the Nomlaki Tuff Member suggest that the dacite unit may represent an early eruptive phase of the Nomlaki. This hypothesis is supported by our radiometric dating and paleomagnetic stratigraphy. Whether the dacite and the Nomlaki Tuff Member were deposited in a single, continuous event or whether they were separated by a significant hiatus is not known.

The maximum exposed thickness of the dacite unit in the mapped area is 21 m in the Thermalito Power Canal. To the west, drill-hole records show a minimum thickness of 31 m in the subsurface adjacent to State Highway 99 (drill record 79–107A), but there may be a problem here with the convergence in the subsurface of the dacite unit with Creely's Mehrten(?) Formation.

Geochronology and Correlation

The age of the dacite unit can be established from stratigraphic and radiometric evidence. It is younger than the Miocene Lovejoy Basalt, because gravel derived from the Lovejoy underlies the dacite. On Meadowview Road, the dacitic section is overlain directly by the 3.4 Ma Nomlaki Tuff Member. The base of the Lovejoy Basalt on South Table Mountain is at 900 to 1,000 ft (270 to 300 m) while the base of the dacitic unit along the regional strike 2 km to the south is 225 to 300 ft (70 to 90 m). This implies a long period of erosion and canyon cutting after eruption of the basalt. By a similar argument the dacite unit could be latest Miocene or Pliocene in age because less than 10 m of erosional relief was cut into the dacite prior to the deposition of the 3.4 Ma Nomlaki Tuff Member of the Laguna Formation.

The paleomagnetic signature of fine dacitic sediments was sampled at three locations (sites 1, 2, and 3 of figs. 2 and 5). The results are of questionable magnetostratigraphic value, because only partial sections were sampled and correlation of strata between sites is speculative.

Four samples, two collected above and two below the fine gravelly dacitic lahar(?) at the Feather River site, have normal magnetic polarity. Other sites had at least one sample with reversed polarity, generally at the highest point sampled in the dacite section (in strata just below the contact with the overlying Laguna Formation). At least two buried soils were observed within the dacitic section. The presence of buried soils and the existence of both normal and reversed polarities can be taken as evidence that deposition of the dacitic sequence took place over an extended period of time, possibly several tens of thousands of years. There also may be more than one silt-lahar-silt sequence in the section.

Three dacite blocks from lahars at two locations were dated by K-Ar radiometric methods (supp. table 9). Duplicate whole-rock age determinations on one sample yield an average age of 3.2±0.1 Ma. Ages derived from hornblende and biotite mineral separates range from 2.8 to 3.4 Ma. Although these are minimum ages, the close stratigraphic association of the dacite unit with the Nomlaki Tuff Member makes it unlikely that these ages are in error by more than 50 percent. Creely (1965) correlated this dacite unit with the andesitic Mehrten(?) Formation that underlies the Lovejoy Basalt at Table Mountain. We have shown from stratigraphic, lithologic, and now radiometric evidence that these two units are not correlative. Dalrymple

(1964) dated a tuff bed within the andesitic conglomerate at Table Mountain (Mehrten(?) Formation) at 23.8 Ma. The revised stratigraphic association of the dacite unit reported above and the new radiometric ages support a middle Pliocene rather than an early Miocene age for this unit, and provides a very different and much younger bracketing age for inception of alluviation in the Feather River area.

Pre-Dacite Cenozoic Units

A series of Eocene to Miocene(?) sedimentary and volcanic units have been described by earlier workers in close proximity to the project area. To the north, in stratigraphic superposition are the Eocene Ione Formation, overlain by the Miocene Mehrten(?) Formation of Creely (1965); and by the Miocene Lovejoy Basalt that forms the prominent Table Mountain near Oroville. South of the Yuba River the pre-dacite Cenozoic units include the Oligocene(?) Reeds Creek Andesite and the Wheatland Formation of Clark and Anderson (1938).

No unequivocal exposures of the Ione Formation or Tertiary auriferous gravel were recognized in the project area, but several outcrops may represent small remnants of the Ione Formation preserved beneath younger Cenozoic cover.

Geologists from the California Department of Water Resources (1968) mapped a sequence of units within the Thermalito Power Canal exposure: the informal "Tertiary Greenstone Gravel," in channels cut into the bedrock, overlain by variegated clay and sand of the Ione Formation, in turn overlain by "unnamed Upper Pliocene(?) volcanic sediments" and capped by the "Red Bluff" Formation.

We have reinterpreted this exposure, in part on the basis of composition of their "Greenstone Gravel." The gravel is not greenstone, but is derived exclusively from the Lovejoy Basalt. In hand specimen and thin section the cobbles are indistinguishable from samples of the Lovejoy collected on nearby (but 300 m topographically higher) South Table Mountain. In thin section, the cobbles are black, microcrystalline olivine basalt containing scattered calcite-filled vesicles. A cobble of basalt collected from the deposit has 48.5 percent SiO₂, 14.5 percent Al₂O₃, 8 percent CaO, and 12.2 percent Fe₂O₃. A fresh sample of Lovejoy Basalt collected on South Table Mountain has 48.5 percent SiO₂, 14.5 percent Al₂O₃, 7.7 percent CaO, and 13.5 percent Fe₂O₃. The gravel deposit, composed of cobbles of Lovejoy Basalt, may be correlative with the New Era Formation of Creely (1965).

On this basis, the varicolored tan to yellow sand and clay that lies above the gravel, which was earlier correlated with the Ione Formation (California Department of Water Resources, 1968), cannot be that, because the Ione at Table Mountain lies stratigraphically below the Lovejoy Basalt. The variegated sediments are highly weathered and are derived from volcanic material. Exposure is poor, but these

Table 4. Comparison of stratigraphic interpretations of an exposure in the Thermalito Power Canal (south side) at Cherokee Bridge (SW¼ sec. 5, T. 19 N., R. 4 E.)

Approximate elevation of top	Approximate thickness	California Department of Water Resources (1968)	This report
305 ft	10 ft (3 m)	Red Bluff Formation	Laguna Formation
295 ft	35 ft (10 m)	Unnamed volcanic sediments	Fresh dacitic lahars and conglomerates
260 ft	35 ft (10 m)	Ione Formation	Highly weathered dacitic sediments with several buried soils
225 ft	0-30 ft (0-9 m)	Greenstone Gravel	Cobble conglomerate derived from Lovejoy Basalt
			Ione Formation (present locally in deep channels cut in bedrock)
202 ft		Bedrock series	Bedrock series
Bottom of canal, 197 ft			

sediments contain sand- and small gravel-size fragments of chalky, white, weathered dacite. We correlate these varicolored sediments with the overlying dacite unit. A comparison of old and new stratigraphic assignments is given in table 4. The presence of at least two buried soils in this lower section of the dacite suggests that deposition was intermittent over an extended period of time.

The relationships laterally along the base of the canal (now underwater) cannot be reexamined, but it is likely that some of the sediments that fill the deepest channels cut in bedrock and that were mapped as Ione are, in fact, the Ione Formation and underlie the Lovejoy Basalt gravel unit (New Era Formation?). This is indirectly suggested by the configuration of the Ione, and of the Greenstone Gravel as shown in geologic section maps of the Thermalito Canal cut (California Department of Water Resources, 1968). Strong postburial alteration by ground water may be responsible for the varicolored staining of both the deep part of the dacite unit and the Ione Formation.

The evidence presented here leads to a reassessment of the section exposed in the Thermalito Power Canal. Sedimentary rocks formerly designated as Eocene in age are here reassigned to the Pliocene based on their relationship to the gravel derived from the Lovejoy Basalt.

Deformation and Tectonism

The foothills and valley margin in the Oroville area were considered until recently to be seismically inactive, and although historic earthquakes have occurred in the surrounding region, the seismic hazards were considered minimal (California Department of Water Resources, 1979). Part of the Foothills fault system (Clark, 1960) does strike north-northwest into the area, and this includes a wide shear zone in metamorphic bedrock in the Yuba River-Browns Valley area. Mesozoic faults that separate contrasting bedrock units were recognized by Creely (1965) and confirmed in studies by the Department of Water Resources (1979). Creely concluded that the Cenozoic rocks were essentially undeformed (1965, p. 79), but he did note that a fault to the east of Oroville had offset deposits of what he called the Red Bluff Formation about 2 m down to the west.

Major late Cenozoic deformation of the Sacramento Valley has recently been documented (Harwood, 1984; Harwood and Helley, 1987). Near the project area, the Pliocene Tuscan Formation is complexly faulted and folded down to the west along the Chico monocline (Harwood and others, 1981; Harwood and Helley, 1987). The monocline extends for more than 75 km from Red Bluff to Chico. Harwood and Helley (1987) demonstrated that the monocline formed in response to movement on a deep-seated, east-dipping, high-angle reverse fault that bounds the east edge of the oceanic basement rocks underneath the Great Valley.

The Oroville earthquake of August 1, 1975, Richter magnitude 5.7, forced a rapid re-evaluation of the potential for seismic activity in the Oroville area. In studies by the California Division of Mines and Geology (Sherburne and Hauge, 1975) and the California Department of Water Resources (1979), geologists reported that the earthquake and ground rupture occurred along a previously unknown fault, which was named the Cleveland Hill fault. The Cleveland Hill fault is an en echelon segment of the longer Swain Ravine lineament fault zone. The Prairie Creek lineament fault zone runs at a slight angle to, and 3 to 6 km west of, the Swain Ravine (fig. 2). These zones trend south-southeast and converge into a single lineament that is on strike with the Bear Mountains fault zone (Clark, 1960) of the Auburn area. The Swain Ravine lineament fault zone displays evidence of late Cenozoic movement in trenches excavated for the earthquake studies. Geomorphic expression takes the form of sag ponds, aligned vegetation, and springs. The Prairie Creek lineament displays bedrock offsets, but no conclusive evidence of Cenozoic movement was found in the project area, although Cenozoic movement has been demonstrated just south of the Yuba River where the Swain Ravine and Prairie Creek zones converge (Woodward-Clyde Consultants, 1977; California Department of Water Resources, 1979). Fault-plane solutions derived from first-motion studies of the 1975 earthquake

and aftershocks yield valley-side-down normal faulting along fault planes that strike approximately N. 10° W. and dip generally about 60° west (California Department of Water Resources, 1979, chapter III). Field evidence suggests that the fault movement was oblique, with both right-lateral and normal, valley-side-down components (Sherburne and Hauge, 1975, p. 70).

The least studied of the three major lineament fault zones is the Prairie Creek lineament, which trends north-northwest through both bedrock and late Cenozoic sediments of the present project area. The lineament is well expressed and easily seen in exposed bedrock, but its trace becomes obscured and ultimately lost in the surficial deposits between Palermo and Oroville (fig. 2).

From our fieldwork and stratigraphic reconstruction, we conclude that upper Cenozoic deposits, primarily the dacite unit and the members of the Laguna Formation, have been significantly deformed by monoclinial and anticlinal folding, and possibly by faulting. The evidence is indirect. We did not observe faults offsetting the described units. This should not be surprising because exposure is poor and the deformation is either old enough or the deformation rate slow enough, or both, that geomorphic expression of it has not been preserved in these erodible, unconsolidated sediments. Our conclusions are based instead on (1) stratigraphic reconstruction, particularly the recognition of and location of the relict and exhumed soils developed on the lower member of the Laguna Formation, (2) the distribution of the surfaces of the units reconstructed from geomorphic and topographic evidence, and (3) reconstruction of projected slopes on stratigraphic marker beds and horizons.

In the paragraphs that follow we use the term slope in the sense of a tectonic inclination of a unit or stratum, not in the sense of the original gradient of a deposit. Projected slopes should be considered approximate, because datum points are widely spaced. Projected slopes were constructed using driller's logs, elevations of stratigraphic units such as the Nomlaki Tuff Member, and elevations of the uppermost outcrops of distinctive units (taken as approximations of the upper surfaces of selected units). All slopes in the Feather River area were constructed using S. 70° W. as the dip orientation.

The slope of the dacite unit is quite steep at the mountain front east and southeast of Oroville, yet relatively shallow in the subsurface west of Oroville: the slope on the upper surface of the dacite east of Oroville is more than 18 m/km and apparently reaches a slope of 70 m/km if the elevations of dacite outcrops in Long Bar Road are compared with those in the Thermalito Power Canal. West of Oroville, slopes of about 4.6 m/km are constructed from the elevation of dacite outcrops on the Feather River and depths to the dacite in the subsurface. Slopes on the dacite between the Feather River and exposures in the borrow pit south of the municipal airport are as low as 2.7 m/km. Much farther to the west, in the subsurface near Highway 99, the slope on the dacite surface appears to steepen again to about 9 m/km

to the west-southwest. Slopes determined from a small number of outcrops of the Nomlaki Tuff Member east and southeast of Oroville are also very steep, 22 to 29 m/km. These steep slopes must also lessen substantially to the west in the subsurface, for the slope of the underlying, older dacite unit flattens there to 4.6 m/km. In contrast, the Nomlaki slopes only about 9 m/km in exposures south of the Yuba River and so may be less deformed there. The slopes near Oroville suggest that there is a relatively narrow zone along the boundary between the valley and mountain front that has been significantly deformed. This may have been achieved by a monoclinial flexure in the unconsolidated Laguna Formation, or possibly by a series of short, en echelon or anastomosing fault segments with net valley-side-down movement. A structure-contour map drawn on the surface of the dacite shows a narrow, north-south-trending zone of closely spaced contours, at a position that suggests that the zone of deformation may be approximately on strike with the short north-south reach of the Feather River due north of Oroville. This zone in turn is on strike with the projection of the Magalia lineament to the north.

A discordance of slopes on the uppermost gravel bed of the upper member of the Laguna Formation north of the Feather River compared to south of it may also reflect deformation at the mountain front. Reconstructions of the surface of this gravel between the Thermalito Power Canal, the Butte County Administrative Center, and the Thermalito Forebay area yield variable slopes of less than 5.5 m/km. Reconstruction of the equivalent gravel surface south of the river at Memorial Park Cemetery yields a slope of more than 11 m/km. This surface appears to flatten valleyward and have a slight concave upward shape (fig. 4A). Differential warping or tilting of this surface is suggested. The apparent concavity of this upper surface, along with the valleyward shallowing of all slopes on older marker horizons, suggests monoclinial flexure along the mountain front. The slopes of older rock units should be steeper than original depositional gradients because of ongoing uplift and westward tilt of the Sierran block. This has been well documented all along the Sierra foothills (Gale and others, 1939; Davis and Hall, 1959; Arkley, 1962; Marchand and Allwardt, 1981); however, slopes of 20 to more than 50 m/km are clearly anomalous for Pliocene and Pleistocene deposits. Slopes calculated for units in the subsurface west of Oroville, which average 5 m/km, are much closer to those reported for Pliocene and Pleistocene units elsewhere along the valley edge (see Marchand and Allwardt, 1981, table 1). The outcrop distribution of the lower member of the Laguna Formation, with its distinctive relict soil profile, is unusual and is best understood in the context of mountain-front deformation. At Hewitt Park in Oroville (NW $\frac{1}{4}$ sec. 17, T. 19 N., R. 4 E.; Oroville 7.5-minute quadrangle), at an elevation of 200 ft (60 m), a remnant of a very strongly developed soil with a bright-red argillic B horizon (10 R Munsell hue) over 4 m thick is preserved on what we interpret as the buried original surface of the lower

Laguna (fig. 4B). This strong soil cannot be associated with the upper member of the Laguna, because the outcrop is much lower than the projection of the 260- to 300-ft-elevation (80 to 90 m) eroded surface of the upper member of the Laguna across the river. At the west end of the park this paleosol appears to be overlain by gravelly alluvium of the upper member. The strong soil profile at Hewitt Park is part of a discontinuous geomorphic surface, remnants of which extend to South Oroville at elevations of 200 to 260 ft (60 to 80 m). This geomorphic surface and its exhumed soil also lie well below the upper surface of the lower member of the Laguna, projected from the higher areas to the northeast (fig. 4B). From this evidence, the older units appear to slope steeply down to the southwest due either to flexure or faulting. Similarly, east of Palermo, the lower member of the Laguna Formation with its distinctive relict soil lies at elevations as high as 600 ft (180 m), and slopes steeply to the west (fig. 4C). To the southwest, across a northerly projection of the Prairie Creek lineament fault zone, the upper member of the Laguna occurs in a syncline-like structure, and farther west it is flanked by an exhumed remnant of the lower member. The bedrock exposed between the lower and upper members suggests that the two are separated by a fault. The north-south linear outcrop pattern of the exhumed lower member of the Laguna and other units (fig. 2) suggests that these remnants describe the axis of a north-south-trending anticline. The Tehama and Red Bluff Formations similarly are exposed well away from the mountain front in the northern Sacramento Valley near Corning, along the axis of the Corning anticline. The overall pattern near Palermo suggests a faulted monocline at the mountain front that merges valleyward into a syncline and anticline. The timing of deformation at the mountain front is important. When did the major deformation occur and is it continuing today? The stratigraphic evidence gives clues, but it may raise more questions than answers. The lower member of the Laguna Formation and the dacite unit are the most strongly deformed; the upper member of the Laguna is less deformed. The intensity of deformation appears to decrease from north to south; it is greatest in the Oroville area and less at the Yuba River.

The deformation history is intertwined with the depositional history of the two members of the Laguna Formation. Deformation probably did not begin until late Pliocene (early Laguna) time. If deformation had begun much earlier, before the lower member was deposited, the slope on the dacite might be significantly greater than that of the lower member of the Laguna, yet steepened slopes on both units are about 18 m/km across the zone of deformation. Very steep apparent slopes on the dacite between Long Bar Road and the Thermalito Power Canal, however, allow the possibility that the dacite is more deformed than the lower member of the Laguna. Deposition of the lower member may have been completed about 3.2 Ma, and deposition of the upper member probably did not begin until about 2.6 Ma or later. During this interval of nondeposition, defor-

mation apparently began in earnest and canyon cutting proceeded rapidly. We conclude this because sediments of the lower member of the Laguna east of the postulated deformation zone (the projection of the Prairie Creek lineament fault zone) were never buried by younger sediments, while areas of the lower member to the west of the zone were completely buried by deposition of the upper member. This was probably the result both of valley-side-down relative displacement of the lower member and of canyon cutting during the time between deposition of the two members, so that the fan-shaped flood plain deposits of the upper member of the Laguna issued from an apex situated at a lower elevation than had the flood plain deposits of the lower member. Deformation continued during and probably after deposition of the upper member of the Laguna, because the slope of the uppermost gravel bed is steepened to 11 m/km just south of the Feather River, and because the upper member is involved in the postulated anticlinal folding that extends from Palermo to south of Honcut Creek. The stratigraphic evidence suggests that the major period of deformation took place between 3 Ma and about 1.0 Ma. Deformation may have begun earlier than 3 Ma and continued more recently than 1.0 Ma, but we lack conclusive evidence to demonstrate this. Harwood and Helley (1987) bracketed most of the deformation of the Chico monocline between about 2.6 and 1.1 Ma because the 2.6 Ma Ishi Tuff Member of the Tuscan Formation is deformed by the monocline, and the 1.1 Ma basalt of Deer Creek, which flowed down a canyon cut into the Tuscan, was not deposited until after folding had ceased; it in fact cascaded over the flexure on its path into the valley. Harwood and Helley (1987) reported a minimum of about 365 m of up-to-the-east offset of the basement surface across a steeply east dipping reverse fault beneath the Chico monocline. The projected trace of the Chico monocline passes between the Campbell Hills and South Table Mountain (figs. 1, 2), and may coincide with the Prairie Creek lineament fault zone.

The outcrop pattern of the younger formations and drainage patterns between Oroville and Honcut Creek may be evidence that anticlinal folding continues to the present day. Outcrops of the lower member of the Riverbank Formation adjacent to the Feather River and south of Oroville (fig. 2) are strikingly linear. Wyman Ravine, Wyandotte Creek, and the Feather River all flow southwest as they exit the mountain front. Each then turns due south, creating a strong north-south alignment of large- and small-scale drainages. The gradient of the Holocene flood plain of the Feather River between Oroville and Yuba City is less than 0.65 m/km, whereas the gradient on the surfaces of the lower member of the Modesto Formation and the basin deposits to the west-southwest of the river is as much as 0.92 m/km. The path of the Feather River may be structurally controlled and the river flow constrained to the south, rather than west-southwest to a confluence with the Sacramento River north of Sutter Buttes.

Significant new work is in progress in the Oroville area to clarify the interplay between tectonics and late Cenozoic sedimentation (Unruh, 1988), and has involved gravity surveys, detailed geologic mapping, analysis of old and many new well logs, and synthesis of published subsurface data. Early findings indicate that bedrock faults indeed have expression in offsets in the late Cenozoic sediments south and east of Oroville and that these faults were reactivated approximately 3.4 Ma (Unruh, 1988). The tectonic regime is interpreted to be one of active east-west extension, with, for example, the north-south course of the Feather River occupying a graben formed by extension. Different faults appear to have been preferentially active through time, resulting in a progressive shift of the trend of the Feather River from west-southwest at 3.4 Ma to due south by 0.7 Ma (Unruh, 1989). Work by Unruh is continuing (Unruh, 1989) in an attempt to relate deformation in the Oroville area to patterns and timing of tectonic activity documented farther north in the Sacramento Valley by Harwood and Helley (1987).

Summary and Discussion of Geologic History and Tectonics

The stratigraphic sequence delineated in this report bears certain similarities to that of the American River area (Shlemon, 1967a, b; 1972) and to that of the northeastern San Joaquin Valley (Marchand, 1977; Marchand and Allwardt, 1981) and yet is unique in several ways (table 1).

The dacite unit that we have described is clearly different from, and younger than, the lower Miocene andesitic Mehrten(?) Formation of Creely (1965), with which the dacite previously had been correlated. We report an average whole-rock K-Ar age of 3.2 Ma for this unit. We have recognized a local stratigraphic sequence of four Pliocene to Holocene alluvial units, and we correlate the pre-Holocene alluvial sequence with the informal units of the Modesto, Riverbank, and Laguna Formations of Marchand and Allwardt (1981).

The sequence of geologic events considered in this study began with eruption of dacitic lava in the late Pliocene. The source of the detritus is not known but is likely to have been in the ancestral upper Feather River basin adjacent to the ancestral Yuba River drainage. The sequence near the Feather River consists of fine tuffaceous sediments, overlain by one or more dacitic mudflows, in turn overlain by fine tuffaceous sand and silt. Deposition was episodic with intervals of nondeposition recorded by two or more buried soils within the section. A period of nondeposition followed, during which the dacite unit was eroded and as much as 10 m of relief appears to have been developed on its surface. Reactivation of Mesozoic shear zones along the mountain front probably began during this time, resulting in the beginning of valley-side-down relative

displacement of the dacite near the point where the modern Feather River leaves its bedrock canyon.

About 3.4 Ma, the Nomlaki Tuff Member was deposited by the ancestral rivers on the Mesozoic bedrock and the dacite, signaling the inception of deposition of the lower member of the Laguna Formation. On the Feather River, the lower member built a fan-shaped flood plain to the south-southwest which had its apex near Sycamore Hill (northeast of Oroville). Remnants of this deposit at its apex now lie at elevations of about 450 to 600 ft (135 to 180 m). A small drainage or embayment to the east of Palermo, which was partially blocked from the Sacramento Valley by a north-south-trending ridge of Mesozoic bedrock, also filled with sediment. Deposits of the stream that appears to have been the source of the alluvium in this embayment (possibly ancestral Honcut Creek) now crop out at elevations as high as 960 ft (290 m) near Bangor. On the Yuba River, alluvium of the lower member spread to the west from an apex near the point where the modern Yuba enters the map area (fig. 2).

Deposition of the lower member ceased about 3.2 Ma. A period of nondeposition was accompanied by valley-side-down displacement of the dacite and lower member of the Laguna. We estimate this period to have been as much as 0.5 million years long because an extremely strong red soil profile formed on stable parts of the landscape of the lower member of the Laguna before it was buried by alluvium of the upper member.

The lower member of the Laguna Formation and possibly also the upper member was deposited in response to tectonic, and not climatic, events: a major period of east-west compression and deformation began 2.6 Ma or before in the southern Sacramento Valley (Harwood and Helley, 1987). The regional compressive stress field and zone of deformation has migrated northward through the valley from that time to the present (Harwood, 1984; Harwood and Helley, 1987). The crest of the Sierra Nevada in the Carson Pass-Sonora Pass area has been rising at a rate which has increased from 0.02 mm/yr 25 million years ago to 0.16 mm/yr at present, and almost half of the total uplift of the crest over the last 25 million years has taken place during the last 5 million years (Huber, 1981). The substantial increase in rate of uplift of the crest beginning about 5 Ma, combined with regional compressive deformation beginning in the southern Sacramento Valley 2.6 Ma, triggered greatly increased rates of erosion and canyon cutting in the northern Sierra, and deposition of the coarse debris that we recognize today as the Laguna Formation. The crest of the northern Sierra in middle or late Pliocene time was probably too low to have sustained ice sheets, should there have been glacial epochs in the Sierra at this time as some glacial stratigraphic evidence from the high southern Sierra suggests, so that a climatic/glacial origin for those deposits appears unlikely. The lower member of the Laguna and the dacite unit were deformed principally in the time interval

between deposition of the lower and upper members of the Laguna or about 3.2 to 2.6 Ma; tectonically steepened slopes on the lower member of the Laguna and the dacite unit appear to be quite similar, whereas slopes on the upper member of the Laguna in the same zone near Oroville are less than half those of the lower member and the dacite unit. Channels were cut deeply into the alluvium of the lower member of the Laguna by the Feather and Yuba Rivers in the period before deposition of the upper member began. The channel cutting was probably enhanced by the west-facing monoclinical flexure of the alluvial and volcanic units that was going on at the same time. When deposition of the upper member of the Laguna began about 2.6 Ma, only the part of the lower Laguna to the west of the monoclinical flexure was buried by alluvium of the upper member. The part that was present to the east of the flexure, which was several tens of meters higher on the landscape, escaped burial, and its remnants persist in the Wyandotte area. Some deformation of the alluvial units continued during and possibly after deposition of the uppermost gravel bed of the upper member had been completed about 1.8 Ma. All units appear to be less deformed near the Yuba River, where the lower and upper members of the Laguna spread westward into a fan-shaped flood plain in which the upper member is inset into the lower. Between about 1.5 and 0.45 Ma, erosional dissection was the dominant geomorphological process along the valley margin. Several erosional geomorphic surfaces were cut into the voluminous sediments of the Laguna Formation between the Feather and Yuba Rivers. These surfaces may have been caused in part by temporary stabilization of base level (either due to climatic or tectonic events) and in part by the position of resistant gravel beds within the deposits. The last period of erosion exhumed the buried surface of the lower member of the Laguna over a large area, as overlying sediments of upper member were stripped away; soil development resumed on these exhumed surfaces. Deposits associated with the erosional events that occurred between about 1.5 and 0.45 Ma have not been recognized in the area. Detritus shed from the eroding landscape was presumably carried farther along the ancestral drainage systems or was buried by younger basin deposits.

The central Sierra and southern Sierra record glacial events at least as far back as 800 to 900 ka (Turlock Lake Formation) (Janda and Croft, 1967; Marchand and Allwardt, 1981), but in the northern Sierra, lower crestal elevations apparently precluded formation of extensive glaciers until early Riverbank time. Mathieson and Sarna-Wojcicki (1982) reported that glaciers probably did not advance into Mohawk Lake (in the upper Feather River basin) before 450 ka, when the Rockland ash bed was deposited in the lakebed sediments, because till or ice-rafted boulders are absent from the strata below this time marker. Evidence of glacial activity older than 450 ka also is absent in the surrounding region. The absence of deposits equiva-

lent to the lower and middle Pleistocene Turlock Lake Formation in the Feather-Yuba rivers area is consistent with this evidence.

Between 250 ka and possibly 450 ka, deposition of the lower member of the Riverbank Formation began, probably in response to a middle Pleistocene glacial advance. By this time the elevation of the northern Sierra was high enough to support extensive glaciers. Interglacial climate brought cessation of deposition and a period of landscape stability, during which soil formation began. Mainstream incision accompanied the interglacial climate, and the lowering of base level led to sculpting of the deposits of the lower member of the Riverbank Formation as side streams eroded into the deposit. In the following glacial period(s), probably corresponding to oxygen isotope stage 6 dated at 127 to 190 ka (Hays and others, 1976; Shackleton and Opdyke, 1976), mainstream alluvium of the upper member of the Riverbank aggraded to moderate thickness and a thin veneer of sediment infilled and buried eroded areas of the lower member of the Riverbank Formation, leaving islands of the original surface of the lower member surrounded by a veneer of sediment of the upper member of the Riverbank. In places, alluvium of the upper member of the Riverbank buried the eroded remnants of various sideslope and swale-filling soils developed on the lower member of the Riverbank. A corresponding interglacial period of landscape stability followed deposition of the upper member, initiating soil development on stable surfaces and incision of river channels along main streams.

Aggradation of the lower member of the Modesto Formation began sometime before 40 ka. The Feather River followed the course it holds today and an extensive system of distributary channels carried flood waters to the southwest across the asymmetrical fan-shaped flood plain to deposit clayey alluvium in the ancestral Butte and Sutter basins. Near the end of the aggradational cycle, Glacial Lake Mohawk was breached, and its lacustrine sediments were transported down the Feather River. This lacustrine silt and clay spread as a sheet of uniform thickness across several hundred square kilometers of the flood plain of the lower member of the Modesto. The last stages of aggradation covered the silt to shallow depth with coarser alluvium.

River incision prior to deposition of the upper member of the Modesto cut channels that correspond essentially to those occupied by the Holocene flood plains. Aggradation of the alluvial cycle of the upper member of the Modesto took place about 10 ka. Alluvium was confined to narrow flood plains on the Feather, Honcut, and Yuba rivers, and did not spread out over the older deposits to form a fan-shaped flood plain within the project area.

Incision of the confined Feather River flood plain during early Holocene time swept out much, if not all, of the deposits of the upper member of the Modesto, although deposits of the upper member were preserved on Honcut Creek. Deposition of the major Holocene flood plain of the

Feather River has been dated at about 3 ka, and radiocarbon ages ranging from 1.775 ka to 0.45 ka record minor channel-building events on the Holocene Honcut Creek and reworking of the flood plain surface on the Feather River.

SOIL CHRONOSEQUENCE SITE SELECTION, EXCAVATION, AND SAMPLING

Nineteen soil pedons were described and sampled from 11 sites for the chronosequence study (fig. 6). The sites were selected after stratigraphic units had been delineated on Honcut Creek. All sites are within a 5-km radius and all are within 1 km of Honcut Creek. Each site had to meet the following criteria: loamy and nongravelly parent materials, absence of major lithologic discontinuities, good internal soil drainage and absence of duripans, slopes of less than 3 percent, and minimal disturbance by erosion, deposition, or farming. The last criterion eliminated the greatest number of potential sites. The lands around Honcut Creek are being used for ever more intensive farming, and land leveling and deep ripping of subsoils has become the norm. The surfaces of some Riverbank-age terrace remnants have been leveled by as much as 2.5 m in order to make possible the cultivation of rice in diked and flooded fields. Disturbance due to agriculture and the small total area of floodplains and terraces on Honcut Creek made it difficult to locate suitable sample sites. Soil profile sample numbers, stratigraphic units, assumed ages and site locations are given in table 5, and the individual soil profiles are described in supplementary table 2.

Sample sites were located in trenches excavated by backhoe and by hand, except for the two sites on the lower member of the Laguna Formation, which were vertical exposures excavated in a bluff adjacent to Honcut Creek. At each of the backhoe trench sites, two soil profiles, separated by at least 6 m, were described and sampled. This paired-pedon sampling scheme required us to find fewer independent sites that met the criteria stated above than we would have had to find without it, while still allowing us to measure the variability of replicate soils on same-age terraces. We described and sampled the soil profiles in the field using standard terms and methods (Soil Survey Staff, 1975, 1981). From each soil horizon we collected a bulk sample weighing about 4 kg for physical and chemical analysis, and three to five undisturbed soil peds for bulk density determination. We analyzed the soils in the lab using methods outlined in Singer and Janitzky (1986).

Four replicate pedons of Holocene soils were described and sampled from two hand-dug pits and two creek-bank exposures. C horizons were described and sampled in the Holocene soils. The replicate Holocene sites (HON-1 to HON-4) are undisturbed and support riparian vegetation. The sites receive some deposition of alluvium during floods, but only HON-4 has a distinct layer of overwash.

Four replicate pedons from the upper member of the Modesto Formation were sampled and described from two sites. The site of HON-5 and HON-6 has not been leveled, is not irrigated, and has been used only for dry farming of grains and legumes. The site of HON-7 and HON-8 is irrigated and is used to grow vegetable and field crops. Care was taken to select a site in this leveled field which had been neither cut nor filled by consulting the original land leveling plan. The deepest sampled horizons were transitional BC horizons of slight pedogenic alteration.

We had difficulty finding suitable sampling sites on the lower member of the Modesto Formation because most of the soils formed on the lower member near Honcut Creek possess duripans that have formed along the stratigraphic boundary that separates the compact silt substratum from overlying sediments. Profile HON-9 is of this type and has a weak duripan. The profile was described and sampled, but at present the profile has been used only to calculate soil development indices (SDI). We described two replicate soil profiles from a second backhoe trench in a uniform but sandy distributary channel deposit (HON-10 and HON-11) in order to avoid duripan development. This site has been used to dry farm grain crops and has not been leveled. Relatively unweathered C-horizons were described and sampled in these profiles of the lower member. All Modesto Formation sites supported annual and perennial grasses and forbs plus scattered oak trees before cultivation.

The claypan and hardpan soils of the Riverbank Formation are widely used to grow rice. The landscape, which is naturally rolling, must be leveled for rice cultivation, and suitable sites were scarce because of the extensive leveling.

We sampled two replicate pedons from a single site on the upper member of the Riverbank Formation (HON-13 and HON-14). A textural discontinuity was recognized in these profiles, but the site met the other established criteria, and no other undisturbed, nonduripan sites were found. The site has been used to dry farm grain for about 50 years but has not been leveled.

We described and sampled four replicate profiles at two sites on nearly level, flat summits of terrace remnants on the lower member of the Riverbank Formation (HON-17, HON-18, HON-19, and HON-20). Both sites have been used in the past to dry farm grain and legumes. The second site has been fallow for 15 years. Neither site has been leveled. We were able to sample only to the depth of BC horizons in these soils. All Riverbank Formation sites supported annual and perennial grasses and forbs, and scattered oak trees before cultivation. A bluff exposure on South Honcut Creek provided the sampling site for two pedons in the lower member of the Laguna Formation. The two pedons (HON-21, HON-22) are about 10 m apart. The face of the bluff was cut back about 1 m to expose fresh soil. Each profile was described and sampled to a depth of about 5 m and an additional sample of C-horizon material was collected from each profile at about 12 m. Relief on this

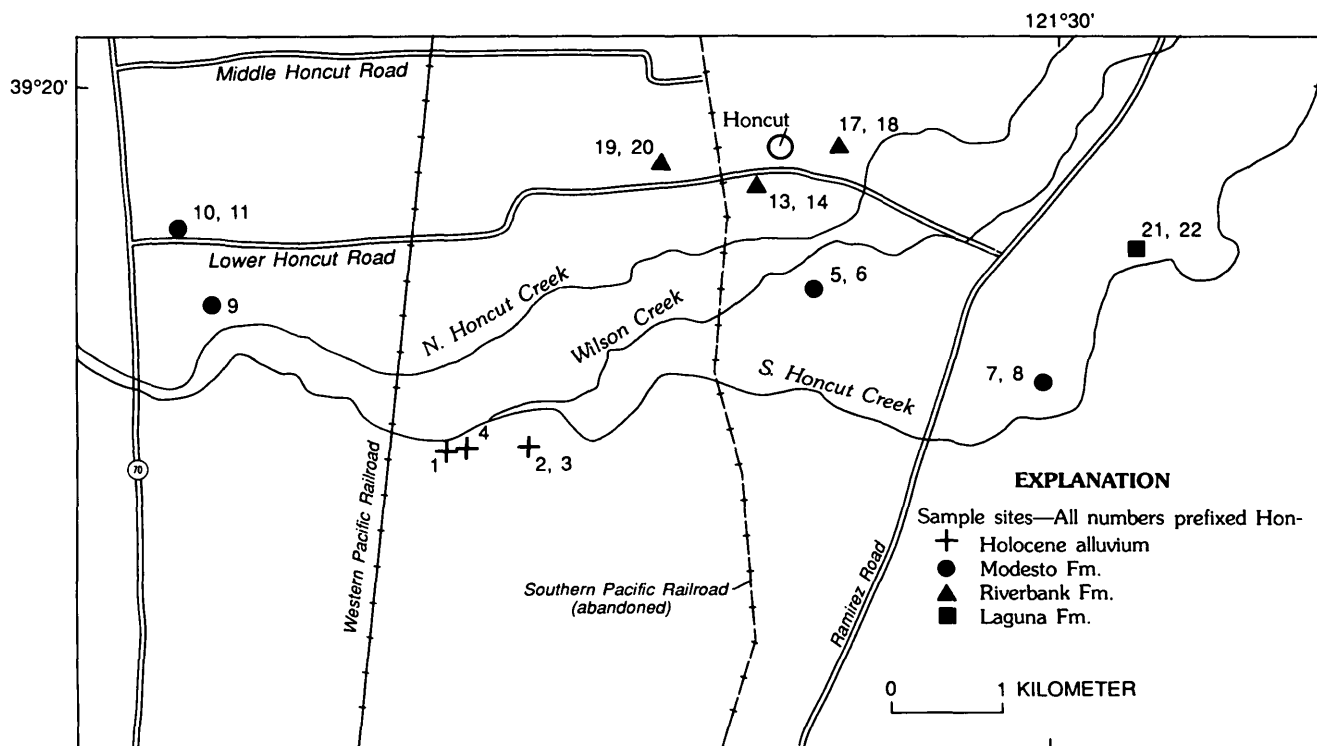


Figure 6. Index map showing sample sites of chronosequence soil profiles.

Table 5. Site locations, assumed ages, and taxonomic subgroups of the soils sampled for the chronosequence study

Profile number	Geologic unit	Approximate age of soil ¹ (ka)	Taxonomic subgroup	Soil profile site locations, Mount Diablo Base and Meridian
HON-1 HON-2 HON-3 HON-4	Holocene alluvium	0.6	Typic Xerorthents	SW ¹ / ₄ NE ¹ / ₄ sec. 30, T. 17 N., R. 4 E. SW ¹ / ₄ NW ¹ / ₄ sec. 31, T. 17 N., R. 4 E. SW ¹ / ₄ NW ¹ / ₄ sec. 31, T. 17 N., R. 4 E. SW ¹ / ₄ NE ¹ / ₄ sec. 31, T. 17 N., R. 4 E.
HON-5 HON-6 HON-7 HON-8	Upper member, Modesto Formation	10	Typic Haploxerolls	NE ¹ / ₄ SW ¹ / ₄ NE ¹ / ₄ sec. 31, T. 17 N., R. 4 E. NE ¹ / ₄ SW ¹ / ₄ NE ¹ / ₄ sec. 31, T. 17 N., R. 4 E. SE ¹ / ₄ SE ¹ / ₄ SE ¹ / ₄ sec. 22, T. 17 N., R. 4 E. SE ¹ / ₄ SE ¹ / ₄ SE ¹ / ₄ sec. 22, T. 17 N., R. 4 E.
HON-9 HON-10 HON-11	Lower member, Modesto Formation	40	Abruptic Durixeralfs Typic Haploxerolls	150 m W. of ctr. sec. 24, T. 17 N., R. 3 E. 150 m W. of ctr. sec. 24, T. 17 N., R. 3 E. SE ¹ / ₄ SW ¹ / ₄ SW ¹ / ₄ sec. 13, T. 17 N., R. 3 E.
HON-13 HON-14	Upper member, Riverbank Formation	130	Mollic Palexeralfs	NE ¹ / ₄ SE ¹ / ₄ sec. 16, T. 17 N., R. 4 E. NE ¹ / ₄ SE ¹ / ₄ sec. 16, T. 17 N., R. 4 E.
HON-17 HON-18 HON-19 HON-20	Lower member, Riverbank Formation	250	Mollic Palexeralfs	NE ¹ / ₄ SE ¹ / ₄ sec. 16, T. 17 N., R. 4 E. NE ¹ / ₄ SE ¹ / ₄ sec. 16, T. 17 N., R. 4 E. SE ¹ / ₄ SE ¹ / ₄ SE ¹ / ₄ sec. 17, T. 17 N., R. 4 E. SE ¹ / ₄ SE ¹ / ₄ SE ¹ / ₄ sec. 17, T. 17 N., R. 4 E.
HON-21 HON-22	Exhumed lower member, Laguna Formation	1,600	Palexerults	NW ¹ / ₄ sec. 23, T. 17 N., R. 4 E. NW ¹ / ₄ sec. 23, T. 17 N., R. 4 E.

¹See table 3 and text for sources of age estimates.

surface is less than 1 m near the sampling site, but as much as 5 to 6 m over longer distances. The site supports a mixed oak-grassland with scattered digger pine and has been used only for grazing.

CHARACTERISTICS OF THE SOIL CHRONOSEQUENCE

Soils form under the influence of five principal state factors or environmental variables: climate, organisms (principally vegetation in these soils), parent material, topography, and time (Jenny, 1980; Birkeland, 1984). Jenny (1980) formulated the equation for an actual, as opposed to idealized, chronosequence as:

$$S \text{ or } s = f(t, cl, o, r, p, \dots)$$

in which *S* is the total soil system, *s* is an individual soil property, *t* is the principal factor time, and *cl*, *o*, *r* and *p* are the ineffectively covarying, as opposed to constant, factors climate, organisms, relief, and parent material, respectively. What Jenny meant by this formulation was that the other four factors need not necessarily be constant or invariant for a single-factor study to be valid. If the range of variation of a secondary factor is small, or if it is large but

of low effectiveness, then that secondary factor will play a subordinate role in soil development (Jenny, 1980). In the Honcut chronosequence, we think that factors other than time have remained relatively similar among sampling sites and it is principally the age of the deposit and soil that has controlled soil formation. If factors other than time have varied among sites, the variation may be random, which adds noise or unexplained variation in soil properties to the time factor analysis. The variation may also be systematic, which could add a secondary systematic trend to soil development that we may or may not correctly recognize and interpret.

Several properties in the Honcut soils change in systematic ways as a function of age, under the influence of ongoing pedogenic processes. Some of these properties are soil profile morphology, clay content of argillic B horizons, and depletion of elements in selected particle-size fractions due to weathering of primary minerals. Other soil properties change in seemingly nonsystematic ways, possibly reflecting the complicating influence of variation among sites in other factors such as climate or parent material.

We analyzed the soils on selected relict alluvial landscapes at Honcut Creek primarily to evaluate their usefulness in stratigraphic correlation. We briefly discuss herein the evidence for constancy of other factors than time and

some of the major trends in soil development. The discussion is intended as an introduction to the many data contained in the soil profile descriptions (supp. table 1), physical properties (supp. table 2), extractive chemical analyses (supp. table 3), clay mineralogy (supp. table 4), total chemical analysis of selected particle-size fractions by X-ray fluorescence spectroscopy (supp. tables 5, 6) and instrumental neutron activation analysis (supp. table 7), and the calculated values of the horizon index and profile index (supp. table 8).

Review of State Factors

Climate

Present climate and paleoclimates need to be considered in any study of relict soils that have developed over hundreds of thousands or millions of years. One possible source of variation in soil properties is the position of the deposits with respect to the present climatic gradient. Chronosequence sampling sites on older terraces generally lie to the east of and closer to the mountain front than sites on the younger terraces, because of the westward progression of alluvial deposition. As a result, sites on the older terraces receive approximately 50 to 70 mm more annual rainfall than do the sites on the younger terraces. The difference in rainfall between sites might therefore constitute a second variable, in addition to time, that has influenced soil development. We consider the effect of the slight difference in rainfall to be minimal.

The climate of the project area has not been constant over the last 4 Ma. Axelrod (1971, 1980) constructed paleoprecipitation curves for central California from paleobotanic evidence. Reconstructions from west-central California demonstrate a gradual secular decrease in precipitation from middle to late Miocene time, followed by a large increase in precipitation in the Pliocene (fig. 7). A precipitation maximum occurred during the late Pliocene, followed by a steady secular decline through the Pleistocene to the Holocene; precipitation in the late Pliocene was about 1.5 times that of the present day (fig. 7). A wetter climate in the late Pliocene may have enhanced development of the soils formed on the Laguna Formation relative to soils formed on the middle and upper Pleistocene Riverbank and Modesto Formations, or a steady secular decline in precipitation through the late Pliocene to the Holocene could impose a second systematic factor on soil development.

Changes in the seasonal distribution of precipitation over geologic time may also be important in the assessment of influences on soil development. Axelrod (1980) reconstructed the middle Pliocene climate at the Turlock Lake paleobotanic site in central California based on species types and diversity. He reported that the climate in the middle Pliocene had a bimodal rainfall distribution with significant summer rain, twice the total precipitation of today, and a slightly lower mean annual temperature. The

change from the bimodal seasonal rainfall pattern that existed in the middle Pliocene to the Mediterranean-type pattern that exists today resulted from the uplift of the Coast Range and exclusion of inland seas beginning in the early or middle Pleistocene.

Relatively little information is available on ranges of precipitation and temperature in the Central Valley during climatic fluctuations of the Pleistocene epoch. From examination of the properties and geographic distribution of soils in California and the Western United States, however, Janda and Croft (1967) and Birkeland and Shroba (1974) reasoned that climatic fluctuations during the Quaternary did not exert a dominant influence on soil development. For example, Janda and Croft (1967) noted that the geographic distribution of Alfisols (Soil Survey Staff, 1975) in California and Oregon corresponds almost exactly to the present-day distribution of grassland and oak-grassland vegetation, and to areas of pronounced summer drought. Further, a transect into Oregon showed that the northern limit of Alfisols corresponded to a decrease in mean annual temperature and an increase in both total annual rainfall and proportion of total rain falling in the warm months. This suggested to Janda and Croft that the climate during the Pleistocene history of soil development in the Sacramento and San Joaquin Valleys was probably within the limits of climatic conditions that correspond to the present-day distribution of Alfisols. They characterized that climate as having a mean precipitation not greater than 860 mm, total summer rain less than 130 mm, and no extended periods of time in which precipitation was low enough for permanent

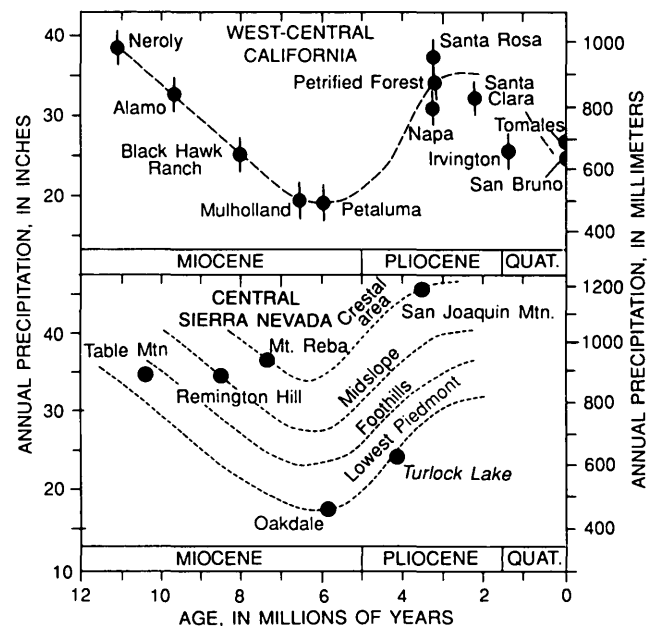


Figure 7. Plots of estimated rainfall from Miocene to Quaternary time in west-central California and central Sierra Nevada. From Axelrod (1980).

accumulation of lime in subsoils. Thus they concluded that the Alfisols which have formed on alluvial terraces in California are the product of long periods of weathering under conditions of climate and vegetation similar to the present, and that Quaternary climatic fluctuations in the Central Valley do not appear to have altered significantly the basic direction of pedogenesis on the alluvial landscapes.

Organisms

Pre-settlement vegetation on wet flood plains was a woodland-savanna populated with perennial grass, valley oak (*Quercus lobata*), and cottonwood (*Populus fremontii*). Low alluvial terraces had (and some still have) perennial grass, scattered valley oak, and interior live oak (*Quercus wislizenii*), whereas high terrace remnants on the margin of the valley supported perennial grass, interior live oak, blue oak (*Quercus douglasii*), a few digger pine (*Pinus sabiniana*), and buckeye (*Aesculus californica*). Little information is available on the movement of ecotone boundaries in this area during the Pliocene and Pleistocene; however, the soils have probably formed under a grass-oak savanna throughout their development.

Parent Material

The alluvial parent materials of the soils in the chronosequence are moderately stratified loam, silt loam, and fine sandy loam (supp. table 2). The parent materials generally are high in silt, fine sand, and very fine sand and are low in clay and coarse sand. Textural and mineralogical variations and discontinuities were recognized both within and between sampling sites. Stratification of texture most directly enhances or impedes the movement of water and, in turn, the movement of soluble or particulate weathering products in soils. Stratification, therefore, may control the depths at which major horizons form. Mineralogical stratification probably has a more complex and subtle effect on soil development through its influence on the types of mineral weathering reactions and on clay formation. The overall texture of a parent material, the proportion of gravel, sand, silt, and clay, can affect rates and processes of soil development because small particles tend to be more reactive to chemical weathering than coarse particles. Over the same period of time, then, a fine-textured parent material may develop a stronger soil profile than a coarse-textured parent material.

Parent material textures vary among the chronosequence soils more than would be considered ideal. We illustrate this with plots of the percentage of sand, calculated on a clay-free basis to minimize the influence of pedogenesis, versus soil depth (fig. 8A-F). The clay-free sand content is useful for visualizing differences in initial texture within and between soil profiles. Busacca (1982) demonstrated that the ratio of silt to sand on a clay-free

basis, and the ratio of medium sand to fine plus very fine sand, on a silt- and clay-free basis, are also useful to distinguish lithologic discontinuities and depositional sequences in these alluvial parent materials. The percentage of sand, on a clay-free basis, ranges from about 20 to 75, considering all A and B horizons together, and ranges as high as 90 in some deep gravelly BC horizons (fig. 8). The gravel content is less than 10 percent in the A and B horizons of all soils, except that the deepest Bt subhorizons of the soils formed on the lower member of the Laguna Formation have up to 30 percent gravel (supp. table 2). The gravel content is from 5 to 70 percent in the deep BC horizons of the soils formed on the lower member of the Riverbank Formation and the lower member of the Laguna Formation.

Replicate profiles of soils formed on each chronosequence member are generally similar to one another in texture and in the position of lithologic discontinuities within the profiles: the soils formed in Holocene alluvium fine upward (fig. 8A). The two profiles sampled from natural levee deposits are more stratified than the two profiles sampled from overbank deposits. The parent materials of the four replicate profiles sampled from the upper member of the Modesto Formation are quite uniform and similar to one another above a depth of 200 cm (fig. 8B), but they become progressively more coarse with increasing depth below this point as basal channel sands of this depositional cycle are encountered. Clay-free silt contents of 55 to 75 percent in the upper 200 cm of these soils corresponds to silt loam parent material textures. These are the finest textured and least stratified parent materials in the chronosequence. In contrast, the two replicate soil profiles sampled from a distributary channel deposit of the lower member of the Modesto Formation have the coarsest parent material textures of any of the chronosequence soils (fig. 8C). The difference in texture between deposits of the upper and lower members of the Modesto Formation may well have influenced relative rates of soil formation at comparable stages, with the rate of development being faster in the finer textured materials.

The two soil profiles sampled on the upper member of the Riverbank Formation show abrupt changes from fine to coarser textures at about 125 and 150 cm, which are superimposed on overall fining-upward patterns (fig. 8D). Parent material textures are silt loam above the discontinuity and stratified loam and sandy loam below it. The argillic B horizon has developed just above the discontinuity in the two replicate profiles, probably as a result of impeded downward flow of water at the discontinuity.

The four soil profiles sampled on the lower member of the Riverbank Formation also have a major textural discontinuity (fig. 8E), but it is at 160 to 200 cm in the profile, and the parent material texture above the discontinuity is loam rather than silt loam. In the soils of the lower member, the maximum development of the argillic B horizon is just above the discontinuity, again suggesting that the dis-

continuity controlled depth and degree of development of the B horizon.

This pattern, in which gravelly or sandy materials fine upward and are overlain abruptly by loam or silt loam materials, is shared by the soils formed on the upper member of the Modesto Formation and those on the upper and lower members of the Riverbank Formation (fig. 8B, D, E). We interpret each of these to be deposits of point-bar

or basal-channel gravel and sand of lateral accretion overlain by overbank loam and silt loam of vertical accretion.

Most of the soils formed on the upper member of the Riverbank Formation at sites away from Honcut Creek have formed in a thin (<2 m) veneer of alluvium deposited over an erosional surface cut into silt strata of the lower member, rather than having formed in alluvium of a single age and depositional cycle. Soils of the *Yokohl* series (*Typic*

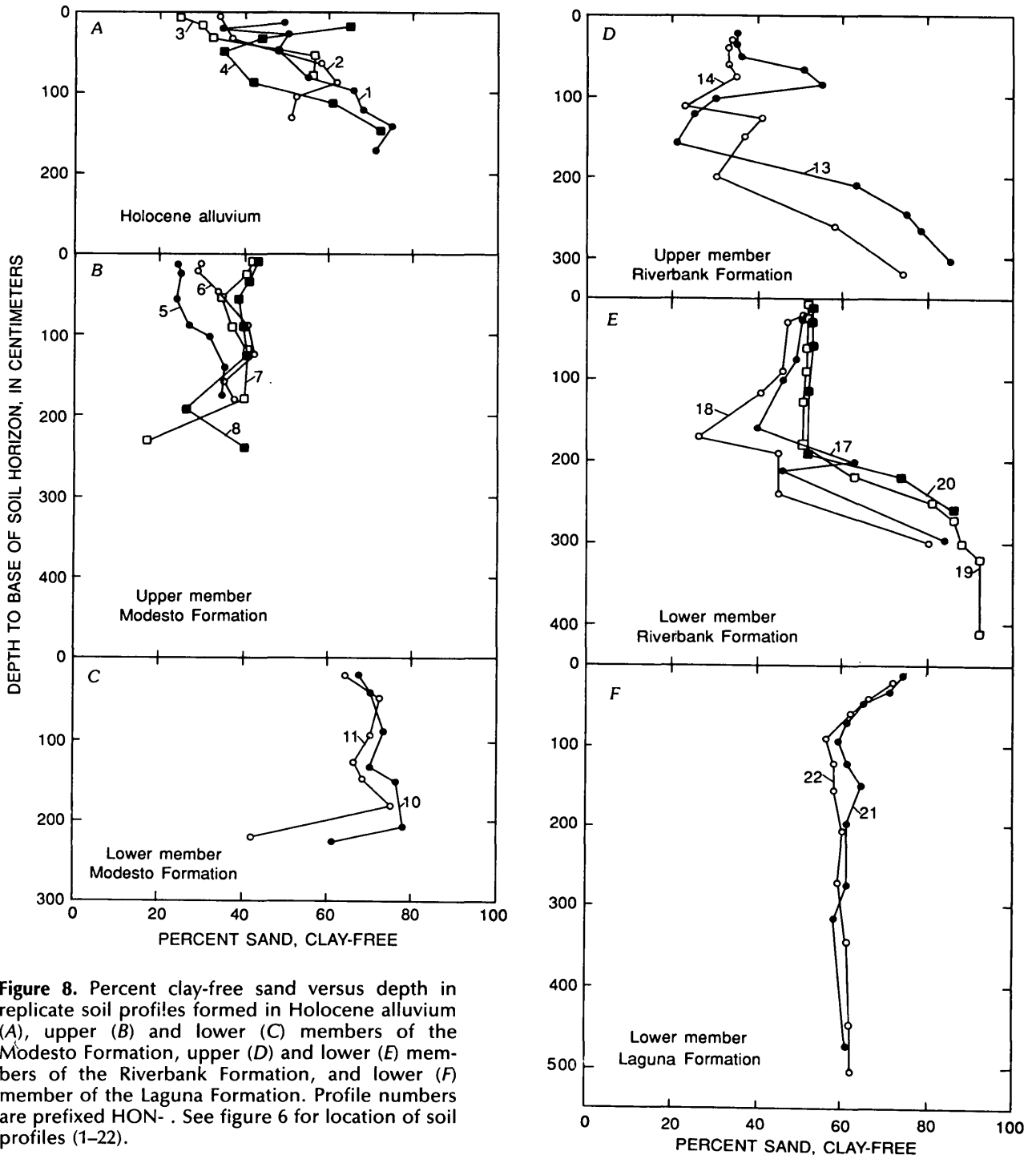


Figure 8. Percent clay-free sand versus depth in replicate soil profiles formed in Holocene alluvium (A), upper (B) and lower (C) members of the Modesto Formation, upper (D) and lower (E) members of the Riverbank Formation, and lower (F) member of the Laguna Formation. Profile numbers are prefixed HON-. See figure 6 for location of soil profiles (1-22).

Durixeralfs)⁶ have formed in the veneer of upper member sediment, and soil development extends across the interface into the older materials. The interface with the older silt has created a sufficient barrier to water movement that a duripan formed in this soil.

Both of the soils sampled from the lower member of the Laguna Formation appear to have formed in a relatively uniform sandy loam parent material similar in texture to the alluvium at the sampling sites of the soils on the lower member of the Modesto Formation (fig. 8C, F). The original texture of the parent materials in the soils of the lower member of the Laguna may be difficult to interpret from particle-size analyses because the extreme depth and degree of weathering in these soils may have altered appreciably the sand and silt content of the horizons.

We analyzed the elemental composition of the fine and coarse silt fractions (2–20 μm and 20–50 μm, respectively) using X-ray fluorescence spectroscopy (XRF) (supp. table 6), and we analyzed the elemental composition of the silt-plus-clay fraction (<50 μm) of selected horizons by XRF and instrumental neutron activation analysis (INAA) (supp. tables 5, 7). Our primary purpose in doing this was to examine pedogenic changes in these reactive size fractions as a function of soil age, but first we used this data to examine the initial uniformity of elemental composition of these fractions both within single deposits and among the chronosequence members. Although we discuss it only briefly here, our analysis of the uniformity of elemental composition in the parent materials was a critical first step in correctly reconstructing pedogenic changes in the elemental chemistry of these size fractions.

We use one of the soil profiles formed in Holocene alluvium to test and illustrate the effect of textural stratification (fig. 8A) on elemental composition (table 6), because pedogenic changes in elemental composition are minimal at this early stage of soil development. We can think of the elemental composition of a particle-size fraction as a proxy for the mineralogical composition of that fraction. Depositional processes can affect the initial mineralogy of a sedimentary layer, and pedogenesis, or soil development, also can affect the mineralogy and elemental composition through dissolution and alteration of the primary minerals.

We have found generally that the textural stratification in these parent materials, even when severe, does not have a strong effect on elemental composition of specific size fractions. This is illustrated in table 6. The silt-to-sand ratio in the horizons of a Holocene soil vary by a factor of almost 5 down the profile, whereas ratios of calcium to zirconium and iron to zirconium in fine and coarse silt of the same horizons vary by a factor of no more than 1.4. Other elemental ratios in these horizons and elemental ratios in little-altered BC and C horizons of other soils confirm

⁶ The Yokohl series was classified as *Abrupt Durixeralfs* in the Yuba area soil survey, but official series classification is as above.

Table 6. Comparison of the effect of stratification in a Holocene soil profile¹ on texture versus elemental composition

Horizon	Basal depth (cm)	Ratio of silt to sand ²	Ratio of (CaO/Zr)×100		Ratio of (Fe ₂ O ₃ /Zr)×100	
			fine silt ³	coarse silt ³	fine silt ³	coarse silt ³
C	17	.54	3.12	2.44	7.70	2.92
2A	32	1.26	3.05	2.54	7.61	2.97
2AC	49	1.83	3.11	2.34	7.55	2.71
2C	86	1.38	3.05	2.46	7.63	3.03
3C1	113	.63	2.94	1.98	7.65	2.45
3C2	147	.39	2.80	1.86	7.20	2.23
H/L ⁴	—	4.7	1.1	1.4	1.1	1.4

¹Profile HON-4.

²Calculated on a clay-free basis.

³Fine silt is 2–20 μm and coarse silt is 20–50 μm.

⁴Ratio of the highest value in a column to the lowest value in column.

this finding. Apparently the grading of grain sizes and of mineralogy are somewhat independent in this alluvial system.

Element concentrations generally are less affected by textural stratification in the fine-silt fraction than in the coarse-silt fraction. The ratios of calcium to zirconium and iron to zirconium in the horizons of the Holocene soil vary by only a factor of 1.1 in the fine-silt fraction but by a factor of 1.4 in the coarse-silt fraction (table 6).

In the soils formed on the lower member of the Modesto Formation, an abrupt textural discontinuity separates the base of the sandy channel deposit from the underlying mica-rich silty sand (between C and 2C horizons in table 7). Although the discontinuity shows as rather large changes in the concentrations of Si, Al, Ca, Zr, and Cr in the coarse-silt fraction, there is but scant evidence of the discontinuity in the concentrations of these elements in the fine-silt fraction.

The elemental composition of the soil parent material not only varies within individual profiles, but also varies between deposits or chronosequence members. The mineralogy of the alluvium deposited by Honcut Creek has changed slightly over the time span of the chronosequence, and the elemental composition of the alluvium reflects this also, although the range of variation is perhaps not greater than that found in other similar alluvial settings. Table 8 summarizes the elemental composition of the coarse- and fine-silt fractions averaged from the least altered horizons in one soil profile from each member of the chronosequence. Deep BC and C horizons were used in these calculations for all but the Holocene soils to minimize the effects of pedogenic alteration. All six horizons were averaged for the Holocene soil, because the degree of alteration of the A and C horizons was judged to be minimal.

Concentrations of Na, K, and Ca in fine silt and of Na, Mg, Si, K, and Ca in coarse silt (table 8) identify the alluvium of the lower member of the Modesto as having had a different source than the other chronosequence members. Cu, Ni, and Cr (supp. table 6) also are good indicators of the different source area. The elemental chemistry in this case confirms field evidence that the alluvium at the sample site for soils of the lower member of the Modesto Formation

Table 7. Comparison of the effect of textural stratification on elemental composition of coarse versus fine silt (20–50 μm versus 2–20 μm) in a soil profile (HON–10) on the lower member of the Modesto Formation

Horizon	Basal depth (cm)	Percent SiO_2		Percent Al_2O_3		Percent CaO		Zr (ppm)		Cr (ppm)	
		coarse silt	fine silt	coarse silt	fine silt	coarse silt	fine silt	coarse silt	fine silt	coarse silt	fine silt
		BC	150	62.6	57.0	15.4	18.9	5.1	2.5	263	140
C	205	61.9	56.5	15.6	18.6	5.2	2.6	275	137	351	299
2C	225	60.1	56.6	16.8	18.9	4.7	2.6	237	130	271	252

was deposited by the Feather River and not Honcut Creek. The data in table 8 demonstrate that the other five chronosequence members did have Honcut Creek as their source.

The differences in parent material composition among chronosequence deposits and compared to fresh stream sediment are large enough (table 8) that we calculated pedogenic gains and losses in these size fractions using the actual C horizon composition of each soil individually. We did not average compositional values among deposits for our calculations. We also placed emphasis on results obtained from the fine-silt fractions because of our finding that initial textural stratification within a deposit or profile caused only relatively small perturbation in elemental composition. In doing these two things we have recognized and attempted to minimize the effect that stratification within a deposit, and variation in mineralogy between deposits, would have on our calculations of pedogenic change over time.

Soil Development

Many of the morphological, physical, chemical, and mineralogical soil properties of the chronosequence change systematically with soil age. For example, the soils become red, clay forms or accumulates in argillic horizons, and profile depth increases to more than 5 m (table 9), although for each of these, the perfection of the trend seemingly is interrupted by variation in factors other than soil age. Different soil properties yield similar or complementary information because the multitude of changes in soil properties over time are interdependent (Busacca, 1982). For example, we can deduce that the formation of secondary clay minerals should be proportional to the dissolution or transformation of primary minerals. As a result we expect the clay content and the morphology of B horizons, and the elemental composition of primary mineral fractions to each change systematically with soil age under the influence of a linked set of pedogenic processes. This is valuable in terms of soil correlation because an interpretation based on the analysis of one soil property can be checked against several other soil properties.

We have selected soil morphology, as quantified by the soil development index of Harden (1982a), mineralogy of

the clay-size fraction ($<2 \mu\text{m}$), and elemental composition of silt fractions (2–20 μm and 20–50 μm) to illustrate some of the systematic changes in the soils over time and also to illustrate some nonsystematic variation imposed by change in other soil-forming factors.

Soil Development Index

The soil development index (Harden, 1982a) has been calculated for the chronosequence soils (supp. table 8), and it has proved to be a very sensitive measure of soil development. We use the index here to illustrate the major developmental steps in the chronosequence soils. The soil development index converts the morphological properties of soils, as recorded in standard field descriptions, into a numerical rating so that soils with differing degrees of development can be compared.

The detailed procedure for calculating the soil development index and the several ways in which the index can be used are discussed by Harden (1982a) and Harden and Taylor (1983). Eight soil properties are used in the original formulation of the soil development index: (1) rubification (reddening of color hue and brightening of chroma), (2) total texture (texture plus wet consistence), (3) structure, (4) dry consistence, (5) moist consistence, (6) clay films, (7) melanization (decrease in color value of A horizons due to the buildup of organic matter), and (8) pH. We substituted laboratory-determined texture and pH for the field-determined equivalents, as did Harden (1982a). With this choice of properties it is clear that this specific formulation of the index has been designed principally for well-drained, freely oxidized soils in which argillic horizon development is a major process. Harden and Taylor (1983) added color-paling, which is the inverse of rubification, and color-lightening, which is the inverse of melanization, specifically for soils that accumulate secondary calcium carbonate.

The soil development index uses a point system in which points are assessed in increments of ten for differences between a property in a soil horizon and that property in the soil's parent material. In the case of dry consistence, ten points are assessed for each step from loose to soft, to slightly hard, to hard, to very hard, to extremely hard: if a soil B horizon has a dry consistence that is extremely hard

Table 8. Average values of element concentration (percent) in coarse (20–50 μm) and fine (2–20 μm) silt fractions of BC and C horizons of the chronosequence soils

[n, number of samples]

Sample data ¹	Na ₂ O	MgO	Al ₂ O ₃	SiO ₂	K ₂ O	CaO	TiO ₂	Fe ₂ O ₃	Zr (ppm)
Fine silt (2–20 μm)									
Holocene alluvium (HON-4), 21-26 n = 6, (A's, C's) ²	2.49	5.15	18.68	52.6	0.805	4.58	1.32	11.52	152.5
Upper member, Modesto Fm. (HON-5), 32-33, n = 2, (BC1, BC2)	2.97	5.50	18.31	53.6	.605	3.98	1.22	10.64	165.5
Lower member, Modesto Fm. (HON-10), 63-65, n = 3, (BC, C, 2C)	2.17	5.79	18.80	56.7	1.85	2.57	1.06	9.23	135.7
Upper and lower members, Riverbank Fm. (HON-14,-18), 93, 94, 109, 110, n = 4, (deep BCt's and CB)	3.18	5.97	17.46	56.5	.875	4.13	.902	9.23	115.3
Lower member, Laguna Fm. 141 (HON-21), 141 (3BC and deep C) ³ 142	2.16 3.20	³ 1.56 5.47	⁴ 21.57 19.17	51.3 ⁵ 52.1	.88 .86	³ 3.30 4.54	.87 1.21	11.74 10.95	120 128
Fresh stream sediment, 156	2.78	4.99	16.09	56.8	.74	5.20	1.33	9.68	137
Coarse silt (20–50 μm)									
Holocene alluvium ⁶	3.95	4.24	15.52	56.2	.617	7.34	1.46	8.80	⁷ 329 (295)
Upper member, Modesto Fm.	4.41	3.48	15.24	58.7	.530	6.43	1.28	7.69	280
Lower Member, Modesto Fm.	3.27	4.41	15.30	62.2	1.12	5.04	1.11	7.14	267
Upper and Lower Members, Riverbank Fm.	4.34	3.24	14.78	60.2	.72	6.95	.75	6.65	⁷ 317 (260)
Lower member, Laguna Fm., ⁵ 141 142	3.80 4.89	³ .70 ² 2.13	⁴ 16.16 15.61	57.7 59.0	.478 .66	7.51 7.19	.74 1.14	⁴ 8.17 7.14	⁴ 300 260
Stream sediment, 156	4.48	2.91	14.70	59.4	.57	7.87	1.23	6.76	262

¹Geologic unit (profile number), sample numbers of horizons used in calculating average values, number of horizons used, and (type of horizons used).

²A horizons were averaged with C horizons in Holocene soil (HON-4) where little or no alteration of elemental composition has yet occurred.

³Concentration depleted by weathering losses.

⁴Concentration enhanced by weathering losses of other elements.

⁵Values for samples 141 and 142 not averaged but reported separately because sample 141, a 3BC horizon, has been altered by soil development.

⁶Samples averaged for coarse silt fraction are as above for fine silt fraction.

⁷Zr concentration is erratic because of stratification. Values shown in parentheses are those used as estimated concentrations in C horizons for calculations of element losses and gains in soil profiles using Zr as a stable element (see text).

and the parent material is loose, 50 points are tallied for the property in that horizon. Once all properties have been evaluated for each horizon in a profile, the quantified properties are normalized to a scale that ranges from 0 to 1, generally by dividing by the maximum points that could be assessed for each property. When the normalized values of the properties are summed for a horizon and divided by the number of properties, a dimensionless quantity between 0 and 1 is obtained called the horizon index. The horizon index is a measure of the development of an individual

horizon relative to its parent material, and the horizons of a profile can be studied as functions of soil depth or soil age. When the horizon index for each horizon is multiplied by the thickness of the horizon, and the values (in index-centimeters) are summed for an entire soil profile, a single quantity, the profile index, is obtained. The profile index of a soil is a measure of the degree of development of the morphology of that soil. Profile indices of two or more soils can be compared, and soil development can be studied as a function of soil age.

Graphs of the horizon index versus soil depth for the chronosequence soils provide a visual summary of the progression of soil development over time (fig. 9A–F). The horizon index values are highest in the A horizons of the Holocene soils and decrease with depth (fig. 9A). Melanization and development of soil structure, which is granular in these A horizons, contribute to the horizon index values. Individual Holocene profiles are highly stratified, and this is reflected in the horizon index plots. C horizons have nonzero horizon indices due to previous weathering of the alluvium deposited in some of the strata and also apparently to rapid oxidation of the sediments once in place. The average profile index for the four replicate Holocene profiles is 12 index-cm (table 10).

A subsoil cambic B horizon has developed in the 10-ka soils of the upper member of the Modesto Formation, and this is reflected in the depth of plots of the horizon index (fig. 9B). The maximum values of the horizon index are in the B, not A, horizons of these soils, and this is primarily due to rubification (reddening and brightening of soil color) and the development of structure and clay films. Large values of rubification and structure extend to more than 2 m in these soils and contribute to large horizon indices at these depths (fig. 9B). As a result of the large horizon index values at depth, the profile index, averaged for the four replicate profiles (the profile index is equivalent to the area under the horizon index plots), is 45 index-cm, a value that is higher than our expectation and higher than the profile index for comparable soils of the upper member of the Modesto Formation on the Merced River (table 10).

The 40-ka soils on the lower member of the Modesto Formation have subsoil argillic horizons. The maximum value of the the horizon index in the B horizons of the soils of the lower member of the Modesto is 0.4, compared to 0.27 in B horizons of soils of the upper member (fig. 9B, C). The B-horizon maximum is more sharply defined in the soils of the lower member than it is in those of the upper member, because of greater clay accumulation (total texture and clay films) and more strongly developed soil structure (structure property).

The presence of a silty substratum and differences in parent material textures between replicate soil sampling sites of the lower member of the Modesto appears to have caused differences in soil development between sites. Two of the soils of the lower member formed in a coarse sandy loam parent material (fig. 9C, profiles 10 and 11), and the third soil formed in a silt loam parent material (profile 9). All three soils overlie a dense silt substratum, the sandy soils at about 2 m, the silty soil at about 1.3 m. The silt substratum restricted deep percolation of water and effectively stopped soil development beneath the discontinuity, in striking contrast to the deep development of the freely drained soils formed on the upper member of the Modesto (compare fig. 9B, C). In 40,000 years, the finer textured parent material in profile 9, which has a larger proportion of weatherable silt- and clay-sized minerals and a higher water

Table 9. Selected morphological and physical properties of the chronosequence soils

Geologic unit	B-horizon color ¹	Pedogenic clay formed ² (g/cm ²)	Total depth of weathering ³ (cm)
Holocene alluvium Modesto Formation	10YR 3/3	-1.6	40
Upper member	7.5YR 3/4	4.5	116
Lower member	5-7.5YR 3/4	9.3	150
Riverbank Formation			
Upper member	5YR 4/6	51.0	263
Lower member	2.5YR 3/6	43.9	>288
Laguna Formation			
Lower member	10R 3/6	105.5	>500

¹Reddest hue and highest chroma reported from B horizons of replicate soil profiles of each stratigraphic unit. A horizon colors used for Holocene soils.

²Calculation of pedogenic clay formed (g clay/cm² land surface/profile) based on: present clay content of each horizon, estimated original clay content of horizons, horizon thickness, and bulk density. Replicate soil profiles averaged.

³Depth of deepest A or AC horizon among Holocene replicate soils; average depth to bottom of Bw horizons used for soils on upper Member of Modesto Formation because of uncertainty as to bottom of solum; average depths to bottom of BC horizon or greatest depth exposed in BC material among replicate soils for all others.

⁴Depth of weathering restricted by subsoil lithologic discontinuity.

holding capacity, has formed a soil with a moderate argillic horizon and with a duripan above the shallow discontinuity. In apparently the same period of time, the sandy parent material in profiles 10 and 11, with a smaller proportion of weatherable silt- and clay-sized minerals and a lower water holding capacity, has formed soils with weak argillic horizons. These differences in B-horizon development are apparent in the plot of horizon index versus depth (fig. 9C) and also in the profile index: the average profile index for the sandy soils of the lower member of the Modesto is 48 index-cm, compared to 56 index-cm for the silty soil. By this measure, the difference in soil development due to difference in texture (and drainage) is about 17 percent at 40 ka.

The soils developed on the two members of the Riverbank Formation have strongly developed, clay-rich argillic B horizons, and significant soil development extends to more than 3 m (fig. 9D, E). The maximum value of the horizon index is similar in the B horizons of both members, about 0.52, compared to 0.4 and 0.27 in the B horizons of the soils of the lower and upper members of the Modesto, respectively. Lithologic discontinuities in soils of both Riverbank members were recognized from field evidence and particle-size data. The discontinuities, silt loam over sandy loam at 1.5 to 2 m in the upper member and loam over gravelly sandy loam at 2 m in the lower member, appear to control the position of maximum B horizon development (fig. 9D, E). Soil development beneath each discontinuity, as measured by the horizon index, decreases markedly with depth into the coarser materials. Retention of water in the finer sediments because of impeded percolation across the discontinuity appears to have concentrated soil development in the B horizons just above the lithologic break (compare figs. 8D, E and 9D, E).

Soils on the lower member of the Riverbank are distinct morphologically from those on the upper member: the

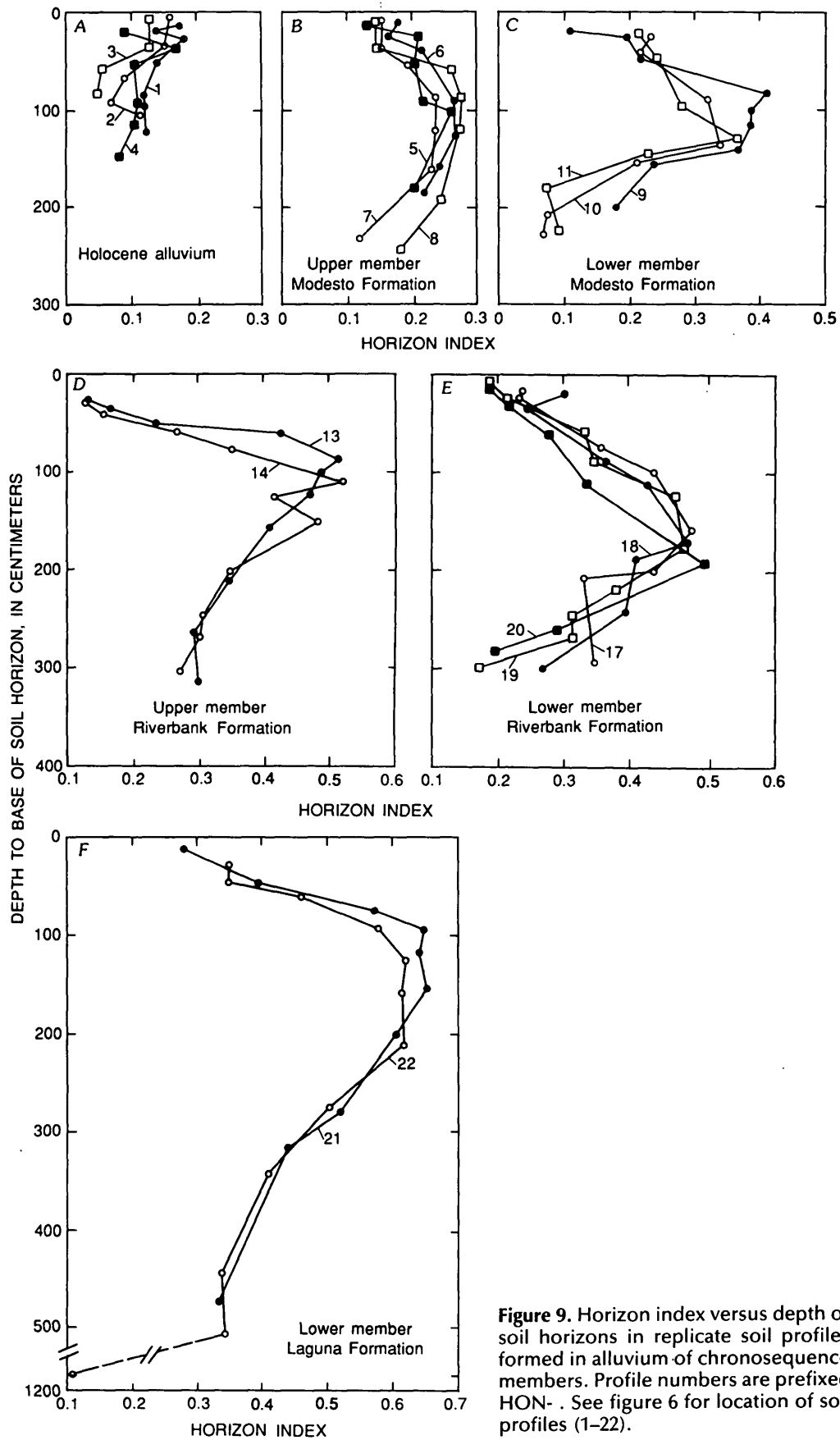


Figure 9. Horizon index versus depth of soil horizons in replicate soil profiles formed in alluvium of chronosequence members. Profile numbers are prefixed HON-. See figure 6 for location of soil profiles (1-22).

soils on the lower member are redder (table 9) and the position of maximum B horizon development is deeper than on the upper member. In the field, these differences were useful in distinguishing the two soils; nevertheless, in terms of the maximum value of horizon index (fig. 9D, E) and in terms of the profile index (table 10), the soils are quite similar in degree of development.

The exhumed soils formed on the lower member of the Laguna Formation display an extreme stage and depth of soil development (table 9); for example the horizon index reaches 0.65 in the B horizon, and it remains greater than 0.3 at a depth of 5 m in the soils (fig. 9F). Particle-size data show that these soils formed in uniform loam or sandy loam parent material (fig. 8F), and the horizon index depth plots indicate smooth changes in soil development from A to B to BC horizons. The average profile index for these soils is 223 index-cm (table 10), more than double the profile index of the next most strongly developed soils on the lower member of the Riverbank Formation.

The very great depth and extent of development of the soils of the lower member of the Laguna Formation is consistent with the geological evidence that the first 0.5 million years of their development, before burial, took place in the wetter climate of the late Pliocene. We might conclude that these soils are so strongly developed because of their early history. Perhaps the gravel abundance in these soils (up to 70 percent), with the attendant decrease in water holding capacity per unit of soil depth, also allowed deep percolation of the available soil water. We believe it likely, as argued by Arkley for a very deep soil in California (1981, p. 672), that the deep weathering of soils is increasingly a function of the wettest years as soils grow older, because with great age the total number of infrequent deep-wetting years becomes very large.

It is informative to overlay depth plots of the horizon index for all six chronosequence members (fig. 10). Each depth plot is an average of the replicate soil profiles for that member. When they are displayed in this way, the changes in soil morphology with age can be compared directly. The development of a B horizon manifests itself within 10,000 years and the B horizon becomes stronger, thicker, and better defined throughout the 1.6 million years of soil development studied here. Of the eight soil properties tracked in the index, clay films, structure, rubification, and total texture contribute most significantly to the increasing horizon index in B horizons.

A horizons do not appear to develop as systematically as B horizons over the full span of the chronosequence. The horizon index of A horizons does increase from Holocene soils to soils of the upper member of the Modesto to the soils of the lower member of the Modesto (fig. 10), largely due to melanization (decreasing color value) and rubification. The horizon indices of the A horizons of the soils of the upper member of the Riverbank are low, comparable to those in the Holocene soils. The A horizons of these soils have weak structure and are not very dark. There is

Table 10. Comparison of profile indices (in index-cm) for soils from Honcut Creek and the Merced River that are approximate stratigraphic equivalents

Geologic unit	Honcut Creek	Merced River ¹
Younger Holocene alluvium (<1000 yr)	12	17
Older Holocene alluvium (>3000 yr)	² —	24
Modesto Formation		
Upper member	45	27
Lower member	³ 51 (56)	69
Riverbank Formation		
Upper member	102	101
Lower member	⁴ 108 (113)	125
Turlock Lake Formation	² —	148
Laguna Formation		
Upper member	² —	⁵ 264
Lower member	⁵ 223	⁶ —

¹Data from Harden (1982a).

²No equivalent soil described at Honcut Creek.

³First value is average of two soils in coarse distributary channels of lower member and one soil in silty overbank materials of lower member. Second value from silty soil only, probably forms a more suitable comparison with soils developed in silt-loam materials on upper member of Modesto.

⁴108 is average of four replicate soils formed on middle member, 113 is average of two most strongly developed soils of four.

⁵Soil at Merced River was estimated by Marchand and Allwardt (1981) and Harden (1982a) to be 3.0 Ma; we estimate that soil at Honcut Creek is 1.6 Ma because, although deposit is older, it has been buried for part of that time. See text for discussion.

⁶No equivalent soil described at Merced River.

morphological evidence that lateral water flow is common in the horizons above the dense claypans. It is possible that leaching and eluviation extends nearly to the surface in these soils that have their argillic B horizons also very near the surface. In other words, these A horizons may be more like E (albic) horizons than A horizons in terms of dominant processes. If this is the case, we should not expect them to lie with the other soils in an ascending sequence of horizon indices. The horizon indices of A horizons of the lower member of the Riverbank and lower member of the Laguna continue in ascending sequence (fig. 10). The indices are large in these A horizons as a result of the development of rubification and structure, in addition to the properties melanization and pH that control the younger A horizons. The very red color and strong structure in the A horizons of the soils of the lower member of the Laguna may be a predictable result of extreme soil development. It is possible, however, that these A horizons formed in material that was once part of the B horizon due to the complex history of soil development, burial, exhumation, and renewal of soil development on the lower member of the Laguna Formation.

The profile indices of the chronosequence describe a smooth, concave-upward curve when they are graphed versus the log of soil age (fig. 11A) and a linear curve on a log-log plot (fig. 11B). The soils formed on Holocene alluvium, and on the Modesto, Riverbank, and Laguna Formations can be distinguished from one another at the 90 percent confidence level, calculated from the profile indices of the replicate soils on each formational member (fig. 11A). The soils formed on different members of the same formation cannot be distinguished from one another using the profile index because the confidence intervals of the indices overlap.

Our inability to distinguish differences in soil development at this level may be due to several factors. First, there could be errors in our age assignments; second, the soils could truly be indistinguishable due to the influence of other soil-forming factors, or due to variations in the rates of soil development with time that we do not understand, and third, the soil development index could itself incorrectly portray or bias our measurements of soil development. Sampling of additional replicate profiles presumably would narrow the confidence intervals for each soil. Lessening

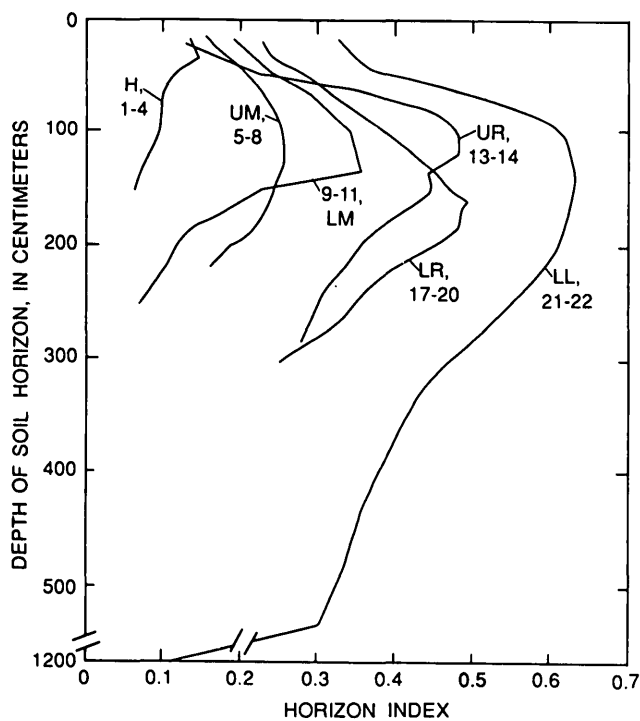


Figure 10. Composite depth plot showing soil development quantified by average values of horizon indices of replicate profiles calculated at 10-cm intervals for soils formed in Holocene alluvium (H), upper (UM) and lower (LM) members of the Modesto Formation, upper (UR) and lower (LR) members of the Riverbank Formation and lower member of the Laguna Formation (LL). Profile numbers are prefixed HON-. See figure 6 for locations of soil profiles (1-22).

the effect of within-member variation could serve to strengthen the soil correlations and also to test the ability of the profile index to resolve smaller differences in soil development.

The data in the profile index-age plots (fig. 11A, B) have a step-and-riser appearance. The two members of the Modesto Formation are not greatly different and form one step, the two members of the Riverbank Formation form another step, and there is a riser or apparent jump in soil development between the formations. Changing assumed soil ages does nothing to potentially improve the separability of the soils in the index, although it should change the fit of the points to the regression line.

Soils of the upper members of both the Modesto and Riverbank Formations appear to be more strongly developed than would be predicted for their ages. The Laguna-age soil could cause this if it is less strongly developed than it should be for its age (fig. 11B). Given the complex history of this soil and the fact that it was exhumed by erosion, our age estimate may be in error, or the soil may be less strongly developed than this age would predict due to the effect of erosion during exhumation.

The greater than predicted degree of development of upper member soils of the Modesto and Riverbank Formations may be caused by nonconstancy of the parent material or topographic factors. Both sets of upper member soils have formed in silt loam parent materials, in contrast to the coarser parent materials of the corresponding sets of lower member soils. Soil development in finer materials can be expected to be more rapid than in coarser materials because smaller mineral particles are more reactive and create soil aggregates that have greater water holding capacity. In addition, the soils of the upper member of the Riverbank were sampled at the base of a slope that descends from a terrace of the lower member because it was the best available site. Lateral flow of extra water into these soils from higher on the slope may have enhanced soil development. The soils on the upper member have skeletans (bleached sand and silt grains on ped faces) and other features of exaggerated leaching or ponding in the A and BA horizons, and have clay-textured Bt horizons. The profile indices of the upper and lower members of the Riverbank Formation are nearly identical at 102 and 108 index-cm, respectively. By this measure, the two sets of soils are indistinguishable. The soils of the upper member are as strongly or even more strongly developed than those of the lower member in terms of elemental depletion in the silt fractions (as shown below) and clay formed in the soil profile (Busacca, 1982). Although we believe that the topographic factor has contributed to the similarity of the soils developed on the two members of the Riverbank Formation, Harden (1982a, b) reported that the soils on upper and middle members of the Riverbank at the Merced River (correlated to our upper and lower members) also are nearly identical in development. Harden speculated that soil development reaches a temporary plateau in the age range

of the Riverbank Formation before continuing in older soils (J.W. Harden, oral commun., 1984). Without sampling additional sites on the upper member in places away from the terrace footslopes, we cannot test Harden's hypothesis. The soil development index itself may in some applications incorrectly portray soil development. For example, because horizon thickness is integrated into the various indices, failing to describe a soil to an adequate depth, or describing similar soils to different depths, may significantly underestimate or incorrectly estimate soil development. Busacca (1982) reported that when replicate profiles of a chronosequence member had been described to different depths, as might commonly occur for Holocene soils, the profile indices were widely different unless the calculations were corrected to similar depths. Harden and Taylor (1983) suggested that the influence of soil thickness can be partly eliminated if the property index or profile index is divided by the total depth of soil description. They called this the weighted mean profile or property index.

The influence of soil thickness on the profile index can be seen by comparing figure 11A and 11C. The profile index versus the log of soil age is strongly concave upward, while the weighted mean profile index versus the log of soil age is very nearly linear. The interaction of increasing soil thickness with increasing property development clearly leads to the strong upward curvature of the profile index (fig. 11A), and removing the effect of thickness gives a more appropriate assessment of the increase in soil properties alone with soil age (fig. 11C). Other differences appear as well. The step-and-riser appearance of the plot of Modesto and Riverbank soils is less pronounced when weighted means are used. In the case of the Riverbank Formation, the soils on the upper member were described to greater depths than soils on the lower member and the weighted means partially compensate for this. Finally, in the transformation to weighted mean values (fig. 11C), some of the replicate profiles appear to be outliers. The two circled points represent the coarse sandy profiles on the lower member of the Modesto. They are considerably less developed than is the soil of the same age formed in silt loam parent material. The weighted mean seems to emphasize the effect of parent material texture on soil development. The two points enclosed in a square represent soils formed on the lower member of the Riverbank Formation. These two soils, sampled from one trench, have an average profile index of 100 index-cm, compared to an average of 113 index-cm for the other two, sampled from a second trench. This difference, which is emphasized in the weighted mean estimate, suggests that there may be significant differences between the two sampling sites in site-specific variables such as erosion or parent texture.

The profile index of soils from the Honcut Creek chronosequence can be compared to the profile indices of the soils from the terraces of the Merced River 200 km to the south (table 10). Although the mineralogy and climate

of the two sites are somewhat different, the profile indices for equivalent stratigraphic units compare well, if discrimination of formations is the objective. If soils that are

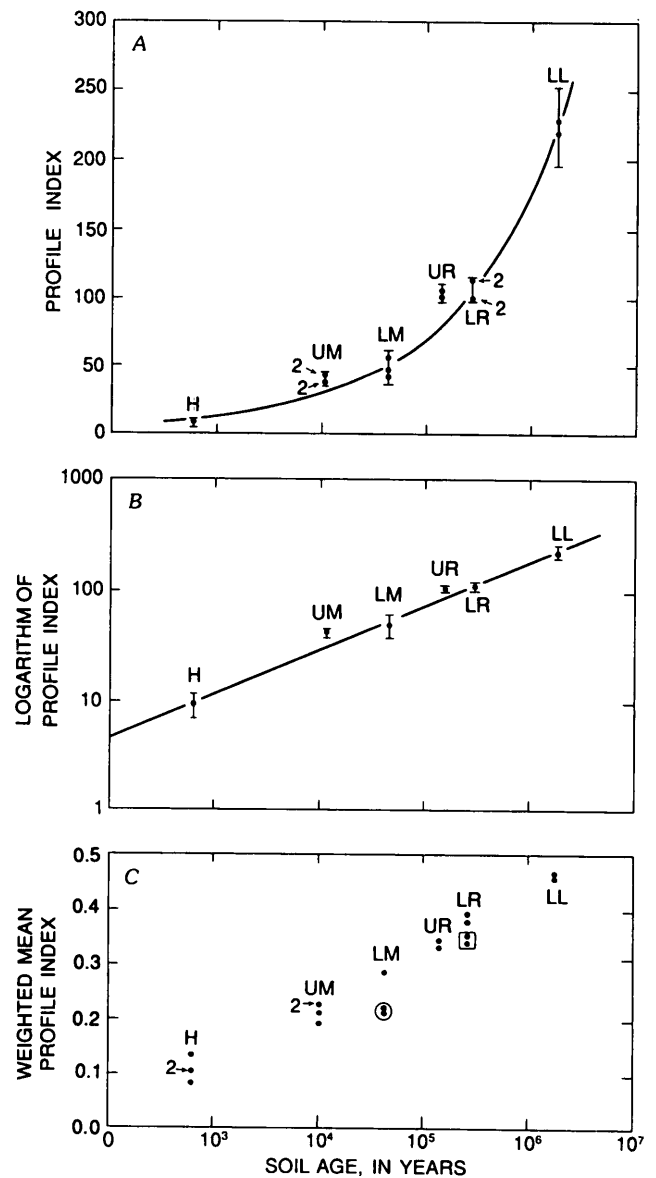


Figure 11. Age trend of soil development showing profile indices versus soil age. Bars are limits of 90-percent confidence intervals for replicate soils of each geologic unit (abbreviations same as in fig. 10). A, Soil age versus profile index. Each point represents one replicate soil except where numbers are shown because points are too close to plot separately. B, Logarithm of soil age versus logarithm of profile index. Each point is the mean of the replicate soils of that geologic unit. C, Soil age versus weighted mean profile index. Each point represents one replicate soil except where numbers are shown because points are too close to plot separately. Points in square and circle are less strongly developed soils formed in coarse-textured alluvium of lower members of Riverbank and Modesto Formations, respectively; see text for discussion.

thought to be correlated between the two areas have greatly different profile indices, the difference may be due to errors in correlation and must be investigated further. Differences between the two sites in the profile index of soils within members of formations may be due to unaccounted-for differences in climate, vegetation, parent material grain size and mineralogy, or even the depths to which the profile index was calculated.

Mineralogy of the Clay Fraction

The clay mineral assemblage in fresh stream sediment from Honcut Creek and in the parent material of older soils is diverse, and consists of vermiculite, kaolinite, smectite, mica, chlorite, and chloritized interlayer clays. This suite of minerals is progressively simplified with increasing soil age. Unstable clay minerals are transformed or dissolved and new, stable minerals are formed. The total quantity of clay in the A horizons does not appear to increase significantly with time, whereas the clay content of B horizons increases greatly due to translocation and neof ormation (formation in place). For example, B horizons in Modesto age soils have 15 to 25 percent clay, depending on parent material texture, and B horizons of the soils of the lower member of the Laguna have up to 54 percent clay.

We have plotted the progressive change in abundance of three of the principal clay minerals with soil age: smectite, kaolinite, and vermiculite (fig. 12A). These graphs are qualitative because they were determined by changes in peak heights on X-ray diffractograms, nevertheless, they portray the changes very clearly. Chlorite, mica, chloritized interlayer clays, and smectite are all progressively lost from A and B horizons with time. Vermiculite in the fine clay of A and B horizons is not present in young soils, reaches maximum abundance in soils of the lower member of the Modesto Formation and upper member of the Riverbank Formation, and then is not detected in the older soils (fig. 12A, C). Kittrick (1973) determined that vermiculite in soils is a fast-forming but unstable intermediate in the weathering of micas. We may be seeing in the soils of Honcut Creek the rapid transformation of fine-clay sized mica (probably biotite) to vermiculite in 10 to 40 ka, and the subsequent slow dissolution of the unstable vermiculite. It is the dominant coarse clay mineral in stream sediments and in the A and B horizons of soils up to those of Riverbank age. It then declines in abundance to trace amounts in soils of the lower member of the Laguna (fig. 12B, D). Vermiculite probably exists in the coarse-clay fraction of stream sediment due to pre-weathering of mica in soils of the sediment source areas. Vermiculite dominates the coarse-clay fraction in soils of the chronosequence until all of the parent mica has been transformed into vermiculite, and thereafter its abundance declines as it dissolves.

Kaolinite is found in moderate to abundant amounts in the stream sediment and in A and B horizons of the young

soils. It increases in abundance with increasing soil age and becomes the dominant clay mineral in both coarse- and fine-clay fractions of A and B horizons in the soils of the lower member of the Laguna. Because the absolute clay content in the B horizons increases with soil age to about 54 percent in these soils, we conclude that a considerable amount of new kaolinite has been formed in these soils over time. The weathering scheme displayed by the clay minerals in the soils of Honcut Creek is one of desilication, in

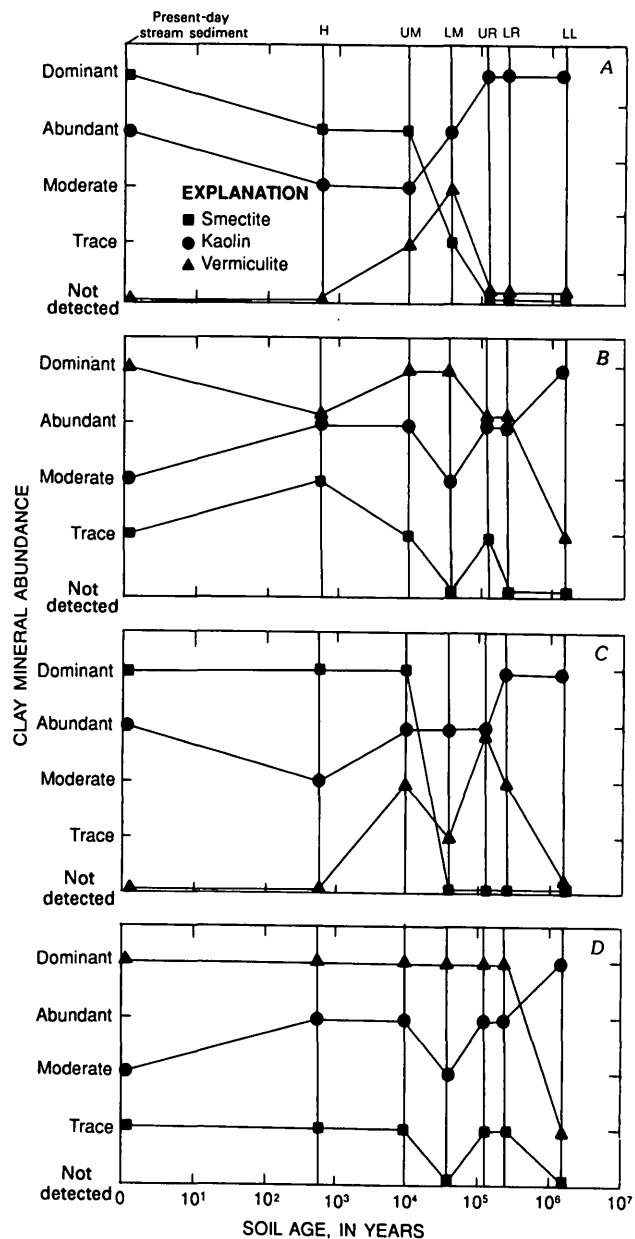


Figure 12. Relative abundance of clay minerals determined by X-ray diffraction versus soil age (abbreviations same as in fig. 10). A, Fine-clay fraction (<0.2 μm) of A horizons. B, Coarse-clay fraction (0.2–2.0 μm) of A horizons. C, Fine-clay fraction of B horizons. D, Coarse-clay fraction of B horizons.

Table 11. Relative enrichment and depletion of elements in the fine-silt fraction (2–20 μm) of A horizons of the chronosequence soils

Geologic Unit	Na ₂ O	MgO	Al ₂ O ₃	SiO ₂	K ₂ O	CaO	TiO ₂	Fe ₂ O ₃	Zr
Holocene alluvium Modesto Formation	1.00	0.98	0.97	1.03	1.05	1.01	0.88	0.97	0.92
Upper member	1.00	.79	1.03	1.01	1.07	1.05	1.06	.98	1.00
Lower member	.86	.82	.93	1.06	1.01	.96	.98	.86	1.07
Riverbank Formation									
Upper member	.73	.15	.89	1.17	1.45	.74	1.23	.72	1.83
Lower member	.60	.26	.93	1.08	1.53	.79	1.20	.78	1.57
Laguna Formation									
Lower member	.12	.14	.91	1.20	1.81	.22	1.23	.73	2.05

¹Calculated as ratio of element in A horizon to that element in C or BC horizon

which there is a progressive shift from 2:1 to 1:1 layer silicate clays and oxide clays with soil age.

Elemental Composition of Silt-Size Fractions

The sand and silt fractions of most soils are dominated by primary aluminosilicate minerals. Because most primary minerals are unstable at earth surface conditions, they are reactants in the weathering scheme of the soil and they supply elements from which secondary aluminosilicate clays and oxide clays are formed. The dissolution of primary minerals also releases a substantial part of the soluble fraction of elements that are lost completely from the soil by leaching. The vertical gradients of temperature, moisture, and biological activity in the soil create vertical gradients of mineral weathering. The stabilities of the common primary minerals vary greatly at the earth's surface, as demonstrated long ago by Goldich (1938), Reiche (1950), and others. Elements that are abundant in weatherable minerals are released at higher rates than elements that are abundant in weathering-resistant minerals. As soil development proceeds, some elements and minerals become depleted relative to others in the soil's framework, and a hierarchy of weathering is created.

We analyzed the elemental composition of the fine- and coarse-silt fractions (2–20 μm and 20–50 μm , respectively) using energy-dispersive X-ray fluorescence (XRF) spectroscopy to examine the changes in these reactive size fractions as a function of soil age. We analyzed only one of the replicate soil profiles from each member of the chronosequence (supp. table 6) because of time and budgetary constraints. We also analyzed the silt-plus-clay fraction (<50 μm) of selected A, B, and C horizons from each member of the chronosequence (supp. tables 5, 7), but we do not discuss these data here.

Four major elements, Si, K, Ti, and Zr, become enriched in the silt fractions of A and B horizons with increasing soil age, whereas five major elements become depleted (table 11). The enrichment of Si, K, Ti, and Zr is

relative, not absolute, and results from the fact that these elements occur in minerals that resist weathering. The weathering-resistant minerals are progressively concentrated with increasing soil age as other more weatherable minerals are destroyed.

The relative enrichment of Si in silt fractions with increasing soil age is not due to silicon-bearing minerals being absolutely stable to weathering. Quartz dominates the fate of silicon because of its moderately high resistance to weathering and its abundance in these soils. It acts as a reservoir of Si. Silicon is lost from the silt fractions in an absolute sense during pedogenesis, as confirmed by Si/Zr ratios of silts in soil horizons (table 12). Absolute losses of Si occur because of the dissolution of feldspars, ferromagnesian minerals, and quartz.

Titanium and potassium also become enriched in a relative sense in the silt fractions of A and B horizons with increasing soil age (table 11), although they too are lost from the silt when measured against Zr as a stable element (table 12). The loss of titanium from weathering of sphene and rutile is important to note in these soils (the Ti/Zr ratios in the soils of the lower member of the Laguna show more than 40 percent loss of Ti) because Ti has been used as a stable element in stable index element studies, although some researchers have found that Ti may be mobilized or lost during pedogenesis (Sudom and St. Arnaud, 1971; Evans and Adams, 1975; Smeck and Wilding, 1981). The relative concentration of K in the silt fraction is unexpected because the most probable source of K is biotite and possibly K-feldspar. Ratios of K to Zr in fine silt of the A, B, and C horizons of the soil of the lower member of the Laguna (table 12) indicate that only about 15 percent of the original K has been lost relative to Zr in 1.6 million years of soil development.

When element loss or gain from the silt fractions is judged by examining the ratios of one element to another, zirconium is found to be the most stable element of the 18 elements in the original analysis group. This is shown for eight major elements in the soil of the lower member of the

Table 12. Ratios of elements to zirconium ($\times 10,000$) in fine-silt fraction (2–20 μm) of selected horizons of soil formed on lower member of Laguna Formation (HON-21)

Horizon	Na ₂ O/Zr	MgO/Zr	Al ₂ O ₃ /Zr	SiO ₂ /Zr	K ₂ O/Zr	CaO/Zr	TiO ₂ /Zr	Fe ₂ O ₃ /Zr
A	24.4	29.0	674	2337	57.6	41.2	56.1	307
Bt1	8.9	27.3	660	2339	57.2	13.3	55.4	275
Bt4	0	22.2	889	2460	59.5	5.7	58.3	371
3BC	61.1	50.3	1471	3008	64.7	58.7	60.5	786
C	250.0	427.0	1498	4073	67.2	355.0	94.5	855

Laguna in table 12. The ratios of these eight elements to Zr are uniformly smaller in all A and B horizons than in the C horizon, indicating net losses in the upper horizons. This pattern of element loss in upper horizons is also found in the soils of the Riverbank Formation; it is expressed for some elements and some horizons of the soils of the Modesto Formation; and element loss is not discernible over the noise related to stratification in the Holocene soil.

Some elements such as Na, Mg, and Ca have been almost totally depleted from the silt fractions of the Riverbank- and Laguna-age soils. For example, the Bt1 and Bt4 horizons of the Laguna-age soil have Na/Zr ratios of 8.9 and 0.0 compared to a ratio of 250 in the C horizon (table 12). Large losses of the alkali and alkaline earth cations are presumably linked to the high weatherability of the ferromagnesian minerals and Na- and Ca-feldspars.

Zirconium is the most highly enriched element in the silt fractions with increasing soil age as a result of greater losses of all other elements relative to Zr. Some Zr also must be lost from the silt fraction during mineral weathering, but we have no way to measure this. Concentration factors for Zr (ratio of average Zr concentration in uppermost three horizons to average Zr concentration in lowermost three horizons) are about 1 in the Holocene soil and soil of the upper member of the Modesto, 1.1 in the soil of the lower member of the Modesto, about 1.6 in the soils of the Riverbank Formation, and about 2.1 and 3.1 in the soil of the lower member of the Laguna (table 13).

Simple plots or regressions of the relative change in elemental concentrations or in elemental ratios with soil age are useful in examining the marked changes in the silt fractions. They are difficult to use, however, in a quantitative analysis because of stratification of parent materials within profiles, and because of differences in parent material composition between chronosequence members. For example, changes in the relative concentration of K or Ca that might have resulted from soil development are hard to interpret because the parent material content of K and Ca varies by as much as a factor of 2 between soils (table 8). Some of the changes in element concentrations with soil age are striking in spite of this problem. For example, Mg has been far more extensively lost from the silt fractions of the soils of the Riverbank Formation than has Na (table 11). Even from these qualitative changes, we can begin to interpret the dynamics of weathering of different primary minerals.

The principal effect of soil age does dominate the secondary effects of parent material heterogeneity for some simple expressions of elemental content. For example, Si increases systematically in silt fractions of surface horizons with increasing soil age due to the very complete weathering losses of other elements (fig. 13). This pattern is similar to those for Ti, Zr, and K, which also become enriched in surface horizons, although it is more systematic than these others. The regularity of the age trend of increasing Si content is interrupted by the high value of the upper member of the Riverbank Formation. Once again the soil of the upper member appears to be more strongly developed than that of the lower member, and we again must speculate about the added influences of parent material or topographic factors. Our ability to interpret these kinds of plots is hampered because we do not have analyses of the replicate soils for each chronosequence member as we did in the case of the soil development index.

The element zirconium and the mineral zircon have been used previously as stable indices by which changes in other elements or minerals can be gauged (for example, Barshad, 1964; Drees and Wilding, 1978; Smeck and Wilding, 1981; Harden, 1987). Age trends of elements compared to Zr are systematic for the Honcut Creek soils. This is especially true of the ratio Fe/Zr in the fine silt fraction of surface horizons (fig. 14). This age trend is one of the clearest derived from a simple elemental ratio, and we think that the reason is that Fe/Zr ratio is less affected by stratification of particle-size than is any other elemental ratio or particle-size ratio, and the fine silt is less affected by stratification than is the coarse silt (table 6). We believe that the changes in this ratio with soil age reflect dominantly pedogenesis and not parent material heterogeneity.

Because of the problems encountered in interpreting simple element abundances or ratios, we calculated losses of elements from the silt fractions by using Zr as a stable index. The differences in parent material composition between soils dictated that any calculation of change within a soil would have to be based on, or normalized to, the initial composition of that soil, not on an average parent material composition for all soils. The most simple and direct calculation of change in elemental composition is:

$$\text{Percent remaining} = \frac{\text{El}_h \times R_{pm}}{\text{El}_{pm} \times R_h} \times 100$$

where El is the element of interest; R is the stable or resistant component, Zr in our case; h is the horizon in which the loss is being calculated; and pm is the parent material; and percent remaining is the percentage of the original content of an element remaining in a soil horizon. A similar calculation of percent loss was first used by Merrill (1921) and has also been used by Harden (1982b; 1987). We used Zr as the stable component because all

Table 13. Concentration ratios for zircon (average concentration in upper three horizons/average concentrations in lower three horizons) in fine- and coarse-silt fraction of chronosequence soils

Geologic unit	Fine silt (2-20 μm)	Coarse silt (20-50 μm)
Holocene alluvium	.96	¹ 1.00
Modesto Formation		
Upper member	.99	.90
Lower member	1.08	1.10
Riverbank Formation		
Upper member	1.78	² 1.63
Lower member	1.48	² 1.58
Laguna Formation		
Lower member	³ 2.08	³ 3.11

¹2C horizon only was used in denominator because stratification strongly affects Zr concentration in two lowest horizons; see table 8 and text for discussion.

²A denominator value of 260 ppm Zr was used because stratification strongly affects Zr concentration in deep horizons; 260 ppm is concentration of Zr in fresh stream sediment on Honcut Creek.

³Lowest horizon only was used in denominator because Zr concentrations of next higher horizons are strongly affected by element loss.

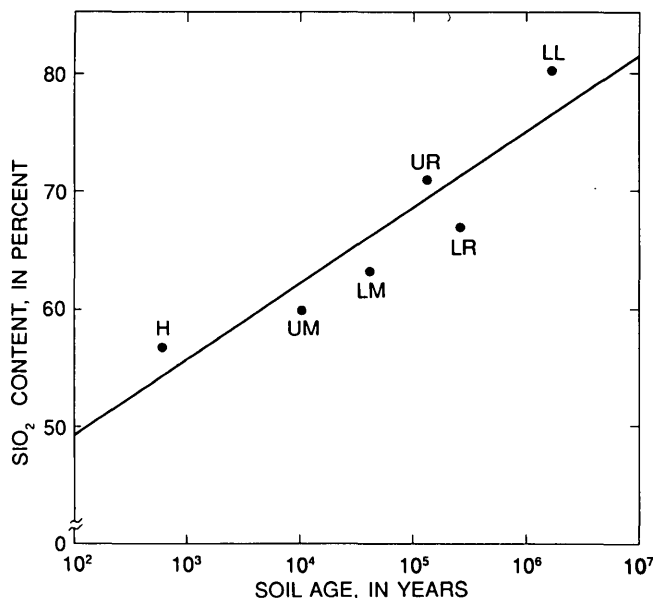


Figure 13. SiO_2 in coarse-silt fraction (20-50 μm) of surface horizons versus soil age; r^2 for linear regression is 0.84 (abbreviations as in fig. 10).

other elements that we analyzed decreased in A and B horizons with soil age when compared to Zr. The assumption in this equation is that the initial distribution of Zr and the element of interest was uniform throughout the soil profile. Our analysis of the stratification in Holocene soils and soils of the Modesto Formation above indicates that this assumption is more reasonable for the elemental distribution in the fine silt than in the coarse silt. We do not assume in this equation that the composition of the parent materials is uniform between chronosequence soils, because each soil is compared only to its own parent material. We used the average elemental concentrations in deep BC or C horizons (table 8) as parent material in these calculations. This method proved valuable in assessing rates of element loss from the soils. The calculated data on percentage of the original content of an element remaining can be considered as depth functions of elemental loss within profiles and as comparisons of loss in A or B horizons with soil age, and can be used to compare relative rates of loss of different elements.

Holocene soils and soils of the upper member of the Modesto provide a check on the method because changes due to soil development are minimal. For example, consider the calculations of "percentage remaining" for eight elements in the fine silts of the Holocene soil (table 14). For Al, Si, Ca, Ti, and Fe, the values range from 92 to 106 percent and cluster around 100 percent as we would expect in an undeveloped soil. Sodium, magnesium, and potassium show more serious effects of stratification. The average of the percentage-remaining values for six horizons and eight elements in table 14 is 99.7 percent. Iron displays values very close to 100 percent for all horizons of the Holocene soil (table 14), and as we have found previously, it appears to be one of the best elements to use in profile reconstructions with Zr. A sedimentological fining-upward pattern in the Holocene and other soils affects Zr in particular, and leads to a subtle depth trend in the fine silt in

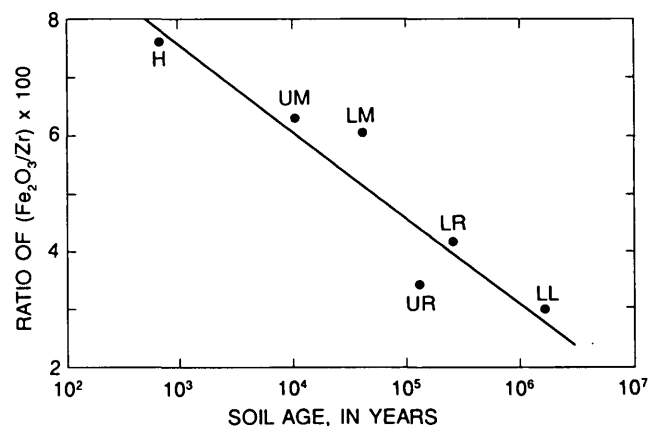


Figure 14. Ratio of Fe_2O_3 in percent to Zr in ppm $\times 100$ in fine-silt fraction (2-20 μm) of surface horizons versus soil age; r^2 for linear regression is 0.89 (abbreviations as in fig. 10).

Table 14. Effect of stratification on the calculation of percentage of original content of elements remaining in the fine-silt fraction (2–20 μm) of a Holocene soil using Zr as a stable index

[If stratification did not affect the index calculation, all values would theoretically be 100]

Horizon	Basal depth (cm)	Percent remaining							
		Na ₂ O	MgO	Al ₂ O ₃	SiO ₂	K ₂ O	CaO	TiO ₂	Fe ₂ O ₃
C	17	103	111	100	101	111	104	104	102
2A	32	95	98	101	102	105	101	97	100
2AC	49	117	103	103	106	101	103	97	100
2C	86	93	95	101	100	98	101	96	101
3C1	113	103	99	98	97	93	97	100	101
3C2	147	88	92	96	92	92	92	102	95

which percentage-remaining values tend to be larger than 100 percent in surface horizons and less than 100 percent in deeper horizons. The trend is more pronounced for some elements than others, and is a serious problem for reconstructions of some elements in the coarse silt. It can be detected in depth plots because its trend is opposite that expected for changes in composition caused by mineral weathering and soil development.

Calculations of percentage of the original content of elements remaining using Zr as a stable index confirm that all elements that we analyzed in both silt fractions are progressively depleted in A and B horizons with increasing soil age (tables 15, 16). Different elements behave differently over the course of soil development and are depleted to different extents over the 1.6 million years of soil development.

Titanium, potassium, and of course zirconium have the smallest percentage losses of the elements in tables 15 and 16. Potassium is very puzzling in its persistence in the silt fractions. Surface horizons of the soils of the lower member of the Laguna retain 84 percent of the original K in the fine silt (table 15) and 57 percent in the coarse silt (table 16). Biotite and possibly small amounts of K-feldspar are the most likely source of K, and both of these minerals would be expected to undergo more severe dissolution in 1.6 million years. The retention of K in primary mineral fractions has also been documented by Harden (1982b) for soils of the Merced River area that contain abundant K-feldspar and muscovite. Weathering losses of Ti, like K, are greater in the coarse silt than fine silt; about 48 percent of the original Ti remains in the coarse silt (table 16), about 58 percent in the fine silt (table 15). Ti is depleted to a depth of more than 4 m in the soil of the lower member of the Laguna. The extent and depth of Ti loss relative to Zr clearly indicates that Ti is mobile in this weathering environment and is unsuitable as a stable index element. The differences in the pattern of loss of Ti with soil age in the coarse versus the fine silt suggest further that two different Ti-bearing minerals with different solubilities may dominate, one in the fine fraction, another in the coarse.

Silicon, aluminum, and iron have weathering losses that are intermediate in extent between the relatively stable

Zr, Ti, and K, and the very unstable Mg, Ca, and Na. The sequential loss of Fe and Al from soil horizons with soil age can be seen in depth plots of element loss in which all 6 chronosequence soils are overlaid (fig. 15A, B).

Holocene soils and soils of the upper member of the Modesto do not show any loss of Al that can be detected over the influence of stratification, but the fine-silt fraction of the 40-ka soil of the lower member of the Modesto has lost about 10 percent of its Al (fig. 15A). About 25–50 percent of the Al has been weathered from the fine silt in the upper 1.5 m of the two Riverbank soils; again the upper member is more strongly weathered than the lower member. As much as 54 percent of the Al in the fine silt and 83 percent in the coarse silt have been weathered from the upper 2 m of the 1.6-Ma soil of the lower member of the Laguna Formation (tables 15 and 16).

The great depth of depletion of elements such as Mg and Ca (fig. 15C, D) in the soil of the lower member of the Laguna could lead to the conclusion that this soil formed under a much wetter, more deeply leaching climatic regime in the late Pliocene than that experienced by any of the younger soils. This assumption is challenged by the depletion patterns of Al and Fe, which are very similar in depth and extent of loss to patterns for these elements in the younger soils. Surprisingly, between depths of 3 and 5 m in the soil of the lower member of the Laguna, Al and Fe in the fine silt actually reach about 125 and 116 percent of original content in the parent material. Either stratification has caused a major error in the profile reconstructions or there has been an actual enrichment of these elements in the fine-silt fraction. This part of the profile coincides with a plinthite-like zone that has red and white reticulate mottling, and we initially concluded that Fe and Al hydrous oxides had crystallized into silt-sized particles at this depth. A pilot study using X-ray diffraction and scanning electron microscopy so far has failed to support this hypothesis, and so its cause is still not known.

The overall pattern of Fe loss from fine silt is similar to that of Al. Note that the depth plots for Fe and Al in the Holocene soil and soil of the upper member of the Modesto (fig. 15A, B) indicate that stratification is not a major problem for reconstructions based on these elements. The

Table 15. Percentage of original content of elements remaining in the fine-silt fraction (2–20 μm), calculated using Zr as a stable index

[Values are averages of the upper three horizons]

Geologic unit	Percent remaining							
	Na ₂ O	MgO	Al ₂ O ₃	SiO ₂	K ₂ O	CaO	TiO ₂	Fe ₂ O ₃
Holocene alluvium	105	104	101	103	106	103	100	101
Modesto Formation								
Upper member	92	80	101	101	105	107	106	99
Lower member	87	84	89	93	100	83	95	88
Riverbank Formation								
Upper member	38	9	52	66	77	38	71	41
Lower member	42	14	62	70	110	56	78	49
Laguna Formation								
Lower member	9	7	46	52	84	10	58	36

Table 16. Percentage of original content of elements remaining in the coarse-silt fraction (20–50 μm), calculated using Zr as a stable index

[Values are averages of the upper three horizons]

Geologic unit	Percent remaining							
	Na ₂ O	MgO	Al ₂ O ₃	SiO ₂	K ₂ O	CaO	TiO ₂	Fe ₂ O ₃
Holocene alluvium	103	99	99	100	100	98	94	96
Modesto Formation								
Upper member	109	108	107	110	109	117	114	105
Lower member	95	86	91	95	91	94	98	93
Riverbank Formation								
Upper member	51	75	7	75	80	50	52	46
Lower member	50	10	60	73	84	60	54	55
Laguna Formation								
Lower member	7	41	7	44	57	8	48	22

increase in Fe content in the middle horizons of the 10-ka soil of the upper member of the Modesto may actually be from secondary Fe oxide coatings precipitated on mineral grains in the cambic B horizon of this soil. Loss of a few percent of Fe seems clear in the soil of the lower member of the Modesto, and depletion continues through the 1.6 million years of soil development.

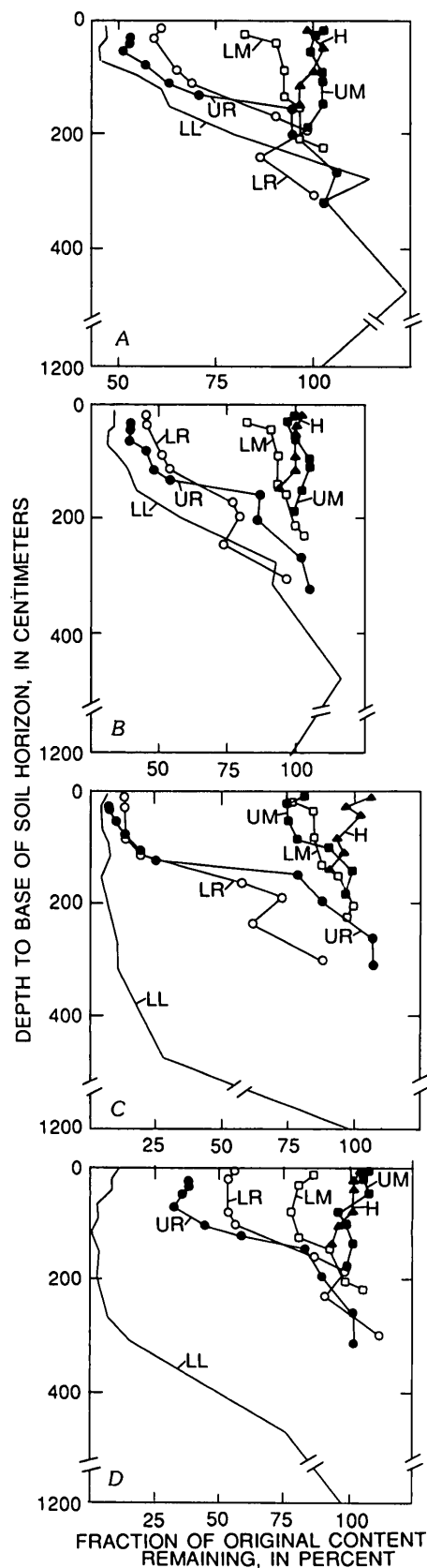
Sodium, magnesium, and calcium are rapidly and extensively depleted from the chronosequence soils because they are bound in the highly weatherable ferromagnesian and Na-Ca feldspar minerals. The “reverse trend” in depth plots caused by fining upward, and the effect of stratification, can be seen for Mg and Ca in the Holocene soil (fig. 15C, D). Magnesium is the most rapidly depleted of the three elements: substantial Mg appears to have been lost from fine silt of the 10-ka soil of the upper member of the Modesto (fig. 15C, table 15), whereas no loss of Ca is evident in the same soil (fig. 15D). Within 130,000 to 250,000 years, Mg-bearing minerals have been virtually eliminated from fine silt in the upper 1.5 m of the soils of the Riverbank Formation. Calcium and sodium are far less

depleted from these same soils (fig. 15D, tables 15 and 16). Calcium, sodium, and magnesium are virtually absent in the fine silt of the upper 4 m of the soil on the lower member of the Laguna Formation.

Profile reconstructions in the coarse-silt fraction are beset by problems of stratification, which obscure the age trends to a greater degree. Some elements appear to behave differently in the two fractions, and these differences may result from the complexity of the size changes that particles undergo as they dissolve or fracture with soil age, or from the possibility that an element is bound principally in one mineral in one size fraction and in another mineral in the other fraction.

The depth of total weathering increases systematically with soil age (table 9), but each element has its own depth-depletion trend (fig. 15A–D). The lithologic discontinuities in the soils of the Riverbank have acted as barriers to deeper elemental losses, and this complicates the results.

Weathering intensities appear to be greatest from about 40 to 150 cm, and less at the surface (see, for example, fig. 15D). The horizons just beneath the soil surface may remain



moist more of each year than those at the surface and become more weathered, but we cannot eliminate the possibility that eolian dust has rejuvenated the mineral suite in the surfaces.

Linear regressions of percentage of an element remaining versus the log of soil age yields results that are comparable to those based on simple relative enrichment or depletion. The trends of element depletion for the major elements in the fine silt are all significant at between the 5 and 1 percent levels, with coefficients of multiple determination (r^2) of between 0.78 and 0.86. The slopes of the linear regressions with respect to the log of soil age for Si, Fe, Na, and Mg are in the order of increasing rate of element release from the silt fractions of the Honcut soils (fig. 16A–D). For Si and Fe, elements that are less strongly influenced by parent material heterogeneity, and for Na, element loss with soil age is very systematic. However, in each of these plots (fig. 16A–D), the soil of the upper member of the Riverbank flaws this pattern and adds further suspicion that topographic and parent material factors have strongly influenced its development.

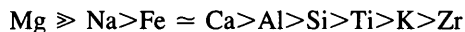
The lack of elemental analyses for the replicate profiles of each member is the greatest limitation to the use of this data in soil correlation. Without the replicates, we cannot estimate confidence intervals of element loss for each member. Analysis of a limited number of replicate soil horizons during XRF methods testing suggested that elemental chemistry would be about as useful as the soil development index in discriminating geologic formations and members by the properties of their soils.

The soil age trends for Si, Fe, Na, and Mg and others not shown suggest that a particular element may be well suited in the correlation of soils in one particular age range and not well suited in other ranges. For example, because of the very large decrease in Mg between 40 and 130 ka, this element may work well to discriminate soils on the Modesto Formation from those on the Riverbank (fig. 16D), whereas Na may be most useful to discriminate soils of the Riverbank from those of the Laguna Formation (fig. 16C).

We examined the element release calculations and determined a mobility or release series for elements in the silt fractions. We used the average element release values for the Riverbank Formation (tables 15 and 16) because depletion is nearly total for several elements in the 1.6 Ma

Figure 15. Fraction of original content of elemental oxides remaining (calculated relative to Zr) in fine-silt fraction (2–20 μm) versus soil depth (0–1200 cm). A, Al_2O_3 ; B, Fe_2O_3 ; C, MgO ; D, CaO . Results over 100 percent due to stratification of parent alluvium and possibly pedogenic accumulation (see text for discussion).

lower Laguna soil. The mobility series are different for the two silt fractions. In the fine silt (2–20 μm):



In the coarse silt (20–50 μm):



The series also is somewhat changed if other time ranges are used. Polynov's (1937) series is $\text{Ca} > \text{Na} > \text{Mg} > \text{K} > \text{Si} > \text{Al} > \text{Fe}$; however, it is based on the ratio of an element in ground water to that element in unweathered bedrock. It is a measure of the elements that escape entirely from the soil by deep leaching. Our series is based only on rate of release from primary minerals in soils and does not take into account the later fate in the soil of those elements, such as Fe, Al, and Si, that are strongly complexed in clay minerals that form concurrent with weathering of primary minerals in the soil profile.

Summary of Trends in Soil Development and Their Use in Soil Correlation

Soils formed on relatively uneroded alluvial terraces at Honcut Creek change systematically with increasing soil age. Differences in soil development here can be used, with some caution, to correlate deposits from site to site in the local area, and to test age correlations with soils and deposits in other areas. Soils on the different deposits can be recognized in the field by key differences in morphology with time: (1) reddening of color hue in B-horizons, (2) increasing depth to fresh parent material, (3) increasing distinctiveness of soil horizons, and (4) sequential development of A horizons, cambic B, weak argillic B, strong argillic B, and extremely strong and thick argillic B horizons. The soil development index of Harden (1982a) integrates many of these properties in a numerical index that can be used in the field. As we gathered stratigraphic and geomorphic evidence of the formations and members, we were able to use the distinctive characteristics of the soils and the soil-landscape patterns to map the distribution of each formation in detail. We used soil morphology, which is the basis for defining soil series, to distinguish between members of a formation in the field (table 2) even when we later found that some quantitative laboratory measures of soil development, such as elemental depletion, failed to do so. For example, we found that the Kimball and Yokohl series soils are consistently associated with the upper member of the Riverbank Formation, and the Kimball-deep variant with the lower member.

At this time, the soil development index of Harden (1982a) is the most useful single measure of soil development that we have tested for distinguishing soils formed on

deposits of different ages. This is in part because it was designed specifically for comparisons of the degree of soil development versus age. Using the index, we have been

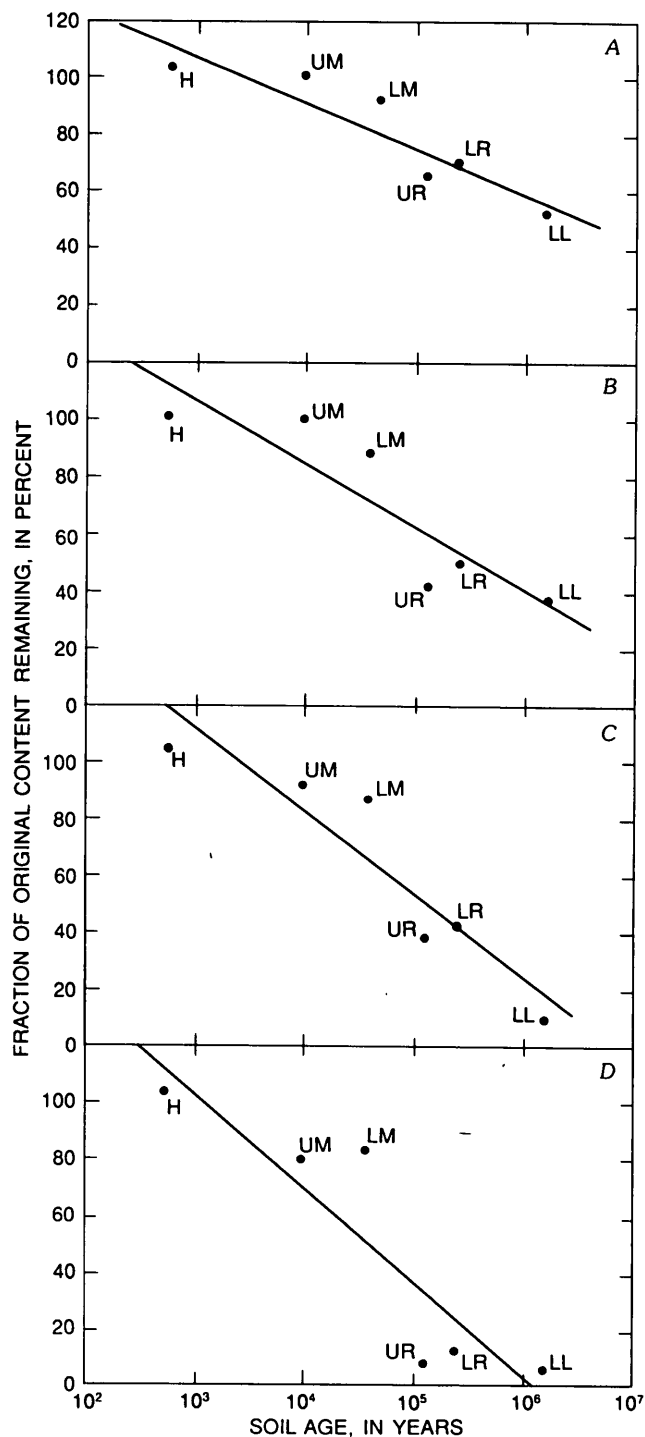


Figure 16. Fraction of original content of elemental oxides remaining (calculated relative to Zr) in fine-silt fraction (2–20 μm) of surface horizons versus soil age (abbreviations as in fig. 10). A, SiO_2 , r^2 for linear regression is 0.84. B, Fe_2O_3 , r^2 is 0.78. C, Na_2O_3 , r^2 is 0.86. D, MgO , r^2 is 0.79. Results over 100 percent due to stratification of parent alluvium.

able to distinguish between the soils developed on the four major alluvial deposits (Holocene, Modesto, Riverbank, and Laguna); however, we are not able to distinguish statistically significant differences in soil development between members of the same formation. We believe that this is the result of uncontrolled variation in other soil-forming factors, principally parent material grain size and mineralogy, and topography, and not of major errors in our stratigraphic or age interpretations. Weighted mean profile indices, which factor out soil depth differences, appear to improve the ability of the soil development index to differentiate small differences in soil development. The small area of the Honcut Creek flood plain and terraces would make it difficult to find new sampling sites at which parent material and topographic factors would be more closely matched, in order to further test the development index.

We offer a comparison of the profile index calculated for soils from Honcut Creek with those calculated by Harden (1982b) for soils on the terraces of the Merced River 200 km to the south (table 10). Profile indices of soils in the two areas match reasonably well when discrimination of formations is the objective. This can be considered to be a test of age and stratigraphic correlations between these two areas. The differences in profile index values between correlative members of formations in the two areas may be due to differences between sites in climate, vegetation, and parent material grain size and mineralogy. The differences may also be significant with respect to soil age assignments and may call certain correlations into question.

Changes in clay mineralogy with soil age reveal much about the developmental history of these soils but are of limited use in correlation studies because they are at best qualitative measures of the minerals present, and because minerals in the clay fraction are, by their nature, both reactants in and products of the pedogenic process.

We believe that depletion of elements from the weathering of primary minerals in silt-sized fractions is a fruitful area of research, both for what we can learn about mineral weathering and soil formation and for its potential in soil correlation. The relationships with soil age tend to be simple and unidirectional because the silt (and sand) fractions are reactants in the weathering process and the scheme is one of loss over time.

X-ray fluorescence analysis of the silt fractions documented systematic changes in soil development over time. Si, Ti, K, and Zr tend to become enriched in silt fractions with increasing soil age because of very complete weathering removal of Ca, Mg, Na, and to a lesser extent Fe and Al. Zr is the most stable element in the silt fractions by a factor of up to 3 in the near-surface horizons of the soil of the lower member of the Laguna. Calculations of change in elemental composition with respect to Zr used as a stable index are successful, and the changes can be evaluated with depth in each soil, or with soil age in selected horizons of all soils.

Trends of element depletion with soil age are systematic for those elements and elemental ratios in which parent material heterogeneity does not cause major interference. Silicon and iron, and calculations of change in these elements with respect to Zr yield among the best results. Lack of X-ray fluorescence data from our replicate soil profiles made it impossible for us to test soil correlations statistically, but we believe that if replicate data were available, elemental chemistry would discriminate geologic formations and members as well as or better than the soil development index.

Profile morphology, clay mineralogy, and elemental chemistry reveal similar, systematic changes in the chronosequence of soils at Honcut Creek. This indicates to us that the major pedogenic processes acting under the climates, parent materials, and vegetation at Honcut Creek are progressive over the 1.6-million year estimated span of soil development rather than cyclic or intermittent. Progressive changes are significant because they provide the best indices of soil and landscape age, and because they provide information about the pedogenic processes that drive soil development over long periods of time.

REFERENCES CITED

- Anderson, C.A., 1933, The Tuscan Formation of northern California with a discussion concerning the origin of volcanic breccias: University of California Publications, Department Geological Science Bulletin, v. 23, p. 215-276.
- Anderson, C.A., and Russell, R.D., 1939, Tertiary formations of the northern Sacramento Valley, California: California Journal of Mines and Geology, v. 35, no. 21, p. 219-253.
- Arkley, R.J., 1954, Soils of eastern Merced County: University of California Agricultural Experiment Station Soil Survey no. 11, 174 p.
- 1962, The geology, geomorphology, and soils of the San Joaquin Valley in the vicinity of the Merced River, California: California Division of Mines and Geology Bulletin 182, p. 25-32.
- 1981, Comments on "Genesis of a Typic Durixeralf of Southern California": Soil Science Society of America Journal, v. 45, p. 672.
- Atwater, B.F., Adam, D.P., Bradbury, J.P., Forester, R.M., Mark, R.K., Lettis, W.R., Fisher, G.R., Gobalet, K.W., and Robinson, S.W., 1986, A fan dam for Tulare Lake, California, and implications for the Wisconsin-glacial history of the Sierra Nevada: Geological Society of America Bulletin, v. 97, p. 97-109.
- Axelrod, D.I., 1971, Fossil plants from the San Francisco Bay region, in Geologic guide to the northern Coast Ranges, Point Reyes region, California: Geological Society of Sacramento Annual Field Trip Guidebook, p. 74-86.
- 1980, Contributions to the Neogene paleobotany of central California: University of California Publications in Geological Sciences, v. 121, 212 p.
- Barshad, Isaac, 1964, Chemistry of soil development, in Bear, F.E., ed., Chemistry of the soil: New York, Reinhold, 515 p.

- Beckett, P.H.T., and Webster, R., 1971, Soil variability, a review: *Soils and Fertilizers*, v. 34, p. 1–15.
- Birkeland, P.W., 1984, *Soils and geomorphology*: New York, Oxford University Press, 372 p.
- Birkeland, P.W., and Shroba, R.R., 1974, The status of the concept of Quaternary soil-forming intervals in the western United States, in Mahaney, W.C., ed., *Quaternary environments, proceedings of a symposium: Geographical Monographs*, no. 5, p. 241–276.
- Bryan, Kirk, 1923, *Geology and ground water resources of the Sacramento Valley, California*: U.S. Geological Survey Water-Supply Paper 495, 285 p.
- Burke, R.M., and Birkeland, P.W., 1979, Reevaluation of multiparameter relative dating techniques and their application to the glacial sequence along the eastern escarpment of the Sierra Nevada, California: *Quaternary Research*, v. 11, no. 1, p. 21–51.
- Busacca, A.J., 1982, *Geologic history and soil development, northeastern Sacramento Valley, California*: Davis, University of California, Ph.D. thesis, 348 p.
- Busacca, A.J., Aniku, J.R., and Singer, M.J., 1984, Dispersion of soils by an ultrasonic method that eliminates probe contact: *Soil Science Society of America Journal*, v. 48, no 5, p. 1125–1129.
- California Department of Water Resources, 1963, Average seasonal isohyetal map, based on or corrected to the period 1910–11 to 1959–60: State of California.
- — — 1968, Final geologic report on the Thermalito Power Canal: Project Geology Report C–26, State of California.
- — — 1979, The August 1, 1975 Oroville earthquake investigations: Bulletin 203–78, State of California.
- Carpenter, E.J., Strahorn, A.T., Glassey, T.W., and Story, R.E., 1926, *Soil survey of the Oroville area, California*: U.S. Department of Agriculture, Bureau of Chemistry and Soils, 63 p.
- Cherven, V.B., 1984, Early Pleistocene glacial outwash deposits in the eastern San Joaquin Valley, California: A model for humid-region alluvial fans: *Sedimentology*, v. 31, p. 823–836.
- Clark, B.L., and Anderson, C.A., 1938, Wheatland Formation and its relation to early Tertiary andesites in the Sierra Nevada: *Geological Society of America Bulletin*, v. 49, no. 6, p. 931–956.
- Clark, L.D., 1960, Foothills fault system, western Sierra Nevada, California: *Geology Society of America Bulletin*, v. 71, p. 483–496.
- Creely, R.S., 1965, *Geology of the Oroville quadrangle, California*: California Division of Mines and Geology Bulletin 184, 86 p.
- Dalrymple, G.B., 1964, *Cenozoic chronology of the Sierra Nevada, California*: University of California Publications in Geological Sciences, v. 47, 35 p.
- Dalrymple, G.B., and Lanphere, M.A., 1969, *Potassium-argon dating: Principles, techniques, and applications to geochronology*: San Francisco, W. H. Freeman, 258 p.
- Davis, G.H., and Olmsted, F.H., 1952, Sutter-Yuba Counties investigation, in *Geologic features and groundwater storage capacity of Sutter-Yuba area*, Appendix B: California State Water Resources Board Bulletin no. 6, p. 89–106.
- Davis, S.N., and Hall, F.R., 1959, *Water quality of eastern Stanislaus and northern Merced Counties, California*: Stanford University Publications in Geological Science, v. 6, no. 1, 26 p.
- Deming, W.E., 1943, *Statistical treatment of data*: New York, John Wiley, 261 p.
- Dethier, D.P., and Bethel, John, 1981, *Surficial deposits along the Cowlitz River near Toledo, Lewis County, Washington*: U.S. Geological Survey Open-File Report 81–1043, 67 p.
- Drees, L.R., and Wilding, L.P., 1978, Elemental distribution in the light mineral isolate of soil separates: *Soil Science Society of America Journal*, v. 42, p. 976–978.
- Evans, L.J., and Adams, W.A., 1975, Quantitative pedological studies on soils derived from Silurian mudstones. V. Redistribution and loss of mobilized constituents: *Journal of Soil Science*, v. 26, p. 327–335.
- Evernden, J.F., Savage, D.E., Curtis, G.H., and James, G.T., 1964, Potassium-argon dates and the Cenozoic mammalian chronology of North America: *American Journal of Science*, v. 262, p. 145–198.
- Gale, H.S., Piper, A.M., and Thomas, H.E., 1939, *Geology*, in Piper, A.M., Gale, H.S., Thomas, H.E., and Robinson, T.W., *Geology and ground water hydrology of the Mokelumne area, California*: U.S. Geological Survey Water-Supply Paper 780, p. 14–100.
- Goldich, S.S., 1938, A study in rock weathering: *Journal of Geology*, v. 46, no. 1, p. 17–58.
- Hansen, R.O., and Begg, E.L., 1970, Age of Quaternary sediments and soils in the Sacramento area, California by uranium and actinium series dating of vertebrate fossils: *Earth and Planetary Science Letters*, v. 8, no. 6, p. 411–419.
- Harden, J.W., 1982a, A quantitative index of soil development from field descriptions: Examples from a chronosequence in central California: *Geoderma*, v. 28, no 1, p. 1–28.
- — — 1982b, A study of soil development using the geochronology of the Merced River deposits, California: Berkeley, University of California, Ph.D. thesis, 237 p.
- — — 1987, Soils developed in granitic alluvium near Merced, California: U.S. Geological Survey Bulletin 1590–A.
- Harden, J.W., and Marchand, D.E., 1977, The soil chronosequence of the Merced River area, in Singer, M.J., ed., *Soil development, geomorphology, and Cenozoic history of the northeastern San Joaquin Valley and adjacent areas, California*: Soil Science Society of America—Geological Society of America joint field session, 1977, guidebook, p. 22–38.
- — — 1980, Quaternary stratigraphy and interpretation of soil data from the Auburn, Oroville, and Sonora areas along the Foothills fault system, western Sierra Nevada, California: U.S. Geological Survey Open-File Report 80–30, 57 p.
- Harden, J.W., and Taylor, E.T., 1983, A quantitative comparison of soil development in four climatic regimes: *Quaternary Research*, v. 20, no. 3, p. 342–359.
- Harwood, D.S., 1984, Evidence for late Cenozoic east-west compressive tectonism in the Sacramento valley, California, in Crouch, J., and Bachman S., eds., *Tectonics and sedimentation along the California margin*: Pacific Section Society of Economic Paleontologists and Mineralogists, v. 38, p. 87–100.
- Harwood, D.S., and Helley, E.J., 1987, Late Cenozoic tectonism of the Sacramento Valley, California: U.S. Geological Survey Professional Paper 1359.
- Harwood, D.S., Helley, E.J., and Doukas, M.P., 1981, *Geologic map of the Chico Monocline and northeastern part of the*

- Sacramento Valley, California: U.S. Geological Survey Miscellaneous Investigation Series Map I-1238, scale 1:62,500.
- Hays, J.D., Imbrie, John, and Shackleton, N.J., 1976, Variation in the earth's orbit: Pacemaker of the ice ages: *Science*, v. 194, no. 4270, p. 1121-1132.
- Helley, E.J., 1979, Preliminary geologic maps of Cenozoic deposits of the Davis, Knights Landing, Lincoln, and Fair Oaks 15-minute quadrangles, California: U.S. Geological Survey Open-File Report 79-483, 4 sheets.
- Helley, E.J., and Harwood, D.S., 1985, Geologic map of the late Cenozoic deposits of the Sacramento Valley and northern Sierran foothills, California: U.S. Geological Survey Miscellaneous Field Studies Map MF-1790, scale 1:62,500.
- Helley, E.J., Harwood, D.S., Barker, J.A., and Griffen, E.A., 1981, Geologic map of the Battle Creek fault zone and adjacent parts of the northern Sacramento Valley, California: U.S. Geological Survey Miscellaneous Field Studies Map MF-1298.
- Herbert, F.W., Jr., and Begg, E.L., 1969, Soils of the Yuba area, California: Davis, University of California, 170 p.
- Huber, N.K., 1981, Amount and timing of late Cenozoic uplift of the central Sierra Nevada, California: Evidence from the upper San Joaquin River basin: U.S. Geological Survey Professional Paper 1197, 28 p.
- Huntington, G.L., 1980, Soil-landform relationships of portions of the San Joaquin River and Kings River alluvial depositional systems in the Great Valley of California: Davis, University of California, Ph.D. thesis, 261 p.
- Ingamells, C.O., 1970, Lithium metaborate flux in silicate analysis: *Analytica Chimica Acta*, v. 52, no. 2, p. 323-334.
- Janda, R.J., 1965, Quaternary alluvium near Friant, California, in *Wahrhaftig, Clyde, and others, eds., International Union for Quaternary Research 7th Congress Guidebook, Field Conference I., Northern Great Basin and California*, Lincoln, Nebraska Academy of Sciences, p. 128-132.
- — — 1966, Pleistocene history and hydrology of the upper San Joaquin River, California: Berkeley, University of California, Ph.D. thesis, 425 p.
- Janda, R.J., and Croft, M.G., 1967, The stratigraphic significance of a sequence of noncalcareous brown soils formed on the Quaternary alluvium of the northeastern San Joaquin Valley, California, in *Morrison, R.B., and Wright, H.E., Jr., eds., Quaternary soils: International Union for Quaternary Research 7th Congress, Proceedings*, v. 9, p. 158-190.
- Jenny, Hans, 1980, *The soil resource; origin and behavior*: New York, Springer-Verlag, 377 p.
- Kittrick, J.A., 1973, Mica-derived vermiculites as unstable intermediates: *Clays and Clay Minerals*, v. 21, p. 479-488.
- Lindgren, Waldemar, 1911, The Tertiary gravels of the Sierra Nevada of California: U.S. Geological Survey Professional Paper 73, 226 p.
- Lytle, Dennis, in press, Soil survey of Sutter County, California: U.S. Department of Agriculture, Soil Conservation Service.
- Machette, M.N., 1983, Geologic map of the southwest quarter of the Beaver quadrangle, Beaver County, Utah: U.S. Geological Survey Miscellaneous Investigations Series Map I-1444, scale 1:24,000.
- Machette, M.N., and Steven, T.A., 1983, Geologic map of the northwest quarter of the Beaver quadrangle, Beaver County: U.S. Geological Survey Miscellaneous Investigations Series-Map I-1445, scale 1:24,000.
- Machette, M.N., Steven, T.A., Cunningham, C.G., and Anderson, J.J., 1984, Geologic map of the Beaver quadrangle, Beaver and Piute Counties, Utah: U.S. Geological Survey Miscellaneous Investigations Series Map I-1520, scale 1:50,000.
- Mankinen, E.A., and Dalrymple, G.B., 1979, Revised geomagnetic polarity time scale for the interval 0-5 m.y. B.P.: *Journal of Geophysical Research*, v. 84, p. 615-626.
- Marchand, D.E., 1977, The Cenozoic history of the San Joaquin Valley and the adjacent Sierra Nevada as inferred from the geology and soils of the eastern San Joaquin Valley, in *Singer, M.J., ed., Soil development, geomorphology, and Cenozoic history of the northeastern San Joaquin Valley and adjacent areas*, California: Soil Science Society—Geological Society of America joint field session, 1977, guidebook, p. 39-50.
- Marchand, D.E., and Allwardt, Alan, 1981, Late Cenozoic stratigraphic units in northeastern San Joaquin Valley, California: U.S. Geological Survey Bulletin 1470, 70 p.
- Matheison, S.A., and Sarna-Wojcicki, A.M., 1982, Ash layer in Mohawk Valley, Plumas County, California, correlated with the 0.45-m.y.-old Rockland Ash—Implications for the glacial and lacustrine history of the region [abs]: *Geological Society America Abstracts with Program, 78th Annual Cordilleran Section Meeting*, p. 184.
- Meixner, R.E., and Singer, M.J., 1981, Use of a field morphology rating system to evaluate soil formation and discontinuities: *Soil Science*, v. 131, no. 2, p. 114-123.
- Merrill, G.P., 1921, *Rocks, rock weathering, and soils*: New York, MacMillan.
- Morrison, R.B., 1978, Quaternary soil stratigraphy—Concepts, methods, problems, in *Mahaney, W.C., ed., Quaternary soils*: Norwich, Geo Abstracts, p. 77-108.
- National Oceanographic and Atmospheric Administration, 1979, *Climatological data, annual summary California*, v. 83: National Oceanographic and Atmospheric Administration, National Climatic Center.
- Olmsted, F.H., and Davis, G.H., 1961, Geologic features and groundwater storage capacity of the Sacramento Valley, California: U.S. Geological Survey Water-Supply Paper 1497.
- Palmer, A.R., 1983, The Decade of North American Geology 1983 geologic time scale: *Geology*, v. 11, p. 503-504.
- Polynov, B.P., 1937, *Cycle of weathering* (translated by A. Muir): London, Murby.
- Reheis, M.C., 1984, Chronologic and climatic control on soil development, northeastern Bighorn Basin, Wyoming and Montana: Boulder, University of Colorado, Ph.D. thesis, 293 p.
- Reiche, Parry, 1950, *A survey of weathering processes and products*: Albuquerque, University of New Mexico Press, 95 p.
- Russell, R.D., 1931, The Tehama Formation of northern California: Berkeley, University of California, Ph.D. thesis, p. 137.
- Russell, R.D., and VanderHoof, V.L., 1931, A vertebrate fauna from a new Pliocene formation in northern California: *University of California Publications in Geological Sciences Bulletin*, v. 20, p. 11-21.
- Sarna-Wojcicki, A.M., 1976, Correlation of late Cenozoic tuffs in the central Coast Ranges of California by means of trace-and-minor-element chemistry: U.S. Geological Survey Pro-

- fessional Paper 972, 30 p.
- Schweickert, R.A., and Cowan, D.S., 1975, Early Mesozoic tectonic evolution of the western Sierra Nevada, California: *Geological Society America Bulletin*, v. 86, p. 1329–1336.
- Shackleton, N.J. and Opdyke, N.D., 1976, Oxygen isotope and paleomagnetic stratigraphy of Pacific core V28–239, late Pliocene to latest Pleistocene: *Geological Society of America Memoir*, v. 145, p. 449–464.
- Sherburne, R.W., and Hauge, C.J., 1975, Oroville California earthquake 1 August 1975: California Division of Mines and Geology Special Report 124, 151 p.
- Shlemon, R.J., 1967a, Landform-soil relationships in northern Sacramento County, California: Berkeley, University of California, Ph.D. thesis, 387 p.
- — — 1967b, Quaternary geology of northern Sacramento County, California: Geological Society of Sacramento, Annual Field Trip Guidebook.
- — — 1972, The lower American River area, California: A model of Pleistocene landscape evolution: *Association of Pacific Coast Geographers Yearbook*, v. 34, p. 61–86.
- Shlemon, R.J., and Begg, E.L., 1972, Quaternary Stony Creek channel system, northwestern Sacramento Valley, California [abs]: *Geological Society American Abstracts with Program*, 68th Annual Cordilleran Section Meeting, v. 4, no. 3, p. 236.
- Singer, M.J., and Janitzky, Peter, 1986, Field and laboratory procedures used in a soil chronosequence study: *U.S. Geologic Survey Bulletin* 1648.
- Smeck, N.E., and Wilding, L.P., 1981, Quantitative evaluation of pedon formation in calcareous glacial till deposits in Ohio: *Geoderma*, v. 24, p. 1–16.
- Soil Survey Staff, 1975, Soil taxonomy, a basic system of soil classification for making and interpreting soil surveys: U.S. Department of Agriculture, Soil Conservation Service, *Agricultural Handbook* 436, 754 p.
- Soil Survey Staff, 1981, Soil survey manual (draft): U.S. Department of Agriculture, Soil Conservation Service.
- Steele, W.C., 1979, Quaternary stream terraces in the northwestern Sacramento Valley, Glenn, Tehama, and Shasta Counties, California: Palo Alto, Stanford University, Ph.D. thesis, 157 p.
- Steiger, R.H., and Jaeger, E.L., 1977, Subcommittee on geochronology: Convention on the use of decay constants in geo- and cosmochronology: *Earth and Planetary Science Letters*, v. 36, p. 359–362.
- Sudom, M.D., and St. Arnaud, R.J., 1971, Use of quartz, zirconium, and titanium as indices in pedological studies: *Canadian Journal of Soil Science*, v. 51, p. 385–396.
- Unruh, J.R., 1988, Reurring late Cenozoic extension in the Oroville area, Sacramento Valley, California [abs]: *Geological Society of America Abstracts with Program*, 84th Annual Cordilleran Section Meeting, p. 239.
- — — 1989, Plio-Pleistocene time-transgressive deformation in the Sacramento Valley and northward migration of the Mendocino triple junction [abs]: *Geological Society of America Abstracts with Program*, 85th Annual Cordilleran Section Meeting (in press).
- Woodward-Clyde Consultants, 1977, Earthquake evaluation studies of the Auburn Dam area: San Francisco, Woodward-Clyde Consultants, 8 v.

**SUPPLEMENTARY TABLES 1–11;
SUPPLEMENTARY FIGURE 1**

EXPLANATION

SOIL TEXTURE

1s	loamy sand	sil	silt loam	scl	sandy clay loam	sg	slightly gravelly
sl	sandy loam	sicl	silty clay loam	sc	sandy clay	gr	gravelly
l	loam	sic	silty clay			vg	very gravelly
+	heavy	cl	clay loam			ext. gr	extremely gravelly
-	light	c	clay				

SOIL CONSISTENCE

Dry		Moist		Wet			
lo	loose	lo	loose	so	nonsticky	po	nonplastic
so	soft	vfr	very friable	ss	slightly sticky	ps	slightly plastic
sh	slightly hard	fr	friable	s	sticky	p	plastic
h	hard	fi	firm	vs	very sticky	vp	very plastic
vh	very hard	vfi	very firm				

SOIL STRUCTURE

Grade		Size		Type			
1	weak	vf	very fine	m	massive	sbk	subangular blocky
2	moderate	f	fine	sg	single grain	abk	angular blocky
3	strong	m	medium	g	granular	pr	prismatic
		c	coarse	cr	crumb	→	parting to
		vc	very coarse	pl	platy		

ROOTS

Abundance		Size		Orientation	
1	few	vf	very fine	h	horizontal
2	common	v	fine	v	vertical
3	many	m	medium	r	random
		c	coarse	on pf	on ped faces

PORES

Abundance		Size		Shape		Orientation	
1	few	vf	very fine	t	tubular	r	random
2	common	f	fine	i	interstitial	h	horizontal
3	many	m	medium			v	vertical
		c	coarse			c	continuous

CLAY FILMS

Frequency		Thickness		Location	
v1	very few	vn	very thin	pf	ped faces
1	few	n	thin	po	pore linings (usually tubular pores)
2	common	mk	moderately thick	br	bridging grains
3	many	k	thick	pc	coating pebbles or gravels
4	continuous				

HORIZON BOUNDARIES

a	abrupt
c	clear
g	gradual
d	diffuse
s	smooth
w	wavy
i	irregular

Supplementary table 1, part 1. Site locations

[Soil-profile sites were originally prefixed HOS-]

Site and soil-profile number	Geologic unit	Soil-profile site locations, Mount Diablo Base and Meridian
HON-1	Holocene alluvium	SW $\frac{1}{4}$ NE $\frac{1}{4}$ sec. 30, T. 17 N., R. 4 E.
HON-2		SW $\frac{1}{4}$ NW $\frac{1}{4}$ sec. 31, T. 17 N., R. 4 E.
HON-3		SW $\frac{1}{4}$ NW $\frac{1}{4}$ sec. 31, T. 17 N., R. 4 E.
HON-4		SW $\frac{1}{4}$ NE $\frac{1}{4}$ sec. 31, T. 17 N., R. 4 E.
HON-5	Upper member, Modesto Formation	NE $\frac{1}{4}$ SW $\frac{1}{4}$ NE $\frac{1}{4}$ sec. 31, T. 17 N., R. 4 E.
HON-6		NE $\frac{1}{4}$ SW $\frac{1}{4}$ NE $\frac{1}{4}$ sec. 31, T. 17 N., R. 4 E.
HON-7		SE $\frac{1}{4}$ SE $\frac{1}{4}$ SE $\frac{1}{4}$ sec. 22, T. 17 N., R. 4 E.
HON-8		SE $\frac{1}{4}$ SE $\frac{1}{4}$ SE $\frac{1}{4}$ sec. 22, T. 17 N., R. 4 E.
HON-9	Lower member, Modesto Formation	150 m W. of Ctr. sec. 24, T. 17 N., R. 3 E.
HON-10		150 m W. of Ctr. sec. 24, T. 17 N., R. 3 E.
HON-11		SE $\frac{1}{4}$ SW $\frac{1}{4}$ SW $\frac{1}{4}$ sec. 13, T. 17 N., R. 3 E.
HON-13	Upper member, Riverbank Formation	NE $\frac{1}{4}$ SW $\frac{1}{4}$ sec. 16, T. 17 N., R. 4 E.
HON-14		NE $\frac{1}{4}$ SW $\frac{1}{4}$ sec. 16, T. 17 N., R. 4 E.
HON-17	Lower member, Riverbank Formation	NE $\frac{1}{4}$ SE $\frac{1}{4}$ sec. 16, T. 17 N., R. 4 E.
HON-18		NE $\frac{1}{4}$ SE $\frac{1}{4}$ sec. 16, T. 17 N., R. 4 E.
HON-19		SE $\frac{1}{4}$ SE $\frac{1}{4}$ SE $\frac{1}{4}$ sec. 17, T. 17 N., R. 4 E.
HON-20		SE $\frac{1}{4}$ SE $\frac{1}{4}$ SE $\frac{1}{4}$ sec. 17, T. 17 N., R. 4 E.
HON-21	Exhumed lower member, Laguna Formation	NW $\frac{1}{4}$ sec. 23, T. 17 N., R. 4 E.
HON-22		NW $\frac{1}{4}$ sec. 23, T. 17 N., R. 4 E.

Supplementary table 1, part 2. Field descriptions

Profile no.	Sample no.	Horizon	Basal depth (cm)	Lower boundary	Moist color	Dry color	Texture	Consistence		
								Dry	Moist	Wet
Holocene alluvium,										
HON-1	1	A	12	a,s	10YR3/3	10YR5/4	1	sh	fr	ss,po
	2	2A1	16	a,s	10YR3/2.5	10YR5/3	sil	h	fr	ss,po
	3	2A2	25	c,s	10YR3/3	10YR5/3	1	sh	fr	ss,ps
	4	2AC	49	c,s	7.5YR4/3	10YR5/4	1	sh	fr	ss,ps
	5	2C	85	c,s	7.5YR4/3	10YR5/4	1	sh	fr	ss,po
	6	3C1	95	a,s	7.5YR4/4	10YR5/4	s1	so	vfr	so,po
	7	3C2	122		7.5YR4/4	10YR5/4	s1	sh	vfr	so,po
HON-2	10	A1	4	a,s	10YR3/2.5	10YR5/3	sil	sh	fr	ss,ps
	11	A2	32	a,w	10YR3/2.5	10YR5/4	sil-1	sh	fr	ss,ps
	12	C	61	c,s	10YR3/3	10YR5/4	1	so	vfr	so,po
	13	2C	92	c,s	10YR4/4	10YR5/4	1-s1	-	vfr	ss,po
	14	3C	103		10YR3/3	10YR5/5	1	-	vfr	ss,ps
HON-3	16	A1	4	a,s	10YR3/3	10YR5/3	sil	sh	vfr	ss,ps
	17	A2	16	g,s	10YR3/3	10YR5/4	sil	sh	fr	ss,ps
	18	AC	31	a,w	10YR3/3	10YR5/4	sil	sh	fr	ss,ps
	19	C	54	a,w	10YR4/3	10YR5.5/4	1	so	vfr	so,po
	20	2C	78		10YR4/3	10YR6/4	1	so	vfr	ss, ps
HON-4	21	C	17	a,s	10YR4/3	10YR6/3	s1	so	vfr	so,po
	22	2A	32	c,s	10YR3/3	10YR5/3	1	sh	vfr	ss,ps
	23	2AC	49	c,s	10YR3/3	10YR5/4	sil	so	vfr	ss,ps
	24	2C	86	g,s	10YR3.5/3	10YR5/4	1	-	vfr	ss,ps
	25	3C1	113	g,s	10YR4/3	10YR5/4	s1	-	vfr	so,po
	26	3C2	147		10YR4/3	10YR5/4	s1	-	vfr	so,po

Structure	Roots	Pores	Clay films	pH	Assumed parent material			
					Texture	Consistence		
						Dry	Moist	Wet
0.6 ka								
1f,mgr	1f,2m	2vf,f i 2m crt	-	6.5	l	lo	lo	so,po
1f,gr	2vf,1f,1m	2vf i 2vf crt	-	6.6	sil	so	vfr	ss,po
1f,mgr	1vf,f,m	2vf,f i 1f,m crt	-	6.5	l	lo	lo	so,po
m	1vf,f,m	1vf i 2f,m crt	-	6.6	l	lo	lo	so,po
m	1vf,m	1f,2m crt	-	6.8	l	lo	lo	so,po
m→sg	1vf,m	1f crt	-	6.7	sl	lo	lo	so,po
m→sg	1vf,f,m,c	1f crt	-	7.0	sl	lo	lo	so,po
2f,mgr	1f,2vf,m	2vf,f i 2vf,f,m crt	-	5.6	sil	so	vfr	ss,po
m→1f,msbk	1f,m,2vf	1vf,f cvt	-	6.2	sil	so	vfr	ss,po
m→sg	1f,2vf	1vf,f cvt	-	6.8	l	lo	lo	so,po
m→sg	1f,2vf	1vf,f crt	-	7.1	l	lo	lo	so,po
m	1vf,f	1vf,f crt	-	7.2	l	lo	lo	so,po
2f,mgr	2f,m,3vf	1vf,f cvt 2vf,fi	-	5.9	sil	so	vfr	ss,po
1f,mgr	2vf,f,m	1vf,m,2f cvt 1vf,f i	-	5.8	sil	so	vfr	ss,po
1m,csbk	2vf,1f	1vf,f,m crt	-	6.1	sil	so	vfr	ss,po
m→sg	1vf,1f	1vf,f crt	-	7.1	l	lo	lo	so,po
m→sg	1vf,f	1vf,f crt	-	7.0	l	lo	lo	so,po
sg	1f,2vf,m r	1vf,1m,2f crt	-	6.5	sl	lo	lo	so,po
2f,mgr	1f,1m,2vf r	3vf ri 1m,c,2vf,f crt	-	6.9	l	lo	lo	so,po
m→1m,csbk	1m,c,2vf,f h	1vf,f crt	-	6.6	sil	so	vfr	ss,po
m	1f,m,c,2vf h	1vf,f,m crt	-	6.7	l	lo	lo	so,po
m	1vf,f,2m,c	1m,2vf,f crt	-	6.8	sl	lo	lo	so,po
m→sg	2vf,f,m,c,h	1f,1m,2vf crt	-	6.7	sl	lo	lo	so,po

Supplementary table 1, part 2. Field descriptions—Continued

Profile no.	Sample no.	Horizon	Basal depth (cm)	Lower boundary	Moist color	Dry color	Texture	Consistence			
								Dry	Moist	Wet	
Modesto Formation,											
HON-5	27	Ap1	13	a,w	7.5YR3/2	7.5YR5/4	sil	vh	fi	ss,ps	
	28	Ap2	23	c,w	7.5YR3/3	7.5YR5/4	sil	h	fi	ss,ps	
	29	BA	54	c,s	7.5YR3/3	7.5YR4/3	sil+	h	fi	ss,ps	
	30	Bw1	88	c,s	7.5YR3/3	7.5YR4/3	sil	h	fr	ss,ps	
	31	Bw2	102	c,s	7.5YR3/4	7.5YR5/4	sil	vh	fr	ss,ps	
	32	BC1	141	g,s	7.5YR4/4	7.5YR5/4, 5/6	sil-1	h	fr	ss,ps	
	33	BC2	180		7.5YR4/4	7.5YR5/4	sil-1	h	fr	ss,ps	
HON-6	34	Ap1	10	a,w	7.5YR3/2	7.5YR5/4	sil	vh	fi	ss,ps	
	35	Ap2	22	c,w	7.5YR3/2	7.5YR5/4	sil	h	fr	ss,ps	
	36	BA	43	c,s	7.5YR3/2	7.5YR4/3	sil	h	fi	ss,ps	
	37	Bw1	91	c,s	7.5YR3/3	7.5YR4/3	l	li	fi	ss,ps	
	38	Bw2	118	c,s	7.5YR3/3	7.5YR5/4	l	li	fr	ss,po	
	39	BC1	151	g,s	7.5YR4/4	7.5YR5/4	l	h	fr	ss,po	
	40	BC2	184		7.5YR4/4	7.5YR5/4	l	h	fr	ss,po	
HON-7	41	Ap1	8	c,s	7.5YR3/3	7.5YR5/4	l	vh	vfr	ss,ps	
	42	Ap2	30	c,s	7.5YR3/3	7.5YR5/4	l	vh	vfr	ss,ps	
	43	BA	54	g,s	7.5YR3/2.5	7.5YR4/4	sil-1	h	fr	ss,ps	
	44	Bw1	88	g,s	7.5YR3/4	7.5YR4/6	l	sh	vfr	ss,ps	
	45	Bw2	118	g,s	7.5YR3/4	7.5YR5/5	l	sh	fr	ss,ps	
	46	BC	180	c,s	7.5YR4/4	7.5YR5.5/5	.	sh	fr	ss,ps	
	47	2BC	230		10YR4/3	10YR5/4	sic1-	sh	fr	ss,ps	
HON-8	51	Ap1	7	a,s	7.5YR3/3	7.5YR5/4	l	vh	fr	so,ps	
	52	Ap2	34	c,s	7.5YR3/3	7.5YR5/4	l	vh	fr	so,ps	
	53	BA	57	c,s	7.5YR3/3	7.5YR4/4	l	h	fr	ss,ps	
	54	Bw1	90	c,w	7.5YR3/4	7.5YR4/6	l	h	fr	ss,ps	
	55	Bw2	126	g,s	7.5YR3/4	7.5YR5/5	l	h	fi	ss,ps	
	56	BC1	191	g,s	7.5YR4/4	7.5YR5/5	l	sh	fi	ss,ps	
	57	BC2	240		7.5YR4/3	7.5YR6/4	l-sil	sh	fr	ss,ps	
Modesto Formation,											
HON-9	none assigned	Ap1	16	c,s	10YR3/3	10YR6/2.5	l-sil	h	fr	ss,ps	
		Ap2	25	g,s	10YR3/3	10YR6/3	l-sil	h	fr	ss,ps	
		BAt1	42	a,s	10YR3/3	10YR5.5/3	l ⁺ -sil	h	fr	ss,ps	
		BAt2	80	a,w	10YR4/3	10YR5/4	c	vh	fi	vs,vp	
		2Bqkm1	99	c,w	10YR4/3	10YR5/3	scl-	cemented-----			
		2Bqkm2	113	c,w	10YR4/3	10YR5/3	scl-	cemented-----			
		2BCqm	137	c,w	10YR4/3	10YR5/3	fs1	weakly cemented-----			
		3BCt	153	c,w	10YR4/3	10YR5/3	l	h	fr	ss,ps	
		3C	198	c,w	10YR6/2.5	10YR7/2	l	h	fr	ss,ps	

Structure	Roots	Miscellaneous	Pores	Clay films	pH	Assumed parent material			
						Texture	Consistence		
							Dry	Moist	Wet
upper member, 10 ka									
m→cloddy	1f,2vf	-	2vf,f,m crt	-	6.2	sil	so	vfr	ss,po
2f,mgr	1f,2vf	-	1vf,f crt 2vf i	-	6.3	sil	so	vfr	ss,po
m→1csbk	1vf,f,m	mn sheen on pf	1m,2vf,f crt	2n pf 1n po	6.7	sil	so	vfr	ss,po
2m,cabk	2vf,f	-	1m,2vf,f crt	3n pf 3n po	7.0	sil	so	vfr	ss,po
2mabk	1f,2vf	-	2vf,2f crt	3vn pf 3vn po	7.1	sil	so	vfr	ss,po
2mabk	1vf,f	-	1f,2vf crt	2vn pf 2vn po	7.2	sil	so	vfr	ss,po
1mabk	1vf,f	-	1vf,f crt	2vn pf 2vn po	7.3	sil	so	vfr	ss,po
m(cloddy)	1f,2vf	-	2vf,f,m crt	-	6.2	sil	so	vfr	ss,po
m→1f,mgr	2vf,f	-	2vf,f,m crt	-	6.4	sil	so	vfr	ss,po
m→1m,csbk	1vf,f,m	mn sheen on pf	1m,2vf,f crt	2n pf 2n po	6.6	sil	so	vfr	ss,po
2m,cabk	2vf,3f,m	-	2vf,f,m crt	3n pf 3n po	7.0	l	lo	lo	so,po
2mabk	2vf,1f	-	2vf,f,m crt	3vn pf 3vn po	7.0	l	lo	lo	so,po
2mabk	2vf,f	-	2vf,f,m crt	2vn pf 2vn po	7.2	l	lo	lo	so,po
1mabk	1vf	Fe mott 7.5YR5/6	1vf,f crt	2vn pf 2vn po	7.4	l	lo	lo	so,po
cloddy	3vf	-	2vf crt	-	5.6	l	lo	lo	so,po
m,compact	3vf	-	2vf crt	-	5.7	l	lo	lo	so,po
m→1,m,csbk	3vf	-	2f,m,3vf crt	2vn br 2vn po	6.6	sil-1	so	vfr	ss,po
2m,cabk 60% 2f,mgr 40%	3vf	-	3vf,f,m,co crt	2vn br 2vn po, 1vn,pf	7.0	l	lo	lo	so,po
2m,cabk	2vf	-	2m,3vf,f crt	2vn po 2vn br	7.2	l	lo	lo	so,po
2m,cabk	1vf	Fe mott: fli	3vf,f,m crt	1vn br 1vn po	7.3	l	lo	lo	so,po
1f,mabk	1vf	Mn shot Fe mott: c2i	2vf,f,m crt	-	7.2	sil-1	so	vfr	ss,po
cloddy, compacted	-	-	-	-	5.6	l	lo	lo	so,po
massive	3vf	-	1m,2f,3vf crt	-	5.8	l	lo	lo	so,po
compacted 1msbk	3vf	-	2f,m,3vf crt	2vn br 2vn po	6.3	l	lo	lo	so,po
2m,csbk 80% 2f,mgr 20%	3vf	-	2c,3vf,f,m crt	3vn br 3vn po	6.8	l	lo	lo	so,po
2m,cabk	3vf on pf	-	2f,m,c,3vf crt	2vn br 3vn po	7.1	l	lo	lo	so,po
2m,cabk	-	Mn stains: fli	2vf,f,m,c crt	1vn br 1vn po	7.3	l	lo	lo	so,po
1m,cabk	-	Mn shot: c2i	2vf,f,m crt	-	7.3	l	lo	lo	so,po
lower member, 40 ka									
cloddy	3vf,2f,1m	-	1vf,f cvt	-	7.0	l	lo	lo	so,po
m→1f,msbk	2vf,f,1m	-	2vf,1f,m crt	v1 vn po v1 vn br	7.2	l	lo	lo	so,po
m→1f,m,c,abk	2vf,1f,1m	-	3vf,2f,1m crt	3n po,1np f v1 mk br	7.4	l	lo	lo	so,po
3m,cabk	2vf 2f, 1m on pf	-	2vf,1f,1m crt	3mk pf,1k pf 3mk po	7.5	l	lo	lo	so,po
3m,cabk	no roots	Mn stains on pf	2vf,f crt	2n br,1mk br in waves	8.2	fs1	lo	lo	so,po
3m,cabk	no roots	Mn stains on pf	2vf,f crt	2n br,1mk br in waves	8.2	fs1	lo	lo	so,po
2m,csbk	no roots	-	3vf,2f,m crt	1n br,1mk br in waves; 3mk po	8.2	fs1	lo	lo	so,po
m→1msbk	no roots	-	3vf,3f,2m crt	1n,mk br 3mk po	8.2	l	lo	lo	so,po
m	no roots	Fe mott: 10YR6/6 D	3vf,f,2m crt	3n,mk po	8.2	l	lo	lo	so,po

Supplementary table 1, part 2. Field descriptions—Continued

Profile no.	Sample no.	Horizon	Basal depth (cm)	Lower boundary	Moist color	Dry color	Texture	Consistence		
								Dry	Moist	Wet
Modesto Formation,										
HON-10	59	Ap	22	c,w	7.5YR3/2	7.5YR5/2	sgsl	sh	fr	ss,po
	60	BA	40	g,s	7.5YR3/3	7.5YR5/3.5	sgsl	vh	fi	so,po
	61	Bt1	86	g,s	7.5YR4/3	7.5YR5/4	sgsl	h	fr	ss,ps
	62	Bt2	132	c,s	5-7.5YR3/4	7.5YR5/5	sgsl	h	fr	ss,ps
	63	BC	150	c,s	7.5YR4/3	7.5YR5/4	sgsl	sh	vfr	ss,po
	64	C	205	a,w	7.5YR4/3	7.5-10YR5/4	sgsl	so	vfr	so,po
	65	2C	225		2.5Y4/3	10YR6/4	fsl	sh	vfr	so,po
HON-11	66	Ap	18	a,w	7.5YR3/2	7.5YR5/2	sgsl	sh	fr	ss,po
	67	BA	45	g,s	7.5YR3/3	7.5YR5/3.5	sgsl	vh	fi	ss,ps
	68	Bt1	94	g,s	7.5YR4/3	7.5YR5/4	sgsl	sh	vfr	ss,ps
	69	Bt2	125	c,w+i	7.5YR3/4	7.5YR4/4	sgsl	h	fi	s,p
	70	BC	145	g,w+i	7.5YR4/4	7.5YR5/5	sgsl	sh	fr	ss,po
	71	C	179	a,w	7.5YR4/4	7.5YR5/5	sgsl	so	vfr	so,po
	72	2C	220		2.5Y5/4	10YR6/4	sil	h	fr	ss,po
Riverbank Formation,										
HON-13	73	Ap	24	a,s	7.5YR4/5	7.5YR6/6	sil	sh	vfr	ss,po
	74	BA	33	c,s	5YR4/4	7.5YR5/6	sil-1	sh	vfr	ss,ps
	75	BAt1	50	c,s	5YR4/4	5YR5/5	sil-1	sh	fr	ss,ps
	76 ¹	BAt2	62	c,s	5YR4/5	5YR5/5	l+	h	fr	s,p
	77	Bt1	86	c,s	5YR4/6	5YR5/6	c-	vh	vfi	vs,vp
	78	Bt2	102	c,s	5YR4/6	5YR5/6	sic	vh	fi	vs,vp
	79	Bt3	123	c,s	5YR4/5	5-7.5YR5/6	sic-	vh	fi	s,vp
	80	BCt	157	g,w	7.5YR4/6	7.5YR6/6	sic1	h	fi	ss,p
	81	2BCt1	208	g,w	5YR5/6, 5YR3/4	7.5YR6/6 peds 5YR4/4 skins	scl	h	fr	ss,ps
	82	2BCt2	245	g,w	5YR4/6, 5YR3/4	7.5YR6/6 peds 7.5YR4/4 skins	cl	h	fr	ss,ps
	83	2BCt3	266	d,w	5YR4/6, 5YR3/4	7.5YR5/6 peds 7.5YR4/4 skins	scl-	sh	fr	ss,ps
	84	2CB	301		5YR4/5	5YR5/6	s1	sh	fr	so,ps
HON-14	85	Ap	28	a,s	7.5YR4/4	7.5YR6/6	sil	sh	vfr	ss,po
	86	BA	39	c,s	7.5YR4/4	7.5YR5/6	sil	sh	vfr	ss,ps
	87	BAt1	59	c,s	5YR4/5	5YR5/5	sil	h	fr	ss,p
	88 ¹	BAt2	76	c,s	5YR4/5	5YR5/5	cl	h	fr	s,p
	89	Bt1	111	c,w	5YR4/6	5YR5/6	sic	vh	vfi	vs,vp
	90	Bt2	126	c,w	5YR4/6	5YR5/5	cl	vh	vfi	s,vp
	91	2BCt1	150	g,w	7.5YR5/6 cF5YR4/4	7.5YR6/6 5YR4/6	cl	h	fr	s,p
	92	2BCt2	200	g,w	7.5YR5/6 cF5YR4/4	7.5YR6/6 5YR4/4	cl-sic1	h	fr	ss,ps
	93	2BCt3	260	d,w	5YR4/6	5,7.5YR 5/6,6/6	cl-	sh	fr	ss,ps
	94	2CB	320		5YR4/6	5YR5/6,6/6	scl-	sh	fr	so,ps

Structure	Roots	Miscellaneous	Pores	Clay films	pH	Assumed parent material			
						Texture	Consistence		
							Dry	Moist	Wet
lower member, 40 ka									
1m,csbk+	3vf,f,m	-	3f,m,c crt	-	6.8	sl	lo	lo	so,po
1f,mgr	root m		2vf,f i						
m,compacted	1m,2f,3vf	-	2c,3f crt	-	6.8	sl	lo	lo	so,po
			3vf,f i						
2m,csbk	2f,3vf	-	2vf,m,3f crt	3n br,1mk br	6.8	sl	lo	lo	so,po
			3vf,f i	1n po,3n pc					
2m,cabk	2f,2vf	-	2vf,f,m,c	3mk br,3mk pc	7.2	sl	lo	lo	so,po
			crt	1n-mk pf,2n po					
2m,csbk	1f,2vf	-	3vf,f,m crt	2n br	7.2	sl	lo	lo	so,po
			3vf,f i						
m+sg	1f,2vf	-	2f,3vf crt	-	7.2	sl	lo	lo	so,po
			3vf,f i						
m	1f,2vf	Fe mott: fli 10YR6/8 D	2vf,f crt	-	7.2	sl	lo	lo	so,po
1m,csbk+	1c,2m,3vf,f	-	2m,c,3vf,f	-	6.6	sl	lo	lo	so,po
2f,mgr			crt; 3vf i						
m,compacted	2m,3vf,f	-	2m,c,3vf,f	1vn po	7.0	sl	lo	lo	so,po
			crt	2n br					
2m,csbk	2f,m,c,3vf	-	3m,c crt	3n br,2n pc	7.0	sl	lo	lo	so,po
			2vf,f i	2n po					
2m,cabk	2f,3vf	-	3vf,f,m,c	3mk br,1mk pf	7.1	sl	lo	lo	so,po
			crt	2mk po					
2m,csbk	2vf,f	-	2m,3vf,f,c	2n br	7.2	sl	lo	lo	so,po
			crt; 2vf,f i						
m+sg	2vf,f	-	2vf,f,1m crt	-	7.3	sl	lo	lo	so,po
			3vf,f i						
m, strat'd	2vf,f	-	2vf,f crt	-	7.3	sil	so	vfr	ss,po
upper member, 130 ka									
cloddy	3vf,f	-	2m,3vf,f crt	-	5.5	sil	so	vfr	ss,po
m+1fmsbk	2f,3vf	Mn shot: c2r	2f,m,3vf crt	2vn po	6.3	sil	so	vfr	ss,po
2m,csbk	2vf,f	Mn shot: c2r	3vf,f,m crt	2n pf	6.5	sil	so	vfr	ss,po
				2n po					
2mpr+2cabk	1f,2vf	Mn shot: c2r	2vf,f,1m	2mk pf,3n pf	6.8	l	lo	lo	so,po
			crt	2mk po,3n po					
3m,cpr+	3vf	Mn shot: flr	3vf on pf	4k pf stress	6.8	l	lo	lo	so,po
3m,cabk			1vf into ped	cutans					
3m,cabk	1vf	few Mn shot	2vf on pf	4k pf stress	6.6	sil	so	vfr	ss,po
			1vf into ped	cutans					
3m,cabk+	1vf	no Mn	2vf on pf	4k pf stress	7.1	sil	so	vfr	ss,po
2fabk			1vf into ped	cutans					
3mabk+	-	Mn shot: clr	1vf on pf	4mk pf	7.1	sil	so	vfr	ss,po
2f,vfabk			1vf into ped	4mk po					
m+2m,cabk	-	Mn stains on pf	1f,m,2vf crt	3mk pf,3mk po	7.2	sl	lo	lo	so,po
				2mk br,2n br					
m+1m,csbk	-	Mn stains on pf	1f,m,2vf crt	1n pf in po	7.1	sl	lo	lo	so,po
				1mkpf,2nbr,2mkbr					
m+1m,csbk	-	Mn stains on pf	1f,m,2vf crt	1n pf,2mk po	6.9	sl	lo	lo	so,po
				3n br					
m+1m,csbk	-	no Mn	1vf i	1mk po	6.7	sl	lo	lo	so,po
			1f,m,2vf crt	3n br					
m+cloddy	2f,3vf	Mn shot: clr	1m,3vf,f crt	-	5.6	sil	so	vfr	ss,po
m+1f,msbk	3vf	Mn shot: clr	1m,c,2f,3vf	1n po	6.1	sil	so	vfr	ss,po
			crt						
2msbk,abk	3vf	Mn shot: c2r	1m,c,2f,3vf	2n pf	6.5	sil	so	vfr	ss,po
			crt	2n po					
2f,mpr+	3vf	Mn shot: c3r	2f,3vf crt	3n pf,3n po	6.7	sil	so	vfr	ss,po
2m,cabk				1mk pf,1mk po					
3m,cpr+	2vf	Mn shot: flr	3vf crt	4k pf stress	6.7	sil	so	vfr	ss,po
3m,cabk				cutans					
3m,cabk	1vf	Mn stains on pf	2vf crt	4k pf stress	7.0	sil	so	vfr	ss,po
				cutans					
3m,cabk+	-	Mn stains on pf	3vf crt	4k pf,4k po	7.1	l	lo	lo	so,po
3vf,fabk				4mk pf,4mk po					
2m,cabk	-	Mn stains on pf	1f,2vf crt	2n pf,2n po	6.9	l	lo	lo	so,po
				2mkpf,2mkpo,3mkbr					
m+1m,cabk	-	Mn stains on pf	1f,2vf crt	1n pf,1n po	6.8	l	lo	lo	so,po
				1mkpf,1mkpo,3mkbr					
m+1m,csbk	-	no Mn	1f,2vf crt	1k po,3mk br	6.8	sl	lo	lo	so,po
				1vn pf					

Supplementary table 1, part 2. Field descriptions—Continued

Profile no.	Sample no.	Horizon	Basal depth (cm)	Lower boundary	Moist color	Dry color	Texture	Consistence		
								Dry	Moist	Wet
Riverbank Formation,										
HON-17	95	Ap1	18	c,w	5YR3/4	5-7.5YR5/4	1	h	fr	ss,ps
	96	Ap2	24	a,w	5YR3/4	5YR5/5	1	sh	fr	ss,ps
	97	BA	76	g,w	2.5YR3/4	2.5YR4/4-5YR4/6	cl-	sh	fr	s,ps
	98	Bt1	100	g,w	2.5YR3/5	2.5YR5/6	cl	vh	fr	s,ps
	99	Bt2	160	c,w	2.5YR3/5	2.5YR5/6 peds 2.5YR4/6 skins	cl	vh	fi	s,ps
	100	2Bct	201	g,w	2.5YR3/5	2.5YR5/6 peds 2.5YR4/6 skins	scl	vh	fi	s,p
	101	3Bct	208	c,s	5YR4/5	5YR5/6	cl-	h	fi	s,ps
	102	4Bct	295		2.5YR4/6	5YR5/6 peds 2.5YR4/5 skins	vg scl	sh	fr	s,ps
HON-18	103	Ap1	19	c,w	5YR3/4	5YR5/4	1	h	fr	ss,ps
	104	Ap2	30	a,w	5YR3/4	5YR5/5	1	sh	fr	ss,ps
	105	BA	90	g,w	2.5YR3/5	5YR4/6	1+	sh	vfr	s,ps
	106	Bt1	113	c,w	2.5YR3/5	2.5YR5/6	cl	vh	fi	s,ps
	107	Bt2	170	g,w	2.5YR3/6	2.5YR5/6, 4/6	sic1	vh	fi	vs,p
	108	2Bct	190	c,w	2.5YR3/6	2.5YR5/6, 4/6	cl-	vh	fi	s,p
	109	3Bct	240	c,s	5YR4/6	5YR5/6, 6/6	cl-	h	fi	s,p
	110	4Bct	300		2.5YR4/6	5YR5/5, 5/6	vg scl-	sh	fr	ss,po
HON-19	111	Ap1	7	c,w	5YR3/4	5YR5/4	1	sh	fr	so,po
	112	Ap2	24	a,w	5YR3/4	5YR5/4, 7.5YR5/4	1	h	fr	so,ps
	113	BA	63	g,w	2.5YR3/5	2.5YR4/5	1+	sh	vfr	ss,ps
	114	Bt1	91	c,w	2.5YR3/5	2.5YR5/6 peds 5YR4/4 skins	1+	sh	fr	s,p
	115 ¹	Bt2	126	g,w	2.5YR3/6	2.5YR5/6 peds 2.5YR4/4 skins	cl	h	fi	s,p
	116	Bt3	176	c,w	2.5YR3/6	2.5YR5/6 peds 2.5YR4/4 skins	cl	vh	fi	s,p
	117	Bct	218	c,s	5YR4/6	5YR6/6 peds 2.5YR4/5 skins	scl-	vh	fi	ss,ps
	118	2Bct1	246	g,s	5YR4/6	5YR5/6	sgs1	sh	fr	ss,ps
	119	2Bct2	268	g,s	5YR4/6	5YR6/6	sgs1	sh	fr	ss,ps
	120	2Bct3	300		5YR4/6	5YR6/6	1	so	vfr	so,po
HON-20	123	Ap1	11	c,w	5YR3/4	5YR5/4	1	sh	vfr	so,po
	124	Ap2	30	a,w	5YR3/4	5YR5/4	1	h	fr	so,ps
	125	BA	60	c,w	5YR3/5	5YR4/5, 5/5	1+	so	vfr	ss,ps
	126	Bt1	114	c,i	2.5YR3/5	2.5YR5/6 peds 2.5YR4/4 skins	1+	sh	fr	ss,p
	127 ¹	Bt2	191	c,w	2.5YR3/6	2.5YR5/6 peds 2.5YR4/6 skins	cl	vh	fi	s,p
	128	2Bct1	223	g,s	5YR5/6 5YR4/6	5YR6/6 peds 5YR5/6 skins	sgscl-	h	fr	ss,p
	129	2Bct2	260	g,s	5YR4/6	5YR5/6 peds 5YR4/4 skins	sgs1+	sh	fr	ss,ps
	130	2CB	283		7.5YR5/6	7.5YR6/6	s1	so	vfr	so,po

Structure	Roots	Miscellaneous	Pores	Clay films	pH	Assumed parent material			
						Texture	Consistence		
							Dry	Moist	Wet
lower member, 250 ka									
cloddy→1fgr	2c,3vf,f,m	-	2c,3vf,f,m i	-	5.7	1	lo	lo	so,po
m→1sbk	2vf,f,3m	-	2m,3vf crt	-	5.7	1	lo	lo	so,po
3vf,f,mcr 30% 2f,msbk	1m,2vf,f	-	2c,3vf,f,m i	-	6.1	1	lo	lo	so,po
2m,csbk 20% fgr	1m,2vf	-	2f,3vf,m crt	2mk pf,4n pf 4n po	6.4	1	lo	lo	so,po
2fpr→2m,cabk	1vf,m	-	1m,3vf,f crt	3mk pf 4k pr	6.6	1	lo	lo	so,po
m→2mabk	1vf	-	2m,3vf crt	2k br,4mk br 1k po	6.8	s1	lo	lo	so,po
m→2mabk	1vf	-	1m,3vf crt	3k br in waves	6.9	1	lo	lo	so,po
m→1m,cabk	1vf	-	1m,2vf crt	1k br in waves 2mk br,1k pc	6.8	vgs1	lo	lo	so,po
2msbk→2f,mcr	2f,3vf	-	2m,3vf,f crt	-	5.5	1	lo	lo	so,po
m→2m,csbk	2f,m,3vf	-	3vf,f,m i 2f,m,3vf crt	-	5.5	1	lo	lo	so,po
2vf,mcr, 10% 2msbk	1f,3vf	-	2f,m,c,3vf crt; 3vf,f i	1mk br,2n po 3n br	6.1	1	lo	lo	so,po
2m,csbk, 30% 2vf,f,mcr	2vfi	-	2f,m,3vf crt	3mk br,3mk pf 1mk po	6.6	1	lo	lo	so,po
3m,cpr→3mabk	2vfi	Mn stains on pf	1f,2vf crt	4k pf 4k br	6.8	sil	so	vfr	ss,po
m→2m,cabk	1vf	Mn stains on pf, in po	1vf,f crt	3mk br,2k br in waves	6.9	1	lo	lo	so,po
m→2m,cabk	-	Mn stains on pf, in po	2vf crt	3mk br,2k br in waves	6.8	1	lo	lo	so,po
m	-	Mn stains on gravels	1vf,f,m crt	3n br,2mk br 1k pc	6.8	vgs1	lo	lo	so,po
cloddy→2f,mcr	3vf,f,m	-	3vf,f i 3vf,f,m crt	-	6.3	1	lo	lo	so,po
m→1m,csbk	2m,3vf,f	-	3vf,f,m crt	-	6.0	1	lo	lo	so,po
2m,csbk→ 2f,mcr	2m,3vf,f	Mn shot: flr	3vf,f i 3vf,f,m crt	2n br	6.1	1	lo	lo	so,po
2m,csbk, 30% 2fcr	2m,3vf,f	Mn stains on pf	3vf,f i 3vf,f,m crt	2n br 2n pf	6.2	1	lo	lo	so,po
3m,cpr→ 3m,cabk	2vf,f	Mn stains on pf	1m,2vf,f crt	2mk pf 3n pf	6.6	1	lo	lo	so,po
3f,m pr 3f,mabk	1vf,2f	-	1m,2vf,f crt	2k pf 2mk pf	7.0	1	lo	lo	so,po
2mabk	1f,2vf	Mn stains in pores	2vf,f crt	1k pf 3mk pf	6.9	1	lo	lo	so,po
m→2mabk	1f,2vf	-	2vf,f crt	v1mk pf in waves;3mk br,3mk pc	7.2	sgs1	lo	lo	so,po
m→2msbk	2vf	-	3vf i 2vf crt	3n br,2mk br 3n pc	7.1	sgs1	lo	lo	so,po
m→1msbk	-	-	3vf i	1n br 1mk pc	6.9	1	lo	lo	so,po
cloddy→ 2c,vccr	3vf,f,m	-	3vf,f i	-	6.2	1	lo	lo	so,po
m→1m,csbk	3vf,f,m	-	3vf,m,2f i	-	6.2	1	lo	lo	so,po
2vf,f,mcr	2f,m,3vf	-	3vf,f i 3vf,f,m,c crt	2n br	6.3	1	lo	lo	so,po
2m,csbk 35% 2f,mcr	2m,3vf,f	-	3vf,f i;2m,c, 3vf,f crt	3n br 2n pf	6.8	1	lo	lo	so,po
3m,cpr→ 3m,cabk	1m,2vf,f	Mn stains on pf and in pores	2vf,f crt	3mk pf,1k pf 2n pf	7.1	1	lo	lo	so,po
2cabk	2vf,f	-	2f,3vf crt	3mk br,2mk pf in waves	6.8	sgs1	lo	lo	so,po
m→2cabk	1vf,f	-	3vf i 1vf,f,m crt	2n br,1mk pf, 2mk pc in waves	6.9	sgs1	lo	lo	so,po
m→1msbk	-	-	3vf i 1vf crt	2n br		1s	lo	lo	so,po

Supplementary table 1, part 2. Field descriptions—Continued

Profile no.	Sample no.	Horizon	Basal depth (cm)	Lower boundary	Moist color	Dry color	Texture	Consistence			
								Dry	Moist	Wet	
Laguna Formation,											
HON-21	131	A	11	c,s	2.5YR3/4	5YR4/4	s1+	sh	vfr	so,po	
	132	AB	33	c,w+c,i	2.5YR3/4	2.5YR4/4	scl	sh	fr	so,ps	
	133	BA	46	a,w+a,i	2.5YR3/4	2.5YR4/5	sgscl-cl	sh	fr	ss,ps	
	134	Bt1	71	c,w	2.5YR3/5	2.5YR3/6	sgc	h	fi	s,p	
	135	Bt2	93	c,w	10R3/5	10R3/6, 4/8	sgc	h	fi	s,p	
	136	Bt3	119	c,w	10R3/6	10R4/6	sgc	h	fi	s,p	
	137	Bt4	148	g,w	10R3/6	10R4/6	sgc	h	fi	s,p	
	138	2Bt1	197	g,w	10R3/6	10R4/6, 4/8	grc	sh	fr	ss,p	
	139	2Bt2	274	d,w	2.5YR3/6	2.5YR4/6	grcl	sh	fr	ss,p	
	140	2BC	315	d,w	2.5YR3/6	2.5YR4/6	grcl	h	fr	ss,po	
	141	3BC	473	a,i	5YR3/4	5YR4/3	extg l+	h	fr	so,po	
	142	"C"	>1200			7.5YR4/3	7.5YR6/3	s1	sh	vfr	so,po
	HON-22	143	A	23	c,w	2.5YR3/4	2.5YR4/4	scl-	sh	fr	ss,ps
144		AB	43	c,w	2.5YR3/5	2.5YR4/5	sgscl	sh	vfr	ss,ps	
145		BA	59	a,w+i	2.5YR3/5	2.5YR4/5	sgc	sh	fr	s,p	
146		Bt1	89	c,w	10R3/5	10R3/6	sgc	h	fr	s,p	
147		Bt2	120	c,w	10R3/6	10R3.5/6	sgc	h	fi	s,p	
148		Bt3	154	g,s	10R3/6	10R3/6, 4/6	sgc	h	fr	s,p	
149		2Bt1	207	g,s	10R3/6	10R3/6, 4/6	grc	sh	fr	s,p	
150		2Bt2	270	g,w	10R3/6	2.5YR3/6, 4/6	grcl++	sh	fr	ss,p	
151		2BCt	342	g,w	2.5-5YR3/4	2.5YR4/4, 4/6	vgrc1	sh	vfr	ss,ps	
152		3BCt1	445	g,w	5YR3/4	5YR3/4	extgcl	sh	vfr	ss,po	
153		3BCt2	505	a,w	5YR4/4	5YR4/4	extg+	sh	fr	ss,po	
154		"C"	>1200			5YR4/4	5YR4/6 5YR4/4 skins	s1	sh	vfr	so,po

¹Sandy skeletons on ped faces.

Structure	Roots	Pores	Clay films	Reticulate mottling		pH	Assumed parent material			
				Abundance	Colors		Consistence			
							Texture	Dry	Moist	Wet
exhumed lower member, 1,600 ka										
2csbk+1f,mgr	1f,3vf	3vf,f i	-	-	-	6.2	s1	lo	lo	so,po
2csbk+2f,mgr	1f,m,3vf	2m,3f crt	1n po	-	-	6.2	s1	lo	lo	so,po
5% 2f,mgr		3vf,f i								
2m,csbk	2vf,f,1m,c	3f,m crt	3n pf	-	-	6.2	sgs1	lo	lo	so,po
		3vf,f i	3n po							
3m,cabk	1f,m,c,2vf	3vf crt	4k pf stress cutans;4k po	-	-	5.7	sgs1	lo	lo	so,po
			" ,4k pc							
1f,mpr+	1vf,f,m	2vf crt		-	-	5.3	sgs1	lo	lo	so,po
3m,cabk										
1mpr+3m,cabk	1vf,f,m,1	2vf crt	" "	5% faint subhor.	5YR6/6 D	5.0	sgs1	lo	lo	so,po
				10%	5YR4/4 M					
1mpr+3m,cabk	1vf	2vf crt	" "		7.5YR7/4,7/2 D	4.9	sgs1	lo	lo	so,po
					7.5YR6/4 M					
3m,cabk	v1vf	1vf crt	4k pf,4k po	20-25%, avg dia 1 cm	as above	5.0	grs1	lo	lo	so,po
			4k pc							
2m,cabk	v1vf	1vf crt	4k pf,4k po	25-30%	7.5YR7/2,7/4,7/6 D	5.3	grs1	lo	lo	so,po
			2vf i		7.4YR6/2,6/4,6/6 M					
2m,fabk	-	2vf,f i	3k pf	as above	as above, plus	5.7	grs1	lo	lo	so,po
			3k pc		7/5YR8/4 D, 7/4 M					
2f,mabk	-	3vf,f,m i	2k pf	>50%	7.5YR8/4 D	6.1	extg s1	lo	lo	so,po
			2mk pc		7.5YR6/6,6/8 M					
m+1csbk	-	-	-			6.2	s1	lo	lo	so,po
2csbk burrows	3vf,f	1f,m,2vf i	1vn pf?	-	-	6.4	s1	lo	lo	so,po
1fgr			1vn po?							
1msbk+	1c,vc,2m,3vf	2m,c,3vf crt	1vn pf,1vn po	-	-	6.7	sgs1	lo	lo	so,po
1vf,f,mgr		3vf i	1vn pc							
2msbk	1vc,2vf,f,m	2m,c,vc	3mk pf,3mk po	-	-	6.7	sgs1	lo	lo	so,po
30% 1fgr		3vf,f crt	3mk pc							
1f,mpr+	1f,m,2vf	1m,2vf,f crt	4k pf stress cutans,4kpo,4kpc	-	-	6.9	sgs1	lo	lo	so,po
3f,m,cabk										
3m,cabk	1f,m,2vf	1f,m,2vf crt	" "	occasional faint mottle	-	5.9	sgs1	lo	lo	so,po
				10% subhor.	7.5YR7/2 D	5.4	sgs1	lo	lo	so,po
3m,cabk	1vf	1vf,f crt	" "	15-25%	7.5YR6/2 M	5.4	grs1	lo	lo	so,po
					7.5YR8/2,7/2,7/4 D					
3fabk	1vf	1vf,f crt	3mk pf,3mk po	25%	7.5YR6/2,6/4 M	5.4	grs1	lo	lo	so,po
			3mk pc		7.5YR7/2,7/6 D					
2m,csbk	-	2f,m,c i	2k br,2k pc	30-50%	7.5YR7/2,6/4 M	5.5	grs1	lo	lo	so,po
			2k po		7.5YR8/2 D					
1f,msbk	-	3f,m,c i	2k po,2k pc	>50%	7.5YR7/2 M	6.1	extg s1	lo	lo	so,po
			2k br		7.5YR6/8,8/2 D					
1f,msbk	-	3f,m,c i	2mk po,2mk br	>75%	7.5YR5/7,7/2 M	6.0	extg s1	lo	lo	so,po
			2kpo,2kbr,2mkpc		7.5YR7/2,6/4 D					
m+1m,csbk	-	3f,m,c i	2n br		7.5YR6/2,5/4 M	6.9	s1	lo	lo	so,po
			2mk br							

Supplementary table 2. Physical properties

[Analysts: A.J. Busacca, K. Trott, and J.R. Anikju]

Sample number	Profile number	Horizon	Basal depth (cm)	>2 mm	Percentage of <2-mm fraction								Bulk density (g/cm ³)
					Total sand	vco sand	co sand	m sand	fi+vfi sand	Silt	<2- μ m clay	<1- μ m clay	
Holocene alluvium, 0.6 ka													
1	Hon-1	A	12	0.0	40.6	0.2	2.2	3.3	34.8	43.0	16.3	12.6	1.26
2	Hon-1	2A1	16	0.0	28.9	0.4	1.8	2.4	24.3	54.0	17.1	12.9	1.30
3	Hon-1	2A2	25	0.0	42.8	0.0	0.6	2.7	39.5	41.0	16.2	12.6	1.34
4	Hon-1	2AC	49	0.0	40.5	0.1	0.7	2.8	36.9	43.9	15.6	12.8	1.41
5	Hon-1	2C	85	0.0	48.0	0.2	0.6	1.8	45.4	39.2	12.8	10.3	1.39
6	Hon-1	3C1	95	0.0	59.4	0.1	1.1	4.3	53.9	30.1	10.5	8.5	1.35
7	Hon-1	3C2	122	0.0	59.9	0.0	2.0	9.8	48.1	28.2	11.9	9.6	1.50
8	Hon-1	4C1	140	0.0	66.4	0.5	15.8	19.0	31.1	22.2	11.4	9.3	1.55
9	Hon-1	4C2	170	0.0	62.3	0.4	16.6	17.0	28.3	24.9	12.8	10.7	1.61
10	Hon-2	A1	4	0.0	27.2	0.3	0.5	0.3	26.1	52.9	19.9	15.9	1.33
11	Hon-2	A2	32	0.0	29.5	0.1	0.2	0.2	29.0	51.0	19.5	15.9	1.48
12	Hon-2	C	61	0.0	50.7	0.0	0.1	0.2	50.4	36.1	13.2	10.7	1.33
13	Hon-2	2C	92	0.0	52.8	0.0	0.1	0.2	52.5	34.2	13.0	10.5	1.30
14	Hon-2	3C	103	0.0	44.0	0.0	0.0	0.1	43.9	40.2	15.8	12.3	1.29
15	Hon-2	4C	130	0.0	43.1	3.0	16.7	8.2	15.1	41.0	15.9	12.4	1.48
16	Hon-3	A1	4	0.0	18.6	0.1	0.2	0.3	18.0	57.7	23.7	18.3	1.16
17	Hon-3	A2	16	0.0	23.8	0.0	0.0	0.2	23.6	54.4	21.8	16.7	1.39
18	Hon-3	AC	31	0.0	25.6	0.0	0.0	0.2	25.4	53.1	21.3	16.5	1.51
19	Hon-3	C	54	0.0	49.6	0.0	0.0	0.2	49.4	37.2	13.2	10.5	1.35
20	Hon-3	2C	78	0.0	47.9	0.0	0.0	0.2	47.7	37.9	14.2	11.5	1.30
21	Hon-4	C	17	0.0	59.0	0.0	0.2	1.5	57.4	31.6	9.4	8.0	1.25
22	Hon-4	2A	32	0.0	37.3	0.1	0.2	0.5	36.5	46.9	15.8	13.0	1.26
23	Hon-4	2AC	49	0.0	29.4	0.0	1.0	0.4	27.9	53.7	16.9	13.7	1.24
24	Hon-4	2C	86	0.0	35.8	0.0	0.2	0.8	34.7	49.3	14.9	12.7	1.33
25	Hon-4	3C1	113	0.0	54.7	0.0	0.1	1.0	53.6	34.5	10.8	9.0	1.35
26	Hon-4	3C2	147	0.0	64.7	0.0	0.6	5.7	58.4	25.4	9.9	7.8	1.42
Upper member of the Modesto Formation, 10 ka													
27	Hon-5	Ap1	13	0.0	18.7	0.2	0.9	1.4	16.2	58.0	23.3	18.7	1.54
28	Hon-5	Ap2	23	0.0	18.0	0.3	0.9	1.4	15.4	58.6	23.4	19.0	1.76
29	Hon-5	BA	54	0.0	18.0	0.2	0.8	1.2	15.8	56.7	25.3	21.0	1.67
30	Hon-5	Bw1	88	0.0	20.7	0.1	0.8	1.2	18.6	55.4	23.9	19.6	1.69
31	Hon-5	Bw2	102	0.0	24.8	0.2	0.7	1.3	22.6	52.6	22.6	18.7	1.58
32	Hon-5	BC1	141	0.0	28.2	0.2	0.8	1.4	25.8	49.4	22.4	18.9	1.77
33	Hon-5	BC2	180	0.0	27.3	0.0	0.8	1.6	24.9	50.9	21.8	18.2	1.80
34	Hon-6	Ap1	10	0.0	23.0	0.5	0.9	1.4	20.2	53.6	23.4	17.9	1.57
35	Hon-6	Ap2	22	0.0	22.5	0.1	0.9	1.4	20.1	54.0	23.5	18.1	1.71
36	Hon-6	BA	43	0.0	25.4	0.2	0.7	1.3	23.2	50.3	24.3	19.6	1.55
37	Hon-6	Bw1	91	0.0	31.6	0.6	1.7	2.1	27.2	46.4	22.0	17.5	1.50
38	Hon-6	Bw2	118	0.0	31.8	0.2	1.7	2.2	27.7	46.9	21.8	17.6	1.72
39	Hon-6	BC1	157	0.0	27.0	0.1	0.7	1.5	24.7	50.2	22.8	18.7	1.81
40	Hon-6	BC2	184	0.0	30.2	0.2	1.0	2.2	26.7	48.2	21.6	17.8	1.83
41	Hon-7	Ap1	8	0.4	34.4	0.8	2.3	2.7	28.6	46.7	18.9	15.2	1.80
42	Hon-7	Ap2	30	1.0	32.8	1.3	2.4	2.4	26.7	47.7	19.5	15.5	1.80

Supplementary table 2. Physical properties—Continued

Sample number	Profile number	Horizon	Basal depth (cm)	>2 mm	Percentage of <2-mm fraction								Bulk density (g/cm ³)
					Total sand	vco sand	co sand	m sand	fi+vfi sand	Silt	<2- μ m clay	<1- μ m clay	
Upper member of the Modesto Formation, 10 ka—Continued													
43	Hon-7	BA	54	0.0	27.8	0.9	2.9	3.0	21.0	51.4	20.8	16.5	1.57
44	Hon-7	Bw1	88	0.0	28.7	1.1	3.0	3.0	21.6	48.5	22.8	18.4	1.54
45	Hon-7	Bw2	118	0.0	32.5	0.8	2.5	3.1	26.1	46.5	21.0	17.6	1.78
46	Hon-7	BC	180	0.0	31.1	0.5	2.0	3.0	25.6	47.3	21.6	17.8	1.74
47	Hon-7	2BC	230	0.0	12.0	0.5	0.9	1.0	9.6	60.4	27.6	21.8	1.64
48	Hon-7	3Cox	290	1.8	42.9	1.4	2.7	1.5	37.3	39.9	17.2	13.9	0.00
49	Hon-7	4Cox	340	0.7	79.4	7.6	27.4	18.8	25.6	12.8	7.8	6.3	0.00
50	Hon-7	4Cn	370	0.3	83.3	9.4	35.0	17.4	21.5	11.2	5.5	4.2	0.00
51	Hon-8	Ap1	7	1.1	34.6	0.9	2.6	3.0	28.1	46.5	18.9	15.1	1.72
52	Hon-8	Ap2	34	2.9	33.4	1.2	2.9	3.1	26.2	47.0	19.6	15.6	1.68
53	Hon-8	BA	57	0.5	29.8	2.0	3.5	3.3	21.0	47.0	23.2	18.7	1.56
54	Hon-8	Bw1	90	0.6	31.4	1.6	4.1	3.3	22.4	47.3	21.3	17.4	1.70
55	Hon-8	Bw2	126	0.0	32.2	1.0	2.9	2.7	25.6	47.3	20.5	16.8	1.73
56	Hon-8	BC1	191	0.0	19.8	0.3	0.8	1.2	17.5	57.1	23.1	18.9	1.70
57	Hon-8	BC2	240	0.0	32.4	0.4	1.2	2.4	28.4	48.9	18.7	15.0	1.63
58	Hon-8	2Cox	390	0.8	88.0	8.7	42.5	20.2	16.6	7.5	4.5	3.4	0.00
Lower member of the Modesto Formation, 40 ka													
59	Hon-10	Ap	22	6.3	59.1	11.1	17.6	8.3	22.1	29.6	11.3	8.0	1.63
60	Hon-10	BA	40	5.9	61.7	12.5	21.1	9.6	18.6	26.1	12.2	9.1	1.79
61	Hon-10	Bt1	86	6.5	64.6	15.7	22.2	9.4	17.3	24.3	12.1	9.1	1.69
62	Hon-10	Bt2	132	5.6	59.9	9.8	20.0	9.4	20.7	26.2	13.9	13.0	1.76
63	Hon-10	BC	150	7.0	68.4	11.4	22.9	12.1	22.0	21.1	10.5	8.3	1.67
64	Hon-10	C	205	10.5	71.4	12.7	23.0	12.5	23.2	20.2	8.4	6.4	1.62
65	Hon-10	2C	225	2.9	50.0	3.8	5.2	2.7	38.3	32.5	7.5	5.3	1.43
66	Hon-11	Ap	18	8.0	55.6	9.2	17.7	8.2	20.5	30.8	13.6	10.0	1.55
67	Hon-11	BA	45	5.0	62.7	12.0	21.6	9.5	19.6	24.9	12.4	9.3	1.94
68	Hon-11	Bt1	94	6.1	60.9	10.4	20.7	9.4	20.3	25.7	13.4	10.5	1.74
69	Hon-11	Bt2	125	4.4	56.3	7.4	19.3	8.8	20.8	28.6	15.1	11.9	1.72
70	Hon-11	BC	145	6.7	64.9	11.8	21.6	10.4	21.1	23.8	11.3	9.0	1.70
71	Hon-11	C	179	14.3	67.7	14.4	21.6	11.3	20.4	22.3	10.0	8.0	1.66
72	Hon-11	2C	220	0.0	39.2	0.3	0.8	0.6	37.5	53.2	7.6	5.2	1.48
Upper member of the Riverbank Formation, 130 ka													
73	Hon-13	Ap	24	0.0	28.9	2.0	4.3	4.1	18.5	54.6	16.5	11.6	1.50
74	Hon-13	BA	33	0.0	28.3	2.0	4.0	4.1	18.2	51.8	19.9	14.5	1.77
75	Hon-13	BAt1	50	0.0	27.6	2.2	4.1	4.2	17.1	49.2	23.2	17.7	1.68
76	Hon-13	BAt2	62	0.0	37.2	2.9	6.9	7.3	20.1	36.4	26.4	21.4	1.80
77	Hon-13	Bt1	86	0.0	31.3	2.7	5.6	6.9	16.0	25.7	43.0	39.1	1.91
78	Hon-13	Bt2	102	0.0	14.5	0.7	1.8	2.6	8.14	34.6	50.9	46.4	1.96
79	Hon-13	Bt3	123	0.0	14.1	0.5	1.3	1.8	10.5	44.1	41.8	35.7	1.93
80	Hon-13	BCt	157	0.0	13.8	0.0	1.0	1.8	11.0	52.7	33.5	29.9	1.87
81	Hon-13	2BCt1	208	0.0	46.9	0.2	1.2	4.2	41.3	27.4	25.7	22.7	1.89
82	Hon-13	2BCt2	245	0.0	56.7	0.2	0.6	7.2	48.7	19.0	24.3	22.0	1.86
83	Hon-13	2BCt3	266	0.0	61.7	0.0	1.0	8.9	51.8	17.1	21.2	19.4	1.83
84	Hon-13	2CB	301	0.0	70.7	0.9	8.6	21.4	39.8	11.9	17.4	16.2	1.78

Supplementary table 2. Physical properties—Continued

Sample number	Profile number	Horizon	Basal depth (cm)	>2 mm	Percentage of <2-mm fraction								Bulk density (g/cm ³)
					Total sand	vco sand	co sand	m sand	fi+vf _i sand	Silt	<2- μ m clay	<1- μ m clay	
Upper member of the Riverbank Formation, 130 ka—Continued													
85	Hon-14	Ap	28	0.0	28.8	1.9	4.2	4.2	18.5	55.2	16.0	10.7	1.55
86	Hon-14	BA	39	0.0	25.8	1.6	4.2	3.8	16.1	52.3	21.9	15.7	1.69
87	Hon-14	BAt1	59	0.0	25.2	1.6	4.4	4.1	15.1	51.4	23.4	17.7	1.65
88	Hon-14	BAt2	76	0.0	24.5	1.0	4.2	4.7	14.6	45.1	30.4	22.7	1.76
89	Hon-14	Bt1	111	0.0	12.8	0.9	2.0	1.9	8.0	42.6	44.6	38.7	1.91
90	Hon-14	Bt2	126	1.0	24.6	1.8	4.6	3.7	15.3	38.5	36.9	32.6	1.95
91	Hon-14	2BCt1	150	0.0	24.4	0.1	0.6	1.3	22.3	41.6	34.0	30.2	1.93
92	Hon-14	2BCt2	200	0.0	21.2	0.4	1.1	1.1	18.5	48.7	30.1	26.5	1.77
93	Hon-14	2BCt3	260	0.0	42.1	0.1	0.8	3.0	38.1	30.5	27.4	24.3	1.73
94	Hon-14	2CB	320	0.4	57.1	0.7	2.5	7.5	46.4	20.3	22.6	19.6	1.78
Lower member of the Riverbank Formation, 250 ka													
95	Hon-17	Ap1	18	3.5	42.1	4.4	7.7	5.8	24.2	40.2	17.7	13.0	1.60
96	Hon-17	Ap2	24	3.4	42.3	4.3	8.5	5.7	23.8	39.9	17.8	13.3	1.64
97	Hon-17	BA	76	1.6	35.6	2.8	6.3	5.1	21.4	37.2	27.2	22.4	1.62
98	Hon-17	Bt1	100	1.1	32.5	2.3	5.8	4.2	20.2	37.9	29.6	24.7	1.76
99	Hon-17	Bt2	160	0.0	26.7	0.8	2.0	1.9	22.0	40.2	33.1	28.7	1.86
100	Hon-17	2BCt	201	0.0	47.7	8.4	23.5	5.4	10.4	27.5	24.8	21.4	1.90
101	Hon-17	3BCt	208	0.0	33.4	2.5	8.1	4.8	18.0	39.7	26.9	22.9	1.88
102	Hon-17	4BCt	295	35.0	66.3	16.2	20.3	14.5	15.3	13.1	20.6	18.1	1.70
103	Hon-18	Ap1	19	4.0	42.3	4.2	7.6	5.9	24.6	40.9	16.8	13.1	1.69
104	Hon-18	Ap2	30	3.0	39.2	3.6	7.3	5.7	22.5	43.7	17.1	13.7	1.58
105	Hon-18	BA	90	1.4	34.5	2.4	6.0	4.7	21.5	40.0	25.5	21.2	1.54
106	Hon-18	Bt1	113	0.7	29.0	1.8	4.3	3.5	19.4	41.9	29.1	25.1	1.76
107	Hon-18	Bt2	170	0.0	17.2	0.6	2.3	1.1	13.2	48.9	33.9	30.2	1.93
108	Hon-18	2BCt	190	0.4	32.6	5.0	16.5	3.2	7.8	39.4	28.0	25.1	1.95
109	Hon-18	3BCt	240	0.3	32.0	0.9	5.5	6.8	18.8	38.9	29.1	25.3	2.20
110	Hon-18	4BCt	300	35.0	63.6	13.1	18.8	14.8	16.8	15.6	20.8	18.8	1.89
111	Hon-19	Ap1	7	1.6	43.6	2.9	7.8	7.1	25.8	40.2	16.2	12.0	1.45
112	Hon-19	Ap2	24	1.5	42.5	3.0	7.6	6.9	25.0	38.4	19.1	14.9	1.64
113	Hon-19	BA	63	1.0	40.6	3.6	7.4	6.3	23.3	35.8	23.6	19.4	1.56
114	Hon-19	Bt1	91	1.0	40.0	2.8	7.6	6.4	23.2	36.2	23.8	20.0	1.75
115	Hon-19	Bt2	126	0.6	34.6	1.7	6.6	4.8	21.5	32.2	33.2	28.6	1.88
116	Hon-19	Bt3	176	1.4	34.6	1.8	4.0	3.6	25.2	31.4	34.0	29.1	1.87
117	Hon-19	BCt	218	0.6	46.1	2.2	4.8	4.1	35.0	27.4	26.5	23.4	1.92
118	Hon-19	2BCt1	246	4.8	65.5	10.7	22.9	12.3	18.6	14.3	20.2	18.6	1.88
119	Hon-19	2BCt2	268	7.4	72.4	9.0	28.5	17.7	17.2	12.2	15.4	12.1	1.77
120	Hon-19	2BCt3	300	6.7	75.7	9.6	31.5	19.0	15.6	10.6	13.7	12.5	1.72
121	Hon-19	3Cox	320	15.2	82.4	24.3	36.9	13.9	7.3	7.1	10.5	9.6	0.00
122	Hon-19	3Cox	410	0.0	79.6	18.8	35.1	15.8	9.9	7.2	13.2	11.9	0.00
123	Hon-20	Ap1	11	1.8	43.8	3.1	7.8	6.9	26.0	39.4	16.8	12.8	1.48
124	Hon-20	Ap2	30	1.2	43.1	2.9	7.9	7.0	25.3	38.7	18.2	14.3	1.63
125	Hon-20	BA	60	1.0	40.1	2.4	7.0	6.6	24.1	36.1	23.8	19.9	1.59
126	Hon-20	Bt1	114	0.7	39.3	2.1	7.3	6.4	23.5	36.0	24.7	20.5	1.73
127	Hon-20	Bt2	191	0.3	34.6	2.0	4.2	3.9	24.5	32.0	33.4	29.1	1.90

Supplementary table 2. Physical properties—Continued

Sample number	Profile number	Horizon	Basal depth (cm)	>2 mm	Percentage of <2-mm fraction								Bulk density (g/cm ³)
					Total sand	vco sand	co sand	m sand	fi+vf _i sand	Silt	<2- μ m clay	<1- μ m clay	
Lower member of the Riverbank Formation, 250 ka—Continued													
128	Hon-20	2BCt1	223	1.8	57.7	5.8	12.6	10.5	28.8	20.3	22.0	19.9	1.88
129	Hon-20	2BCt2	260	9.9	70.3	11.2	23.5	17.8	17.9	11.5	18.2	16.6	1.78
130	Hon-20	2CB	283	8.5	81.9	17.4	36.5	17.3	10.7	6.7	11.4	10.7	1.77
Exhumed lower member of the Laguna Formation, 1,600 ka													
131	Hon-21	A	11	4.0	60.1	3.4	14.8	13.6	28.3	21.6	18.3	15.2	1.62
132	Hon-21	AB	33	1.0	53.0	2.8	13.8	12.1	24.3	22.1	24.9	21.1	1.78
133	Hon-21	BA	46	7.0	45.7	2.1	10.4	10.0	23.2	24.8	29.5	25.5	1.57
134	Hon-21	Bt1	71	7.0	29.5	2.0	6.9	5.9	14.7	19.6	50.9	47.2	1.71
135	Hon-21	Bt2	93	7.0	26.7	1.7	6.9	5.5	12.6	18.8	54.5	50.3	1.84
136	Hon-21	Bt3	119	7.0	29.9	2.7	8.3	5.9	13.0	19.4	50.7	46.5	1.81
137	Hon-21	Bt4	148	7.0	33.2	3.3	9.2	6.8	13.9	18.8	48.0	43.4	1.78
138	Hon-21	2Bt1	197	20.0	33.9	3.6	9.8	7.5	13.0	21.3	44.6	39.2	1.80
139	Hon-21	2Bt2	274	20.0	39.8	4.8	12.5	9.1	13.4	25.1	35.2	30.5	1.72
140	Hon-21	2BC	315	25.0	38.8	4.6	11.4	7.7	15.0	27.7	33.4	28.9	1.66
141	Hon-21	3BC	473	55.0	44.5	5.6	12.9	9.2	16.8	28.8	26.4	22.6	1.72
142	Hon-21	C	1300	0.0	78.3	20.1	33.9	12.8	11.6	9.6	11.5	8.1	0.00
143	Hon-22	A	23	3.0	56.4	2.8	14.8	13.6	25.2	21.7	21.5	17.9	1.74
144	Hon-22	AB	43	7.0	46.6	2.0	10.2	11.0	23.4	24.1	29.1	25.1	1.36
145	Hon-22	BA	59	7.0	34.7	2.1	8.7	7.8	16.1	21.5	43.9	39.9	1.63
146	Hon-22	Bt1	89	7.0	25.0	2.0	6.2	5.3	12.3	19.5	54.5	50.6	1.83
147	Hon-22	Bt2	120	7.0	28.1	2.6	7.4	5.9	12.1	20.3	51.4	46.7	1.83
148	Hon-22	Bt3	154	7.0	28.4	2.0	7.6	5.2	13.5	20.2	51.4	47.1	1.82
149	Hon-22	2Bt1	207	20.0	32.5	2.5	10.0	7.3	12.7	20.4	47.2	41.8	1.93
150	Hon-22	2Bt2	270	30.0	36.0	3.8	12.1	7.5	12.6	24.6	39.4	33.8	1.68
151	Hon-22	2BCt	342	35.0	43.0	6.5	15.6	8.0	12.8	26.9	30.2	25.8	1.62
152	Hon-22	3BCt1	445	60.0	47.4	10.8	10.4	7.5	18.7	29.2	23.4	20.2	1.73
153	Hon-22	3BCt2	505	70.0	40.5	9.1	9.9	6.4	15.0	25.1	34.4	30.7	2.12
154	Hon-22	C	1300	0.0	69.3	16.3	37.8	8.0	7.2	13.0	17.7	16.2	0.00
Modern alluvium, 0 ka													
155	Hon-71	Cn	0	0.0	86.2	17.1	35.4	17.0	16.7	8.0	5.8	4.6	0.00
156	Hon-72	Cn	0	0.0	93.5	1.4	32.7	44.5	14.9	3.7	2.8	2.3	0.00

Supplementary table 3. Extractive chemical analyses

[Analysts: A.J. Busacca and P. Janitzky]

Sample number	Profile number	Horizon	Basal depth (cm)	Percent of <2-mm fraction		
				Organic carbon	Fe _d	mags (pct)
Holocene alluvium, 0.6 ka						
1	Hon-1	A	12	2.20	2.12	—
2	Hon-1	2A1	16	2.22	2.16	—
3	Hon-1	2A2	25	1.38	1.94	—
4	Hon-1	2AC	49	1.08	2.04	—
5	Hon-1	2C	85	.85	2.06	—
6	Hon-1	3C1	95	.64	1.86	—
7	Hon-1	3C2	122	.47	1.53	—
8	Hon-1	4C1	140	.11	1.38	—
9	Hon-1	4C2	170	2.33	2.43	—
10	Hon-2	A1	4	.58	1.46	—
11	Hon-2	A2	32	1.67	2.29	—
12	Hon-2	C	61	.60	2.00	—
13	Hon-2	2C	92	.60	2.01	—
14	Hon-2	3C	103	.54	2.09	—
15	Hon-2	4C	130	.26	1.67	—
16	Hon-3	A1	4	3.27	2.41	—
17	Hon-3	A2	16	1.60	2.43	—
18	Hon-3	AC	31	1.25	2.37	—
19	Hon-3	C	54	.58	1.98	—
20	Hon-3	2C	78	.56	1.99	—
21	Hon-4	C	17	.81	1.66	0.58
22	Hon-4	2A	32	1.87	2.06	.18
23	Hon-4	2AC	49	1.43	2.27	.12
24	Hon-4	2C	86	.64	2.09	.11
25	Hon-4	3C1	113	.43	1.88	.44
26	Hon-4	3C2	147	.48	1.77	.48
Upper member of the Modesto Formation, 10 ka						
27	Hon-5	Ap1	13	1.52	2.69	0.02
28	Hon-5	Ap2	23	1.38	2.71	.02
29	Hon-5	BA	54	.87	2.89	.01
30	Hon-5	Bw1	88	.51	2.79	.03
31	Hon-5	Bw2	102	.35	2.75	.05
32	Hon-5	BC1	141	.20	2.67	.02
33	Hon-5	BC2	180	.18	2.46	.02
34	Hon-6	Ap1	10	1.50	2.63	—
35	Hon-6	Ap2	22	1.27	2.65	—
36	Hon-6	BA	43	.97	2.74	—
37	Hon-6	Bw1	91	.59	2.54	—
38	Hon-6	Bw2	118	.40	2.52	—
39	Hon-6	BC1	157	.21	2.46	—
40	Hon-6	BC2	184	.18	2.22	—
41	Hon-7	Ap1	8	1.13	2.41	—
42	Hon-7	Ap2	30	1.06	2.46	—
43	Hon-7	BA	54	.58	2.76	—
44	Hon-7	Bw1	88	.51	2.63	—
45	Hon-7	Bw2	118	.27	2.41	—
46	Hon-7	BC	180	.15	2.27	—
47	Hon-7	2BC	230	.19	2.08	—
48	Hon-7	3Cox	290	.21	1.59	—
49	Hon-7	4Cox	340	.11	1.06	—
50	Hon-7	4Cn	370	.10	.96	—

Sample number	Profile number	Horizon	Basal depth (cm)	Percent of <2-mm fraction		
				Organic carbon	Fe _d	mags (pct)
Upper member of the Modesto Formation, 10 ka—Continued						
51	Hon-8	Ap1	7	1.22	2.47	—
52	Hon-8	Ap2	34	1.21	2.46	—
53	Hon-8	BA	57	.56	2.67	—
54	Hon-8	Bw1	90	.39	2.58	—
55	Hon-8	Bw2	126	.19	2.33	—
56	Hon-8	BC1	191	.39	2.23	—
57	Hon-8	BC2	240	.30	1.89	—
58	Hon-8	2Cox	390	.03	.94	—
Lower member of the Modesto Formation, 40 ka						
59	Hon-10	Ap	22	2.08	1.13	0.60
60	Hon-10	BA	40	.62	1.35	.55
61	Hon-10	Bt1	86	.40	1.35	.78
62	Hon-10	Bt2	132	.49	1.47	.75
63	Hon-10	BC	150	.39	1.31	.87
64	Hon-10	C	205	.28	1.22	1.13
65	Hon-10	2C	225	.16	1.27	.29
66	Hon-11	Ap	18	2.07	1.13	—
67	Hon-11	BA	45	.37	1.31	—
68	Hon-11	Bt1	94	.24	1.43	—
69	Hon-11	Bt2	125	.17	1.47	—
70	Hon-11	BC	145	.16	1.37	—
71	Hon-11	C	179	.13	1.18	—
72	Hon-11	2C	220	.14	1.38	—
Upper member of the Riverbank Formation, 130 ka						
73	Hon-13	Ap	24	.92	2.44	—
74	Hon-13	BA	33	.31	2.69	—
75	Hon-13	BAt1	50	.24	2.81	—
76	Hon-13	BAt2	62	.13	2.73	—
77	Hon-13	Bt1	86	.18	2.64	—
78	Hon-13	Bt2	102	.19	2.25	—
79	Hon-13	Bt3	123	.12	2.30	—
80	Hon-13	BCt	157	.11	2.35	—
81	Hon-13	2BCt1	208	.08	1.75	—
82	Hon-13	2BCt2	245	.08	1.84	—
83	Hon-13	2BCt3	266	.07	1.70	—
84	Hon-13	2CB	301	.07	1.65	—
85	Hon-14	Ap	28	.82	2.38	.01
86	Hon-14	BA	39	.35	2.68	.00
87	Hon-14	BAt1	59	.23	2.79	.01
88	Hon-14	BAt2	76	.24	3.07	.00
89	Hon-14	Bt1	111	.17	2.59	.01
90	Hon-14	Bt2	126	.11	2.27	.00
91	Hon-14	2BCt1	150	.09	2.08	.01
92	Hon-14	2BCt2	200	.07	1.76	.02
93	Hon-14	2BCt3	260	.07	1.86	.03
94	Hon-14	2CB	320	.08	1.72	—
Lower member of the Riverbank Formation, 250 ka						
95	Hon-17	Ap1	18	.89	1.99	—
96	Hon-17	Ap2	24	.74	2.18	—

Supplementary table 3. Extractive chemical analyses—Continued

Sample number	Profile number	Horizon	Basal depth (cm)	Percent of <2-mm fraction		
				Organic carbon	Fe _d	mags (pct)
Lower member of the Riverbank Formation, 250 ka—Continued						
97	Hon-17	BA	76	.26	2.82	—
98	Hon-17	Bt1	100	.16	2.88	—
99	Hon-17	Bt2	160	.11	2.78	—
100	Hon-17	2BCt	201	.09	2.21	—
101	Hon-17	3BCt	208	.07	2.16	—
102	Hon-17	4BCt	295	.07	1.89	—
103	Hon-18	Ap1	19	.88	2.14	.03
104	Hon-18	Ap2	30	.77	2.23	.02
105	Hon-18	BA	90	.23	2.71	.02
106	Hon-18	Bt1	113	.15	2.82	.01
107	Hon-18	Bt2	170	.09	1.93	.00
108	Hon-18	2BCt	190	.08	2.11	.01
109	Hon-18	3BCt	240	.09	2.07	.00
110	Hon-18	4BCt	300	.06	1.90	.01
111	Hon-19	Ap1	7	1.73	1.97	—
112	Hon-19	Ap2	24	.68	2.22	—
113	Hon-19	BA	63	.27	2.54	—
114	Hon-19	Bt1	91	.23	2.52	—
115	Hon-19	Bt2	126	.14	2.88	—
116	Hon-19	Bt3	176	.13	2.86	—
117	Hon-19	BCt	218	.12	2.28	—
118	Hon-19	2BCt1	246	.11	1.84	—
119	Hon-19	2BCt2	268	.09	1.64	—
120	Hon-19	2BCt3	300	.08	1.67	—
121	Hon-19	3Cox	320	.08	1.42	—
122	Hon-19	3Cox	410	.08	1.69	—
123	Hon-20	Ap1	11	1.57	2.14	—
124	Hon-20	Ap2	30	.62	2.28	—
125	Hon-20	BA	60	.26	2.59	—
126	Hon-20	Bt1	114	.17	2.63	—
127	Hon-20	Bt2	191	.04	1.99	—
128	Hon-20	2BCt1	223	.10	2.93	—

Sample number	Profile number	Horizon	Basal depth (cm)	Percent of <2-mm fraction		
				Organic carbon	Fe _d	mags (pct)
Lower member of the Riverbank Formation, 250 ka—Continued						
129	Hon-20	2BCt2	260	.04	1.78	—
130	Hon-20	2CB	283	.13	1.59	—
Exhumed lower member of the Laguna Formation, 1,600 ka						
131	Hon-21	A	11	1.23	2.49	0.13
132	Hon-21	AB	33	.80	2.89	.06
133	Hon-21	BA	46	.55	3.50	.10
134	Hon-21	Bt1	71	.37	4.35	.04
135	Hon-21	Bt2	93	.25	4.71	.03
136	Hon-21	Bt3	119	.22	4.67	.04
137	Hon-21	Bt4	148	.23	4.88	.02
138	Hon-21	2Bt1	197	.21	5.01	.01
139	Hon-21	2Bt2	274	.17	4.79	.01
140	Hon-21	2BC	315	.20	4.39	.02
141	Hon-21	3BC	473	.15	2.61	.02
142	Hon-21	C	1300	.05	1.66	.90
143	Hon-22	A	23	1.22	2.74	—
144	Hon-22	AB	43	.68	3.46	—
145	Hon-22	BA	59	.18	4.31	—
146	Hon-22	Bt1	89	.19	4.83	—
147	Hon-22	Bt2	120	.16	4.79	—
148	Hon-22	Bt3	154	.18	4.86	—
149	Hon-22	2Bt1	207	.15	4.90	—
150	Hon-22	2Bt2	270	.16	4.64	—
151	Hon-22	2BCt	342	.13	3.91	—
152	Hon-22	3BCt1	445	.13	2.23	—
153	Hon-22	3BCt2	505	.14	2.04	—
154	Hon-22	C	1300	.05	1.49	—
Modern alluvium, 0 ka						
155	Hon-71	Cn	0	.62	1.06	—
156	Hon-72	Cn	0	.13	.51	—

Supplementary table 4, part 1. Clay mineralogy of the coarse (0.2–2 μm) fraction

[Clay minerals: +, trace; ++, moderate; +++, abundant; +++++, clearly dominant; —, not determined. Primary minerals: X, moderate; XX, abundant; —, not determined. Analysts: H. Foolad and A.J. Busacca]

Sample number	Profile	Horizon	Basal depth (cm)	Kaolin	Chlorite	Chloritized vermiculite	Vermiculite	Mica	Smectite	Talc	Quartz	Feldspar
Holocene alluvium, 0.6 ka												
1	Hon-1	A	12	—	—	—	—	—	—	—	—	—
2	Hon-1	2A1	16	—	—	—	—	—	—	—	—	—
3	Hon-1	2A2	25	—	—	—	—	—	—	—	—	—
4	Hon-1	2AC	49	—	—	—	—	—	—	—	—	—
5	Hon-1	2C	85	—	—	—	—	—	—	—	—	—
6	Hon-1	3C1	95	—	—	—	—	—	—	—	—	—
7	Hon-1	3C2	122	—	—	—	—	—	—	—	—	—
8	Hon-1	4C1	140	—	—	—	—	—	—	—	—	—
9	Hon-1	4C2	170	—	—	—	—	—	—	—	—	—
10	Hon-2	A1	4	—	—	—	—	—	—	—	—	—
11	Hon-2	A2	32	—	—	—	—	—	—	—	—	—
12	Hon-2	C	61	—	—	—	—	—	—	—	—	—
13	Hon-2	2C	92	—	—	—	—	—	—	—	—	—
14	Hon-2	3C	103	—	—	—	—	—	—	—	—	—
15	Hon-2	4C	130	—	—	—	—	—	—	—	—	—
16	Hon-3	A1	4	—	—	—	—	—	—	—	—	—
17	Hon-3	A2	16	—	—	—	—	—	—	—	—	—
18	Hon-3	AC	31	—	—	—	—	—	—	—	—	—
19	Hon-3	C	54	—	—	—	—	—	—	—	—	—
20	Hon-3	2C	78	—	—	—	—	—	—	—	—	—
21	Hon-4	C	17	—	—	—	—	—	—	—	—	—
22	Hon-4	2A	32	+++	+++	++	+++	+	++	++	X	X
23	Hon-4	2AC	49	—	—	—	—	—	—	—	—	—
24	Hon-4	2C	86	+++	+	++	++++	+	+	—	X	X
25	Hon-4	3C1	113	—	—	—	—	—	—	—	—	—
26	Hon-4	3C2	147	—	—	—	—	—	—	—	—	—
Upper member of the Modesto Formation, 10 ka												
27	Hon-5	Ap1	13	—	—	—	—	—	—	—	—	—
28	Hon-5	Ap2	23	+++	+	++	++++	—	+	—	X	X
29	Hon-5	BA	54	—	—	—	—	—	—	—	—	—
30	Hon-5	Bw1	88	+++	—	++	++++	—	+	—	X	X
31	Hon-5	Bw2	102	—	—	—	—	—	—	—	—	—
32	Hon-5	BC1	141	—	—	—	—	—	—	—	—	—
33	Hon-5	BC2	180	—	—	++	++++	+	+	—	X	X
34	Hon-6	Ap1	10	—	—	—	—	—	—	—	—	—
35	Hon-6	Ap2	22	—	—	—	—	—	—	—	—	—
36	Hon-6	BA	43	—	—	—	—	—	—	—	—	—
37	Hon-6	Bw1	91	—	—	—	—	—	—	—	—	—
38	Hon-6	Bw2	118	—	—	—	—	—	—	—	—	—
39	Hon-6	BC1	157	—	—	—	—	—	—	—	—	—
40	Hon-6	BC2	184	—	—	—	—	—	—	—	—	—
41	Hon-7	Ap1	8	—	—	—	—	—	—	—	—	—
42	Hon-7	Ap2	30	—	—	—	—	—	—	—	—	—

Supplementary table 4, part 1. Clay mineralogy of the coarse (0.2–2 μm) fraction—Continued

Sample number	Profile number	Horizon	Basal depth (cm)	Kaolin	Chlorite	Chloritized vermiculite	Vermiculite	Mica	Smectite	Talc	Quartz	Feldspar
Upper member of the Modesto Formation, 10 ka—Continued												
43	Hon-7	BA	54	—	—	—	—	—	—	—	—	—
44	Hon-7	Bw1	88	—	—	—	—	—	—	—	—	—
45	Hon-7	Bw2	118	—	—	—	—	—	—	—	—	—
46	Hon-7	BC	180	—	—	—	—	—	—	—	—	—
47	Hon-7	2BC	230	—	—	—	—	—	—	—	—	—
48	Hon-7	3Cox	290	—	—	—	—	—	—	—	—	—
49	Hon-7	4Cox	340	—	—	—	—	—	—	—	—	—
50	Hon-7	4Cn	370	—	—	—	—	—	—	—	—	—
51	Hon-8	Ap1	7	—	—	—	—	—	—	—	—	—
52	Hon-8	Ap2	34	—	—	—	—	—	—	—	—	—
53	Hon-8	BA	57	—	—	—	—	—	—	—	—	—
54	Hon-8	Bw1	90	—	—	—	—	—	—	—	—	—
55	Hon-8	Bw2	126	—	—	—	—	—	—	—	—	—
56	Hon-8	BC1	191	—	—	—	—	—	—	—	—	—
57	Hon-8	BC2	240	—	—	—	—	—	—	—	—	—
58	Hon-8	2Cox	390	—	—	—	—	—	—	—	—	—
Lower member of the Modesto Formation, 40 ka												
59	Hon-10	Ap	22	++	+	++	++++	+++	—	+	X	X
60	Hon-10	BA	40	—	—	—	—	—	—	—	—	—
61	Hon-10	Bt1	86	—	—	—	—	—	—	—	—	—
62	Hon-10	Bt2	132	++	+	++	++++	+++	—	+	X	X
63	Hon-10	BC	150	—	—	—	—	—	—	—	—	—
64	Hon-10	C	205	++	+	++	++++	+++	—	+	X	X
65	Hon-10	2C	225	—	—	—	—	—	—	—	—	—
66	Hon-11	Ap	18	—	—	—	—	—	—	—	—	—
67	Hon-11	BA	45	—	—	—	—	—	—	—	—	—
68	Hon-11	Bt1	94	—	—	—	—	—	—	—	—	—
69	Hon-11	Bt2	125	—	—	—	—	—	—	—	—	—
70	Hon-11	BC	145	—	—	—	—	—	—	—	—	—
71	Hon-11	C	179	—	—	—	—	—	—	—	—	—
72	Hon-11	2C	220	—	—	—	—	—	—	—	—	—
Upper member of the Riverbank Formation, 130 ka												
73	Hon-13	Ap	24	—	—	—	—	—	—	—	—	—
74	Hon-13	BA	33	—	—	—	—	—	—	—	—	—
75	Hon-13	BAt1	50	—	—	—	—	—	—	—	—	—
76	Hon-13	BAt2	62	—	—	—	—	—	—	—	—	—
77	Hon-13	Bt1	86	—	—	—	—	—	—	—	—	—
78	Hon-13	Bt2	102	—	—	—	—	—	—	—	—	—
79	Hon-13	Bt3	123	—	—	—	—	—	—	—	—	—
80	Hon-13	BCt	157	—	—	—	—	—	—	—	—	—
81	Hon-13	2BCt1	208	—	—	—	—	—	—	—	—	—
82	Hon-13	2BCt2	245	—	—	—	—	—	—	—	—	—
83	Hon-13	2BCt3	266	—	—	—	—	—	—	—	—	—
84	Hon-13	2CB	301	—	—	—	—	—	—	—	—	—
85	Hon-14	Ap	28	+++	—	+	+++	++	+	+	XX	X
86	Hon-14	BA	39	—	—	—	—	—	—	—	—	—

Supplementary table 4, part 1. Clay mineralogy of the coarse (0.2–2 μm) fraction—Continued

Sample number	Profile number	Horizon	Basal depth (cm)	Kaolin	Chlorite	Chloritized vermiculite	Vermiculite	Mica	Smectite	Talc	Quartz	Feldspar
Upper member of the Riverbank Formation, 130 ka—Continued												
87	Hon-14	BA _{t1}	59	—	—	—	—	—	—	—	—	—
88	Hon-14	BA _{t2}	76	—	—	—	—	—	—	—	—	—
89	Hon-14	B _{t1}	111	+++	—	+	++++	+	+	+	XX	X
90	Hon-14	B _{t2}	126	—	—	—	—	—	—	—	—	—
91	Hon-14	2BC _{t1}	150	—	—	—	—	—	—	—	—	—
92	Hon-14	2BC _{t2}	200	—	—	—	—	—	—	—	—	—
93	Hon-14	2BC _{t3}	260	++	+	+	++++	+	+	+	X	XX
94	Hon-14	2CB	320	—	—	—	—	—	—	—	—	—
Lower member of the Riverbank Formation, 250 ka												
95	Hon-17	Ap ₁	18	—	—	—	—	—	—	—	—	—
96	Hon-17	Ap ₂	24	—	—	—	—	—	—	—	—	—
97	Hon-17	BA	76	—	—	—	—	—	—	—	—	—
98	Hon-17	B _{t1}	100	—	—	—	—	—	—	—	—	—
99	Hon-17	B _{t2}	160	—	—	—	—	—	—	—	—	—
100	Hon-17	2BC _t	201	—	—	—	—	—	—	—	—	—
101	Hon-17	3BC _t	208	—	—	—	—	—	—	—	—	—
102	Hon-17	4BC _t	295	—	—	—	—	—	—	—	—	—
103	Hon-18	Ap ₁	19	—	—	—	—	—	—	—	—	—
104	Hon-18	Ap ₂	30	+++	+	+	+++	+++	—	+	XX	X
105	Hon-18	BA	90	—	—	—	—	—	—	—	—	—
106	Hon-18	B _{t1}	113	+++	—	++	++++	++	+	—	XX	X
107	Hon-18	B _{t2}	170	+++	—	—	++++	+	+	—	X	XX
108	Hon-18	2BC _t	190	—	—	—	—	—	—	—	—	—
109	Hon-18	3BC _t	240	—	—	—	—	—	—	—	—	—
110	Hon-18	4BC _t	300	—	—	—	—	—	—	—	—	—
111	Hon-19	Ap ₁	7	—	—	—	—	—	—	—	—	—
112	Hon-19	Ap ₂	24	—	—	—	—	—	—	—	—	—
113	Hon-19	BA	63	—	—	—	—	—	—	—	—	—
114	Hon-19	B _{t1}	91	—	—	—	—	—	—	—	—	—
115	Hon-19	B _{t2}	126	—	—	—	—	—	—	—	—	—
116	Hon-19	B _{t3}	176	—	—	—	—	—	—	—	—	—
117	Hon-19	BC _t	218	—	—	—	—	—	—	—	—	—
118	Hon-19	2BC _{t1}	246	—	—	—	—	—	—	—	—	—
119	Hon-19	2BC _{t2}	268	—	—	—	—	—	—	—	—	—
120	Hon-19	2BC _{t3}	300	—	—	—	—	—	—	—	—	—
121	Hon-19	3Cox	320	—	—	—	—	—	—	—	—	—
122	Hon-19	3Cox	410	—	—	—	—	—	—	—	—	—
123	Hon-20	Ap ₁	11	—	—	—	—	—	—	—	—	—
124	Hon-20	Ap ₂	30	—	—	—	—	—	—	—	—	—
125	Hon-20	BA	60	—	—	—	—	—	—	—	—	—
126	Hon-20	B _{t1}	114	—	—	—	—	—	—	—	—	—
127	Hon-20	B _{t2}	191	—	—	—	—	—	—	—	—	—
128	Hon-20	2BC _{t1}	223	—	—	—	—	—	—	—	—	—
129	Hon-20	2BC _{t2}	260	—	—	—	—	—	—	—	—	—
130	Hon-20	2CB	283	—	—	—	—	—	—	—	—	—

Supplementary table 4, part 1. Clay mineralogy of the coarse (0.2–2 μm) fraction—Continued

Sample number	Profile number	Horizon	Basal depth (cm)	Kaolin	Chlorite	Chloritized vermiculite	Vermiculite	Mica	Smectite	Talc	Quartz	Feldspar
Exhumed lower member of the Laguna Formation, 1,600 ka												
131	Hon-21	A	11	++++	—	—	+	++	—	+	XX	X
132	Hon-21	AB	33	—	—	—	—	—	—	—	—	—
133	Hon-21	BA	46	—	—	—	—	—	—	—	—	—
134	Hon-21	Bt1	71	—	—	—	—	—	—	—	—	—
135	Hon-21	Bt2	93	++++	—	—	+	++	—	+	XX	X
136	Hon-21	Bt3	119	—	—	—	—	—	—	—	—	—
137	Hon-21	Bt4	148	—	—	—	—	—	—	—	—	—
138	Hon-21	2Bt1	197	—	—	—	—	—	—	—	—	—
139	Hon-21	2Bt2	274	—	—	—	—	—	—	—	—	—
140	Hon-21	2BC	315	—	—	—	—	—	—	—	—	—
141	Hon-21	3BC	473	+++	—	+	++++	+	—	—	X	X
142	Hon-21	C	1300	—	—	—	—	—	—	—	—	—
143	Hon-22	A	23	—	—	—	—	—	—	—	—	—
144	Hon-22	AB	43	—	—	—	—	—	—	—	—	—
145	Hon-22	BA	59	—	—	—	—	—	—	—	—	—
146	Hon-22	Bt1	89	—	—	—	—	—	—	—	—	—
147	Hon-22	Bt2	120	—	—	—	—	—	—	—	—	—
148	Hon-22	Bt3	154	—	—	—	—	—	—	—	—	—
149	Hon-22	2Bt1	207	—	—	—	—	—	—	—	—	—
150	Hon-22	2Bt2	270	—	—	—	—	—	—	—	—	—
151	Hon-22	2BCt	342	—	—	—	—	—	—	—	—	—
152	Hon-22	3BCt1	445	—	—	—	—	—	—	—	—	—
153	Hon-22	3BCt2	505	—	—	—	—	—	—	—	—	—
154	Hon-22	C	1300	—	—	—	—	—	—	—	—	—
Modern alluvium, 0 ka												
155	Hon-71	Cn	0	—	—	—	—	—	—	—	—	—
156	Hon-72	Cn	0	—	—	—	—	—	—	—	—	—

Supplementary table 4, part 2. Clay mineralogy of the fine (<0.2 μm) fraction

[Clay Minerals: +, trace; ++, moderate; +++, abundant; +++++, clearly dominant; —, not determined. Primary minerals: X, moderate; XX, abundant; —, not determined. Analysts: H. Foolad and A.J. Busacca]

Sample number	Profile number	Horizon	Basal depth (cm)	Kaolin	Chlorite	vermiculite	Vermiculite	Mica	Smectite	Talc	Quartz	Feldspar
Holocene alluvium, 0.6 ka												
1	Hon-1	A	12	—	—	—	—	—	—	—	—	—
2	Hon-1	2A1	16	—	—	—	—	—	—	—	—	—
3	Hon-1	2A2	25	—	—	—	—	—	—	—	—	—
4	Hon-1	2AC	49	—	—	—	—	—	—	—	—	—
5	Hon-1	2C	85	—	—	—	—	—	—	—	—	—
6	Hon-1	3C1	95	—	—	—	—	—	—	—	—	—
7	Hon-1	3C2	122	—	—	—	—	—	—	—	—	—
8	Hon-1	4B1b	140	—	—	—	—	—	—	—	—	—
9	Hon-1	4B2b	170	—	—	—	—	—	—	—	—	—
10	Hon-2	A1	4	—	—	—	—	—	—	—	—	—
11	Hon-2	A2	32	—	—	—	—	—	—	—	—	—
12	Hon-2	C	61	—	—	—	—	—	—	—	—	—
13	Hon-2	2C	92	—	—	—	—	—	—	—	—	—
14	Hon-2	3C	103	—	—	—	—	—	—	—	—	—
15	Hon-2	4B2tb	130	—	—	—	—	—	—	—	—	—
16	Hon-3	A1	4	—	—	—	—	—	—	—	—	—
17	Hon-3	A2	16	—	—	—	—	—	—	—	—	—
18	Hon-3	AC	31	—	—	—	—	—	—	—	—	—
19	Hon-3	C	54	—	—	—	—	—	—	—	—	—
20	Hon-3	2C	78	—	—	—	—	—	—	—	—	—
21	Hon-4	C	17	—	—	—	—	—	—	—	—	—
22	Hon-4	2A	32	++	—	—	—	—	+++	—	X	X
23	Hon-4	2AC	49	—	—	—	—	—	—	—	—	—
24	Hon-4	2C	86	++	—	—	—	—	++++	—	XX	X
25	Hon-4	3C1	113	—	—	—	—	—	—	—	—	—
26	Hon-4	3C2	147	—	—	—	—	—	—	—	—	—
Upper member of the Modesto Formation, 10 ka												
27	Hon-5	AP1	13	—	—	—	—	—	—	—	—	—
28	Hon-5	AP2	23	++	—	—	+	—	+++	—	X	X
29	Hon-5	BA	54	—	—	—	—	—	—	—	—	—
30	Hon-5	Bw1	88	+++	—	—	++	—	++++	—	X	X
31	Hon-5	Bw2	102	—	—	—	—	—	—	—	—	—
32	Hon-5	BC1	141	—	—	—	—	—	—	—	—	—
33	Hon-5	BC2	180	+++	—	—	++	—	++++	—	XX	X
34	Hon-6	AP1	10	—	—	—	—	—	—	—	—	—
35	Hon-6	AP2	22	—	—	—	—	—	—	—	—	—
36	Hon-6	BA	43	—	—	—	—	—	—	—	—	—
37	Hon-6	Bw1	91	—	—	—	—	—	—	—	—	—
38	Hon-6	Bw2	118	—	—	—	—	—	—	—	—	—
39	Hon-6	BC1	157	—	—	—	—	—	—	—	—	—
40	Hon-6	BC2	184	—	—	—	—	—	—	—	—	—
41	Hon-7	AP1	8	—	—	—	—	—	—	—	—	—
42	Hon-7	AP2	30	—	—	—	—	—	—	—	—	—

Supplementary table 4, part 2. Clay mineralogy of the fine (<0.2 μm) fraction—Continued

Sample number	Profile number	Horizon	Basal depth (cm)	Kaolin	Chlorite	Chloritized vermiculite	Vermiculite	Mica	Smectite	Talc	Quartz	Feldspar
Upper member of the Modesto Formation, 10 ka—Continued												
43	Hon-7	BA	54	—	—	—	—	—	—	—	—	—
44	Hon-7	Bw1	88	—	—	—	—	—	—	—	—	—
45	Hon-7	Bw2	118	—	—	—	—	—	—	—	—	—
46	Hon-7	BC	180	—	—	—	—	—	—	—	—	—
47	Hon-7	2BC	230	—	—	—	—	—	—	—	—	—
48	Hon-7	3Cox	290	—	—	—	—	—	—	—	—	—
49	Hon-7	4Cox	340	—	—	—	—	—	—	—	—	—
50	Hon-7	4Cn	370	—	—	—	—	—	—	—	—	—
51	Hon-8	AP1	7	—	—	—	—	—	—	—	—	—
52	Hon-8	AP2	34	—	—	—	—	—	—	—	—	—
53	Hon-8	BA	57	—	—	—	—	—	—	—	—	—
54	Hon-8	Bw1	90	—	—	—	—	—	—	—	—	—
55	Hon-8	Bw2	126	—	—	—	—	—	—	—	—	—
56	Hon-8	BC1	191	—	—	—	—	—	—	—	—	—
57	Hon-8	BC2	240	—	—	—	—	—	—	—	—	—
58	Hon-8	2Cox	390	—	—	—	—	—	—	—	—	—
Lower member of the Modesto Formation, 40 ka												
59	Hon-10	Ap	22	+++	—	+	++	+	+	—	X	X
60	Hon-10	BA	40	—	—	—	—	—	—	—	—	—
61	Hon-10	Bt1	86	—	—	—	—	—	—	—	—	—
62	Hon-10	Bt2	132	+++	—	—	+	+	—	—	X	X
63	Hon-10	BC	150	—	—	—	—	—	—	—	—	—
64	Hon-10	C	205	+++	—	+	++	+	+++	—	X	X
65	Hon-10	2C	225	—	—	—	—	—	—	—	—	—
66	Hon-11	Ap	18	—	—	—	—	—	—	—	—	—
67	Hon-11	BA	45	—	—	—	—	—	—	—	—	—
68	Hon-11	Bt1	94	—	—	—	—	—	—	—	—	—
69	Hon-11	Bt2	125	—	—	—	—	—	—	—	—	—
70	Hon-11	BC	145	—	—	—	—	—	—	—	—	—
71	Hon-11	C	179	—	—	—	—	—	—	—	—	—
72	Hon-11	2C	220	—	—	—	—	—	—	—	—	—
Upper member of the Riverbank Formation, 130 ka												
73	Hon-13	Ap	24	—	—	—	—	—	—	—	—	—
74	Hon-13	BA	33	—	—	—	—	—	—	—	—	—
75	Hon-13	BAt1	50	—	—	—	—	—	—	—	—	—
76	Hon-13	BAt2	62	—	—	—	—	—	—	—	—	—
77	Hon-13	Bt1	86	—	—	—	—	—	—	—	—	—
78	Hon-13	Bt2	102	—	—	—	—	—	—	—	—	—
79	Hon-13	Bt3	123	—	—	—	—	—	—	—	—	—
80	Hon-13	BCt	157	—	—	—	—	—	—	—	—	—
81	Hon-13	2BCt1	208	—	—	—	—	—	—	—	—	—
82	Hon-13	2BCt2	245	—	—	—	—	—	—	—	—	—
83	Hon-13	2BCt3	266	—	—	—	—	—	—	—	—	—
84	Hon-13	2CB	301	—	—	—	—	—	—	—	—	—

Supplementary table 4, part 2. Clay mineralogy of the fine (<0.2 μm) fraction—Continued

Sample number	Profile number	Horizon	Basal depth (cm)	Kaolin	Chlorite	Chloritized vermiculite	Vermiculite	Mica	Smectite	Talc	Quartz	Feldspar
Upper member of the Riverbank Formation, 130 km—Continued												
85	Hon-14	Ap	28	++++	—	—	—	—	—	—	X	X
86	Hon-14	BA	39	—	—	—	—	—	—	—	—	—
87	Hon-14	BAt1	59	—	—	—	—	—	—	—	—	—
88	Hon-14	BA2	76	—	—	—	—	—	—	—	—	—
89	Hon-14	Bt1	111	+++	+	—	+++	—	—	+	X	X
90	Hon-14	Bt2	126	—	—	—	—	—	—	—	—	—
91	Hon-14	2BCt1	150	—	—	—	—	—	—	—	—	—
92	Hon-14	2BCt2	200	—	—	—	—	—	—	—	—	—
93	Hon-14	2BCt3	260	+++	+	—	+	+	+++	—	X	X
94	Hon-14	2CB	320	—	—	—	—	—	—	—	—	—
Lower member of the Riverbank Formation, 250 ka												
95	Hon-17	Ap1	18	—	—	—	—	—	—	—	—	—
96	Hon-17	Ap2	24	—	—	—	—	—	—	—	—	—
97	Hon-17	BA	76	—	—	—	—	—	—	—	—	—
98	Hon-17	Bt1	100	—	—	—	—	—	—	—	—	—
99	Hon-17	Bt2	160	—	—	—	—	—	—	—	—	—
100	Hon-17	2BCt	201	—	—	—	—	—	—	—	—	—
101	Hon-17	3BCt	208	—	—	—	—	—	—	—	—	—
102	Hon-17	4BCt	295	—	—	—	—	—	—	—	—	—
103	Hon-18	Ap1	19	—	—	—	—	—	—	—	—	—
104	Hon-18	Ap2	30	++++	—	—	—	+	—	+	X	X
105	Hon-18	BA	90	—	—	—	—	—	—	—	—	—
106	Hon-18	Bt1	113	++++	—	+	++	+	—	—	X	X
107	Hon-18	Bt2	170	+++	—	—	+++	—	++	—	X	X
108	Hon-18	2BCt	190	—	—	—	—	—	—	—	—	—
109	Hon-18	3BCt	240	—	—	—	—	—	—	—	—	—
110	Hon-18	4BCt	300	—	—	—	—	—	—	—	—	—
111	Hon-19	Ap1	7	—	—	—	—	—	—	—	—	—
112	Hon-19	Ap2	24	—	—	—	—	—	—	—	—	—
113	Hon-19	BA	63	—	—	—	—	—	—	—	—	—
114	Hon-19	Bt1	91	—	—	—	—	—	—	—	—	—
115	Hon-19	Bt2	126	—	—	—	—	—	—	—	—	—
116	Hon-19	Bt3	176	—	—	—	—	—	—	—	—	—
117	Hon-19	BCt	218	—	—	—	—	—	—	—	—	—
118	Hon-19	2BCt1	246	—	—	—	—	—	—	—	—	—
119	Hon-19	2BCt2	268	—	—	—	—	—	—	—	—	—
120	Hon-19	2BCt3	300	—	—	—	—	—	—	—	—	—
121	Hon-19	3Cox	320	—	—	—	—	—	—	—	—	—
122	Hon-19	3Cox	410	—	—	—	—	—	—	—	—	—
123	Hon-20	Ap1	11	—	—	—	—	—	—	—	—	—
124	Hon-20	Ap2	30	—	—	—	—	—	—	—	—	—
125	Hon-20	BA	60	—	—	—	—	—	—	—	—	—
126	Hon-20	Bt1	114	—	—	—	—	—	—	—	—	—
127	Hon-20	Bt2	191	—	—	—	—	—	—	—	—	—
128	Hon-20	2BCt1	223	—	—	—	—	—	—	—	—	—
129	Hon-20	2BCt2	260	—	—	—	—	—	—	—	—	—
130	Hon-20	2CB	283	—	—	—	—	—	—	—	—	—

Supplementary table 4, part 2. Clay mineralogy of the fine (<0.2 μm) fraction—Continued

Sample number	Profile number	Horizon	Basal depth (cm)	Kaolin	Chlorite	Chloritized vermiculite	Vermiculite	Mica	Smectite	Talc	Quartz	Feldspar
Exhumed lower member of the Laguna Formation, 1,600 ka												
131	Hon-21	A	11	++++	—	—	—	+	—	—	X	X
132	Hon-21	AB	33	—	—	—	—	—	—	—	—	—
133	Hon-21	BA	46	—	—	—	—	—	—	—	—	—
134	Hon-21	Bt1	71	—	—	—	—	—	—	—	—	—
135	Hon-21	Bt2	93	++++	—	—	—	+	—	—	X	X
136	Hon-21	Bt3	119	—	—	—	—	—	—	—	—	—
137	Hon-21	Bt4	148	—	—	—	—	—	—	—	—	—
138	Hon-21	2Bt1	197	—	—	—	—	—	—	—	—	—
139	Hon-21	2Bt2	274	—	—	—	—	—	—	—	—	—
140	Hon-21	2BC	315	—	—	—	—	—	—	—	—	—
141	Hon-21	3BC	473	+++	—	—	—	+	++	+	X	X
142	Hon-21	C	1300	—	—	—	—	—	—	—	—	—
143	Hon-22	A	23	—	—	—	—	—	—	—	—	—
144	Hon-22	AB	43	—	—	—	—	—	—	—	—	—
145	Hon-22	BA	59	—	—	—	—	—	—	—	—	—
146	Hon-22	Bt1	89	—	—	—	—	—	—	—	—	—
147	Hon-22	Bt2	120	—	—	—	—	—	—	—	—	—
148	Hon-22	Bt3	154	—	—	—	—	—	—	—	—	—
149	Hon-22	2Bt1	207	—	—	—	—	—	—	—	—	—
150	Hon-22	2Bt2	270	—	—	—	—	—	—	—	—	—
151	Hon-22	2BCt	342	—	—	—	—	—	—	—	—	—
152	Hon-22	3BCt1	445	—	—	—	—	—	—	—	—	—
153	Hon-22	3BCt2	505	—	—	—	—	—	—	—	—	—
154	Hon-22	C	1300	—	—	—	—	—	—	—	—	—
Modern alluvium, 0 ka												
155	Hon-71	Cn	0	—	—	—	—	—	—	—	—	—
156	Hon-72	Cn	0	—	—	—	—	—	—	—	—	—

Supplementary table 5. Total chemical analyses of the fine (<50 μm) fraction by X-ray fluorescence

[All values in weight percent. Analysts: J. Baker, A. Bartell, J. Taggart, and J.S. Wahlberg]

Sample number	Profile number	Horizon	Basal depth (cm)	SiO ₂	Al ₂ O ₃	Fe ₂ O ₃	MgO	CaO	Na ₂ O	K ₂ O	TiO ₂	P ₂ O ₅	MnO
Holocene alluvium, 0.6 ka													
1	Hon-1	A	12	—	—	—	—	—	—	—	—	—	—
2	Hon-1	2A1	16	—	—	—	—	—	—	—	—	—	—
3	Hon-1	2A2	25	50.4	17.9	11.0	2.94	4.81	1.96	0.64	1.35	0.15	0.18
4	Hon-1	2AC	49	—	—	—	—	—	—	—	—	—	—
5	Hon-1	2C	85	49.7	18.1	11.4	2.95	5.04	1.86	.57	1.39	.13	.20
6	Hon-1	3C1	95	—	—	—	—	—	—	—	—	—	—
7	Hon-1	3C2	122	—	—	—	—	—	—	—	—	—	—
8	Hon-1	4B1b	140	—	—	—	—	—	—	—	—	—	—
9	Hon-1	4B2b	170	—	—	—	—	—	—	—	—	—	—
10	Hon-2	A1	4	—	—	—	—	—	—	—	—	—	—
11	Hon-2	A2	32	50.3	18.2	10.9	2.86	4.64	1.95	.65	1.29	.17	.19
12	Hon-2	C	61	—	—	—	—	—	—	—	—	—	—
13	Hon-2	2C	92	49.0	18.2	11.3	2.80	4.87	1.89	.59	1.39	.13	.21
14	Hon-2	3C	103	—	—	—	—	—	—	—	—	—	—
15	Hon-2	4B2tb	130	—	—	—	—	—	—	—	—	—	—
16	Hon-3	A1	4	—	—	—	—	—	—	—	—	—	—
17	Hon-3	A2	16	50.9	18.3	10.6	2.85	4.60	1.99	.65	1.26	.17	.17
18	Hon-3	AC	31	—	—	—	—	—	—	—	—	—	—
19	Hon-3	C	54	48.8	18.2	11.3	2.85	4.80	1.80	.60	1.34	.13	.22
20	Hon-3	2C	78	—	—	—	—	—	—	—	—	—	—
21	Hon-4	C	17	—	—	—	—	—	—	—	—	—	—
22	Hon-4	2A	32	49.9	18.0	11.0	2.83	4.88	1.93	.60	1.32	.26	.17
23	Hon-4	2AC	49	—	—	—	—	—	—	—	—	—	—
24	Hon-4	2C	86	49.5	18.2	11.4	2.95	4.95	1.90	.58	1.37	.14	.20
25	Hon-4	3C1	113	—	—	—	—	—	—	—	—	—	—
26	Hon-4	3C2	147	—	—	—	—	—	—	—	—	—	—
Upper member of the Modesto Formation, 10 ka													
27	Hon-5	AP1	13	—	—	—	—	—	—	—	—	—	—
28	Hon-5	AP2	23	50.4	18.6	10.9	2.54	4.10	1.99	.50	1.32	.15	.18
29	Hon-5	BA	54	—	—	—	—	—	—	—	—	—	—
30	Hon-5	Bw1	88	50.2	18.3	10.9	2.60	4.25	2.06	.45	1.35	.10	.20
31	Hon-5	Bw2	102	—	—	—	—	—	—	—	—	—	—
32	Hon-5	BC1	141	—	—	—	—	—	—	—	—	—	—
33	Hon-5	BC2	180	—	—	—	—	—	—	—	—	—	—
34	Hon-6	AP1	10	—	—	—	—	—	—	—	—	—	—
35	Hon-6	AP2	22	50.4	18.6	11.0	2.48	4.07	2.01	.49	1.33	.14	.18
36	Hon-6	BA	43	—	—	—	—	—	—	—	—	—	—
37	Hon-6	Bw1	91	52.2	17.6	10.0	2.67	4.85	2.36	.46	1.39	.12	.17
38	Hon-6	Bw2	118	—	—	—	—	—	—	—	—	—	—
39	Hon-6	BC1	157	—	—	—	—	—	—	—	—	—	—
40	Hon-6	BC2	184	—	—	—	—	—	—	—	—	—	—
41	Hon-7	AP1	8	—	—	—	—	—	—	—	—	—	—
42	Hon-7	AP2	30	51.7	18.4	10.7	2.25	4.43	2.19	.57	1.46	.14	.20

Supplementary table 5. Total chemical analyses of the fine (<50 μm) fraction by X-ray fluorescence—Continued

Sample number	Profile number	Horizon	Basal depth (cm)	SiO ₂	Al ₂ O ₃	Fe ₂ O ₃	MgO	CaO	Na ₂ O	K ₂ O	TiO ₂	P ₂ O ₅	MnO
Upper member of the Modesto Formation, 10 ka—Continued													
43	Hon-7	BA	54	—	—	—	—	—	—	—	—	—	—
44	Hon-7	Bw1	88	50.2	18.7	11.0	2.38	4.00	2.03	.48	1.37	.11	.22
45	Hon-7	Bw2	118	—	—	—	—	—	—	—	—	—	—
46	Hon-7	BC	180	—	—	—	—	—	—	—	—	—	—
47	Hon-7	2BC	230	—	—	—	—	—	—	—	—	—	—
48	Hon-7	3Cox	290	—	—	—	—	—	—	—	—	—	—
49	Hon-7	4Cox	340	—	—	—	—	—	—	—	—	—	—
50	Hon-7	4Cn	370	—	—	—	—	—	—	—	—	—	—
51	Hon-8	AP1	7	—	—	—	—	—	—	—	—	—	—
52	Hon-8	AP2	34	51.5	18.5	10.8	2.23	4.36	2.10	.58	1.49	.14	.19
53	Hon-8	BA	57	—	—	—	—	—	—	—	—	—	—
54	Hon-8	Bw1	90	50.4	18.5	10.8	2.44	4.13	2.11	.48	1.38	.10	.22
55	Hon-8	Bw2	126	—	—	—	—	—	—	—	—	—	—
56	Hon-8	BC1	191	—	—	—	—	—	—	—	—	—	—
57	Hon-8	BC2	240	53.2	17.5	9.69	2.77	3.71	2.35	.54	1.22	.05	.20
58	Hon-8	2Cox	390	—	—	—	—	—	—	—	—	—	—
Lower member of the Modesto Formation, 40 ka													
59	Hon-10	Ap	22	54.5	17.5	8.84	2.95	2.87	1.63	1.66	1.09	0.41	0.14
60	Hon-10	BA	40	—	—	—	—	—	—	—	—	—	—
61	Hon-10	Bt1	86	—	—	—	—	—	—	—	—	—	—
62	Hon-10	Bt2	132	51.5	19.9	9.81	3.09	2.40	1.38	1.69	1.04	.30	.20
63	Hon-10	BC	150	—	—	—	—	—	—	—	—	—	—
64	Hon-10	C	205	52.1	19.1	9.76	3.31	2.78	1.54	1.55	1.05	.22	.20
65	Hon-10	2C	225	—	—	—	—	—	—	—	—	—	—
66	Hon-11	Ap	18	54.6	17.3	8.67	2.84	2.71	1.57	1.64	1.07	.37	.13
67	Hon-11	BA	45	—	—	—	—	—	—	—	—	—	—
68	Hon-11	Bt1	94	—	—	—	—	—	—	—	—	—	—
69	Hon-11	Bt2	125	51.6	20.0	9.78	3.02	2.46	1.42	1.62	1.03	.30	.20
70	Hon-11	BC	145	—	—	—	—	—	—	—	—	—	—
71	Hon-11	C	179	51.9	19.1	9.81	3.36	2.75	1.48	1.59	1.05	.23	.20
72	Hon-11	2C	220	—	—	—	—	—	—	—	—	—	—
Upper member of the Riverbank Formation, 130 ka													
73	Hon-13	Ap	24	60.5	16.9	7.64	.77	3.24	1.75	1.05	1.17	.12	.20
74	Hon-13	BA	33	—	—	—	—	—	—	—	—	—	—
75	Hon-13	BAt1	50	—	—	—	—	—	—	—	—	—	—
76	Hon-13	BAt2	62	—	—	—	—	—	—	—	—	—	—
77	Hon-13	Bt1	86	—	—	—	—	—	—	—	—	—	—
78	Hon-13	Bt2	102	50.2	20.2	10.5	2.00	2.24	1.32	.50	.95	.05	.05
79	Hon-13	Bt3	123	—	—	—	—	—	—	—	—	—	—
80	Hon-13	BCt	157	—	—	—	—	—	—	—	—	—	—
81	Hon-13	2BCt1	208	—	—	—	—	—	—	—	—	—	—
82	Hon-13	2BCt2	245	—	—	—	—	—	—	—	—	—	—
83	Hon-13	2BCt3	266	—	—	—	—	—	—	—	—	—	—
84	Hon-13	2CB	301	—	—	—	—	—	—	—	—	—	—

Supplementary table 5. Total chemical analyses of the fine (<50 µm) fraction by X-ray fluorescence—Continued

Sample number	Profile number	Horizon	Basal depth (cm)	SiO ₂	Al ₂ O ₃	Fe ₂ O ₃	MgO	CaO	Na ₂ O	K ₂ O	TiO ₂	P ₂ O ₅	MnO
Upper member of the Riverbank Formation, 130 ka—Continued													
85	Hon-14	Ap	28	60.0	16.9	7.76	.80	3.16	1.71	1.05	1.18	.12	.20
86	Hon-14	BA	39	—	—	—	—	—	—	—	—	—	—
87	Hon-14	BAt1	59	—	—	—	—	—	—	—	—	—	—
88	Hon-14	BAt2	76	—	—	—	—	—	—	—	—	—	—
89	Hon-14	Bt1	111	51.3	20.6	10.2	1.62	2.06	1.19	.93	1.11	.07	.21
90	Hon-14	Bt2	126	—	—	—	—	—	—	—	—	—	—
91	Hon-14	2BCt1	150	—	—	—	—	—	—	—	—	—	—
92	Hon-14	2BCt2	200	—	—	—	—	—	—	—	—	—	—
93	Hon-14	2BCt3	260	—	—	—	—	—	—	—	—	—	—
94	Hon-14	2CB	320	—	—	—	—	—	—	—	—	—	—
Lower member of the Riverbank Formation, 250 ka													
95	Hon-17	Ap1	18	—	—	—	—	—	—	—	—	—	—
96	Hon-17	Ap2	24	55.5	18.9	9.08	1.10	3.85	1.47	1.34	1.20	.16	.20
97	Hon-17	BA	76	—	—	—	—	—	—	—	—	—	—
98	Hon-17	Bt1	100	—	—	—	—	—	—	—	—	—	—
99	Hon-17	Bt2	160	49.9	20.5	10.7	1.69	3.34	1.50	.74	1.07	.08	.19
100	Hon-17	2BCt	201	—	—	—	—	—	—	—	—	—	—
101	Hon-17	3BCt	208	51.7	19.3	10.0	1.92	3.56	1.73	.71	1.01	.06	.17
102	Hon-17	4BCt	295	—	—	—	—	—	—	—	—	—	—
103	Hon-18	Ap1	19	—	—	—	—	—	—	—	—	—	—
104	Hon-18	Ap2	30	55.7	18.6	8.98	1.08	3.90	1.49	1.32	1.21	.16	.18
105	Hon-18	BA	90	—	—	—	—	—	—	—	—	—	—
106	Hon-18	Bt1	113	—	—	—	—	—	—	—	—	—	—
107	Hon-18	Bt2	170	51.5	19.8	10.4	1.98	3.53	1.75	.62	1.02	.06	.18
108	Hon-18	2BCt	190	—	—	—	—	—	—	—	—	—	—
109	Hon-18	3BCt	240	52.1	19.1	10.4	2.21	3.45	1.78	.68	1.01	.06	.16
110	Hon-18	4BCt	300	—	—	—	—	—	—	—	—	—	—
111	Hon-19	Ap1	7	55.2	18.8	9.03	1.06	3.35	1.36	1.39	1.23	.14	.26
112	Hon-19	Ap2	24	—	—	—	—	—	—	—	—	—	—
113	Hon-19	BA	63	—	—	—	—	—	—	—	—	—	—
114	Hon-19	Bt1	91	—	—	—	—	—	—	—	—	—	—
115	Hon-19	Bt2	126	49.2	20.9	11.3	1.83	2.86	1.33	.78	1.11	.08	.20
116	Hon-19	Bt3	176	—	—	—	—	—	—	—	—	—	—
117	Hon-19	BCt	218	—	—	—	—	—	—	—	—	—	—
118	Hon-19	2BCt1	246	—	—	—	—	—	—	—	—	—	—
119	Hon-19	2BCt2	268	—	—	—	—	—	—	—	—	—	—
120	Hon-19	2BCt3	300	—	—	—	—	—	—	—	—	—	—
121	Hon-19	3Cox	320	—	—	—	—	—	—	—	—	—	—
122	Hon-19	3Cox	410	—	—	—	—	—	—	—	—	—	—
123	Hon-20	Ap1	11	—	—	—	—	—	—	—	—	—	—
124	Hon-20	Ap2	30	55.6	18.7	8.98	1.04	3.35	1.43	1.39	1.22	0.14	0.23
125	Hon-20	BA	60	—	—	—	—	—	—	—	—	—	—
126	Hon-20	Bt1	114	—	—	—	—	—	—	—	—	—	—
127	Hon-20	Bt2	191	48.9	20.8	11.1	1.69	2.83	1.33	.81	1.11	.08	.17
128	Hon-20	2BCt1	223	—	—	—	—	—	—	—	—	—	—

Supplementary table 5. Total chemical analyses of the fine (<50 μm) fraction by X-ray fluorescence—Continued

Sample number	Profile number	Horizon	Basal depth (cm)	SiO ₂	Al ₂ O ₃	Fe ₂ O ₃	MgO	CaO	Na ₂ O	K ₂ O	TiO ₂	P ₂ O ₅	MnO
Lower member of the Riverbank Formation, 250 ka—Continued													
129	Hon-20	2BCt2	260	—	—	—	—	—	—	—	—	—	—
130	Hon-20	2CB	283	—	—	—	—	—	—	—	—	—	—
Exhumed lower member of the Laguna Formation, 1,600 ka													
131	Hon-21	A	11	53.7	20.1	10.3	.63	.84	.29	1.19	1.47	.25	.14
132	Hon-21	AB	33	—	—	—	—	—	—	—	—	—	—
133	Hon-21	BA	46	—	—	—	—	—	—	—	—	—	—
134	Hon-21	Bt1	71	—	—	—	—	—	—	—	—	—	—
135	Hon-21	Bt2	93	47.5	26.0	10.9	.54	.15	.15	.87	1.10	.16	.07
136	Hon-21	Bt3	119	—	—	—	—	—	—	—	—	—	—
137	Hon-21	Bt4	148	—	—	—	—	—	—	—	—	—	—
138	Hon-21	2Bt1	197	45.3	27.0	12.0	.51	.16	.15	.72	.96	.14	.03
139	Hon-21	2Bt2	274	—	—	—	—	—	—	—	—	—	—
140	Hon-21	2BC	315	—	—	—	—	—	—	—	—	—	—
141	Hon-21	3BC	473	—	—	—	—	—	—	—	—	—	—
142	Hon-21	C	1300	—	—	—	—	—	—	—	—	—	—
143	Hon-22	A	23	52.0	20.5	10.3	.60	.97	.29	1.16	1.45	.25	.18
144	Hon-22	AB	43	—	—	—	—	—	—	—	—	—	—
145	Hon-22	BA	59	—	—	—	—	—	—	—	—	—	—
146	Hon-22	Bt1	89	47.6	25.9	11.0	.55	.24	.15	.88	1.12	.18	.09
147	Hon-22	Bt2	120	—	—	—	—	—	—	—	—	—	—
148	Hon-22	Bt3	154	—	—	—	—	—	—	—	—	—	—
149	Hon-22	2Bt1	207	—	—	—	—	—	—	—	—	—	—
150	Hon-22	2Bt2	270	—	—	—	—	—	—	—	—	—	—
151	Hon-22	2BCt	342	—	—	—	—	—	—	—	—	—	—
152	Hon-22	3BCt1	445	—	—	—	—	—	—	—	—	—	—
153	Hon-22	3BCt2	505	—	—	—	—	—	—	—	—	—	—
154	Hon-22	C	1300	47.7	21.3	10.7	1.97	2.75	1.66	.51	.92	.07	.14
Modern alluvium, 0 ka													
155	Hon-71	Cn	0	—	—	—	—	—	—	—	—	—	—
156	Hon-72	Cn	0	—	—	—	—	—	—	—	—	—	—

Supplementary table 6, part 1. Total chemical analyses of the 2–20 μm fraction by X-ray fluorescence for major oxides

[All values in weight percent. Analyst: A.J. Busacca]

Sample number	Profile number	Horizon	Basal depth (cm)	SiO ₂	Al ₂ O ₃	Fe ₂ O ₃	MgO	CaO	Na ₂ O	K ₂ O	TiO ₂	P ₂ O ₅	MnO
Holocene alluvium, 0.6 ka													
1	Hon-1	A	12	—	—	—	—	—	—	—	—	—	—
2	Hon-1	2A1	16	—	—	—	—	—	—	—	—	—	—
3	Hon-1	2A2	25	—	—	—	—	—	—	—	—	—	—
4	Hon-1	2AC	49	—	—	—	—	—	—	—	—	—	—
5	Hon-1	2C	85	—	—	—	—	—	—	—	—	—	—
6	Hon-1	3C1	95	—	—	—	—	—	—	—	—	—	—
7	Hon-1	3C2	122	—	—	—	—	—	—	—	—	—	—
8	Hon-1	4B1b	140	—	—	—	—	—	—	—	—	—	—
9	Hon-1	4B2b	170	—	—	—	—	—	—	—	—	—	—
10	Hon-2	A1	4	—	—	—	—	—	—	—	—	—	—
11	Hon-2	A2	32	—	—	—	—	—	—	—	—	—	—
12	Hon-2	C	61	—	—	—	—	—	—	—	—	—	—
13	Hon-2	2C	92	—	—	—	—	—	—	—	—	—	—
14	Hon-2	3C	103	—	—	—	—	—	—	—	—	—	—
15	Hon-2	4B2tb	130	—	—	—	—	—	—	—	—	—	—
16	Hon-3	A1	4	—	—	—	—	—	—	—	—	—	—
17	Hon-3	A2	16	—	—	—	—	—	—	—	—	—	—
18	Hon-3	AC	31	—	—	—	—	—	—	—	—	—	—
19	Hon-3	C	54	—	—	—	—	—	—	—	—	—	—
20	Hon-3	2C	78	—	—	—	—	—	—	—	—	—	—
21	Hon-4	C	17	52.90	18.50	11.63	5.69	4.71	2.55	0.89	1.37	—	0.22
22	Hon-4	2A	32	53.12	18.69	11.41	4.97	4.58	2.33	.83	1.27	—	.20
23	Hon-4	2AC	49	53.68	18.42	11.02	5.09	4.54	2.81	.78	1.23	—	.21
24	Hon-4	2C	86	52.34	18.67	11.52	4.85	4.60	2.29	.78	1.26	—	.24
25	Hon-4	3C1	113	51.91	18.48	11.78	5.19	4.52	2.61	.76	1.34	—	.25
26	Hon-4	3C2	147	51.76	19.30	11.74	5.10	4.55	2.34	.79	1.45	—	.23
Upper member of the Modesto Formation, 10 ka													
27	Hon-5	AP1	13	55.04	18.37	10.29	4.43	4.21	2.88	.66	1.28	—	.20
28	Hon-5	AP2	23	54.19	18.72	10.47	4.33	4.19	2.97	.64	1.30	—	.21
29	Hon-5	BA	54	53.07	18.22	10.59	4.31	4.34	2.31	.60	1.30	—	.21
30	Hon-5	Bw1	88	52.49	19.65	11.69	4.61	3.98	2.48	.60	1.33	—	.26
31	Hon-5	Bw2	102	52.79	19.08	11.26	5.03	4.02	2.93	.58	1.32	—	.26
32	Hon-5	BC1	141	53.64	18.47	10.62	5.51	3.97	2.96	.61	1.21	—	.24
33	Hon-5	BC2	180	53.55	18.15	10.67	5.50	3.98	2.98	.60	1.23	—	.25
34	Hon-6	AP1	10	—	—	—	—	—	—	—	—	—	—
35	Hon-6	AP2	22	—	—	—	—	—	—	—	—	—	—
36	Hon-6	BA	43	—	—	—	—	—	—	—	—	—	—
37	Hon-6	Bw1	91	—	—	—	—	—	—	—	—	—	—
38	Hon-6	Bw2	118	—	—	—	—	—	—	—	—	—	—
39	Hon-6	BC1	157	—	—	—	—	—	—	—	—	—	—
40	Hon-6	BC2	184	—	—	—	—	—	—	—	—	—	—
41	Hon-7	AP1	8	—	—	—	—	—	—	—	—	—	—
42	Hon-7	AP2	30	—	—	—	—	—	—	—	—	—	—

Supplementary table 6, part 1. Total chemical analyses of the 2–20 μm fraction by X-ray fluorescence for major oxides—*Continued*

Sample number	Profile number	Horizon	Basal depth (cm)	SiO ₂	Al ₂ O ₃	Fe ₂ O ₃	MgO	CaO	Na ₂ O	K ₂ O	TiO ₂	P ₂ O ₅	MnO
Upper member of the Modesto Formation, 10 ka—Continued													
43	Hon-7	BA	54	—	—	—	—	—	—	—	—	—	—
44	Hon-7	Bw1	88	—	—	—	—	—	—	—	—	—	—
45	Hon-7	Bw2	118	—	—	—	—	—	—	—	—	—	—
46	Hon-7	BC	180	—	—	—	—	—	—	—	—	—	—
47	Hon-7	2BC	230	—	—	—	—	—	—	—	—	—	—
48	Hon-7	3Cox	290	—	—	—	—	—	—	—	—	—	—
49	Hon-7	4Cox	340	—	—	—	—	—	—	—	—	—	—
50	Hon-7	4Cn	370	—	—	—	—	—	—	—	—	—	—
51	Hon-8	AP1	7	—	—	—	—	—	—	—	—	—	—
52	Hon-8	AP2	34	—	—	—	—	—	—	—	—	—	—
53	Hon-8	BA	57	—	—	—	—	—	—	—	—	—	—
54	Hon-8	Bw1	90	—	—	—	—	—	—	—	—	—	—
55	Hon-8	Bw2	126	—	—	—	—	—	—	—	—	—	—
56	Hon-8	BC1	191	—	—	—	—	—	—	—	—	—	—
57	Hon-8	BC2	240	—	—	—	—	—	—	—	—	—	—
58	Hon-8	2Cox	390	—	—	—	—	—	—	—	—	—	—
Lower member of the Modesto Formation, 40 ka													
59	Hon-10	Ap	22	59.73	17.28	8.08	4.97	2.49	2.04	1.96	1.08	—	0.14
60	Hon-10	BA	40	57.46	18.95	9.21	5.50	2.30	2.05	2.04	1.12	—	.20
61	Hon-10	Bt1	86	57.01	18.76	9.26	5.44	2.20	2.08	2.05	1.12	—	.18
62	Hon-10	Bt2	132	56.82	18.98	9.22	5.59	2.27	2.15	2.05	1.10	—	.17
63	Hon-10	BC	150	56.99	18.89	9.24	5.77	2.51	2.06	2.02	1.11	—	.18
64	Hon-10	C	205	56.54	18.60	9.35	6.07	2.59	2.37	1.94	1.10	—	.18
65	Hon-10	2C	225	56.60	18.90	9.10	5.54	2.60	2.08	1.60	.97	—	.18
66	Hon-11	Ap	18	—	—	—	—	—	—	—	—	—	—
67	Hon-11	BA	45	—	—	—	—	—	—	—	—	—	—
68	Hon-11	Bt1	94	—	—	—	—	—	—	—	—	—	—
69	Hon-11	Bt2	125	—	—	—	—	—	—	—	—	—	—
70	Hon-11	BC	145	—	—	—	—	—	—	—	—	—	—
71	Hon-11	C	179	—	—	—	—	—	—	—	—	—	—
72	Hon-11	2C	220	—	—	—	—	—	—	—	—	—	—
Upper member of the Riverbank Formation, 130 ka													
73	Hon-13	Ap	24	—	—	—	—	—	—	—	—	—	—
74	Hon-13	BA	33	—	—	—	—	—	—	—	—	—	—
75	Hon-13	BAt1	50	—	—	—	—	—	—	—	—	—	—
76	Hon-13	BAt2	62	—	—	—	—	—	—	—	—	—	—
77	Hon-13	Bt1	86	—	—	—	—	—	—	—	—	—	—
78	Hon-13	Bt2	102	—	—	—	—	—	—	—	—	—	—
79	Hon-13	Bt3	123	—	—	—	—	—	—	—	—	—	—
80	Hon-13	BCt	157	—	—	—	—	—	—	—	—	—	—
81	Hon-13	2BCt1	208	—	—	—	—	—	—	—	—	—	—
82	Hon-13	2BCt2	245	—	—	—	—	—	—	—	—	—	—
83	Hon-13	2BCt3	266	—	—	—	—	—	—	—	—	—	—
84	Hon-13	2CB	301	—	—	—	—	—	—	—	—	—	—

Supplementary table 6, part 1. Total chemical analyses of the 2–20 μm fraction by X-ray fluorescence for major oxides—*Continued*

Sample number	Profile number	Horizon	Basal depth (cm)	SiO ₂	Al ₂ O ₃	Fe ₂ O ₃	MgO	CaO	Na ₂ O	K ₂ O	TiO ₂	P ₂ O ₅	MnO
Upper member of the Riverbank Formation, 130 ka—Continued													
85	Hon-14	Ap	28	65.58	15.68	6.74	.91	2.85	2.18	1.16	1.08	—	.20
86	Hon-14	BA	39	64.26	16.01	6.85	.92	2.67	2.08	1.16	1.13	—	.22
87	Hon-14	BAt1	59	63.71	15.84	7.01	1.03	2.61	1.97	1.18	1.12	—	.20
88	Hon-14	BAt2	76	62.01	16.87	7.70	1.55	2.34	2.20	1.23	1.18	—	.22
89	Hon-14	Bt1	111	61.86	16.67	7.42	1.79	2.84	2.71	1.09	1.05	—	.23
90	Hon-14	Bt2	126	62.17	17.23	7.52	2.10	3.40	2.83	1.05	.99	—	.21
91	Hon-14	2BCt1	150	57.22	17.51	9.13	5.07	3.67	3.21	.82	.91	—	.15
92	Hon-14	2BCt2	200	58.52	16.91	8.58	5.41	3.76	3.06	.72	.86	—	.16
93	Hon-14	2BCt3	260	57.41	17.56	9.39	6.13	3.87	3.00	.80	.88	—	.21
94	Hon-14	2CB	320	55.96	17.49	10.02	6.46	4.04	3.39	.86	.93	—	.28
Lower member of the Riverbank Formation, 250 ka													
95	Hon-17	Ap1	18	—	—	—	—	—	—	—	—	—	—
96	Hon-17	Ap2	24	—	—	—	—	—	—	—	—	—	—
97	Hon-17	BA	76	—	—	—	—	—	—	—	—	—	—
98	Hon-17	Bt1	100	—	—	—	—	—	—	—	—	—	—
99	Hon-17	Bt2	160	—	—	—	—	—	—	—	—	—	—
100	Hon-17	2BCt	201	—	—	—	—	—	—	—	—	—	—
101	Hon-17	3BCt	208	—	—	—	—	—	—	—	—	—	—
102	Hon-17	4BCt	295	—	—	—	—	—	—	—	—	—	—
103	Hon-18	Ap1	19	62.01	16.44	7.15	1.31	3.69	2.31	1.50	1.05	—	.14
104	Hon-18	Ap2	30	60.11	16.43	7.34	1.40	3.60	1.95	1.50	1.09	—	.19
105	Hon-18	BA	90	59.76	17.09	7.76	1.27	3.45	1.96	1.45	1.09	—	.26
106	Hon-18	Bt1	113	59.46	17.40	7.79	1.70	3.50	2.66	1.20	1.07	—	.22
107	Hon-18	Bt2	170	56.51	17.84	8.50	3.95	4.02	3.01	.80	.91	—	.20
108	Hon-18	2BCt	190	56.30	17.45	8.00	4.44	4.08	2.97	.81	.84	—	.20
109	Hon-18	3BCt	240	57.21	17.07	8.12	4.07	4.07	3.12	.86	.89	—	.19
110	Hon-18	4BCt	300	55.42	17.74	9.39	5.32	4.55	3.23	.98	.91	—	.26
111	Hon-19	Ap1	7	—	—	—	—	—	—	—	—	—	—
112	Hon-19	Ap2	24	—	—	—	—	—	—	—	—	—	—
113	Hon-19	BA	63	—	—	—	—	—	—	—	—	—	—
114	Hon-19	Bt1	91	—	—	—	—	—	—	—	—	—	—
115	Hon-19	Bt2	126	—	—	—	—	—	—	—	—	—	—
116	Hon-19	Bt3	176	—	—	—	—	—	—	—	—	—	—
117	Hon-19	BCt	218	—	—	—	—	—	—	—	—	—	—
118	Hon-19	2BCt1	246	—	—	—	—	—	—	—	—	—	—
119	Hon-19	2BCt2	268	—	—	—	—	—	—	—	—	—	—
120	Hon-19	2BCt3	300	—	—	—	—	—	—	—	—	—	—
121	Hon-19	3Cox	320	—	—	—	—	—	—	—	—	—	—
122	Hon-19	3Cox	410	—	—	—	—	—	—	—	—	—	—
23	Hon-20	Ap1	11	—	—	—	—	—	—	—	—	—	—
124	Hon-20	Ap2	30	—	—	—	—	—	—	—	—	—	—
125	Hon-20	BA	60	—	—	—	—	—	—	—	—	—	—
126	Hon-20	Bt1	114	—	—	—	—	—	—	—	—	—	—
127	Hon-20	Bt2	191	—	—	—	—	—	—	—	—	—	—

Supplementary table 6, part 1. Total chemical analyses of the 2–20 μm fraction by X-ray fluorescence for major oxides—*Continued*

Sample number	Profile number	Horizon	Basal depth (cm)	SiO ₂	Al ₂ O ₃	Fe ₂ O ₃	MgO	CaO	Na ₂ O	K ₂ O	TiO ₂	P ₂ O ₅	MnO
Lower member of the Riverbank Formation, 250 ka—Continued													
128	Hon-20	2BCt1	223	—	—	—	—	—	—	—	—	—	—
129	Hon-20	2BCt2	260	—	—	—	—	—	—	—	—	—	—
130	Hon-20	2CB	283	—	—	—	—	—	—	—	—	—	—
Exhumed lower member of the Laguna Formation, 1,600 ka													
131	Hon-21	A	11	61.23	17.67	8.04	.76	1.08	.64	1.51	1.47	—	.21
132	Hon-21	AB	33	62.75	17.54	8.00	.75	.98	.37	1.56	1.49	—	.19
133	Hon-21	BA	46	64.21	17.86	7.91	.84	.99	.78	1.59	1.55	—	.18
134	Hon-21	Bt1	71	65.03	18.35	7.64	.76	.37	.25	1.59	1.54	—	.10
135	Hon-21	Bt2	93	62.19	20.36	8.30	.77	.14	.22	1.44	1.47	—	.08
136	Hon-21	Bt3	119	61.04	21.33	8.78	.71	.11	.24	1.36	1.35	—	.06
137	Hon-21	Bt4	148	60.77	22.20	9.16	.55	.14	.00	1.47	1.44	—	.07
138	Hon-21	2Bt1	197	55.24	24.35	10.90	.68	.16	.26	1.30	1.28	—	.07
139	Hon-21	2Bt2	274	50.12	26.68	12.80	.70	.38	.55	.99	1.02	—	.07
140	Hon-21	2BC	315	50.23	24.56	13.12	.84	.98	1.02	1.08	1.01	—	.08
141	Hon-21	3BC	473	51.27	21.57	11.79	1.56	3.30	2.16	.88	.87	—	.13
142	Hon-21	C	1300	52.13	19.17	10.95	5.47	4.54	3.20	.86	1.21	—	.25
143	Hon-22	A	23	—	—	—	—	—	—	—	—	—	—
144	Hon-22	AB	43	—	—	—	—	—	—	—	—	—	—
145	Hon-22	BA	59	—	—	—	—	—	—	—	—	—	—
146	Hon-22	Bt1	89	—	—	—	—	—	—	—	—	—	—
147	Hon-22	Bt2	120	—	—	—	—	—	—	—	—	—	—
148	Hon-22	Bt3	154	—	—	—	—	—	—	—	—	—	—
149	Hon-22	2Bt1	207	—	—	—	—	—	—	—	—	—	—
150	Hon-22	2Bt2	270	—	—	—	—	—	—	—	—	—	—
151	Hon-22	2BCt	342	—	—	—	—	—	—	—	—	—	—
152	Hon-22	3BCt1	445	—	—	—	—	—	—	—	—	—	—
153	Hon-22	3BCt2	505	—	—	—	—	—	—	—	—	—	—
154	Hon-22	C	1300	—	—	—	—	—	—	—	—	—	—
Modern alluvium, 0 ka													
155	Hon-71	Cn	0	56.82	16.09	9.68	4.99	5.20	2.78	.74	1.33	—	.20
156	Hon-72	Cn	0	—	—	—	—	—	—	—	—	—	—

Supplementary table 6, part 2. Total chemical analyses of the 20–50 μm fraction by X-ray fluorescence for major oxides

[All values in weight percent. Analyst: A.J. Busacca]

Sample number	Profile number	Horizon	Basal depth (cm)	SiO ₂	Al ₂ O ₃	Fe ₂ O ₃	MgO	CaO	Na ₂ O	K ₂ O	TiO ₂	P ₂ O ₅	MnO
Holocene alluvium, 0.6 ka													
1	Hon-1	A	12	—	—	—	—	—	—	—	—	—	—
2	Hon-1	2A1	16	—	—	—	—	—	—	—	—	—	—
3	Hon-1	2A2	25	—	—	—	—	—	—	—	—	—	—
4	Hon-1	2AC	49	—	—	—	—	—	—	—	—	—	—
5	Hon-1	2C	85	—	—	—	—	—	—	—	—	—	—
6	Hon-1	3C1	95	—	—	—	—	—	—	—	—	—	—
7	Hon-1	3C2	122	—	—	—	—	—	—	—	—	—	—
8	Hon-1	4B1b	140	—	—	—	—	—	—	—	—	—	—
9	Hon-1	4B2b	170	—	—	—	—	—	—	—	—	—	—
10	Hon-2	A1	4	—	—	—	—	—	—	—	—	—	—
11	Hon-2	A2	32	—	—	—	—	—	—	—	—	—	—
12	Hon-2	C	61	—	—	—	—	—	—	—	—	—	—
13	Hon-2	2C	92	—	—	—	—	—	—	—	—	—	—
14	Hon-2	3C	103	—	—	—	—	—	—	—	—	—	—
15	Hon-2	4B2tb	130	—	—	—	—	—	—	—	—	—	—
16	Hon-3	A1	4	—	—	—	—	—	—	—	—	—	—
17	Hon-3	A2	16	—	—	—	—	—	—	—	—	—	—
18	Hon-3	AC	31	—	—	—	—	—	—	—	—	—	—
19	Hon-3	C	54	—	—	—	—	—	—	—	—	—	—
20	Hon-3	2C	78	—	—	—	—	—	—	—	—	—	—
21	Hon-4	C	17	56.97	15.69	8.66	4.30	7.21	4.11	0.61	1.42	—	0.18
22	Hon-4	2A	32	56.82	15.69	8.46	4.20	7.23	3.98	.62	1.36	—	.17
23	Hon-4	2AC	49	56.69	15.11	8.43	4.13	7.28	4.19	.63	1.39	—	.18
24	Hon-4	2C	86	55.70	15.77	8.73	4.25	7.10	3.93	.64	1.41	—	.18
25	Hon-4	3C1	113	55.78	15.80	9.26	4.22	7.50	3.78	.60	1.57	—	.20
26	Hon-4	3C2	147	55.49	15.09	9.29	4.34	7.73	3.74	.60	1.64	—	.20
Upper member of the Modesto Formation, 10 ka													
27	Hon-5	AP1	13	59.69	14.89	7.32	3.32	6.78	4.37	.53	1.31	—	.15
28	Hon-5	AP2	23	59.83	15.04	7.36	3.60	6.90	4.63	.54	1.33	—	.16
29	Hon-5	BA	54	59.19	14.99	7.49	3.44	6.95	4.22	.52	1.36	—	.16
30	Hon-5	Bw1	88	58.57	15.25	8.02	3.58	6.54	4.76	.52	1.39	—	.17
31	Hon-5	Bw2	102	57.90	15.17	8.11	3.41	6.57	4.34	.50	1.41	—	.17
32	Hon-5	BC1	141	59.55	15.75	7.58	3.65	6.54	4.37	.54	1.25	—	.16
33	Hon-5	BC2	180	57.87	14.74	7.80	3.30	6.32	4.45	.52	1.30	—	.16
34	Hon-6	AP1	10	—	—	—	—	—	—	—	—	—	—
35	Hon-6	AP2	22	—	—	—	—	—	—	—	—	—	—
36	Hon-6	BA	43	—	—	—	—	—	—	—	—	—	—
37	Hon-6	Bw1	91	—	—	—	—	—	—	—	—	—	—
38	Hon-6	Bw2	118	—	—	—	—	—	—	—	—	—	—
39	Hon-6	BC1	157	—	—	—	—	—	—	—	—	—	—
40	Hon-6	BC2	184	—	—	—	—	—	—	—	—	—	—
41	Hon-7	AP1	8	—	—	—	—	—	—	—	—	—	—
42	Hon-7	AP2	30	—	—	—	—	—	—	—	—	—	—

Supplementary table 6, part 2. Total chemical analyses of the 20–50 μm fraction by X-ray fluorescence for major oxides—*Continued*

Sample number	Profile number	Horizon	Basal depth (cm)	SiO ₂	Al ₂ O ₃	Fe ₂ O ₃	MgO	CaO	Na ₂ O	K ₂ O	TiO ₂	P ₂ O ₅	MnO
Upper member of the Modesto Formation, 10 ka—Continued													
43	Hon-7	BA	54	—	—	—	—	—	—	—	—	—	—
44	Hon-7	Bw1	88	—	—	—	—	—	—	—	—	—	—
45	Hon-7	Bw2	118	—	—	—	—	—	—	—	—	—	—
46	Hon-7	BC	180	—	—	—	—	—	—	—	—	—	—
47	Hon-7	2BC	230	—	—	—	—	—	—	—	—	—	—
48	Hon-7	3Cox	290	—	—	—	—	—	—	—	—	—	—
49	Hon-7	4Cox	340	—	—	—	—	—	—	—	—	—	—
50	Hon-7	4Cn	370	—	—	—	—	—	—	—	—	—	—
51	Hon-8	AP1	7	—	—	—	—	—	—	—	—	—	—
52	Hon-8	AP2	34	—	—	—	—	—	—	—	—	—	—
53	Hon-8	BA	57	—	—	—	—	—	—	—	—	—	—
54	Hon-8	Bw1	90	—	—	—	—	—	—	—	—	—	—
55	Hon-8	Bw2	126	—	—	—	—	—	—	—	—	—	—
56	Hon-8	BC1	191	—	—	—	—	—	—	—	—	—	—
57	Hon-8	BC2	240	—	—	—	—	—	—	—	—	—	—
58	Hon-8	2Cox	390	—	—	—	—	—	—	—	—	—	—
Lower member of the Modesto Formation, 40 ka													
59	Hon-10	Ap	22	63.69	14.49	6.55	3.62	5.20	3.17	1.08	1.10	—	0.12
60	Hon-10	BA	40	62.90	15.03	7.25	4.32	4.98	3.25	1.09	1.18	—	.14
61	Hon-10	Bt1	86	62.35	14.91	7.38	4.24	4.91	3.46	1.09	1.20	—	.13
62	Hon-10	Bt2	132	62.03	14.95	7.17	4.45	4.77	3.26	1.15	1.14	—	.13
63	Hon-10	BC	150	62.62	15.37	7.07	4.28	5.13	3.42	1.09	1.11	—	.13
64	Hon-10	C	205	61.92	15.59	7.19	4.50	5.21	3.13	1.13	1.08	—	.13
65	Hon-10	2C	225	60.07	16.84	7.29	4.53	4.69	2.77	1.10	1.03	—	.13
66	Hon-11	Ap	18	—	—	—	—	—	—	—	—	—	—
67	Hon-11	BA	45	—	—	—	—	—	—	—	—	—	—
68	Hon-11	Bt1	94	—	—	—	—	—	—	—	—	—	—
69	Hon-11	Bt2	125	—	—	—	—	—	—	—	—	—	—
70	Hon-11	BC	145	—	—	—	—	—	—	—	—	—	—
71	Hon-11	C	179	—	—	—	—	—	—	—	—	—	—
72	Hon-11	2C	220	—	—	—	—	—	—	—	—	—	—
Upper member of the Riverbank Formation, 130 ka													
73	Hon-13	Ap	24	—	—	—	—	—	—	—	—	—	—
74	Hon-13	BA	33	—	—	—	—	—	—	—	—	—	—
75	Hon-13	BAt1	50	—	—	—	—	—	—	—	—	—	—
76	Hon-13	BAt2	62	—	—	—	—	—	—	—	—	—	—
77	Hon-13	Bt1	86	—	—	—	—	—	—	—	—	—	—
78	Hon-13	Bt2	102	—	—	—	—	—	—	—	—	—	—
79	Hon-13	Bt3	123	—	—	—	—	—	—	—	—	—	—
80	Hon-13	BCt	157	—	—	—	—	—	—	—	—	—	—
81	Hon-13	2BCt1	208	—	—	—	—	—	—	—	—	—	—
82	Hon-13	2BCt2	245	—	—	—	—	—	—	—	—	—	—
83	Hon-13	2BCt3	266	—	—	—	—	—	—	—	—	—	—
84	Hon-13	2CB	301	—	—	—	—	—	—	—	—	—	—

Supplementary table 6, part 2. Total chemical analyses of the 20–50 μm fraction by X-ray fluorescence for major oxides—*Continued*

Sample number	Profile number	Horizon	Basal depth (cm)	SiO ₂	Al ₂ O ₃	Fe ₂ O ₃	MgO	CaO	Na ₂ O	K ₂ O	TiO ₂	P ₂ O ₅	MnO
Upper member of the Riverbank Formation, 130 ka—Continued													
85	Hon-14	Ap	28	72.09	13.21	4.71	.37	5.55	3.44	.90	.88	—	.11
86	Hon-14	BA	39	70.93	13.06	4.81	.36	5.36	3.49	.89	.88	—	.11
87	Hon-14	BAt1	59	69.44	12.98	4.75	.36	5.24	3.47	.87	.90	—	.11
88	Hon-14	BAt2	76	68.12	13.38	5.16	.53	5.30	3.26	.87	.88	—	.12
89	Hon-14	Bt1	111	67.94	13.73	4.94	.56	5.56	4.23	.83	.78	—	.13
90	Hon-14	Bt2	126	64.74	13.62	5.19	.79	6.10	4.12	.82	.77	—	.12
91	Hon-14	2BCt1	150	61.05	14.77	6.04	1.66	6.43	4.68	.69	.74	—	.11
92	Hon-14	2BCt2	200	62.51	15.04	5.78	2.80	6.05	4.97	.66	.72	—	.11
93	Hon-14	2BCt3	260	60.86	15.33	6.45	3.16	6.51	4.42	.68	.76	—	.14
94	Hon-14	2CB	320	60.16	14.63	6.64	3.47	6.95	4.55	.68	.77	—	.16
Lower member of the Riverbank Formation, 250 ka													
95	Hon-17	Ap1	18	—	—	—	—	—	—	—	—	—	—
96	Hon-17	Ap2	24	—	—	—	—	—	—	—	—	—	—
97	Hon-17	BA	76	—	—	—	—	—	—	—	—	—	—
98	Hon-17	Bt1	100	—	—	—	—	—	—	—	—	—	—
99	Hon-17	Bt2	160	—	—	—	—	—	—	—	—	—	—
100	Hon-17	2BCt	201	—	—	—	—	—	—	—	—	—	—
101	Hon-17	3BCt	208	—	—	—	—	—	—	—	—	—	—
102	Hon-17	4BCt	295	—	—	—	—	—	—	—	—	—	—
103	Hon-18	Ap1	19	67.08	13.30	5.53	.48	6.36	3.41	.93	.89	—	.10
104	Hon-18	Ap2	30	67.43	13.52	5.53	.49	6.36	3.38	.91	.89	—	.10
105	Hon-18	BA	90	65.78	13.63	5.71	.44	6.38	3.14	.90	.93	—	.12
106	Hon-18	Bt1	113	66.26	13.56	5.24	.36	6.06	3.96	.86	.88	—	.11
107	Hon-18	Bt2	170	64.36	13.98	5.41	1.01	6.50	4.27	.80	.73	—	.11
108	Hon-18	2BCt	190	61.23	14.38	5.40	1.44	6.63	4.59	.70	.69	—	.11
109	Hon-18	3BCt	240	61.26	14.33	5.47	1.43	6.63	4.26	.74	.71	—	.12
110	Hon-18	4BCt	300	58.60	14.85	6.87	3.10	7.72	4.12	.75	.76	—	.17
111	Hon-19	Ap1	7	—	—	—	—	—	—	—	—	—	—
112	Hon-19	Ap2	24	—	—	—	—	—	—	—	—	—	—
113	Hon-19	BA	63	—	—	—	—	—	—	—	—	—	—
114	Hon-19	Bt1	91	—	—	—	—	—	—	—	—	—	—
115	Hon-19	Bt2	126	—	—	—	—	—	—	—	—	—	—
116	Hon-19	Bt3	176	—	—	—	—	—	—	—	—	—	—
117	Hon-19	BCt	218	—	—	—	—	—	—	—	—	—	—
118	Hon-19	2BCt1	246	—	—	—	—	—	—	—	—	—	—
119	Hon-19	2BCt2	268	—	—	—	—	—	—	—	—	—	—
120	Hon-19	2BCt3	300	—	—	—	—	—	—	—	—	—	—
121	Hon-19	3Cox	320	—	—	—	—	—	—	—	—	—	—
122	Hon-19	3Cox	410	—	—	—	—	—	—	—	—	—	—
123	Hon-20	Ap1	11	—	—	—	—	—	—	—	—	—	—
124	Hon-20	Ap2	30	—	—	—	—	—	—	—	—	—	—
125	Hon-20	BA	60	—	—	—	—	—	—	—	—	—	—
126	Hon-20	Bt1	114	—	—	—	—	—	—	—	—	—	—
127	Hon-20	Bt2	191	—	—	—	—	—	—	—	—	—	—

Supplementary table 6, part 2. Total chemical analyses of the 20–50 μm fraction by X-ray fluorescence for major oxides—*Continued*

Sample number	Profile number	Horizon	Basal depth (cm)	SiO ₂	Al ₂ O ₃	Fe ₂ O ₃	MgO	CaO	Na ₂ O	K ₂ O	TiO ₂	P ₂ O ₅	MnO
Lower member of the Riverbank Formation, 250 kaa—<i>Continued</i>													
128	Hon-20	2BCt1	223	—	—	—	—	—	—	—	—	—	—
129	Hon-20	2BCt2	260	—	—	—	—	—	—	—	—	—	—
130	Hon-20	2CB	283	—	—	—	—	—	—	—	—	—	—
Exhumed lower member of the Laguna Formation, 1,600 ka													
131	Hon-21	A	11	80.01	7.69	4.67	0.27	1.68	0.73	1.18	1.65	—	0.09
132	Hon-21	AB	33	80.47	8.50	5.12	.40	1.83	1.06	1.19	1.70	—	.10
133	Hon-21	BA	46	79.64	8.38	5.14	.43	1.93	1.19	1.16	1.71	—	.10
134	Hon-21	Bt1	71	82.72	7.26	4.58	.25	.77	.48	1.31	1.72	—	.08
135	Hon-21	Bt2	93	85.90	6.70	4.30	.15	.18	.19	1.38	1.66	—	.06
136	Hon-21	Bt3	119	85.30	7.05	4.92	.23	.10	.38	1.34	1.74	—	.60
137	Hon-21	Bt4	148	85.28	6.75	4.16	.25	.18	.34	1.40	1.69	—	.60
138	Hon-21	2Bt1	197	81.86	7.89	5.46	.30	.32	.52	1.48	1.62	—	.60
139	Hon-21	2Bt2	274	67.06	14.53	8.50	.32	1.46	1.28	1.25	1.26	—	.70
140	Hon-21	2BC	315	62.03	15.51	9.17	.37	3.95	1.80	1.05	.96	—	.90
141	Hon-21	3BC	473	57.68	16.16	8.17	.70	7.51	3.80	.78	.74	—	.12
142	Hon-21	C	1300	59.01	15.61	7.14	2.13	7.19	4.89	.66	1.14	—	.18
143	Hon-22	A	23	—	—	—	—	—	—	—	—	—	—
144	Hon-22	AB	43	—	—	—	—	—	—	—	—	—	—
145	Hon-22	BA	59	—	—	—	—	—	—	—	—	—	—
146	Hon-22	Bt1	89	—	—	—	—	—	—	—	—	—	—
147	Hon-22	Bt2	120	—	—	—	—	—	—	—	—	—	—
148	Hon-22	Bt3	154	—	—	—	—	—	—	—	—	—	—
149	Hon-22	2Bt1	207	—	—	—	—	—	—	—	—	—	—
150	Hon-22	2Bt2	270	—	—	—	—	—	—	—	—	—	—
151	Hon-22	2BCt	342	—	—	—	—	—	—	—	—	—	—
152	Hon-22	3BCt1	445	—	—	—	—	—	—	—	—	—	—
153	Hon-22	3BCt2	505	—	—	—	—	—	—	—	—	—	—
154	Hon-22	C	1300	—	—	—	—	—	—	—	—	—	—
Modern alluvium, 0 ka													
155	Hon-71	Cn	0	59.43	14.71	6.76	2.91	7.87	4.48	.57	1.23	—	.15
156	Hon-72	Cn	0	—	—	—	—	—	—	—	—	—	—

Supplementary table 6, part 3. Total chemical analyses of the 2–20 μm fraction by X-ray fluorescence for trace elements

[All values in parts per million. Analyst: A.J. Busacca]

Sample number	Profile number	Horizon	Basal depth (cm)	Cr	Ni	Cu	Zn	Rb	Sr	Nb	Zr
Holocene alluvium, 0.6 ka											
1	Hon-1	A	12	—	—	—	—	—	—	—	—
2	Hon-1	2A1	16	—	—	—	—	—	—	—	—
3	Hon-1	2A2	25	—	—	—	—	—	—	—	—
4	Hon-1	2AC	49	—	—	—	—	—	—	—	—
5	Hon-1	2C	85	—	—	—	—	—	—	—	—
6	Hon-1	3C1	95	—	—	—	—	—	—	—	—
7	Hon-1	3C2	122	—	—	—	—	—	—	—	—
8	Hon-1	4B1b	140	—	—	—	—	—	—	—	—
9	Hon-1	4B2b	170	—	—	—	—	—	—	—	—
10	Hon-2	A1	4	—	—	—	—	—	—	—	—
11	Hon-2	A2	32	—	—	—	—	—	—	—	—
12	Hon-2	C	61	—	—	—	—	—	—	—	—
13	Hon-2	2C	92	—	—	—	—	—	—	—	—
14	Hon-2	3C	103	—	—	—	—	—	—	—	—
15	Hon-2	4B2tb	130	—	—	—	—	—	—	—	—
16	Hon-3	A1	4	—	—	—	—	—	—	—	—
17	Hon-3	A2	16	—	—	—	—	—	—	—	—
18	Hon-3	AC	31	—	—	—	—	—	—	—	—
19	Hon-3	C	54	—	—	—	—	—	—	—	—
20	Hon-3	2C	78	—	—	—	—	—	—	—	—
21	Hon-4	C	17	192	84	79	139	30	196	11	151
22	Hon-4	2A	32	198	83	86	146	31	185	10	150
23	Hon-4	2AC	49	184	80	69	120	23	183	9	146
24	Hon-4	2C	86	186	86	80	128	30	190	11	151
25	Hon-4	3C1	113	202	77	86	127	28	194	10	154
26	Hon-4	3C2	147	193	83	77	119	27	193	10	163
Upper member of the Modesto Formation, 10 ka											
27	Hon-5	AP1	13	167	71	63	112	31	190	8	163
28	Hon-5	AP2	23	169	73	67	117	25	185	8	167
29	Hon-5	BA	54	157	64	75	109	27	189	9	166
30	Hon-5	Bw1	88	175	92	96	122	22	175	9	173
31	Hon-5	Bw2	102	198	91	88	110	21	183	8	167
32	Hon-5	BC1	141	196	93	83	113	20	183	9	164
33	Hon-5	BC2	157	180	89	82	113	23	187	8	167
34	Hon-6	AP1	10	—	—	—	—	—	—	—	—
35	Hon-6	AP2	22	—	—	—	—	—	—	—	—
36	Hon-6	BA	43	—	—	—	—	—	—	—	—
37	Hon-6	Bw1	91	—	—	—	—	—	—	—	—
38	Hon-6	Bw2	118	—	—	—	—	—	—	—	—
39	Hon-6	BC1	157	—	—	—	—	—	—	—	—
40	Hon-6	BC2	184	—	—	—	—	—	—	—	—
41	Hon-7	AP1	8	—	—	—	—	—	—	—	—
42	Hon-7	AP2	30	—	—	—	—	—	—	—	—

Supplementary table 6, part 3. Total chemical analyses of the 2–20 μm fraction by X-ray fluorescence for trace elements—*Continued*

Sample number	Profile number	Horizon	Basal depth (cm)	Cr	Ni	Cu	Zn	Rb	Sr	Nb	Zr
Upper member of the Modesto Formation, 10 ka—<i>Continued</i>											
43	Hon-7	BA	54	—	—	—	—	—	—	—	—
44	Hon-7	Bw1	88	—	—	—	—	—	—	—	—
45	Hon-7	Bw2	118	—	—	—	—	—	—	—	—
46	Hon-7	BC	180	—	—	—	—	—	—	—	—
47	Hon-7	2BC	230	—	—	—	—	—	—	—	—
48	Hon-7	3Cox	290	—	—	—	—	—	—	—	—
49	Hon-7	4Cox	340	—	—	—	—	—	—	—	—
50	Hon-7	4Cn	370	—	—	—	—	—	—	—	—
51	Hon-8	AP1	7	—	—	—	—	—	—	—	—
52	Hon-8	AP2	34	—	—	—	—	—	—	—	—
53	Hon-8	BA	57	—	—	—	—	—	—	—	—
54	Hon-8	Bw1	90	—	—	—	—	—	—	—	—
55	Hon-8	Bw2	126	—	—	—	—	—	—	—	—
56	Hon-8	BC1	191	—	—	—	—	—	—	—	—
57	Hon-8	BC2	240	—	—	—	—	—	—	—	—
58	Hon-8	2Cox	390	—	—	—	—	—	—	—	—
Lower member of the Modesto Formation, 40 ka											
59	Hon-10	Ap	22	241	212	92	146	73	224	10	147
60	Hon-10	BA	40	275	280	90	130	76	207	10	148
61	Hon-10	Bt1	86	283	286	89	124	79	205	10	145
62	Hon-10	Bt2	132	285	269	83	121	75	211	10	144
63	Hon-10	BC	150	278	260	82	125	72	235	9	140
64	Hon-10	C	205	299	278	85	127	68	237	9	137
65	Hon-10	2C	225	252	256	86	111	49	243	9	130
66	Hon-11	Ap	18	—	—	—	—	—	—	—	—
67	Hon-11	BA	45	—	—	—	—	—	—	—	—
68	Hon-11	Bt1	94	—	—	—	—	—	—	—	—
69	Hon-11	Bt2	125	—	—	—	—	—	—	—	—
70	Hon-11	BC	145	—	—	—	—	—	—	—	—
71	Hon-11	C	179	—	—	—	—	—	—	—	—
72	Hon-11	2C	220	—	—	—	—	—	—	—	—
Upper member of the Riverbank Formation, 130 ka											
73	Hon-13	Ap	24	—	—	—	—	—	—	—	—
74	Hon-13	BA	33	—	—	—	—	—	—	—	—
75	Hon-13	BAt1	50	—	—	—	—	—	—	—	—
76	Hon-13	BAt2	62	—	—	—	—	—	—	—	—
77	Hon-13	Bt1	86	—	—	—	—	—	—	—	—
78	Hon-13	Bt2	102	—	—	—	—	—	—	—	—
79	Hon-13	Bt3	123	—	—	—	—	—	—	—	—
80	Hon-13	BCt	157	—	—	—	—	—	—	—	—
81	Hon-13	2BCt1	208	—	—	—	—	—	—	—	—
82	Hon-13	2BCt2	245	—	—	—	—	—	—	—	—
83	Hon-13	2BCt3	266	—	—	—	—	—	—	—	—
84	Hon-13	2CB	301	—	—	—	—	—	—	—	—

Supplementary table 6, part 3. Total chemical analyses of the 2–20 μm fraction by X-ray fluorescence for trace elements—*Continued*

Sample number	Profile	Horizon	Basal depth (cm)	Cr	Ni	Cu	Zn	Rb	Sr	Nb	Zr
Upper member of the Riverbank Formation, 130 ka—<i>Continued</i>											
85	Hon-14	Ap	28	151	67	57	90	56	168	7	196
86	Hon-14	BA	39	163	73	60	70	55	164	7	198
87	Hon-14	BAt1	59	163	79	62	74	56	163	10	201
88	Hon-14	BAt2	76	158	83	61	81	55	151	12	193
89	Hon-14	Bt1	111	149	73	59	72	37	170	9	175
90	Hon-14	Bt2	126	179	72	62	77	38	187	6	159
91	Hon-14	2BCt1	150	202	94	83	102	21	172	7	122
92	Hon-14	2BCt2	200	176	92	80	101	19	168	5	116
93	Hon-14	2BCt3	260	175	98	88	120	23	161	7	107
94	Hon-14	2CB	320	205	108	96	121	23	159	5	111
Lower member of the Riverbank Formation, 250 ka											
95	Hon-17	Ap1	18	—	—	—	—	—	—	—	—
96	Hon-17	Ap2	24	—	—	—	—	—	—	—	—
97	Hon-17	BA	76	—	—	—	—	—	—	—	—
98	Hon-17	Bt1	100	—	—	—	—	—	—	—	—
99	Hon-17	Bt2	160	—	—	—	—	—	—	—	—
100	Hon-17	2BCt	201	—	—	—	—	—	—	—	—
101	Hon-17	3BCt	208	—	—	—	—	—	—	—	—
102	Hon-17	4BCt	295	—	—	—	—	—	—	—	—
103	Hon-18	Ap1	19	153	65	65	91	70	197	8	176
104	Hon-18	Ap2	30	172	84	73	90	72	199	8	181
105	Hon-18	BA	90	171	78	72	86	69	192	8	174
106	Hon-18	Bt1	113	167	80	66	77	48	188	6	167
107	Hon-18	Bt2	170	178	78	73	92	23	195	6	129
108	Hon-18	2BCt	190	169	75	68	83	18	196	5	116
109	Hon-18	3BCt	240	164	84	69	85	25	191	6	128
110	Hon-18	4BCt	300	192	93	80	110	28	179	8	115
111	Hon-19	Ap1	7	—	—	—	—	—	—	—	—
112	Hon-19	Ap2	24	—	—	—	—	—	—	—	—
113	Hon-19	BA	63	—	—	—	—	—	—	—	—
114	Hon-19	Bt1	91	—	—	—	—	—	—	—	—
115	Hon-19	Bt2	126	—	—	—	—	—	—	—	—
116	Hon-19	Bt3	176	—	—	—	—	—	—	—	—
117	Hon-19	BCt	218	—	—	—	—	—	—	—	—
118	Hon-19	2BCt1	246	—	—	—	—	—	—	—	—
119	Hon-19	2BCt2	268	—	—	—	—	—	—	—	—
120	Hon-19	2BCt3	300	—	—	—	—	—	—	—	—
121	Hon-19	3Cox	320	—	—	—	—	—	—	—	—
122	Hon-19	3Cox	410	—	—	—	—	—	—	—	—
123	Hon-20	Ap1	11	—	—	—	—	—	—	—	—
124	Hon-20	Ap2	30	—	—	—	—	—	—	—	—
125	Hon-20	BA	60	—	—	—	—	—	—	—	—
126	Hon-20	Bt1	114	—	—	—	—	—	—	—	—
127	Hon-20	Bt2	191	—	—	—	—	—	—	—	—
128	Hon-20	2BCt1	223	—	—	—	—	—	—	—	—

Supplementary table 6, part 3. Total chemical analyses of the 2–20 μm fraction by X-ray fluorescence for trace elements—*Continued*

Sample number	Profile number	Horizon	Basal depth (cm)	Cr	Ni	Cu	Zn	Rb	Sr	Nb	Zr
Lower member of the Riverbank Formation, 250 ka—Continued											
129	Hon-20	2BCt2	260	—	—	—	—	—	—	—	—
130	Hon-20	2CB	283	—	—	—	—	—	—	—	—
Exhumed lower member of the Laguna Formation, 1,600 ka											
131	Hon-21	A	11	190	82	87	90	77	78	13	262
132	Hon-21	AB	33	209	79	82	78	76	73	13	263
133	Hon-21	BA	46	211	80	79	74	79	82	11	274
134	Hon-21	Bt1	71	200	86	75	69	78	46	15	278
135	Hon-21	Bt2	93	228	115	62	75	64	31	11	255
136	Hon-21	Bt3	119	181	101	63	67	57	25	10	246
137	Hon-21	Bt4	148	197	89	71	79	55	23	10	247
138	Hon-21	2Bt1	197	210	88	64	53	43	20	7	214
139	Hon-21	2Bt2	274	208	92	76	56	32	29	8	162
140	Hon-21	2BC	315	199	88	78	69	39	70	7	167
141	Hon-21	3BC	473	182	66	85	84	31	167	5	120
142	Hon-21	C	1300	173	84	93	169	25	187	9	128
143	Hon-22	A	23	—	—	—	—	—	—	—	—
144	Hon-22	AB	43	—	—	—	—	—	—	—	—
145	Hon-22	BA	59	—	—	—	—	—	—	—	—
146	Hon-22	Bt1	89	—	—	—	—	—	—	—	—
147	Hon-22	Bt2	120	—	—	—	—	—	—	—	—
148	Hon-22	Bt3	154	—	—	—	—	—	—	—	—
149	Hon-22	2Bt1	207	—	—	—	—	—	—	—	—
150	Hon-22	2Bt2	270	—	—	—	—	—	—	—	—
151	Hon-22	2BCt	342	—	—	—	—	—	—	—	—
152	Hon-22	3BCt1	445	—	—	—	—	—	—	—	—
153	Hon-22	3BCt2	505	—	—	—	—	—	—	—	—
154	Hon-22	C	1300	—	—	—	—	—	—	—	—
Modern alluvium, 0 ka											
155	Hon-71	Cn	0	150	73	71	124	24	209	10	137
156	Hon-72	Cn	0	—	—	—	—	—	—	—	—

Supplementary table 6, part 4. Total chemical analyses of the 20–50 μm fraction by X-ray fluorescence for trace elements

[All values in parts per million. Analyst: A.J. Busacca]

Sample number	Profile number	Horizon	Basal depth (cm)	Cr	Ni	Cu	Zn	Rb	Sr	Nb	Zr
Holocene alluvium, 0.6 ka											
1	Hon-1	A	12	—	—	—	—	—	—	—	—
2	Hon-1	2A1	16	—	—	—	—	—	—	—	—
3	Hon-1	2A2	25	—	—	—	—	—	—	—	—
4	Hon-1	2AC	49	—	—	—	—	—	—	—	—
5	Hon-1	2C	85	—	—	—	—	—	—	—	—
6	Hon-1	3C1	95	—	—	—	—	—	—	—	—
7	Hon-1	3C2	122	—	—	—	—	—	—	—	—
8	Hon-1	4B1b	140	—	—	—	—	—	—	—	—
9	Hon-1	4B2b	170	—	—	—	—	—	—	—	—
10	Hon-2	A1	4	—	—	—	—	—	—	—	—
11	Hon-2	A2	32	—	—	—	—	—	—	—	—
12	Hon-2	C	61	—	—	—	—	—	—	—	—
13	Hon-2	2C	92	—	—	—	—	—	—	—	—
14	Hon-2	3C	103	—	—	—	—	—	—	—	—
15	Hon-2	4B2tb	130	—	—	—	—	—	—	—	—
16	Hon-3	A1	4	—	—	—	—	—	—	—	—
17	Hon-3	A2	16	—	—	—	—	—	—	—	—
18	Hon-3	AC	31	—	—	—	—	—	—	—	—
19	Hon-3	C	54	—	—	—	—	—	—	—	—
20	Hon-3	2C	78	—	—	—	—	—	—	—	—
21	Hon-4	C	17	163	29	43	62	12	272	6	296
22	Hon-4	2A	32	143	28	45	69	12	282	7	285
23	Hon-4	2AC	49	147	24	40	61	14	278	7	311
24	Hon-4	2C	86	146	41	42	54	12	274	8	288
25	Hon-4	3C1	113	138	29	43	56	13	287	8	378
26	Hon-4	3C2	147	136	21	45	57	12	298	6	416
Upper member of the Modesto Formation, 10 ka											
27	Hon-5	AP1	13	125	32	34	48	11	257	5	255
28	Hon-5	AP2	23	115	24	38	46	9	255	7	249
29	Hon-5	BA	54	152	32	36	47	10	260	6	268
30	Hon-5	Bw1	88	137	24	46	60	10	272	5	276
31	Hon-5	Bw2	102	126	22	39	49	11	269	4	299
32	Hon-5	BC1	141	156	37	39	48	10	247	7	279
33	Hon-5	BC2	180	148	20	43	51	8	269	4	282
34	Hon-6	AP1	10	—	—	—	—	—	—	—	—
35	Hon-6	AP2	22	—	—	—	—	—	—	—	—
36	Hon-6	BA	43	—	—	—	—	—	—	—	—
37	Hon-6	Bw1	91	—	—	—	—	—	—	—	—
38	Hon-6	Bw2	118	—	—	—	—	—	—	—	—
39	Hon-6	BC1	157	—	—	—	—	—	—	—	—
40	Hon-6	BC2	184	—	—	—	—	—	—	—	—
41	Hon-7	AP1	8	—	—	—	—	—	—	—	—
42	Hon-7	AP2	30	—	—	—	—	—	—	—	—

Supplementary table 6, part 4. Total chemical analyses of the 20–50 μm fraction by X-ray fluorescence for trace elements—*Continued*

Sample number	Profile number	Horizon	Basal depth (cm)	Cr	Ni	Cu	Zn	Rb	Sr	Nb	Zr
Upper member of the Modesto Formation, 10 ka—Continued											
43	Hon-7	BA	54	—	—	—	—	—	—	—	—
44	Hon-7	Bw1	88	—	—	—	—	—	—	—	—
45	Hon-7	Bw2	118	—	—	—	—	—	—	—	—
46	Hon-7	BC	180	—	—	—	—	—	—	—	—
47	Hon-7	2BC	230	—	—	—	—	—	—	—	—
48	Hon-7	3Cox	290	—	—	—	—	—	—	—	—
49	Hon-7	4Cox	340	—	—	—	—	—	—	—	—
50	Hon-7	4Cn	370	—	—	—	—	—	—	—	—
51	Hon-8	AP1	7	—	—	—	—	—	—	—	—
52	Hon-8	AP2	34	—	—	—	—	—	—	—	—
53	Hon-8	BA	57	—	—	—	—	—	—	—	—
54	Hon-8	Bw1	90	—	—	—	—	—	—	—	—
55	Hon-8	Bw2	126	—	—	—	—	—	—	—	—
56	Hon-8	BC1	191	—	—	—	—	—	—	—	—
57	Hon-8	BC2	240	—	—	—	—	—	—	—	—
58	Hon-8	2Cox	390	—	—	—	—	—	—	—	—
Lower member of the Modesto Formation, 40 ka											
59	Hon-10	Ap	22	316	97	46	77	26	360	9	281
60	Hon-10	BA	40	365	133	48	81	27	324	9	280
61	Hon-10	Bt1	86	376	133	51	72	26	332	9	292
62	Hon-10	Bt2	132	356	135	56	74	27	332	8	263
63	Hon-10	BC	150	331	125	53	76	26	356	8	263
64	Hon-10	C	205	351	139	56	77	29	365	8	275
65	Hon-10	2C	225	271	137	57	82	26	351	9	237
66	Hon-11	Ap	18	—	—	—	—	—	—	—	—
67	Hon-11	BA	45	—	—	—	—	—	—	—	—
68	Hon-11	Bt1	94	—	—	—	—	—	—	—	—
69	Hon-11	Bt2	125	—	—	—	—	—	—	—	—
70	Hon-11	BC	145	—	—	—	—	—	—	—	—
71	Hon-11	C	179	—	—	—	—	—	—	—	—
72	Hon-11	2C	220	—	—	—	—	—	—	—	—
Upper member of the Riverbank Formation, 130 ka											
73	Hon-13	Ap	24	—	—	—	—	—	—	—	—
74	Hon-13	BA	33	—	—	—	—	—	—	—	—
75	Hon-13	BAt1	50	—	—	—	—	—	—	—	—
76	Hon-13	BAt2	62	—	—	—	—	—	—	—	—
77	Hon-13	Bt1	86	—	—	—	—	—	—	—	—
78	Hon-13	Bt2	102	—	—	—	—	—	—	—	—
79	Hon-13	Bt3	123	—	—	—	—	—	—	—	—
80	Hon-13	BCt	157	—	—	—	—	—	—	—	—
81	Hon-13	2BCt1	208	—	—	—	—	—	—	—	—
82	Hon-13	2BCt2	245	—	—	—	—	—	—	—	—
83	Hon-13	2BCt3	266	—	—	—	—	—	—	—	—
84	Hon-13	2CB	301	—	—	—	—	—	—	—	—

Supplementary table 6, part 4. Total chemical analyses of the 20–50 μm fraction by X-ray fluorescence for trace elements—*Continued*

Sample number	Profile number	Horizon	Basal depth (cm)	Cr	Ni	Cu	Zn	Rb	Sr	Nb	Zr
Upper member of the Riverbank Formation, 130 ka—Continued											
85	Hon-14	Ap	28	175	11	35	47	21	255	5	414
86	Hon-14	BA	39	179	11	36	29	21	254	6	423
87	Hon-14	BAt1	59	196	14	37	36	22	255	7	431
88	Hon-14	BAt2	76	199	13	41	30	21	250	5	399
89	Hon-14	Bt1	111	171	15	43	34	15	260	5	370
90	Hon-14	Bt2	126	184	12	40	30	16	279	6	348
91	Hon-14	2BCt1	150	206	22	44	41	11	275	3	321
92	Hon-14	2BCt2	200	174	29	45	42	10	262	3	278
93	Hon-14	2BCt3	260	170	30	46	47	12	268	4	313
94	Hon-14	2CB	320	212	30	51	48	12	272	5	322
Lower member of the Riverbank Formation, 250 ka											
95	Hon-17	Ap1	18	—	—	—	—	—	—	—	—
96	Hon-17	Ap2	24	—	—	—	—	—	—	—	—
97	Hon-17	BA	76	—	—	—	—	—	—	—	—
98	Hon-17	Bt1	100	—	—	—	—	—	—	—	—
99	Hon-17	Bt2	160	—	—	—	—	—	—	—	—
100	Hon-17	2BCt	201	—	—	—	—	—	—	—	—
101	Hon-17	3BCt	208	—	—	—	—	—	—	—	—
102	Hon-17	4BCt	295	—	—	—	—	—	—	—	—
103	Hon-18	Ap1	19	195	14	35	32	21	276	6	404
104	Hon-18	Ap2	30	180	7	31	27	20	273	5	405
105	Hon-18	BA	90	199	13	39	32	22	278	7	424
106	Hon-18	Bt1	113	203	9	37	27	19	264	4	372
107	Hon-18	Bt2	170	143	12	35	30	13	278	3	310
108	Hon-18	2BCt	190	147	17	39	28	10	282	4	264
109	Hon-18	3BCt	240	125	17	39	30	13	281	3	301
110	Hon-18	4BCt	300	217	30	49	44	15	288	5	332
111	Hon-19	Ap1	7	—	—	—	—	—	—	—	—
112	Hon-19	Ap2	24	—	—	—	—	—	—	—	—
113	Hon-19	BA	63	—	—	—	—	—	—	—	—
114	Hon-19	Bt1	91	—	—	—	—	—	—	—	—
115	Hon-19	Bt2	126	—	—	—	—	—	—	—	—
116	Hon-19	Bt3	176	—	—	—	—	—	—	—	—
117	Hon-19	BCt	218	—	—	—	—	—	—	—	—
118	Hon-19	2BCt1	246	—	—	—	—	—	—	—	—
119	Hon-19	2BCt2	268	—	—	—	—	—	—	—	—
120	Hon-19	2BCt3	300	—	—	—	—	—	—	—	—
121	Hon-19	3Cox	320	—	—	—	—	—	—	—	—
122	Hon-19	3Cox	410	—	—	—	—	—	—	—	—
123	Hon-20	Ap1	11	—	—	—	—	—	—	—	—
124	Hon-20	Ap2	30	—	—	—	—	—	—	—	—
125	Hon-20	BA	60	—	—	—	—	—	—	—	—
126	Hon-20	Bt1	114	—	—	—	—	—	—	—	—
127	Hon-20	Bt2	191	—	—	—	—	—	—	—	—
128	Hon-20	2BCt1	223	—	—	—	—	—	—	—	—

Supplementary table 6, part 4. Total chemical analyses of the 20–50 μm fraction by X-ray fluorescence for trace elements—*Continued*

Sample number	Profile number	Horizon	Basal depth (cm)	Cr	Ni	Cu	Zn	Rb	Sr	Nb	Zr
Lower member of the Riverbank Formation, 250 ka—<i>Continued</i>											
129	Hon-20	2BCt2	260	—	—	—	—	—	—	—	—
130	Hon-20	2CB	283	—	—	—	—	—	—	—	—
Exhumed lower member of the Laguna Formation, 1,600 ka											
131	Hon-21	A	11	277	6	39	34	25	93	9	843
132	Hon-21	AB	33	329	14	41	41	26	99	9	797
133	Hon-21	BA	46	320	12	40	39	24	103	7	784
134	Hon-21	Bt1	71	333	10	45	40	27	55	9	790
135	Hon-21	Bt2	93	257	7	45	34	26	26	9	828
136	Hon-21	Bt3	119	324	35	46	36	23	23	8	947
137	Hon-21	Bt4	148	301	5	47	41	23	23	7	920
138	Hon-21	2Bt1	197	276	7	50	34	23	25	6	906
139	Hon-21	2Bt2	274	224	23	66	39	23	72	4	625
140	Hon-21	2BC	315	160	24	61	31	21	170	3	459
141	Hon-21	3BC	473	157	8	65	42	15	314	6	300
142	Hon-21	C	1300	173	15	43	43	12	302	6	260
143	Hon-22	A	23	—	—	—	—	—	—	—	—
144	Hon-22	AB	43	—	—	—	—	—	—	—	—
145	Hon-22	BA	59	—	—	—	—	—	—	—	—
146	Hon-22	Bt1	89	—	—	—	—	—	—	—	—
147	Hon-22	Bt2	120	—	—	—	—	—	—	—	—
148	Hon-22	Bt3	154	—	—	—	—	—	—	—	—
149	Hon-22	2Bt1	207	—	—	—	—	—	—	—	—
150	Hon-22	2Bt2	270	—	—	—	—	—	—	—	—
151	Hon-22	2BCt	342	—	—	—	—	—	—	—	—
152	Hon-22	3BCt1	445	—	—	—	—	—	—	—	—
153	Hon-22	3BCt2	505	—	—	—	—	—	—	—	—
154	Hon-22	C	1300	—	—	—	—	—	—	—	—
Modern alluvium, 0 ka											
155	Hon-71	Cn	0	138	28	32	41	10	310	5	262
156	Hon-72	Cn	0	—	—	—	—	—	—	—	—

Supplementary table 7, part 1. Total chemical analyses of the fine (<50 μm) fraction by instrumental neutron activation, elements Ba to Mn

[Fe and K values in weight percent; all other values in parts per million. Analysts: J. Budahn, D.M. McKown, and R. Knight]

Sample number	Profile number	Horizon	Basal depth (cm)	Ba	Ce	Co	Cr	Cs	Dy	Eu	Fe	Gd	Hf	K	La	Lu	Mn
Holocene alluvium, 0.6 ka																	
1	Hon-1	A	12	—	—	—	—	—	—	—	—	—	—	—	—	—	—
2	Hon-1	2A1	16	—	—	—	—	—	—	—	—	—	—	—	—	—	—
3	Hon-1	2A2	25	213	27.0	26.8	118	0.902	4.83	1.29	7.44	5.00	4.28	0.57	12.8	0.486	1400
4	Hon-1	2AC	49	—	—	—	—	—	—	—	—	—	—	—	—	—	—
5	Hon-1	2C	85	252	30.5	31.6	113	0.912	5.18	1.39	8.21	5.20	4.36	0.50	13.8	0.532	1490
6	Hon-1	3C1	95	—	—	—	—	—	—	—	—	—	—	—	—	—	—
7	Hon-1	3C2	122	—	—	—	—	—	—	—	—	—	—	—	—	—	—
8	Hon-1	4B1b	140	—	—	—	—	—	—	—	—	—	—	—	—	—	—
9	Hon-1	4B2b	170	—	—	—	—	—	—	—	—	—	—	—	—	—	—
10	Hon-2	A1	4	—	—	—	—	—	—	—	—	—	—	—	—	—	—
11	Hon-2	A2	32	246	30.7	29.8	109	0.871	5.41	1.33	7.72	6.12	3.97	0.50	13.2	0.521	1450
12	Hon-2	C	61	—	—	—	—	—	—	—	—	—	—	—	—	—	—
13	Hon-2	2C	92	265	32.9	34.3	113	0.945	5.45	1.39	7.81	5.30	4.95	0.50	15.4	0.556	1560
14	Hon-2	3C	103	—	—	—	—	—	—	—	—	—	—	—	—	—	—
15	Hon-2	4B2tb	130	—	—	—	—	—	—	—	—	—	—	—	—	—	—
16	Hon-3	A1	4	—	—	—	—	—	—	—	—	—	—	—	—	—	—
17	Hon-3	A2	16	250	25.4	27.2	101	0.850	4.91	1.34	7.10	4.90	3.87	0.76	12.8	0.501	1240
18	Hon-3	AC	31	—	—	—	—	—	—	—	—	—	—	—	—	—	—
19	Hon-3	C	54	252	34.2	36.5	114	0.926	5.57	1.44	8.02	5.78	4.74	0.50	15.1	0.565	1800
20	Hon-3	2C	78	—	—	—	—	—	—	—	—	—	—	—	—	—	—
21	Hon-4	C	17	—	—	—	—	—	—	—	—	—	—	—	—	—	—
22	Hon-4	2A	32	232	28.7	27.2	118	0.926	4.89	1.34	7.66	5.21	4.29	0.55	12.9	0.499	1390
23	Hon-4	2AC	49	—	—	—	—	—	—	—	—	—	—	—	—	—	—
24	Hon-4	2C	86	267	28.7	30.7	116	0.958	5.75	1.43	7.95	—	4.68	0.59	13.5	0.577	1590
25	Hon-4	3C1	113	—	—	—	—	—	—	—	—	—	—	—	—	—	—
26	Hon-4	3C2	147	—	—	—	—	—	—	—	—	—	—	—	—	—	—
Upper member of the Modesto Formation, 10 ka																	
27	Hon-5	AP1	13	—	—	—	—	—	—	—	—	—	—	—	—	—	—
28	Hon-5	AP2	23	234	27.3	30.0	107	1.16	5.65	1.41	7.81	5.64	3.81	0.50	12.2	0.553	1460

Supplementary table 7, part 1. Total chemical analyses of the fine (<50 μm) fraction by instrumental neutron activation, elements Ba to Mn—Continued

Sample number	Profile number	Horizon	Basal depth (cm)	Ba	Ce	Co	Cr	Cs	Dy	Eu	Fe	Gd	Hf	K	La	Lu	Mn
Upper member of the Modesto Formation, 10 ka—Continued																	
29	Hon-5	BA	54	—	—	—	—	—	—	—	—	—	—	—	—	—	—
30	Hon-5	Bw1	88	190	25.5	35.7	117	1.15	5.74	1.45	8.20	6.15	3.93	0.50	12.2	0.573	1580
31	Hon-5	Bw2	102	—	—	—	—	—	—	—	—	—	—	—	—	—	—
32	Hon-5	BC1	141	—	—	—	—	—	—	—	—	—	—	—	—	—	—
33	Hon-5	BC2	180	—	—	—	—	—	—	—	—	—	—	—	—	—	—
34	Hon-6	AP1	10	—	—	—	—	—	—	—	—	—	—	—	—	—	—
35	Hon-6	AP2	22	220	24.4	29.2	106	1.17	5.54	1.37	7.70	5.22	3.80	0.50	12.0	0.541	1390
36	Hon-6	BA	43	—	—	—	—	—	—	—	—	—	—	—	—	—	—
37	Hon-6	Bw1	91	214	23.3	30.2	110	0.928	5.19	1.40	7.10	5.15	4.27	0.50	11.6	0.552	1410
38	Hon-6	Bw2	118	—	—	—	—	—	—	—	—	—	—	—	—	—	—
39	Hon-6	BC1	157	—	—	—	—	—	—	—	—	—	—	—	—	—	—
40	Hon-6	BC2	184	—	—	—	—	—	—	—	—	—	—	—	—	—	—
41	Hon-7	AP1	8	—	—	—	—	—	—	—	—	—	—	—	—	—	—
42	Hon-7	AP2	30	258	27.9	28.5	117	1.33	5.35	1.41	7.47	—	4.47	0.50	13.1	0.551	1550
43	Hon-7	BA	54	—	—	—	—	—	—	—	—	—	—	—	—	—	—
44	Hon-7	Bw1	88	246	26.7	36.4	126	1.38	6.30	1.47	7.82	—	4.30	0.54	13.3	0.579	1750
45	Hon-7	Bw2	118	—	—	—	—	—	—	—	—	—	—	—	—	—	—
46	Hon-7	BC	180	—	—	—	—	—	—	—	—	—	—	—	—	—	—
47	Hon-7	2BC	230	—	—	—	—	—	—	—	—	—	—	—	—	—	—
48	Hon-7	3Cox	290	—	—	—	—	—	—	—	—	—	—	—	—	—	—
49	Hon-7	4Cox	340	—	—	—	—	—	—	—	—	—	—	—	—	—	—
50	Hon-7	4Cn	370	—	—	—	—	—	—	—	—	—	—	—	—	—	—
51	Hon-8	AP1	7	—	—	—	—	—	—	—	—	—	—	—	—	—	—
52	Hon-8	AP2	34	243	31.5	29.7	125	1.42	5.08	1.49	7.90	5.44	4.80	0.53	13.6	0.565	1540
53	Hon-8	BA	57	—	—	—	—	—	—	—	—	—	—	—	—	—	—
54	Hon-8	Bw1	90	197	27.6	35.1	127	1.38	5.50	1.49	7.73	5.10	4.33	0.50	13.0	0.569	1670
55	Hon-8	Bw2	126	—	—	—	—	—	—	—	—	—	—	—	—	—	—
56	Hon-8	BC1	191	—	—	—	—	—	—	—	—	—	—	—	—	—	—
57	Hon-8	BC2	240	227	28.9	30.8	123	1.32	5.51	1.39	6.88	5.27	3.94	0.60	13.7	0.534	1580
58	Hon-8	2Cox	390	—	—	—	—	—	—	—	—	—	—	—	—	—	—

Supplementary table 7, part 1. Total chemical analyses of the fine (<50 μm) fraction by instrumental neutron activation, elements Ba to Mn—Continued

Sample number	Profile number	Horizon	Basal depth (cm)	Ba	Ce	Co	Cr	Cs	Dy	Eu	Fe	Gd	Hf	K	La	Lu	Mn
Upper member of the Riverbank Formation, 130 ka—Continued																	
88	Hon-14	BA2	76	—	—	—	—	—	—	—	—	—	—	—	—	—	—
89	Hon-14	Bt1	111	316	30.8	36.8	160	2.83	4.42	1.10	6.99	4.63	3.98	0.876	15.2	0.451	1620
90	Hon-14	Bt2	126	—	—	—	—	—	—	—	—	—	—	—	—	—	—
91	Hon-14	2BCt1	150	—	—	—	—	—	—	—	—	—	—	—	—	—	—
92	Hon-14	2BCt2	200	—	—	—	—	—	—	—	—	—	—	—	—	—	—
93	Hon-14	2BCt3	260	—	—	—	—	—	—	—	—	—	—	—	—	—	—
94	Hon-14	2CB	320	—	—	—	—	—	—	—	—	—	—	—	—	—	—
Lower member of the Riverbank Formation, 250 ka																	
95	Hon-17	Ap1	18	—	—	—	—	—	—	—	—	—	—	—	—	—	—
96	Hon-17	Ap2	24	379	44.4	28.7	179	2.52	5.84	1.61	6.42	5.60	6.02	1.15	19.1	0.586	1590
97	Hon-17	BA	76	—	—	—	—	—	—	—	—	—	—	—	—	—	—
98	Hon-17	Bt1	100	—	—	—	—	—	—	—	—	—	—	—	—	—	—
99	Hon-17	Bt2	160	288	30.1	37.0	168	1.50	5.77	1.36	7.57	5.60	4.21	0.560	13.9	0.542	1460
100	Hon-17	2BCt	201	—	—	—	—	—	—	—	—	—	—	—	—	—	—
101	Hon-17	3BCt	208	254	25.9	35.0	161	1.35	5.24	1.23	6.97	5.11	4.01	0.708	12.4	0.524	1300
102	Hon-17	4BCt	295	—	—	—	—	—	—	—	—	—	—	—	—	—	—
103	Hon-18	Ap1	19	—	—	—	—	—	—	—	—	—	—	—	—	—	—
104	Hon-18	Ap2	30	385	43.5	26.7	180	2.58	5.50	1.54	6.26	5.46	6.08	1.32	18.5	0.579	1490
105	Hon-18	BA	90	—	—	—	—	—	—	—	—	—	—	—	—	—	—
106	Hon-18	Bt1	113	—	—	—	—	—	—	—	—	—	—	—	—	—	—
107	Hon-18	Bt2	170	274	30.5	35.7	172	1.29	5.65	1.37	7.49	4.77	4.01	0.615	13.3	0.538	1480
108	Hon-18	2BCt	190	—	—	—	—	—	—	—	—	—	—	—	—	—	—
109	Hon-18	3BCt	240	253	24.3	32.7	172	1.40	5.25	1.26	7.47	4.99	3.73	0.556	12.6	0.561	1340
110	Hon-18	4BCt	300	—	—	—	—	—	—	—	—	—	—	—	—	—	—
111	Hon-19	Ap1	7	—	—	—	—	—	—	—	—	—	—	—	—	—	—
112	Hon-19	Ap2	24	430	46.3	35.0	186	2.76	5.92	1.53	6.28	5.36	5.98	1.17	20.2	0.585	2010
113	Hon-19	BA	63	—	—	—	—	—	—	—	—	—	—	—	—	—	—
114	Hon-19	Bt1	91	—	—	—	—	—	—	—	—	—	—	—	—	—	—
115	Hon-19	Bt2	126	—	—	—	—	—	—	—	—	—	—	—	—	—	—
116	Hon-19	Bt3	176	265	31.1	41.7	175	1.60	—	1.32	8.08	5.08	3.94	0.656	13.6	0.518	1590

Supplementary table 7, part 2. Total chemical analyses of the fine (<50 µm) fraction by instrumental neutron activation, elements Na to Zr

[Na value in weight percent; all other values in parts per million. Analysts: J. Budahn, D.M. McKown, and R. Knight]

Sample number	Profile number	Horizon	Basal depth (cm)	Na	Nd	Rb	Sb	Sc	Sm	Sr	Ta	Tb	Th	Tm	U	Yb	Zr
Holocene alluvium, 0.6 ka																	
1	Hon-1	A	12	—	—	—	—	—	—	—	—	—	—	—	—	—	—
2	Hon-1	2A1	16	—	—	—	—	—	—	—	—	—	—	—	—	—	—
3	Hon-1	2A2	25	1.67	18.3	20.5	0.580	31.8	4.33	130	0.551	0.789	2.63	—	1.09	2.97	160
4	Hon-1	2AC	49	—	—	—	—	—	—	—	—	—	—	—	—	—	—
5	Hon-1	2C	85	1.38	17.7	18.2	.498	33.8	4.81	132	.636	.819	2.84	0.513	1.09	3.14	—
6	Hon-1	3C1	95	—	—	—	—	—	—	—	—	—	—	—	—	—	—
7	Hon-1	3C2	122	—	—	—	—	—	—	—	—	—	—	—	—	—	—
8	Hon-1	4B1b	140	—	—	—	—	—	—	—	—	—	—	—	—	—	—
9	Hon-1	4B2b	170	—	—	—	—	—	—	—	—	—	—	—	—	—	—
10	Hon-2	A1	4	—	—	—	—	—	—	—	—	—	—	—	—	—	—
11	Hon-2	A2	32	1.56	20.4	26.6	.468	33.3	4.75	136	.570	.826	2.67	—	1.17	3.52	151
12	Hon-2	C	61	—	—	—	—	—	—	—	—	—	—	—	—	—	—
13	Hon-2	2C	92	1.51	19.5	22.9	.606	32.7	5.11	150	.654	.833	2.93	—	1.18	3.43	156
14	Hon-2	3C	103	—	—	—	—	—	—	—	—	—	—	—	—	—	—
15	Hon-2	4B2tb	130	—	—	—	—	—	—	—	—	—	—	—	—	—	—
16	Hon-3	A1	4	—	—	—	—	—	—	—	—	—	—	—	—	—	—
17	Hon-3	A2	16	1.60	16.8	22.3	.520	31.0	4.44	150	.564	.762	2.48	—	1.03	3.06	179
18	Hon-3	AC	31	—	—	—	—	—	—	—	—	—	—	—	—	—	—
19	Hon-3	C	54	1.54	21.3	19.6	.440	33.8	4.94	220	.656	.944	3.00	.493	1.36	3.40	200
20	Hon-3	2C	78	—	—	—	—	—	—	—	—	—	—	—	—	—	—
21	Hon-4	C	17	—	—	—	—	—	—	—	—	—	—	—	—	—	—
22	Hon-4	2A	32	1.61	19.0	24.0	.605	32.3	4.46	340	.570	.880	2.53	.457	1.16	3.00	160
23	Hon-4	2AC	49	—	—	—	—	—	—	—	—	—	—	—	—	—	—
24	Hon-4	2C	86	1.68	20.0	22.0	.495	33.5	4.67	178	.614	.966	2.80	—	1.20	3.65	187
25	Hon-4	3C1	113	—	—	—	—	—	—	—	—	—	—	—	—	—	—
26	Hon-4	3C2	147	—	—	—	—	—	—	—	—	—	—	—	—	—	—
Upper member of the Modesto Formation, 10 ka																	
27	Hon-5	AP1	13	—	—	—	—	—	—	—	—	—	—	—	—	—	—
28	Hon-5	AP2	23	1.66	18.1	10.0	.405	33.2	4.89	150	.473	.904	2.21	—	1.14	3.27	142

Supplementary table 7, part 2. Total chemical analyses of the fine (<50 μm) fraction by instrumental neutron activation, elements Na to Zr—Continued

Sample number	Profile number	Horizon	Basal depth (cm)	Na	Nd	Rb	Sb	Sc	Sm	Sr	Ta	Tb	Th	Tm	U	Yb	Zr
Upper member of the Modesto Formation, 10 ka—Continued																	
29	Hon-5	BA	54	—	—	—	—	—	—	—	—	—	—	—	—	—	—
30	Hon-5	Bw1	88	1.49	15.5	21.6	.430	36.2	4.78	150	.431	.890	2.29	—	.973	3.75	135
31	Hon-5	Bw2	102	—	—	—	—	—	—	—	—	—	—	—	—	—	—
32	Hon-5	BC1	141	—	—	—	—	—	—	—	—	—	—	—	—	—	—
33	Hon-5	BC2	180	—	—	—	—	—	—	—	—	—	—	—	—	—	—
34	Hon-6	AP1	10	—	—	—	—	—	—	—	—	—	—	—	—	—	—
35	Hon-6	AP2	22	1.60	16.6	22.2	.359	32.9	4.68	120	.413	.860	2.12	.680	.853	3.44	123
36	Hon-6	BA	43	—	—	—	—	—	—	—	—	—	—	—	—	—	—
37	Hon-6	Bw1	91	1.95	17.2	23.7	.431	32.3	4.50	139	.448	.840	1.99	.569	.918	3.50	163
38	Hon-6	Bw2	118	—	—	—	—	—	—	—	—	—	—	—	—	—	—
39	Hon-6	BC1	157	—	—	—	—	—	—	—	—	—	—	—	—	—	—
40	Hon-6	BC2	184	—	—	—	—	—	—	—	—	—	—	—	—	—	—
41	Hon-7	AP1	8	—	—	—	—	—	—	—	—	—	—	—	—	—	—
42	Hon-7	AP2	30	1.75	17.7	30.7	.520	31.8	4.59	145	.474	.850	2.58	.546	1.08	3.52	148
43	Hon-7	BA	54	—	—	—	—	—	—	—	—	—	—	—	—	—	—
44	Hon-7	Bw1	88	1.71	18.7	30.3	.462	34.6	4.94	138	.520	.890	2.61	—	1.10	3.72	145
45	Hon-7	Bw2	118	—	—	—	—	—	—	—	—	—	—	—	—	—	—
46	Hon-7	BC	180	—	—	—	—	—	—	—	—	—	—	—	—	—	—
47	Hon-7	2BC	230	—	—	—	—	—	—	—	—	—	—	—	—	—	—
48	Hon-7	3Cox	290	—	—	—	—	—	—	—	—	—	—	—	—	—	—
49	Hon-7	4Cox	340	—	—	—	—	—	—	—	—	—	—	—	—	—	—
50	Hon-7	4Cn	370	—	—	—	—	—	—	—	—	—	—	—	—	—	—
51	Hon-8	AP1	7	—	—	—	—	—	—	—	—	—	—	—	—	—	—
52	Hon-8	AP2	34	1.80	20.1	32.0	.549	33.0	4.89	160	.533	.920	2.62	—	1.16	3.76	217
53	Hon-8	BA	57	—	—	—	—	—	—	—	—	—	—	—	—	—	—
54	Hon-8	Bw1	90	1.72	17.1	20.6	.464	34.5	4.72	110	.481	.900	2.58	.574	1.08	3.61	172
55	Hon-8	Bw2	126	—	—	—	—	—	—	—	—	—	—	—	—	—	—
56	Hon-8	BC1	191	—	—	—	—	—	—	—	—	—	—	—	—	—	—
57	Hon-8	BC2	240	1.84	18.1	15.6	—	30.2	4.71	116	.476	.890	3.07	—	.915	3.52	175
58	Hon-8	2Cox	390	—	—	—	—	—	—	—	—	—	—	—	—	—	—

Late Cenozoic Stratigraphy of the Feather and Yuba Rivers Area, California

Supplementary table 7, part 2. Total chemical analyses of the fine (<50 μm) fraction by instrumental neutron activation, elements Na to Zr—Continued

Sample number	Profile number	Horizon	Basal depth (cm)	Na	Nd	Rb	Sb	Sc	Sm	Sr	Ta	Tb	Th	Tm	U	Yb	Zr
Upper member of the Riverbank Formation, 130 ka—Continued																	
87	Hon-14	BA1	59	—	—	—	—	—	—	—	—	—	—	—	—	—	—
88	Hon-14	BA2	76	—	—	—	—	—	—	—	—	—	—	—	—	—	—
89	Hon-14	Bt1	111	1.01	14.3	42.3	.720	33.4	3.98	—	.463	.700	4.44	.560	1.48	2.70	156
90	Hon-14	Bt2	126	—	—	—	—	—	—	—	—	—	—	—	—	—	—
91	Hon-14	2BCt1	150	—	—	—	—	—	—	—	—	—	—	—	—	—	—
92	Hon-14	2BCt2	200	—	—	—	—	—	—	—	—	—	—	—	—	—	—
93	Hon-14	2BCt3	260	—	—	—	—	—	—	—	—	—	—	—	—	—	—
94	Hon-14	2CB	320	—	—	—	—	—	—	—	—	—	—	—	—	—	—
Lower member of the Riverbank Formation, 250 ka																	
95	Hon-17	Ap1	18	—	—	—	—	—	—	—	—	—	—	—	—	—	—
96	Hon-17	Ap2	24	1.24	24.0	60.8	1.13	31.6	5.49	170	.503	.942	4.74	.647	1.94	3.66	253
97	Hon-17	BA	76	—	—	—	—	—	—	—	—	—	—	—	—	—	—
98	Hon-17	Bt1	100	—	—	—	—	—	—	—	—	—	—	—	—	—	—
99	Hon-17	Bt2	160	1.25	19.6	27.8	.726	37.5	—	100	.335	.894	3.30	.623	1.44	3.42	141
100	Hon-17	2BCt	201	—	—	—	—	—	—	—	—	—	—	—	—	—	—
101	Hon-17	3BCt	208	1.48	16.4	28.0	.775	34.7	4.24	100	.316	.803	3.16	.548	1.06	3.19	155
102	Hon-17	4BCt	295	—	—	—	—	—	—	—	—	—	—	—	—	—	—
103	Hon-18	Ap1	19	—	—	—	—	—	—	—	—	—	—	—	—	—	—
104	Hon-18	Ap2	30	1.26	24.6	62.1	.969	30.9	5.49	100	.519	.900	4.47	—	2.16	3.65	240
105	Hon-18	BA	90	—	—	—	—	—	—	—	—	—	—	—	—	—	—
106	Hon-18	Bt1	113	—	—	—	—	—	—	—	—	—	—	—	—	—	—
107	Hon-18	Bt2	170	1.45	19.5	23.0	.688	38.2	4.88	—	.323	.866	3.13	—	1.20	3.42	160
108	Hon-18	2BCt	190	—	—	—	—	—	—	—	—	—	—	—	—	—	—
109	Hon-18	3BCt	240	1.46	19.5	26.8	.666	36.5	4.54	160	.316	.884	3.11	.569	.915	3.47	140
110	Hon-18	4BCt	300	—	—	—	—	—	—	—	—	—	—	—	—	—	—
111	Hon-19	Ap1	7	—	—	—	—	—	—	—	—	—	—	—	—	—	—
112	Hon-19	Ap2	24	1.14	24.0	76.1	.745	29.5	5.57	100	.586	.961	5.26	.630	2.21	3.55	223
113	Hon-19	BA	63	—	—	—	—	—	—	—	—	—	—	—	—	—	—
114	Hon-19	Bt1	91	—	—	—	—	—	—	—	—	—	—	—	—	—	—
115	Hon-19	Bt2	126	—	—	—	—	—	—	—	—	—	—	—	—	—	—
116	Hon-19	Bt3	176	1.10	16.6	28.8	.733	37.1	4.57	100	.333	.812	3.41	.559	1.22	3.22	150

Supplementary table 8. Calculated values of the Soil Development Index

[HI is horizon index; PI is profile index. Analyst, A. J. Busacca]

Horizon	Basal depth (cm)	HI	Horizon	Basal depth (cm)	Hi	Horizon	Basal depth (cm)	HI
Profile: HON-1			Profile: HON-2			Profile: HON-3		
A	12	0.172	A	4	0.158	A1	4	0.128
2A1	16	.136	A2	32	.153	A2	16	.131
2A2	25	.179	C	61	.090	AC	31	.131
2AC	49	.137	2C	92	.080	C	54	.053
2C	85	.117	3C	103	.113	2C	78	.048
3C1	95	.119						
3C2	122	.122						
	PI	= 16.22		PI	= 11.23		PI	= 6.42
	PI _{85 cm}	= 11.73		PI _{92 cm}	= 9.99			
Profile: HON-4			Summary: HON-1, -2, -3, -4					
C	17	0.088				$\bar{X}_{full\ depth}$	=	12.32
2A	32	.170				σ	=	4.50
2AC	49	.101				cv	=	36.5 pct
2C	86	.112				$\bar{X}_{subequal\ depths}$	=	9.51
3C1	113	.103				σ	=	2.22
3C2	147	.080				cv	=	23.4 pct
	PI	= 15.40						
	PI _{86 cm}	= 9.89						
Profile: HON-5			Profile: HON-6			Profile: HON-7		
Ap1	13	.181	Ap1	10	.177	Ap1	8	.153
Ap2	23	.208	Ap2	22	.158	Ap2	30	.153
BA	54	.203	BA	43	.211	BA	54	.200
Bw1	88	.216	Bw1	91	.267	Bw1	88	.237
Bw2	102	.258	Bw2	118	.242	Bw2	118	.236
BC1	141	.234	BC1	157	.240	BC	180	.229
BC2	180	.204	BC2	184	.214	2BC	230	.116
	PI	= 37.73		PI	= 42.45		PI	= 44.53
							PI _{180 cm}	= 38.71
Profile: HON-8			Summary: HON-5, -6, -7, -8					
Ap1	7	.151				$\bar{X}_{full\ depth}$	=	44.72
Ap2	34	.151				σ	=	6.91
BA	57	.259				cv	=	15.5 pct
Bw1	90	.273				$\bar{X}_{subequal\ depth}$	=	41.5
Bw2	126	.264				σ	=	3.51
BC1	191	.243				cv	=	8.5 pct
BC2	240	.179						
	PI	= 54.17						
	PI _{191 cm}	= 45.41						
Profile: HON-9			Summary: HON-9, -10, -11					
Ap1	16	.152				$\bar{X}_{subequal\ depth}$	=	50.52
Ap2	25	.168				σ	=	5.14
BAt1	42	.218				cv	=	10.2 pct
BAt2	80	.407						
2Bqkm1	99	.384						
2Bqkm2	113	.384						
2BCqm	137	.369						
3BCt	153	.237						
3C	198	.176						
	PI	= 56.3						
Profile: HON-10			Profile: HON-11			Summary: HON-10,-11		
Ap	22	.233	Ap	18	.208	$\bar{X}_{full\ depth}$	=	47.65
BA	40	.212	BA	45	.251	σ	=	1.68
Bt1	86	.324	Bt1	94	.277	cv	=	3.5 pct
Bt2	132	.344	Bt2	125	.368	$\bar{X}_{subequal\ depth}$	=	45.01
BC	150	.208	BC	145	.230	σ	=	3.44
C	205	.073	C	179	.074	cv	=	7.6 pct
2C	225	.069	2C	220	.094			
	PI	= 48.82		PI	= 46.45			
	PI _{205 cm}	= 47.44		PI _{179 cm}	= 42.58			

Supplementary table 8. Calculated values of the Soil Development Index—Continued

Horizon	Basal depth (cm)	HI	Horizon	Basal depth (cm)	HI	Horizon	Basal depth (cm)	HI
Profile: HON-13			Profile: HON-14			Summary: HON-13,-14		
Ap	24	.133	Ap	28	.129	$\bar{X}_{\text{full depth}}$	=	101.52
BA	33	.169	BA	39	.182	σ	=	1.28
BA1	50	.238	BA1	59	.270	cv	=	1.3 pct
BA12	62	.426	BA12	76	.352			
Bt1	86	.518	Bt1	111	.522			
Bt2	102	.490	Bt2	126	.415			
Bt3	123	.473	2BC1	150	.483			
BCt	157	.408	2BC2	200	.349			
2BC1	208	.345	2BC3	260	.292			
2BC2	245	.302	2CB	320	.239			
3BC3	266	.295						
3BC	301	.220	PI	=	102.42			
PI	=	100.61						
Profile: HON-17			Profile: HON-18			Profile: HON-19		
Ap1	18	.236	Ap1	19	.304	Ap1	7	.189
Ap2	24	.233	Ap2	30	.248	Ap2	24	.213
BA	76	.356	BA	90	.365	BA	63	.330
Bt1	100	.437	Bt1	113	.429	Bt1	91	.346
Bt2	160	.493	Bt2	170	.491	Bt2	126	.468
2BCt	201	.436	2BCt	190	.412	Bt3	176	.489
3BCt	208	.328	3BCt	240	.394	BCt	218	.378
4BCt	295	.346	4BCt	300	.265	2BC1	246	.312
						2BC2	268	.315
PI	=	114.48	PI	=	112.08	2BC3	300	.174
						PI	=	105.41
Profile: HON-20			Summary: HON-17, -18, -19, -20					
Ap1	11	.186	\bar{X}	=	107.84			
Ap2	30	.216	σ	=	6.76			
BA	60	.277	cv	=	6.3 pct			
Bt1	114	.337						
Bt2	191	.511						
2BC1	223	.382						
2BC2	260	.293						
2CB	283	.194						
PI	=	99.52						
Profile: HON-21			Profile: HON-22			Summary: HON-21,-22		
A	11	.276	A	23	.347	\bar{X}	=	223.36
AB	33	.350	AB	43	.348	σ	=	6.54
BA	46	.394	BA	59	.460	cv	=	2.9 pct
Bt1	71	.572	Bt1	89	.576			
Bt2	93	.646	Bt2	120	.617			
Bt3	119	.638	Bt3	154	.599			
Bt4	148	.651	2Bt1	207	.584			
2Bt1	197	.605	2Bt2	270	.501			
2Bt2	274	.523	2BCt	342	.410			
2BC	315	.446	3BC1	445	.338			
3BC	473	.331	3BC2	505	.341			
PI	=	220.29	PI	=	226.43			

Supplementary table 9, part 1. Radiocarbon ages

[Analyst, Beta Analytic]

Sample	Laboratory number	Location	C-14 age (yr B.P.) $\pm 1\sigma$
HOO-21	Beta-1649	SE ¹ / ₄ sec. 23, T. 17 N., R. 3 E. 400 m due west of State Highway 70, in northeast bank of North Honcut Creek, at depth of 2.5 m.	1,625 \pm 90
HON-4	Beta-1650	Sec. 18, T. 17 N., R. 4 E.; 700 m east of Western Pacific Railroad, south bank of southernmost channel of South Honcut Creek, at depth of 1.2 m in C horizon of soil profile HON-4.	625 \pm 60
HOO-25A	Beta-1651	NE ¹ / ₄ sec. 15, T. 17 N., R. 4 E.; 70 m east of westernmost high power line, in north bank of Honcut Creek at a depth of 2.1 m.	450 \pm 45
LRO-2	Beta-1652	400 m west-northwest of center of sec. 23, T. 17 N., R. 4 E.; east bank of north-south reach of South Honcut Creek, 6 m south of old east-west fenceline at a depth of 96 cm.	1,110 \pm 95
HOO-25B	Beta-1653	Same as HOO-25A, at depth of 40 cm.	595 \pm 70
HOO-19-1	Beta-1654	SE ¹ / ₄ SE ¹ / ₄ sec. 16, T. 17 N., R. 4 E., south bank of North Honcut Creek, where creek turns from south to southwest, at a depth of 2.8 m.	1,045 \pm 95
LRO-1	Beta-1655	Near southeast corner, sec. 14, T. 17 N., R. 3 E.; directly across the channel from HOO-21, at 25 cm depth.	1,775 \pm 110

Supplementary table 9, part 2. K-Ar radiometric ages of dacite blocks from lahar of the dacite unit

[ORO-9A,B consisted of 2 samples of fresh dacite blocks in a lahar unit, SE¹/4NE¹/4 sec. 15, T. 19 N., R. 4 E., roadcut on Olive Highway at church. ORO-21 consisted of 1 sample of fresh dacite from a lahar unit, NW¹/4NW¹/4 sec. 9, T. 19 N., R. 4 E., Long Bar Road approximately 150 m south of Y-split. All ages obtained by analyses performed at the U.S. Geological Survey laboratories in Menlo Park, California between 1982 and 1984. Potassium was analyzed by S. Neil and D. Vivit by flame photometry, using lithium metaborate fusion, with lithium serving as an internal standard (Ingamells, 1970). Argon was analyzed by Wendy Hillhouse by the standard isotope-dilution and mass-spectrometry techniques described by Dalrymple and Lanphere (1969). Mineral separates were prepared by D.H. Sorg. Constants used in the calculations are: $\lambda\epsilon + \lambda\epsilon = 0.581 \times 10^{-10} \text{yr}^{-1}$, $\lambda\beta = 4.962 \times 10^{-10} \text{yr}^{-1}$, and $^{40}\text{K}/\text{K}_{\text{total}} = 1.167 \times 10^{-4} \text{mol/mol}$]

Field number	Material analyzed	K ₂ O			Argon		Apparent age (Ma)	Age (Ma) ±σ	Locality	
		Weight percent	σ	Number of values	⁴⁰ Ar _{rad} (mol/g)	100 rad ⁴⁰ Ar / total ⁴⁰ Ar			Lat N.	Long W.
Oro-9A	Dacite	1.913	3.60	4	8.84188x10 ⁻¹²	58.73	3.2	3.2±0.1 (3 pct)	39°30'20"	121°30'52"
					8.71626x10 ⁻¹²	27.20	3.2			
Oro-9B	Biotite	7.58	.62	4	3.72008x10 ⁻¹¹	29.92	3.4	3.4±0.2 (5 pct)	39°30'20"	121°30'52"
	Hornblende	.406	.603	4	1.61132x10 ⁻¹²	4.10	2.8			
					1.95173x10 ⁻¹²	6.14	3.3	3.3±0.3 (10 pct)		
Oro-21	Biotite	8.105	.236	4	3.97022x10 ⁻¹¹	20.16	3.4	3.4±0.2 (5 pct)	39°31'21"	121°32'10"
	Hornblende	.444	.216	4	2.06710x10 ⁻¹²	3.41	3.2			

Supplementary table 10. Tephra correlation

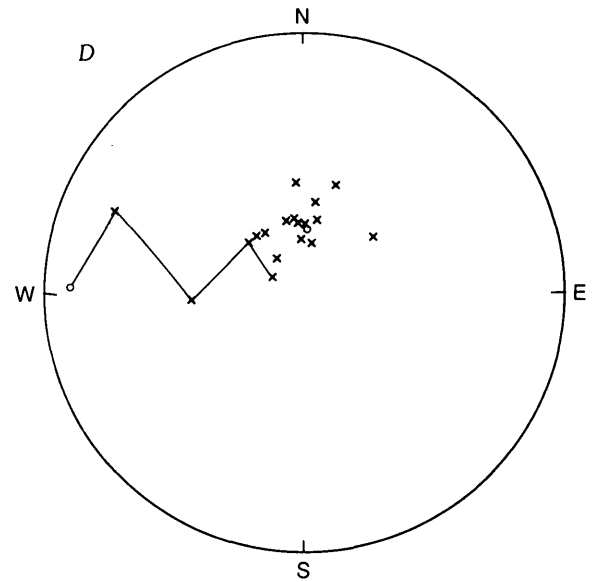
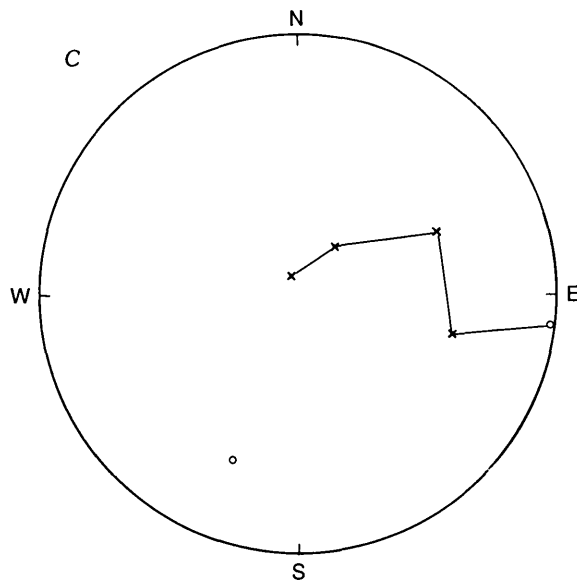
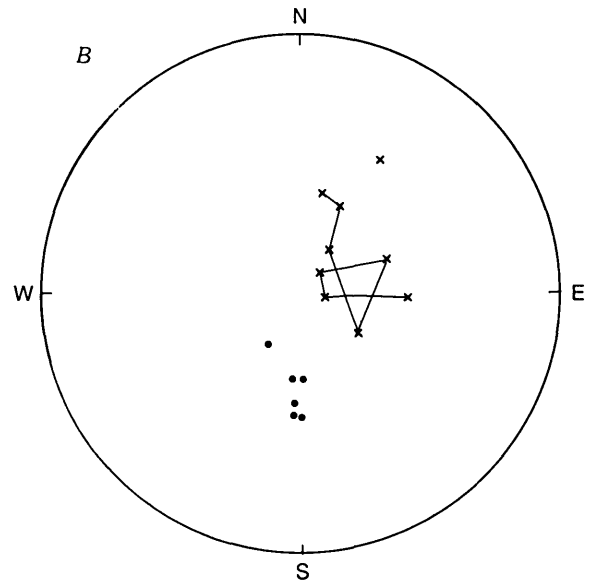
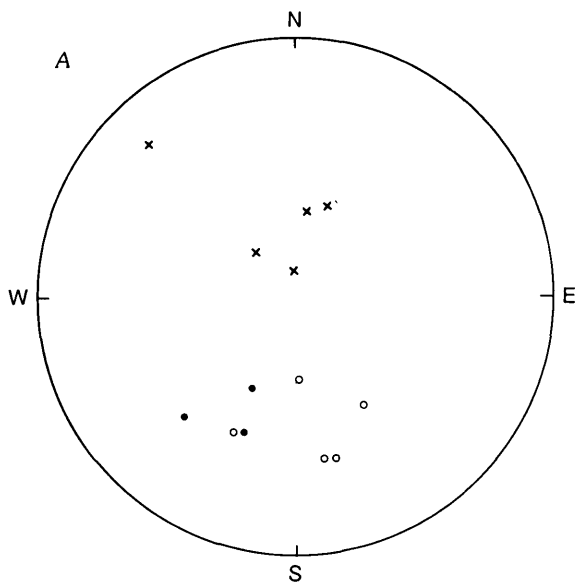
[Results based on comparison of minor- and trace-element chemistry of glass from tuff samples using similarity-coefficient analysis (Sama-Wojcicki, 1976); analyst, A.N. Sama-Wojcicki]

Sample	Location and description	Result
BVO-5	Blue-gray subrounded pumice pebbles in a fluvially derived crystal-vitric matrix; collected at 4 m in backhoe pit, NE $\frac{1}{4}$ NE $\frac{1}{4}$ sec. 8, T. 15 N., R. 5 E., Browns Valley 7 $\frac{1}{2}$ -minute quadrangle.	Correlated with the Nomlaki Tuff Member of the Tehama Formation.
81F-11	Sample of tuffaceous(?) silt; collected by geologists of California Department of Water Resources from a depth of 21 m (69 ft) beneath a deposit mapped as the Laguna Formation; elevation, 186 ft; Thermalito Forebay Dam at toe. SW $\frac{1}{4}$ sec. 10, T. 19 N., R. 3 E., Shippee 7 $\frac{1}{2}$ -minute quadrangle.	Diatomaceous silt.
Therm-1	Sample of white pumice pebbles in tuffaceous sand collected by a geologist of California Department of Water Resources from a depth of 4.6 m (15 ft) beneath a deposit mapped as the lower member of the Riverbank Formation; elevation, 115 ft; Thermalito Afterbay perimeter dam at toe. SW $\frac{1}{4}$ sec. 19, T. 19 N., R. 3 E., Biggs 7 $\frac{1}{2}$ -minute quadrangle.	Not correlated; similarity coefficient approx. 0.90 for comparison with Rockland ash bed; approx. 0.85-0.90 for comparison with Nomlaki Tuff Member of the Tehama Formation.

Supplementary table 11. Paleomagnetic determinations

[A total of 40 samples from the four sites were collected for paleomagnetic study; analyst K.L. Verosub. Each sample consisted of a pedestal of sediment carved in the outcrop and collected in a small plastic box. Because the purpose of the study was only to ascertain the magnetic-polarity zonation, the orientations of the samples were determined with an accuracy of only about $\pm 5^\circ$. All the samples were subjected to at least five levels of alternating field demagnetization (0, 10, 20, 30 and 40 mT), and many samples were studied at intermediate and higher levels as well. After each demagnetization, the samples were measured with a spinner magnetometer operating in a six-spin mode. The initial intensities of the samples ranged from 1.3×10^{-3} to 5.6×10^{-5} emu, and the median destructive fields ranged from 10 to 30 mT. The results are shown in figure 5. Detailed stereographic projections are shown in the supplementary figure. The behavior of the samples upon demagnetization indicated that the magnetic carrier was magnetite and that the magnetization of the samples was a detrital remanent magnetization acquired at or shortly after deposition. With three exceptions, all the samples showed minimal directional changes after the initial demagnetization to 10 mT. For all these samples, the direction at a representative demagnetization level of 20 mT is shown in the supplementary figure. For each sample, the polarity can be unambiguously determined to be either normal (down and northward) or reversed (up and southward). The three samples that did not have stable end points above 10 mT (queried in fig. 5) are: the sample above the buried soil at the Western Pacific Railroad site (site 2), the lowest sample at that site, and a sample near the base of the upper member of the Laguna Formation at the same site. The complete demagnetization behavior for the first sample is shown in supplementary figure B. Although the directions are not particularly stable, there appears to be no tendency toward a reversed direction, and so this sample has been classified as probably normal. The second sample (fig. C), and the third sample (fig. D), however, both show a clear progression to a reversed direction and so they have been classified as probably reversed]

Site	Location and description
Feather River, site 1	SE $\frac{1}{4}$ sec. 13, T. 19 N., R. 3 E. Composite section from Bluff exposure on west bank of Feather River; samples taken in stratigraphic succession at sites a few meters south to 80 m north of old railroad-bridge piers. Section sampled exposes very coarse cobble conglomerate of the upper member of the Laguna Formation overlying thin-bedded volcanoclastic silt and sand and a thin lahar belonging to the dacite unit.
Western Pacific Railroad, site 2	NE $\frac{1}{4}$ sec. 31, and SE $\frac{1}{4}$ sec. 30, T. 19 N., R. 4 E. This is a composite section that includes from the top of the section to the bottom, the north face of the roadcut in Ophir Road, the southeast-facing sideslope of the adjacent hill, the west side of the Western Pacific Railroad cut, and the roadcut in Baggett-Palermo Road. This section is described on p. G26 and consists of the upper member of the Laguna Formation unconformably overlying volcanic sediment of the dacite unit.
Meadowview Road, site 3	NW $\frac{1}{4}$ NE $\frac{1}{4}$ sec. 15, T. 19 N., R. 4 E. This section exposes the Nomlaki Tuff Member of the Laguna Formation overlying volcanic sediment and a dacitic lahar of the dacite unit. The contact zone between the dacite unit and the Nomlaki Tuff Member may be gradational. The exposure starts at the intersection of Oro-Quincy Highway and Meadowview Road and extends eastward on Meadowview Road. This section is described on p. G34-G35.
Wyandotte Road, site 4	Approximately 60 m north of the E $\frac{1}{4}$ cor. NW $\frac{1}{4}$ sec. 21, T. 19 N., R. 4 E. Samples were taken from the east side of a roadcut on Wyandotte Road that exposes several meters of thin-bedded, fluvial, pumice-pebble-bearing sediment of the Nomlaki Tuff Member of the Laguna Formation.



Supplementary figure 1. Stereographic projections of data from paleomagnetic studies. Each point represents direction of magnetization of a single sample after demagnetization to 20 mT; crosses, data points on lower hemisphere; circles and dots, data points on upper hemisphere. *A*, Samples from Feather River (site 1) are crosses; from Meadowview Road (site 3), circles; from Wyandotte Road (site 4), dots. *B*, Top eight samples from

Western Pacific Railroad site (site 2), showing complete demagnetization behavior of queried normal sample above buried soil. *C*, Bottom two samples from Western Pacific Railroad site, showing complete demagnetization behavior of lowest sample. *D*, Remaining samples from Western Pacific Railroad site, showing complete demagnetization behavior of queried normal sample from near base of upper member of Laguna Formation.

SELECTED SERIES OF U.S. GEOLOGICAL SURVEY PUBLICATIONS

Periodicals

Earthquakes & Volcanoes (issued bimonthly).

Preliminary Determination of Epicenters (issued monthly).

Technical Books and Reports

Professional Papers are mainly comprehensive scientific reports of wide and lasting interest and importance to professional scientists and engineers. Included are reports on the results of resource studies and of topographic, hydrologic, and geologic investigations. They also include collections of related papers addressing different aspects of a single scientific topic.

Bulletins contain significant data and interpretations that are of lasting scientific interest but are generally more limited in scope or geographic coverage than Professional Papers. They include the results of resource studies and of geologic and topographic investigations; as well as collections of short papers related to a specific topic.

Water-Supply Papers are comprehensive reports that present significant interpretive results of hydrologic investigations of wide interest to professional geologists, hydrologists, and engineers. The series covers investigations in all phases of hydrology, including hydrogeology, availability of water, quality of water, and use of water.

Circulars present administrative information or important scientific information of wide popular interest in a format designed for distribution at no cost to the public. Information is usually of short-term interest.

Water-Resources Investigations Reports are papers of an interpretive nature made available to the public outside the formal USGS publications series. Copies are reproduced on request unlike formal USGS publications, and they are also available for public inspection at depositories indicated in USGS catalogs.

Open-File Reports include unpublished manuscript reports, maps, and other material that are made available for public consultation at depositories. They are a nonpermanent form of publication that may be cited in other publications as sources of information.

Maps

Geologic Quadrangle Maps are multicolor geologic maps on topographic bases in 7 1/2- or 15-minute quadrangle formats (scales mainly 1:24,000 or 1:62,500) showing bedrock, surficial, or engineering geology. Maps generally include brief texts; some maps include structure and columnar sections only.

Geophysical Investigations Maps are on topographic or planimetric bases at various scales; they show results of surveys using geophysical techniques, such as gravity, magnetic, seismic, or radioactivity, which reflect subsurface structures that are of economic or geologic significance. Many maps include correlations with the geology.

Miscellaneous Investigations Series Maps are on planimetric or topographic bases of regular and irregular areas at various scales; they present a wide variety of format and subject matter. The series also includes 7 1/2-minute quadrangle photogeologic maps on planimetric bases which show geology as interpreted from aerial photographs. Series also includes maps of Mars and the Moon.

Coal Investigations Maps are geologic maps on topographic or planimetric bases at various scales showing bedrock or surficial geology, stratigraphy, and structural relations in certain coal-resource areas.

Oil and Gas Investigations Charts show stratigraphic information for certain oil and gas fields and other areas having petroleum potential.

Miscellaneous Field Studies Maps are multicolor or black-and-white maps on topographic or planimetric bases on quadrangle or irregular areas at various scales. Pre-1971 maps show bedrock geology in relation to specific mining or mineral-deposit problems; post-1971 maps are primarily black-and-white maps on various subjects such as environmental studies or wilderness mineral investigations.

Hydrologic Investigations Atlases are multicolored or black-and-white maps on topographic or planimetric bases presenting a wide range of geohydrologic data of both regular and irregular areas; principal scale is 1:24,000 and regional studies are at 1:250,000 scale or smaller.

Catalogs

Permanent catalogs, as well as some others, giving comprehensive listings of U.S. Geological Survey publications are available under the conditions indicated below from the U.S. Geological Survey, Books and Open-File Reports Section, Federal Center, Box 25425, Denver, CO 80225. (See latest Price and Availability List.)

"**Publications of the Geological Survey, 1879- 1961**" may be purchased by mail and over the counter in paperback book form and as a set of microfiche.

"**Publications of the Geological Survey, 1962- 1970**" may be purchased by mail and over the counter in paperback book form and as a set of microfiche.

"**Publications of the U.S. Geological Survey, 1971- 1981**" may be purchased by mail and over the counter in paperback book form (two volumes, publications listing and index) and as a set of microfiche.

Supplements for 1982, 1983, 1984, 1985, 1986, and for subsequent years since the last permanent catalog may be purchased by mail and over the counter in paperback book form.

State catalogs, "List of U.S. Geological Survey Geologic and Water-Supply Reports and Maps For (State)," may be purchased by mail and over the counter in paperback booklet form only.

"**Price and Availability List of U.S. Geological Survey Publications**," issued annually, is available free of charge in paperback booklet form only.

Selected copies of a monthly catalog "New Publications of the U.S. Geological Survey" available free of charge by mail or may be obtained over the counter in paperback booklet form only. Those wishing a free subscription to the monthly catalog "New Publications of the U.S. Geological Survey" should write to the U.S. Geological Survey, 582 National Center, Reston, VA 22092.

Note---Prices of Government publications listed in older catalogs, announcements, and publications may be incorrect. Therefore, the prices charged may differ from the prices in catalogs, announcements, and publications.

